THE JOURNAL
OF
CHEMICAL PHYSICS

VOLUME 16, NUMBER 8 AUGUST, 1948

The Mechanism of Flame Propagation

M. F. HOARE AND J. W. LINNETT
Inorganic Chemistry Laboratory, University Museum, Oxford, England

(Received February 23, 1948)

Recently Tanford and Pease have shown that in a number of carbon monoxide flames the burning velocity increases as the calculated equilibrium concentration of hydrogen atoms in the flame front increases. They point out that this would be so if the propagation of the flame were dependent on the diffusion of hydrogen atoms ahead of the flame. It is shown in the present paper that, by combining calculated ignition and flame temperatures, the variation in burning velocity with composition can also be accounted for on an essentially thermal theory of flame propagation.

IN a recent paper Tanford and Pease[1] have calculated the equilibrium concentrations of hydrogen atoms, hydroxyl, radicals and oxygen atoms in carbon monoxide flames to which have been added nitrogen, water, and hydrogen. Using burning velocities measured by Jahn[2] they show that the burning velocity increases regularly, on the whole, with the hydrogen atom concentration (see Fig. 1, reference 1). This most interesting and striking result is consistent with the view that the flame is carried from one layer to the next by the diffusion of the light and fast-moving hydrogen atoms ahead of the flame, for the flame will be expected to move more quickly the higher the equilibrium concentration of hydrogen atoms in the flame front. They have followed up this idea in two subsequent papers.[3,4] In the first of these[3] Tanford states that "this correlation is not readily explained by theories of burning velocity based on heat conduction."

The object of this communication is to show that the variation in burning velocity observed by Jahn is quite consistent with an essentially thermal conception of flame propagation.

The three main features of Jahn's results are that the burning velocity increases (a) when the percentage of carbon monoxide is increased, the

TABLE I. Flame temperatures, T_f; ignition temperatures, T_e; and burning velocities, V_b, for carbon monoxide-oxygen flames. The burning velocities are given in cm/sec.

Percentage composition				T_e[a]						V_b
CO	O_2	N_2	T_f	A	B	C	D	E	F	Jahn
35**	8.5	56.5	1730	947	1212	968	1247	984	1273	25.5
26½**	44.1	29.4	2320	1100	1475	1057	1398	1028	1347	29.5
40*	12.6	47.4	2320	1003	1304	1002	1303	1001	1302	30
40**	12.6	47.4	2320	955	1224	973	1255	986	1277	40
40*	59.1	0.9	2720	1118	1507	1067	1415	1032	1355	48
40**	24	36	2660	996	1293	997	1296	999	1298	50.5
45**	22	33	2710	975	1258	985	1275	992	1287	57
40**	59.1	0.9	2720	1059	1402	1034	1359	1017	1329	60
60*	39.4	0.6	2930	1025	1343	1015	1325	1007	1313	68
50**	30	20	2810	996	1268	989	1281	994	1291	72
80*	19.7	0.3	2860	943	1206	966	1243	982	1271	72
60**	24	16	2850	945	1208	967	1244	983	1272	83
60**	39.4	0.6	2930	975	1258	985	1275	993	1288	93
70**	24	6	2900	927	1179	955	1226	977	1262	98
80**	19.7	0.3	2860	901	1137	939	1199	968	1247	106

* CO contains 1.35 percent H_2O.
** CO contains 1.35 percent H_2O and 1.5 percent H_2.
[a] Six columns of T_e:—*A*: E=30,000, T_e~1000; *B*: E=30,000, T_e~1300; *C*: E=50,000, T_e~1000; *D*: E=50,000, T_e~1300; *E*: E=100,000, T_e~1000; *F*: E=100,000, T_e~1300. All temperatures are in °K, and activation energies, E, in cal. per g mole.

[1] C. Tanford and R. N. Pease, J. Chem. Phys **15**, 431 (1947).
[2] G. Jahn, *Der Zundvorgang in Gasgemischen* (Oldenbourg, Berlin, 1942).
[3] C. Tanford, J. Chem. Phys. **15**, 433 (1947).
[4] C. Tanford and R. N. Pease, J. Chem. Phys. **15**, 861 (1947).

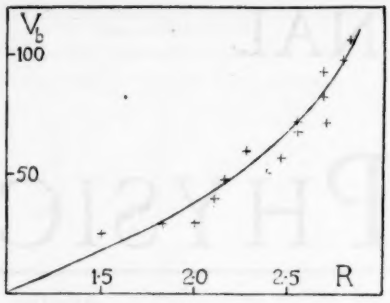

FIG. 1. Graph of the burning velocity, V_b, in cm/sec. against $R=(T_f-T_0)/(T_e-T_0)$ for moist carbon monoxide-oxygen flames.

percentage of oxygen being kept constant; (b) when the oxygen percentage is increased, the percentage of carbon monoxide being kept constant; (c) when hydrogen is added, the carbon monoxide and oxygen percentages being kept constant. The effect of (a) and (b) is to make the flame hotter and the effect of (c) is to increase the rate of reaction, i.e., the rate of heat release. Both would be expected to increase the flame speed according to a thermal theory.

Let us suppose that the reaction becomes thermally uncontrolled (i.e., explosive) at a temperature, T_e, when the rate of heat release reaches a value H. The value of H may be assumed to be a constant independent of composition because carbon monoxide, oxygen, and nitrogen have approximately the same heat capacities and thermal conductivities. On the basis of the kinetic results of Hadman, Thompson, and Hinshelwood[5] (which have been interpreted in terms of a radical chain mechanism[6]) and because the rate of heat release is proportional to the rate of reaction, we may write

$$H=k.\frac{p_{CO}.p_{H_2O}}{p_{O_2}}.e^{-E/RT_e}=k.P.e^{-E/RT_e}, \quad (1)$$

where

$$P=\frac{p_{CO}.p_{H_2O}}{p_{O_2}},$$

where k is the transformation constant to convert reaction rate to rate of heat liberation and involves the heat of reaction, E is the energy of activation, and H is that rate of heat release (assumed constant) at which the reaction just becomes explosive. We shall make the simplifying assumption in what follows that the effect of the added hydrogen is equal to that of an equivalent amount of water because the hydrogen will be rapidly converted to water. From (1) we may write

$$T_e=E/R(\log_e P-\log_e H'), \quad (2)$$

where $H'=H/k$ and is also a constant independent of composition. We have calculated the way in which T_e is expected to change with composition according to (2) for three values of E (30,000, 50,000 and 100,000 cal. per g mole) using for each value of E two values of the constant H', one being chosen so that T_e is in the neighborhood of 1000°K, and the other so that T_e is in the neighborhood of 1300°K. These temperatures were chosen because they may be considered likely extremes for what is usually called the ignition temperature. The energy of activation is not likely to be greater than 100,000 or less than 30,000 cal. per g mole. The values of T_e calculated for the six combinations of E and H' are shown in Table I together with the compositions, the flame temperatures, T_f, given by Tanford and Pease, and the burning velocities of Jahn, V_b.

On a thermal conception of flame propagation we have to consider the time that will be taken in heating a portion of gas ahead of the flame up to the temperature, T_e, at which the reaction becomes thermally self-sustaining. This time will be longer the more closely (T_e-T_0) (T_0 being the initial temperature) approaches (T_f-T_0). So an increase in $(T_e-T_0)/(T_f-T_0)$ should lead to a decrease in V_b. Or, alternatively, V_b should increase as $(T_f-T_0)/(T_e-T_0)$ (represented by R) increases.[7] In Fig. 1 V_b is plotted against R for E equal to 50,000 and H' selected so that T_e is about 1300°K or about 1000°C (middle of the range of values). It will be seen that all the points lie close to a smooth curve drawn through them. That is, V_b does increase in the fairly regular manner with R that is to be expected

[5] G. Hadman, H. W. Thompson, and C. N. Hinshelwood, Proc. Roy. Soc. **A137**, 87 (1932).

[6] C. N. Hinshelwood, *Kinetics of Chemical Change in Gaseous Systems* (Oxford University Press, London, 1933), p. 286; B. Lewis and G. von Elbe, *Combustion, Flames and Explosions in Gases* (Cambridge University Press, Teddington, England, 1938), p. 74.

[7] Cf. Mallard and LeChatelier, Ann. des. Mines **4**, 274 (1883); also reference 6, p. 208.

from a thermal theory. The correlation between V_b and R obtained here is quite as satisfactory as that between V_b and p_H pointed out by Tanford and Pease.[1] Moreover, the correlation is also satisfactory for the other combinations of E and H' (rather better for E equal to 50,000 and T_e about 1000°K and for both values of T_e when E is 100,000; rather less good for both values of T_e (i.e., H') when E is 30,000). The interpretation is therefore hardly at all dependent on the exact values assumed for E and H'.

There is one point that may be added here. The line in Fig. 1 can reasonably be extrapolated to pass through $V_b=0$, $R=1$, which is to be expected theoretically on the thermal theory since no flame could propagate if T_f were less than T_e, according to this theory.

Our general conclusion, therefore, is that the results of Jahn do not enable us to decide whether thermal conduction or radical diffusion is more important in the propagation of carbon monoxide-oxygen flames. We are, at the moment, carrying out determinations of burning velocities which we hope will help in deciding the relative importance of these two factors in the propagation of certain flames.

THE JOURNAL OF CHEMICAL PHYSICS VOLUME 16, NUMBER 8 AUGUST, 1948

Symmetry Matrices in Normal Coordinate Analysis

JOHN E. KILPATRICK
Department of Chemistry, The Rice Institute, Houston, Texas

(Received March 2, 1948)

A general symmetry matrix, U_n, has been derived which may be used to combine n equivalent coordinates in a molecule having the symmetry of any cyclic or dihedral point group of multiplicity n. The direct products $U_2 \times U_n$ and $U_2 \times U_2 \times U_n$ may be used in the cases of $2n$ and $4n$ equivalent coordinates. The symmetry type of each row of the symmetry matrices used has been determined.

THE secular equation necessary for a normal coordinate treatment of the vibrations of a molecule with N degrees of freedom may be represented by a polynomial equation of degree N, a determinantal equation of degree N or a matrix of order N. The superficial form of the secular equation varies with the choice of coordinates but the roots (which are simply related to the vibrational frequencies of the molecule) are independent of this choice. Wilson[1] has given a very convenient method by which the secular equation can be set up in terms of any given set of coordinates.

A set of valence-bond and valence-angle increases is usually not the best choice of coordinates that can be made. The use instead of certain linear combinations of these elementary coordinates may lead to a considerably factored form of the secular equation. Just which combinations, if any, are suitable is dependent on the symmetry of the molecule. This factorization decreases considerably the number of terms that need be calculated and replaces one equation of high degree with several of lower degree.

The choice of these linear combinations of elementary valence coordinates (symmetry coordinates) has frequently been left to the experience and intuition of the worker. Wilson[1] has given some rules which must be satisfied by a set of symmetry coordinates. Venkatarayudu[2] has given a method for determining symmetry coordinates that is related to the method given in this paper. Eyring, Walter and Kimball[3] have given a method which was derived for use with wave functions but may be applied to the problem of symmetry coordinates. In this method it is necessary to investigate the action of each of the symmetry operations of the point group appro-

[1] E. Bright Wilson, Jr., J. Chem. Phys. **9**, 97 (1941).

[2] T. Venkatarayudu, Proc. Ind. Acad. Sci. **17a**, 50 (1943).

[3] H. Eyring, J. Walter and G. Kimball, *Quantum Chemistry* (John Wiley and Sons, Inc., New York), Eq. (10.47), p. 189.

TABLE I. General character table for C_{nv} and D_n.

C_{nv}* / D_n	C_n^m / C_n^m	(*Fused into one class for n odd.*) $(n/2)\sigma_v$ / $(n/2)C_2$	$(n/2)\sigma_v'$ / $(n/2)C_2'$
A_1	1	1	1
A_2	1	−1	−1
E_1	$2\cos m\omega$	0	0
E_2	$2\cos 2m\omega$	0	0
...	...	...	...
E_p	$2\cos pm\omega$	0	0
B_1**	$(-1)^m$	1	−1
B_2**	$(-1)^m$	−1	1

* The first column of characters represents the characters for n elements. $m=1, 2, \ldots n$. $p=(n-2)/2$ for n even, $(n-1)/2$ for n odd, $\omega=2\pi/n$ radiians. The two A representations may be regarded as a degenerate E_0; the two B representations as $E_{\frac{1}{2}n}$ (when $\frac{1}{2}n$ is integral).
** Drop out for n odd.

priate to the system under consideration upon the elementary valence coordinates. Glockler[4] has used a similar method for determining nondegenerate symmetry coordinates.

It is the purpose of this paper to discuss a method which, in very many cases, leads immediately to a suitable set of symmetry coordinates. An $n\times n$ matrix (U_n) is given as a function of n. U_n may be used to combine n equivalent coordinates in any of the common cyclic or dihedral groups of order n. The first row of U_n always gives an A symmetry coordinate, the next two an E_1 doubly degenerate pair, the next two an E_2 pair, etc., and the last row (present only when n is even) a B coordinate. Similarly, the direct products $U_2\times U_n$ and $U_2\times U_2\times U_n$ may be used to combine $2n$ and $4n$, respectively, equivalent coordinates in a group of multiplicity n (C_{nv}, D_n, D_{nh}, etc.). In the three cases just mentioned (n, $2n$, and $4n$ equivalent coordinates), the rows of the symmetry matrix occur in one, two and four sets of n rows. The auxiliary superscripts ($'$ and $''$) are always the same for every symmetry coordinate in any one set of n.

Although the proofs of these properties are somewhat lengthy, the symmetry matrices here defined may be used immediately in any appropriate problem.

EQUIVALENT COORDINATES

A molecule is said to have the symmetry G if the permutations of the sets of equivalent atoms in the molecule form a representation of the point group G. Certain bonds and certain angles will also be permuted among themselves by the action of a given permutation P of G. A set of bonds or a set of angles which are completely permuted among themselves by the elements P of G are called a set of equivalent bonds or angles, respectively. Internal coordinates, however, are increases in bond lengths and valence angles. It is possible to associate a set of equivalent points, not necessarily coinciding with any set of equivalent atoms, with each set of equivalent bonds or angles. These sets are useful in calculating, for example, how many C−H stretching vibrations there are in a given symmetry type in a given molecule. However, for our present purpose, we need a set of vectors to associate with each set of equivalent coordinates (changes in sets of equivalent bonds or angles). For a given set of equivalent bond length changes, a unit vector may be associated with each bond, with some uniform convention as to direction. For a set of equivalent angles changes, the vectors may be oriented perpendicular to the planes of the angles, also with a uniform convention as to direction. A similar convention may be devised for other types of deformation, such as torsion.

It does not follow that a given permutation P (of G) will merely permute the vectors associated with a set of equivalent coordinates among themselves. There may be, in addition, changes of sign. That is, if a given P moves the atoms which define vector $\mathbf{R}_i$ to the position formerly occupied by the atoms which define $\mathbf{R}_j$, we say $PR_i=R_j$. On the other hand, if $\mathbf{R}_i$ moves to the former position of $\mathbf{R}_j$ but is oriented in the opposite direction, we have $PR_i=-R_j$.

We can readily express the whole family of such equations in matrix notation. Let R be the column matrix with elements R_i and R^* be the column matrix with the elements PR_i. We then have

$$R^*=PR. \tag{1}$$

There will be a square matrix P for each element of G and together they form a reducible representation of G. In the case of the cyclic and dihedral groups, the elements of the matrices P consist of zero or plus or minus unity. There will be not more than one unity in any one row or column.

[4] G. Glockler, Rev. Mod. Phys. **15**, 111 (1943).

It is informative to set up such matrices in a few actual cases but we shall show that it is not usually necessary to do so in order to choose suitable symmetry coordinates.

The matrices P will always be blocked out along the main diagonal at least to the extent necessary to separate the sets of equivalent coordinates. Corresponding diagonal minors from each P also are reducible representations of G and frequently it is convenient to treat them separately. A representation of G consisting of one or more diagonal minors of the complete P's will be designated P_q, where the subscript will indicate the coordinates involved, except when no confusion is likely to arise by the omission of the subscript.

Let U be some square matrix that when multiplied on R, generates a new set of coordinates $\mathfrak{R}$:

$$\mathfrak{R} = UR. \tag{2}$$

If we require that U be ortho-normal, in place of Eq. (1) we have

$$\mathfrak{R}^* = (UPU')\mathfrak{R} \tag{3}$$

Eq. (3) obviously can also be written in terms of $\mathfrak{R}_q$ and P_q.

Now if a matrix U can be found that will transform the reducible representations P to the irreducible representations of G, that matrix U consists of just the symmetry coefficients we need. How this can be done in many cases will be shown in the following sections.

POINT GROUPS C_{nv} AND D_n

These two families may be treated together since, for any particular value of n, C_{nv} is isomorphic with D_n. Both have $2n$ elements: n are proper rotations about the main symmetry axis (C_n); the remaining n are dihedral elements.

The first n elements may be represented by C_n^m, where m takes the values 1, 2, 3, $\cdots n$. C_n^m is the mth power of C_n and represents a rotation of $m(2\pi/n)$ radians. The way in which these elements separate into classes is not important for our present purposes.

The n dihedral elements consist of reflections through n vertical planes (σ_v) in the case of C_{nv} and of rotations about n dihedral twofold axes (C_2) in the case of D_n. In both cases these n elements fall into a single class when n is odd but divide into two classes ($n/2$ elements to each) when n is even.

The characters of the irreducible representations of both of these groups are given in a condensed notation in Table I.

It is now time to introduce a matrix which will be the basis for all of our symmetry combinations. Let $\omega = 2\pi/n$, where n is some integer. Write the following array of terms:

cos0	cos0	cos0	cos0	
sin0	sin0	sin0	sin0	
cos0	cosω	cos2ω	cos3ω	$\cdots$.
sin0	sinω	sin2ω	sin3ω	
cos0	cos2ω	cos4ω	cos6ω	
sin0	sin2ω	sin4ω	sin6ω	
$\cdots$	$\cdots$	$\cdots$	$\cdots$	

After n columns the terms will repeat; consequently retain only the first n columns. Cross out all rows consisting wholly of zeros and retain only the first n rows which remain. This square array we will call the matrix V_n. The first row will always have $+1$ for every element and will be followed, according to whether n is even or odd, by $(n-2)/2$ or $(n-1)/2$ pairs of cosine-sine rows. If n is even, there will be a final row consisting alternatingly of $+1$ and -1. We will refer to the first row and the last row (when n is even) as odd rows.

V_n is normalized by the factor $(1/n)^{\frac{1}{2}}$ for the odd rows and by $(2/n)^{\frac{1}{2}}$ for each of the other rows. A matrix N_n that will normalize V_n by premultiplication is diagonal and has for elements $(1/n)^{\frac{1}{2}}$, followed by $(2/n)^{\frac{1}{2}}$ for each row of the cosine-sine row pairs. If n is even, there will be a final element $(1/n)^{\frac{1}{2}}$. The normalized form of V_n we will call U_n:

$$U_n = N_n V_n. \tag{4}$$

The preceding discussion is illustrated by the two examples, $n=3$ and $n=6$:*

* A number of special cases of U_n have been used before. U_2, U_3, U_4* and U_6 are well known (although not always written in the order given here). U_5 has been used in a treatment of cyclopentane (Kilpatrick, Pitzer and Spitzer, J. Am. Chem. Soc. 69, 2483 (1947)).

$$V_3=\begin{bmatrix}1 & 1 & 1\\ 1 & \cos 2\pi/3 & \cos 4\pi/3\\ 0 & \sin 2\pi/3 & \sin 4\pi/3\end{bmatrix}=\begin{bmatrix}1 & 1 & 1\\ 1 & -1/2 & -1/2\\ 0 & (3/4)^{\frac{1}{2}} & -(3/4)^{\frac{1}{2}}\end{bmatrix}, \tag{5}$$

$$U_3=\begin{bmatrix}(1/3)^{\frac{1}{2}} & 0 & 0\\ 0 & (2/3)^{\frac{1}{2}} & 0\\ 0 & 0 & (2/3)^{\frac{1}{2}}\end{bmatrix}\begin{bmatrix}1 & 1 & 1\\ 1 & -1/2 & -1/2\\ 0 & (3/4)^{\frac{1}{2}} & -(3/4)^{\frac{1}{2}}\end{bmatrix}=\begin{bmatrix}(1/3)^{\frac{1}{2}} & (1/3)^{\frac{1}{2}} & (1/3)^{\frac{1}{2}}\\ (2/3)^{\frac{1}{2}} & -(1/6)^{\frac{1}{2}} & -(1/6)^{\frac{1}{2}}\\ 0 & (1/2)^{\frac{1}{2}} & -(1/2)^{\frac{1}{2}}\end{bmatrix}, \tag{6}$$

$$V_6=\begin{bmatrix}1 & 1 & 1 & 1 & 1 & 1\\ 1 & \cos 2\pi/6 & \cos 4\pi/6 & \cos 6\pi/6 & \cos 8\pi/6 & \cos 10\pi/6\\ 0 & \sin 2\pi/6 & \sin 4\pi/6 & \sin 6\pi/6 & \sin 8\pi/6 & \sin 10\pi/6\\ 1 & \cos 4\pi/6 & \cos 8\pi/6 & \cos 12\pi/6 & \cos 16\pi/6 & \cos 20\pi/6\\ 0 & \sin 4\pi/6 & \sin 8\pi/6 & \sin 12\pi/6 & \sin 16\pi/6 & \sin 20\pi/6\\ 1 & -1 & 1 & -1 & 1 & -1\end{bmatrix}, \tag{7}$$

$$U_6=\begin{bmatrix}(1/6)^{\frac{1}{2}} & (1/6)^{\frac{1}{2}} & (1/6)^{\frac{1}{2}} & (1/6)^{\frac{1}{2}} & (1/6)^{\frac{1}{2}} & (1/6)^{\frac{1}{2}}\\ (1/3)^{\frac{1}{2}} & 1/2(1/3)^{\frac{1}{2}} & -1/2(1/3)^{\frac{1}{2}} & -(1/3)^{\frac{1}{2}} & -1/2(1/3)^{\frac{1}{2}} & 1/2(1/3)^{\frac{1}{2}}\\ 0 & 1/2 & 1/2 & 0 & -1/2 & -1/2\\ (1/3)^{\frac{1}{2}} & -1/2(1/3)^{\frac{1}{2}} & -1/2(1/3)^{\frac{1}{2}} & (1/3)^{\frac{1}{2}} & -1/2(1/3)^{\frac{1}{2}} & -1/2(1/3)^{\frac{1}{2}}\\ 0 & 1/2 & -1/2 & 0 & 1/2 & -1/2\\ (1/6)^{\frac{1}{2}} & -(1/6)^{\frac{1}{2}} & (1/6)^{\frac{1}{2}} & -(1/6)^{\frac{1}{2}} & (1/6)^{\frac{1}{2}} & -(1/6)^{\frac{1}{2}}\end{bmatrix}. \tag{8}$$

U_n is readily seen to be orthonormal from the trigonometric identities of Appendix I. We shall now show how it may be used as a symmetry matrix.

Case 1. n equivalent coordinates

The coordinates should be numbered and oriented so that the rotation C_n^m merely permutes the several R_i cyclically: $C_n^m R_i = R_{i+m}$. For example, if $n=5$, $m=2$:

$$\begin{bmatrix}0 & 0 & 0 & 1 & 0\\ 0 & 0 & 0 & 0 & 1\\ 1 & 0 & 0 & 0 & 0\\ 0 & 1 & 0 & 0 & 0\\ 0 & 0 & 1 & 0 & 0\end{bmatrix}\begin{bmatrix}R_1\\ R_2\\ R_3\\ R_4\\ R_5\end{bmatrix}=\begin{bmatrix}R_4\\ R_5\\ R_1\\ R_2\\ R_3\end{bmatrix}. \tag{9}$$

The elements of P for C_n^m are given by

$$P_{ij}=\delta_{i,\,j+m}. \tag{10}$$

We are using the convention that subscripts i, $i\pm n$, $i\pm 2n$, etc., are equivalent.

Let A be defined by

$$A=U_nPU_n'=N_nV_nPV_n'N_n'=N_n^2V_nPV_n'. \tag{11}$$

We shall prove that

$$A=\Gamma=(\Gamma_1+\Gamma_2+\Gamma_3+\cdots) \tag{12}$$

where the right hand member is the direct sum of the irreducible representations of the group G, i.e., a matrix composed of square blocks along its main diagonal and with each block an irreducible representation of G.

On expanding Eq. (6) we have

$$\begin{aligned}(N^{-2}A)_{ij}&=\sum_r\sum_s V_{ir}P_{rs}V_{sj}\\ &=\sum_r\sum_s V_{ir}V_{js}\delta_{r,\,s+m}\\ &=\sum_{r=1}^{n}V_{i,\,r}V_{j,\,r-m}.\end{aligned} \tag{13}$$

The elements A_{11} and (if n is even) A_{nn} are readily evaluated. They are

$$A_{11}=1,\quad A_{nn}=(-1)^m \text{ (if } n \text{ is even)}. \tag{14}$$

The general form of the cosine-sine elements of V may be written as

$$V_{i,\,r}=\begin{Bmatrix}\cos(i/2)(r-1)\omega\\ \sin((i-1)/2)(r-1)\omega\end{Bmatrix}, \quad \text{according to } i\begin{Bmatrix}\text{even}\\ \text{odd}\end{Bmatrix}. \tag{15}$$

Therefore for the as yet undetermined elements of A,

$$A_{ij}=-\frac{2}{n}\sum_{r=1}^{n}\begin{Bmatrix}\cos(i/2)(r-1)\omega\\ \sin((i-1)/2)(r-1)\omega\end{Bmatrix}\times\begin{Bmatrix}\cos(i/2)(r-m-1)\omega\\ \sin((j-1)/2)(r-m-1)\omega\end{Bmatrix}$$
$$=-\frac{2}{n}\sum_{r=1}^{n}\begin{Bmatrix}\cos(i/2)r\omega\\ \sin((i-1)/2)r\omega\end{Bmatrix}\times\begin{Bmatrix}\cos(j/2)(r-m)\omega\\ \sin((j-1)/2)(r-m)\omega\end{Bmatrix} \tag{16}$$

where again the upper or lower term is to be used according to whether i or j, as the case may be, is even or odd.

When Eq. (11) is reduced by means of the identities of Appendix I, we are able to write:

$$A=\begin{bmatrix}1&0&0&0&0&\\0&\cos m\omega&-\sin m\omega&0&0&\\0&\sin m\omega&\cos m\omega&0&0&\cdots\\0&0&0&\cos 2m\omega&-\sin 2m\omega&\\0&0&0&\sin 2m\omega&\cos 2m\omega&\\0&0&0&0&0&\\&&&\cdots&&\end{bmatrix}. \tag{17}$$

If n is even, the final diagonal term is $(-1)^m$.

This matrix is composed of the irreducible representations of C_{nv} or D_n for the elements C_n^m. The traces of each of the diagonal blocks correspond, in order, to the characters for C_n^m of Table I.

In a very similar fashion it can be shown that, for any of the dihedral elements, A is blocked off at least as much as in Eq. (17) and that the traces are as follows: for the first and last (if n is even) elements, corresponding to the odd rows of U, $+1$ or -1; for each of the cosine-sine row pairs of U, zero.

We have now established the following result: U_n is a suitable symmetry matrix for combining n equivalent coordinates in molecules of symmetry C_{nv} or D_n. The first row pair is identified with E_1, the second with E_2, and so on to E_p. The first row of U_n is A_1 or A_2 and the final odd row, if it occurs, B_1 or B_2. This final identification of the odd rows is probably most easily made by inspection.

Case 2. $2n$ equivalent coordinates

It will always be found that a set of $2n$ equivalent coordinates can be resolved into two sets of n each and into n sets of 2 each. They can be numbered according to two conventions, (1), number the first set of n cyclically from 1 to n and the second set from $n+1$ to $2n$, with the ith coordinate of the first set paired with its mate, the $n+i$th of the second set, (2), assign odd index numbers to the first set and even numbers to the second, using a similar cyclic convention.

With index numbers assigned by the first convention, a suitable symmetry matrix is the direct product[5] of U_2 and U_n:

$$U_2\times U_n=\begin{bmatrix}(1/2)^{\frac{1}{2}}U_n, & (1/2)^{\frac{1}{2}}U_n\\ (1/2)^{\frac{1}{2}}U_n, & -(1/2)^{\frac{1}{2}}U_n\end{bmatrix}. \tag{18}$$

There will now be two rows corresponding to each row of U_n. Following the argument of case 1, we see that rows 1 and $n+1$ will correspond to A-modes (one will be A_1 and the other A_2) and that rows n and $2n$ (if there is a final odd row in U_n) will correspond to B_1 or B_2. Similarly, the two pairs of rows formed from the ith cosine-sine pair of U_n will both correspond to E_i.

This procedure corresponds to taking n-fold combinations of the two sets of n coordinates and then taking symmetric and antisymmetric combinations of these combinations. The second numbering convention would require the opposite direct product, U_n and U_2, and corresponds to first taking symmetric-antisymmetric combinations, followed by n-fold combinations of each type. The two differ only in the order of the

[5] J. E. Rosenthal and G. M. Murphy, Rev. Mod. Phys., 8, 317 (1936).

TABLE II. Condensed character tables for D_{nh}.

D_{nh}, n odd ($p=(n-1)/2$)	C_n^m	nC_2	S_n^m	$n\sigma_v$
A_1'	1	1	1	1
A_2'	1	−1	1	−1
E_1'	$2\cos m\omega$	0	$2\cos m\omega$	0
...	...	...	...	...
E_p'	$2\cos pm\omega$	0	$2\cos pm\omega$	0
A_1''	1	1	−1	−1
A_2''	1	−1	−1	−1
E_1''	$2\cos m\omega$	0	$-2\cos m\omega$	0
...	...	...	...	...
E_p''	$2\cos pm\omega$	0	$-2\cos pm\omega$	0

D_{nh}, n even ($p=(n-2)/2$)	C_n^m	$\frac{1}{2}nC_2$	$\frac{1}{2}nC_2'$	S_n^m	$\frac{1}{2}n\sigma_v$	$\frac{1}{2}n\sigma_{v'}$
A_1'	1	1	1	1	1	1
A_2'	1	−1	−1	1	−1	−1
E_1'	$2\cos m\omega$	0	0	$2\cos m\omega$	0	0
...	...	...	...	...	...	...
E_p'	$2\cos pm\omega$	0	0	$2\cos pm\omega$	0	0
B_1'	$(-1)^m$	1	−1	$(-1)^m$	1	−1
B_2'	$(-1)^m$	−1	1	$(-1)^m$	−1	1
A_1''	1	1	1	−1	−1	−1
A_2''	1	−1	−1	−1	1	1
E_1''	$2\cos m\omega$	0	0	$-2\cos m\omega$	0	0
...	...	...	...	...	...	...
E_p''	$2\cos pm\omega$	0	0	$-2\cos pm\omega$	0	0
B_1''	$(-1)^m$	+1	−1	$-(-1)^m$	−1	1
B_2''	$(-1)^m$	−1	1	$-(-1)^m$	1	−1

terms in the rows and columns of the symmetry matrix. The second convention has the disadvantage of separating the cosine-sine pairs.

POINT GROUP D_{nh}

There are $4n$ elements in D_{nh}; the $2n$ elements of D_n and $2n$ others, formed by multiplying the elements of D_n by a horizontal reflection, σ_h. There are also twice as many symmetry types as in D_n, since each type in D_n splits into two types in D_{nh}, symmetric and antisymmetric, respectively, to the additional symmetry elements. The condensed character tables for D_{nh}, n even or odd, are given in Table II. In this case it is too complicated to write the characters for n both even and odd together in one table.

The conventional way of writing the character table for D_{nh}, n even, differs from that for D_{nh}, n odd. Since D_{nh} is formed from D_n by adding a horizontal plane of symmetry, we write the character table as the direct product of C_h and D_n, for n either even or odd. This convention makes the use of our symmetry matrix somewhat simpler. However, when n is even, D_{nh} contains an element of inversion ($S_n^{\frac{1}{2}n}\equiv I$). A classification of symmetry types with respect to inversion rather than with respect to reflection in a horizontal plane is generally more useful. This classification can be made as follows. Symmetry types symmetric to inversion (g) have a positive character for $S_n^{\frac{1}{2}n}(\equiv I)$. Thus, $A_1'=A_{1g}$, $A_2'=A_{2g}$, $A_1''=A_{1u}$ and $A_2''=A_{2u}$ for all values of n. When $\frac{1}{2}n$ is even, $B_1'=B_{1g}$, $B_2'=B_{2g}$, $B_1''=B_{1u}$, $B_2''=B_{2u}$. For $\frac{1}{2}n$ odd, the subscripts g and u are interchanged. The E' types with even subscripts are g and those with odd subscripts are u. The reverse is true for E''.

In D_{nh}, sets of n, $2n$ or $4n$ equivalent coordinates are possible.

Case 1. n equivalent coordinates

The analysis for n coordinates in D_n applies here for the first $2n$ elements of D_{nh}. We need, then, merely to investigate the properties of the second $2n$ elements. The P matrix for σ_h for n equivalent coordinates can consist only of either plus or minus the identity matrix, that is, the operation σ_h will either leave the R_i unchanged or merely reverse their signs without permuting them. It follows that the matrix A for each of the second $2n$ elements is either plus or minus the A matrix for the corresponding element from the first group of $2n$ elements. By reference to Table II, we see that this means that the n symmetry coordinates all correspond to either the upper half or the lower half of the character table. It is therefore actually necessary to investigate the symmetry properties of only the symmetry coordinate formed from the first row (the simple sum of the n coordinates) of U_n with respect to only one of the second $2n$ elements. The most convenient choice is $\sigma_h(\equiv S_n^n)$.

We now have the results: matrix U_n is suitable for combining n equivalent coordinates in a molecule of symmetry D_{nh}. The first row of U_n has the symmetry A and the last odd row, if present, symmetry B, with subscripts 1 or 2 according to their behavior with respect to the dihedral two-fold axes (C_2) of symmetry. The row pairs are E_1, E_2, etc., in the order in which they are written in the matrix. So far these results are identical with those of C_{nv} and D_n. The whole set of n symmetry coordinates is symmetric or antisymmetric to σ_h ($'$ or $''$) ac-

cording to the behavior of the first symmetry coordinate (the first row of U_n) with respect to σ_h. When n is even, the primes of the symmetry type symbols may be replaced with g and u, according to the rules already given.

Case 2. $2n$ equivalent coordinates

A convenient numbering and orientation convention is the first one mentioned for $2n$ coordinates in C_{nv}. The operation C_n^m then raises the index number of a coordinate in the first set of n coordinates by m, within a cycle of n. Similarly, C_n^m also increases the index number of a coordinate in the second set of n coordinates by m, within its cycle of n. For example, if $n=5$, $C_5^2R_1=R_3$, $C_5^2R_4=R_1$, $C_5^2R_6=R_8$ and $C_5^2R_9=R_6$. The result of $S_n^m(\equiv\sigma_h C_n^m)$ is a little more complicated. The index number of R_i is increased by m, within the cycle of its own set of n; it is then increased by n, within a cycle of $2n$, which changes it to a coordinate of the other set. For example, for $n=5$, $S_5^2R_1=R_8$ and $S_5^2R_9=R_1$.

If we let P_n be the matrix of degree n defined by Eq. (5), the permutation matrix for C_n^m is

$$\begin{bmatrix} P_n & 0 \\ 0 & P_n \end{bmatrix}$$

and for S_n^m,

$$\begin{bmatrix} 0 & P_n \\ P_n & 0 \end{bmatrix}$$

It immediately follows that $U_2\times U_n$ is a suitable symmetry matrix:

$$\begin{bmatrix} (1/2)^{\frac{1}{2}}U_n & (1/2)^{\frac{1}{2}}U_n \\ (1/2)^{\frac{1}{2}}U_n & -(1/2)^{\frac{1}{2}}U_n \end{bmatrix}\begin{bmatrix} P_n & 0 \\ 0 & P_n \end{bmatrix} \times\begin{bmatrix} (1/2)^{\frac{1}{2}}U_n' & (1/2)^{\frac{1}{2}}U_n' \\ (1/2)^{\frac{1}{2}}U_n' & -(1/2)^{\frac{1}{2}}U_n' \end{bmatrix} =\begin{bmatrix} U_nP_nU_n' & 0 \\ 0 & U_nP_nU_n' \end{bmatrix}$$

$$\begin{bmatrix} (1/2)^{\frac{1}{2}}U_n & (1/2)^{\frac{1}{2}}U_n \\ (1/2)^{\frac{1}{2}}U_n & -(1/2)^{\frac{1}{2}}U_n \end{bmatrix}\begin{bmatrix} 0 & P_n \\ P_n & 0 \end{bmatrix} \times\begin{bmatrix} (1/2)^{\frac{1}{2}}U_n' & (1/2)^{\frac{1}{2}}U_n' \\ (1/2)^{\frac{1}{2}}U_n' & -(1/2)^{\frac{1}{2}}U_n' \end{bmatrix} =\begin{bmatrix} U_nP_nU_n' & 0 \\ 0 & -U_nP_nU_n' \end{bmatrix}. \quad (20)$$

We have already evaluated $U_nP_nU_n'$ (Eqs. (6), (12)). By comparison with the character table for D_{nh}, we see that the first row of $U_2\times U_n$ is A_1' or A_2' and the $n+1$th row, A_1'' or A_2''. The first set of cosine-sine pairs are E_1', E_2', $\cdots$, in order and the second set of row pairs, E_1'', E_2'', etc. When n is even, the nth row is B_1' or B_2' and the $2n$th row, B_1'' or B_2''. As before, the subscripts 1 and 2 on A and B coordinates are determined by the symmetry properties of these coordinates with respect to the dihedral elements of symmetry. This is always easy to determine in the case of nondegenerate coordinates.

Case 3. $4n$ equivalent coordinates

In this case it is difficult to make a general statement concerning numbering the coordinates. There will be four sets of n each and n sets of four each. It is probably best to number each set of n cyclically as usual. The ambiguity comes in the choice of which set of n to be the first set, which to be the second set, etc.

It might be expected that $U_4\times U_n$ would be a suitable symmetry matrix. This is not exactly the case. A slight modification of U_4 may, however, be used.

The reader may have observed that an alternative form of U_n could be written with imaginary exponentials. It is not quite so obvious that an arbitrary phase angle may be added to each element of any cosine-sine row pair. The standard form of U_4 is:

$$U_4=\begin{bmatrix} 1/2 & 1/2 & 1/2 & 1/2 \\ (1/2)^{\frac{1}{2}} & 0 & -(1/2)^{\frac{1}{2}} & 0 \\ 0 & (1/2)^{\frac{1}{2}} & 0 & -(1/2)^{\frac{1}{2}} \\ 1/2 & -1/2 & 1/2 & -1/2 \end{bmatrix}. \quad (21)$$

The addition of a phase angle of 45° to the middle row pair changes U_4 to a somewhat more symmetric form:

$$U_4^*=\begin{bmatrix} 1/2 & 1/2 & 1/2 & 1/2 \\ 1/2 & -1/2 & -1/2 & 1/2 \\ 1/2 & 1/2 & -1/2 & -1/2 \\ 1/2 & -1/2 & 1/2 & -1/2 \end{bmatrix}. \quad (22)$$

This matrix, U_4^*, happens to be the direct product of U_2 on U_2 with the last two columns interchanged. It is for this reason that $U_4^*\times U_n$ is suitable in this case. The four sets of equivalent coordinates are equivalent to each other in pairs, in different ways, according to the symmetry

element considered. Symmetric-antisymmetric combinations of symmetric-antisymmetric combinations are called for.

$U_4^* \times U_n$ is divided into four sets of n rows. The methods of the preceding sections show that within any one set of n rows, the identification is A, E_1, E_2, $\cdots$, B, as before. Each set of n rows is $'$ or $''$, according to their symmetry with respect to σ_h. This question can be answered in the following way. Let R_i be a typical coordinate from the first set of n coordinates and R_j, R_k and R_l be the corresponding coordinates from the other three sets of n, i.e., R_i, R_j, R_k and R_l form a typical set of four. These four coordinates (or more generally, the four sets of n to which they belong) can be identified with the four columns of U_4^* (Eq. (22)). The four rows of U_4^* correspond to the four sets of n rows of the whole symmetry matrix. The behavior of R_i, R_j, R_k and R_l with respect to σ_h tells us the symmetry of each row of U_4^* to this same operation and in turn, the symmetry of each of the four sets of n rows of the whole symmetry matrix. For example, let R_i, R_j, R_k and R_l be, respectively, from the first, second, third and fourth sets of n coordinates. They therefore correspond to the first, second, third, and fourth columns of U_4^*, in order. Now assume that σ_h interchanges R_i and R_j and also R_k and R_l. It is obvious that rows one and three of U_4^* are symmetric to this operation and rows two and four, antisymmetric. Therefore, the first and third sets of n rows of $U_4^* \times U_n$ are symmetric to $\sigma_h(')$ and the second and fourth sets, antisymmetric ($''$). The subscripts of the non-degenerate rows are determined as before by reference to the dihedral elements. Of course, $U_2 \times U_2$ may be used instead of U_4^*.

OTHER POINT GROUPS

It does not seem worth while to treat the point groups C_n, C_{nh}, S_n, S_{nv} or D_{nd} in a general fashion, since so few examples of each occur in nature. The matrices appropriate to the first four families are quite similar to those already discussed. The only important example of D_{nd} is D_{3d}. In this case, $U_2 \times U_3$ is suitable for 6 equivalent coordinates.

The matrix U_n was designed particularly for the cyclic and dihedral groups. It is useful, however, in some other cases. For example, in the case of methane (T_d), a set of four equivalent C−H stretchings and a set of six H−C−H bendings occur. U_4 and U_6 are suitable modes of combination respectively, for either of the two sets alone. The former gives one A combination and the three components of a T_2 combination. The latter gives one redundant (identically zero) combination, an E and a T_2. However, the two T_2 modes are not oriented similarly in space. This defect can be remedied by taking three-fold combinations of the last three rows of U_4,

$$\begin{bmatrix} 1 & 0 \\ 0 & U_3 \end{bmatrix} [U_4] \begin{bmatrix} 1 & 0 \\ 0 & U_3' \end{bmatrix}.$$

This new four-fold set of symmetry coordinates gives a T_2 family that is aligned with the T_2 from the six angular coordinates by means of U_6.

In conclusion, a few suggestions are appropriate as to symmetry combinations that may be used in certain cases other than the basic ones previously treated.

Frequently, it is desirable to combine certain symmetry coordinates, formed from different sets of equivalent coordinates, by means of U_2, U_3 or U_4 in order to force a redundant combination of elementary coordinates to appear. A case of this sort occurs in CH_3X. There are four elementary bond stretchings and two sets of three angle bendings, a total of ten. There are only nine internal degrees of freedom. If the three-fold combinations of HCH bendings are combined with the three-fold combinations of HCX bendings in symmetric-antisymmetric pairs, the symmetric combination of the A_1 coordinates from each source will be a null or redundant combination and can be dropped. If in place of this procedure, one or the other of these two A_1 coordinates were dropped, a fallacious interaction potential term would be necessary in the potential expression for the molecule.

Sometimes several groups of atoms, each group with the same symmetry G' which may be different from the symmetry of whole molecule, G, are found in one molecule. It is then desirable to take combinations of the coordinates equivalent under G', whether or not these are equivalent under G, and then to combine these combinations under G. As an example, in the case of isobutane,

the three CH stretchings and the six angular bendings of each methyl group (C_{3v}) may be combined as in the preceding paragraph. These combinations may then be combined, respectively, under the symmetry of whole molecule (C_{3v} again in this case).

A case of misalignment of degenerate coordinates, analogous to the case mentioned in methane, may appear in ring molecules. If the components of two or more degenerate symmetry coordinates of the same symmetry type are not oriented similarly in the plane perpendicular to the main symmetry axis, the secular equation will not factor properly. This situation may be cured by introducing a phase angle into one or the other of the symmetry matrices. The angle required can often be found by inspection.

APPENDIX I

Let

$$z = e^{i\omega} = \cos\omega + i\sin\omega,$$

$$z^{rm} = \cos rm\omega + i\sin rm\omega,$$

$$\sum_{r=1}^{n} z^{rm} = z^m + z^{2m} + z^{3m} + \cdots + z^{nm},$$

$$= 1 + z^m + z^{2m} + \cdots + z^{(n-1)m},$$

$$(1-z^m)\sum z^{rm} = 1 - z^{nm} = 0,$$

since

$$z^{nm} = e^{inm\omega} = e^{2\pi m i} = 1.$$

If $m \neq 0, \pm n, \pm 2n, \cdots$, we have $\sum z^{rm} = 0$. Since both the real and imaginary parts of this complex number are zero,

$$\sum_{r=1}^{n} \cos rm\omega = \sum_{r=1}^{n} \sin rm\omega = 0.$$

In the same manner, from

$$\sum z^{2rm} = \sum z^{rm} z^{rm}$$
$$= \sum \cos^2 rm\omega - \sum \sin^2 rm\omega + 2i \sum \cos rm\omega \cdot \sin rm\omega$$

we find

$$\sum \cos^2 rm\omega - \sum \sin^2 rm\omega = 0,$$
$$\sum \cos rm\omega \cdot \sin rm\omega = 0.$$

From

$$\sum z^{rm} z^{-rm} = n,$$

we have

$$\sum \cos^2 rm\omega + \sum \sin^2 rm\omega = n.$$

Therefore,

$$\sum_{r=1}^{n} \cos^2 rm\omega = \sum \sin^2 rm\omega = \tfrac{1}{2}n$$

with the restriction $m \neq 0, \pm\frac{1}{2}n, \pm n, \pm\frac{3}{2}n, \cdots$.

The following identities may be proved in a similar manner:

$$\sum_{r=1}^{n} \cos rs\omega \cdot \cos rt\omega = 0,$$

$$\sum_{r=1}^{n} \sin rs\omega \cdot \sin rt\omega = 0,$$

$$\sum_{r=1}^{n} \cos rs\omega \cdot \sin rt\omega = 0,$$

with the restriction $s \pm t \neq 0, \pm n, \pm 2n, \cdots$.

THE JOURNAL OF CHEMICAL PHYSICS VOLUME 16, NUMBER 8 AUGUST, 1948

Consideration of the Gibbs Theory of Surface Tension

RICHARD C. TOLMAN
California Institute of Technology, Pasadena, California

(Received April 15, 1948)

The Gibbs theory of surface tension is discussed. Detailed consideration is given to the structure of transition layers between phases. This provides theoretical information, as to the magnitude of surface tension and as to the location of the surface of tension, which can be used in making applications of the Gibbs theory.

I. DISCUSSION OF THE GIBBS THEORY

1. Introduction

IN his treatise on heterogeneous equilibrium,[1] Gibbs has developed a comprehensive and valid theory for treating the phenomena of surface tension by the methods of thermodynamics. Various applications of thermodynamics to particular problems in the field of surface phenomena can be made without employing the complete theory of Gibbs, and simplified theories can be developed for the thermodynamic treatment of plane surfaces. Nevertheless, to obtain the full results that can be expected from thermodynamics, especially in the case of curved surfaces, it is essential to employ the complete theory of Gibbs or its equivalent.

In Part I of this article we present a brief review which will assist in furnishing a clear appreciation of the nature and consequences of the Gibbs theory. This includes in Sections 2–5 a resume of fundamental notions, such as those of dividing surface, decomposition of quantities, surface of tension, etc., that are introduced in the Gibbs development. In Section 6 we then derive two well-known consequences of the Gibbs theory needed in Part II and in a proposed later application. In Section 7 we comment on certain aspects of the Gibbs theory that need emphasis in order to prevent misconceptions and secure full understanding. And, finally, in Section 8 we consider the status of certain simplified treatments of surface tension.

In Part II of the article we undertake a detailed treatment of transition layers in order to gain added insight into the mechanisms underlying surface phenomena, and to provide theoretical information as to the magnitude of surface tension and as to the location of the surface of tension. This information can be of value in making applications of the Gibbs theory and will be so employed in a proposed later application. We devote Sections 9–12 to the rather complicated deduction needed to obtain our two theoretical expressions (12.6) and (12.7) for the magnitude of surface tension and for the location of surface of tension. In Sections 13 and 14 we then show that these detailed expressions can themselves be used as the starting point to derive the two consequences of the Gibbs theory presented in Part I. In Section 15 we give general consideration to different kinds of possibilities for the detailed treatment of transition layers. And, finally, in Section 16 we discuss the extent to which we may ascribe validity to the particular detailed treatment that we have presented.

2. Introduction of Dividing Surface

We may begin our discussion of the Gibbs theory by giving attention to the fundamental notion of "dividing surface." For this purpose let us consider the conditions for equilibrium in systems consisting of two fluid phases which meet at a surface of discontinuity. In accordance with the known conditions for equilibrium within a single phase, and with the short range of molecular force, we can regard such a system as composed of two phases which have substantially uniform distributions of matter throughout their interiors but which meet in a thin layer of physical inhomogeneity where a transition takes place from the distribution in one phase to that in the other.

In order to obtain a simple treatment of the

[1] J. W. Gibbs, *Collected Works* (Longmans Green and Company, New York, 1928), Vol. I, pp. 55–353.

thermodynamic properties of such a system, it is convenient to regard the system as precisely separated into two parts by the construction of an imaginary geometrical surface, which lies within the layer of physical inhomogeneity, and which passes through points in that layer which are similarly located with respect to the condition of neighborhing matter. Such a surface, which gives a precise separation of the system into two parts, with the homogeneous portions of the two phases located on its opposite sides, was called by Gibbs a *dividing surface.*

It is evident that a variety of choices for such a dividing surface can be made, according as one or another condition of the neighboring matter is selected for the construction of the surface. It will be noted, however, that the different dividing surfaces which we might choose in any given case can be thought of as "parallel" to each other and to the tangible physical surface of discontinuity. Hence we can regard the properties of the whole transition layer as determined by the area and configuration of the particular dividing surface that we are using. (For further discussion see Section 7.)

3. Decomposition of Quantities Having Extensive Magnitude

Having made some particular choice for the dividing surface, the whole volume v occupied by a two-phase system may then be regarded as thereby precisely divided into two volumes v' and v'', which have boundaries determined by the physical boundaries of the system itself and by the location of the dividing surface, and which have magnitudes exactly satisfying the equation

$$v=v'+v''. \tag{3.1}$$

As a consequence of this division it will be seen that v' will contain the matter in one of the homogeneous regions together with a part of the small amount of matter in the transition layer, and v'' will contain the matter in the other homogeneous region together with the rest of that in the transition layer.

In view of the nature of the contents of the two volumes v' and v'', it then appears natural, and actually proves useful, to express the total energy E of the system as the sum of the energies E' and E'' which the two phases would have if they remained strictly homogeneous right to the surface of separation, plus an additional term E^s which gives the necessary correction arising from the actual presence of the homogeneous transition layer. Thus for the total energy of the system we shall write

$$E=E'+E''+E^s. \tag{3.2}$$

Similarly, for other quantities having extensive magnitude, we shall write for the total entropy of the system

$$S=S'+S''+S^s, \tag{3.3}$$

and for the total amounts $m_1, m_2, \cdots m_h$, of the h different independent components of which the system is regarded as composed, we shall write

$$\begin{aligned} m_1&=m_1'+m_1''+m_1^s,\\ m_2&=m_2'+m_2''+m_2^s,\\ &\cdots\cdots\cdots\cdots\\ m_h&=m_h'+m_h''+m_h^s. \end{aligned} \tag{3.4}$$

The terms without superscript on the left-hand side of these equations give the actual total amounts of the quantities in question for the two-phase system as a whole. The terms with single and double accents give the amounts of those quantities, computed as though the two phases were strictly homogeneous right to the geometrical dividing surface, and the terms with the superscript S (not to be confused with an exponent) give the corrections, arising from the actual presence of a transition layer, that have to be introduced to make the equations true. Thus the above equations may be taken as defining those quantities, indicated by the superscript S, which we assign to the presence of the transition layer.

4. Variation of Energy for a System at Equilibrium

Let us now consider variations in the state of a two-phase system originally in a condition of equilibrium. We shall take the state of such a system, and hence its energy E, as determined by its entropy S, by the masses $m_1, m_2, \cdots m_h$ of the various independent components which compose it, by the volumes v' and v'' which contain the two phases, and by the area s and principal curvatures c_1 and c_2 of the dividing surface

between the phases, where this is assumed sufficient in accordance with Section 2 to complete the determination of the state of the whole system.[2]

Considering a small variation in the state of the system, we may then evidently write for the variation in its energy

$$\delta E = T\delta S + \mu_1\delta m_1 + \mu_2\delta m_2 + \cdots - p'\delta v' - p''\delta v'' + \sigma\delta s + C_1\delta c_1 + C_2\delta c_2, \quad (4.1)$$

where in the first instance we regard the quantities T, μ_1, μ_2, $\cdots\mu_h$, p', p'', σ, C_1, and C_2 merely as coefficients having values determined by the initial equilibrium state of the system.

Introducing our previous expressions (3.2–4), however, we may rewrite the above equation in the form

$$\begin{aligned}\delta E &= \delta E' + \delta E'' + \delta E^s \\ &= T\delta S' + \mu_1\delta m_1' + \mu_2\delta m_2' + \cdots - p'\delta v' \\ &+ T\delta S'' + \mu_1\delta m_1'' + \mu_2\delta m_2'' + \cdots - p''\delta v'' \\ &+ T\delta S^s + \mu_1\delta m_1^s + \mu_2\delta m_2^s + \cdots \\ &+ \sigma\delta s + C_1\delta c_1 + C_2\delta c_2. \quad (4.2)\end{aligned}$$

Furthermore, for any single homogeneous phase at equilibrium we have the known dependence (see reference 1, Eq. (12), p. 63) of energy on heat absorption, change in material contents, and work done,

$$\delta E = T\delta S + \mu_1\delta m_1 + \mu_2\delta m_2 + \cdots - p\delta v, \quad (4.3)$$

where T, μ_1, μ_2, $\cdots\mu_h$, and p have their usual significance. Hence comparing with (4.2), we now see that the coefficient T appearing therein may actually be taken as the temperature of the system having a value which can be determined by usual methods in either of the homogeneous regions, that the coefficients μ_1, μ_2, $\cdots\mu_h$ may be taken as the Gibbs potentials for the components of the system also having values determinable in the homogeneous parts of the system, and that the coefficients p' and p'' may be taken as the pressures in the homogeneous parts of the two phases. The coefficients σ, C_1, and C_2 in Eqs. (4.1) and (4.2) are, however, new quantities to the consideration of which we must now turn.

5. Introduction of the Surface of Tension

In order to proceed, it will be advantageous to introduce a rearrangement of the last two terms in Eq. (4.1), and rewrite our expression for variation in energy of the system in a form

$$\begin{aligned}\delta E = T\delta S + \mu_1\delta m_1 + \mu_2\delta m_2 + \cdots - p'\delta v' - p''\delta v'' \\ + \sigma\delta s + \tfrac{1}{2}(C_1+C_2)\delta(c_1+c_2) \\ + \tfrac{1}{2}(C_1-C_2)\delta(c_1-c_2), \quad (5.1)\end{aligned}$$

which will make it easier to analyze the effects of changes in curvature.

In accordance with this equation, we see that the last three terms of (5.1),

$$\sigma\delta s + \tfrac{1}{2}(C_1+C_2)\delta(c_1+c_2) + \tfrac{1}{2}(C_1-C_2)\delta(c_1-c_2), \quad (5.2)$$

give the variation in the energy of the system which would accompany a variation in the area and curvatures of the dividing surface, without absorption of heat, change in composition, or change in the volumes containing the two phases. It is evident that the sum of these three terms would have a value determined by the actual variation in the condition of the surface layer and independent of the choice of dividing surface, but that the values of the individual terms therein would be dependent on the particular choice made. Hence it now becomes natural to introduce any simplification that can be obtained by a special choice for the location of the dividing surface.

To obtain such a simplification we shall choose the location of the dividing surface in such a manner as to make the coefficient $\frac{1}{2}(C_1+C_2)$ of the second term in (5.2) equal to zero. A special investigation to show the possibility of such a location for the dividing surface was made by Gibbs (see reference 1, pp. 226–227), and in Part II of this article we shall obtain a specific expression (12.7) determining this location in

[2] This treats the dividing surface as having constant curvatures c_1 and c_2 throughout. The procedure actually adopted by Gibbs in this connection was somewhat more general. He starts by treating elements of the transition layer which are small enough so that the corresponding elements of dividing surface can be regarded as having uniform curvature throughout (see reference 1, p. 225). After showing the possibility of choosing the dividing surface for any such element in a manner to secure the desired simplification, corresponding to our later reduction from (5.1) to (5.3), he then introduces the idea that the dividing surface for the whole transition layer can be regarded as composed of elements of surface all consonant with the desired simplification (see reference 1, p. 227). It has not seemed desirable to introduce this increased generality into the exposition given in the text, partly since it would require considerable space to give a rigorous development, and partly since our contemplated later applications will be to spherical surfaces of uniform curvature throughout.

terms of the distribution of fluid pressures in the layer. Moreover, since change in curvature of the dividing surface would lead to increase in the lamelliform distribution of matter on one side of the surface and decrease on the other, it would seem reasonable, in general, to expect that a location for the dividing surface could be found which would make $\frac{1}{2}(C_1+C_2)$ equal to zero through a balancing of the consequences of such opposing changes in distribution. Hence, we shall assume that we can indeed eliminate the second term in (5.2) by a suitable choice of our dividing surface.

Having made this simplification, let us now consider the third term in (5.2), which depends on the coefficient $\frac{1}{2}(C_1-C_2)$. We note at once that this coefficient would be equal to zero for a plane surface, because of the equality of C_1 and C_2 for that case. Hence, with Gibbs (see reference 1, p. 228) we may conclude that the third term can also be dropped, without danger of sensible error, whenever the curvature of the actual transition layer is small enough compared with its thickness so that we can regard it as composed of parts which are essentially plane. Furthermore, since in proposed applications we shall actually be interested in the treatment of spherical surfaces of small radius, we also note that the coefficient $\frac{1}{2}(C_1-C_2)$ would be precisely equal to zero for spherical surfaces in general.

In accordance with the preceding two paragraphs, we now see that, by a suitable choice of dividing surface, we can write our Eq. (5.1) for variation in energy in the simplified form

$$\delta E=T\delta S+\mu_1\delta m_1+\mu_2\delta m_2+\cdots -p'\delta v'-p''\delta v''+\sigma\delta s. \quad (5.3)$$

Furthermore, since the conditions for thermodynamic equilibrium require a minimum of energy, with a given entropy, composition, and total volume for the system as a whole, we see—making use of the restrictions on the volumes v' and v'' given by (3.1)—that equilibrium requires validity of the equation

$$(p'-p'')\delta v'=\sigma\delta s. \quad (5.4)$$

This, however, is the form of equation which would apply to a system of two homogeneous fluids at pressures p' and p'', separated by a membrane without rigidity having a tension σ uniform in all directions. Hence, we may now designate the particular dividing surface that we have chosen as *the surface of tension*, and may define σ as *the surface tension* thereof.

Introducing the Helmholtz expression defining the free energy of a system

$$A=E-TS, \quad (5.5)$$

we can also write (5.3) in the form

$$\delta A=-S\delta T+\mu_1\delta m_1+\mu_2\delta m_2+\cdots -p'\delta v'-p''\delta v''+\sigma\delta s. \quad (5.6)$$

In accordance with (5.3) and (5.6), we then see that we can regard the surface tension σ either as the rate of change of energy with surface area at constant entropy, constant composition, and constant volumes for the two phases measured to the surface of tension, or as the rate of change of free energy with surface area at constant temperature, composition, and volumes. In both cases it will be appreciated that the surface area to be considered is that for the surface of tension within the transition layer.

Introducing a thermodynamic potential defined by

$$F=E-TS+p'v'+p''v'', \quad (5.7)$$

it would also be possible to write

$$\delta F=-S\delta T+\mu_1\delta m_1+\mu_2\delta m_2+\cdots +v'\delta p'+v''\delta p''+\sigma\delta s. \quad (5.8)$$

Such an expression, however, was not employed by Gibbs, and we shall make use of it only for purpose of comparison with an equation given by Lewis and Randall. (See Section 9.)

6. Two Consequences of the Gibbs Theory

We may now complete this brief resumé of the Gibbs theory by considering the derivation of two well-known consequences of special interest.

The first consequence that we wish to consider can be immediately obtained by applying Eq. (5.4), connecting variations in volume and surface, to the special case of a uniform displacement of the surface of tension everywhere normal to itself. As can be readily seen (see reference 1, Eq. (500), p. 229), this at once leads to the familiar equation of Kelvin

$$p'-p''=(c_1+c_2)\sigma, \quad (6.1)$$

connecting the pressures p' and p'' in the two phases with surface tension σ and with the principal curvatures c_1 and c_2 of the surface of tension. With a spherical surface, having the curvature c and radius r, this reduces to the form

$$p'-p''=2c\sigma=2\sigma/r. \qquad (6.2)$$

With positive values for the surface tension as are experimentally found, the higher pressure p' occurs in the so-called interior phase on the concave side of the surface, and the lower pressure p'' in the exterior phase on the convex side. We shall adopt the general convention of using a single accent to denote quantities applying to the interior phase and a double accent to denote those applying to the exterior phase.

The Kelvin relation between the pressures in the two phases given by (6.1) may be regarded as replacing the familiar equilibrium condition of uniform pressure throughout a system which is obtained when surface effects are neglected. It will be noted that equal pressures will prevail in the two phases only when they are separated by a plane surface and, *vice versa*, that maintenance of equality between these pressures is the condition for maintenance of a plane surface of separation.

In obtaining the second consequence of the Gibbs theory that will interest us, we shall be concerned with reversible[3] changes in the state of our two-phase system, rather than in arbitrary variations, and shall indicate this by replacing the sign of variation δ by the sign of differentiation d in Eq. (5.3). For the change in energy accompanying a reversible change from the original equilibrium state, we can then write in agreement with (5.3)

$$dE=TdS+\mu_1dm_1+\mu_2dm_2+\cdots \\ -p'dv'-p''dv''+\sigma ds, \qquad (6.3)$$

which, in accordance with the discussion of Section 3, can also be written in the more detailed form

$$\begin{aligned} dE&=dE'+dE''+dE^s \\ &=TdS'+\mu_1dm_1'+\mu_2dm_2'+\cdots-p'dv' \\ &+TdS''+\mu_1dm_1''+\mu_2dm_2''+\cdots-p''dv'' \\ &+TdS^s+\mu_1dm_1^s+\mu_2dm_2^s+\cdots+\sigma ds, \end{aligned} \qquad (6.4)$$

[3] The term reversible is used here in the usual thermodynamic sense, rather than in the special sense employed by Gibbs (reference 1, p. 222).

which shows the distribution of changes in energy, entropy, etc., among the different parts of the system.

Let us now consider the application of this equation to a calculation of the energy increase which would be brought about by an increase in the area of the surface of tension, *without* changes in the volumes v' and v'', or in the idealized homogeneous distributions of fluid in those volumes. Under such circumstances it is evident that the expression given by (6.4) would reduce to the form

$$dE^s=TdS^s+\mu_1dm_1^s+\mu_2dm_2^s+\cdots+\sigma ds, \qquad (6.5)$$

where dE^s is the increase in energy of the system, TdS^s is the heat that has to be absorbed, dm_1, dm_2, $\cdots dm_h$ are the additions that have to be made to the h components of the system, and σds the work that has to be done to increase the surface by the amount ds, without affecting the homogeneous distributions in the volumes v' and v''. Furthermore, since the coefficients T, μ_1, μ_2, $\cdots\mu_h$, and σ which appear in this equation would evidently maintain constant values if we make a finite change in area maintaining uniform properties throughout the extent of the surface, we see that we can now integrate (6.5) between $s=0$ and some finite value $s=s$, and obtain

$$E^s=TS^s+\mu_1m_1^s+\mu_2m_2^s+\cdots+\sigma s, \qquad (6.6)$$

as a correct expression for the total correction term E^s which has to be added to E' and E'', as discussed in Section 3, to get the total energy of a system of two fluid phases separated by a surface of tension of finite area s.

This equation now makes it possible to obtain one of the most important consequences of the Gibbs theory. Since (6.6) gives an analytically correct expression for E^s, we may now differentiate it with respect to all the variables on the right-hand side, and by comparing with (6.5) readily obtain the relation

$$-sd\sigma=S^sdT+m_1^sd\mu_1+m_2^sd\mu_2\cdots. \qquad (6.7)$$

Or if for simplicity we define the *superficial densities* of entropy and matter by

$$S_S=S^s/s, \quad \Gamma_1=m_1^s/s, \quad \Gamma_2=m_2^s/s\cdots, \qquad (6.8)$$

we can write the desired result

$$-d\sigma=S_SdT+\Gamma_1d\mu_1+\Gamma_2d\mu_2+\cdots. \qquad (6.9)$$

This consequence of the Gibbs theory, which is now sometimes called the Gibbs adsorption equation, has the important function of expressing the dependence of surface tension on the temperature of our two-phase system and on the potential of the components of which it is composed. The analogy of (6.9) with the Gibbs expression (reference 1, Eq. (98), p. 88) for the dependence of pressure, in a single-phase system of volume v, on temperature and potentials,

$$dp = (S/v)dT + (m_1/v)d\mu_1 + (m_2/v)d\mu_2 + \cdots, \quad (6.10)$$

will be appreciated.

7. Comments on Certain Aspects of the Gibbs Theory

The theory of surface tension given by Gibbs was developed with a minimum of hypothesis as to the detailed structure of the transition layer, this being reduced essentially to the assumption that all the properties of the layer can be regarded as determined by the area and curvature of some selected imaginary dividing surface. This procedure has the advantage of providing a very general theory, which is valid for a wide range of possible kinds of transition layer. The procedure also carries the consequence, however, that the theory will not itself provide information as to the detailed structure of transition layers. It is for this reason that we shall consider a more detailed treatment of transition layers in Part II.

The idea of using changes in the area and curvature of a single imaginary dividing surface to specify changes in the state of the whole transition layer may need elucidation. Any given dividing surface is defined by its passage through points within the transition layer where the fluid is locally in some given specified condition, the same for all points. Furthermore, the entire series of possible "parallel" dividing surfaces can be regarded as corresponding to the series of different values which can be assigned to the specified condition of the fluid. Hence, in a condition of equilibrium, the area and curvature of any one of the possible dividing surfaces may be regarded as determining the areas and curvatures of all the surfaces in the series, if we neglect edge effects in the case of transition layers of large extent, or take lateral boundaries normal to the dividing surfaces in the case of transition layers of small extent and in the case of small portions of a large layer. (Compare reference 1, pp. 219–220.) Thus, a variation in the area and curvature of any one dividing surface may be regarded as "controlling" the variation in state of the whole transition layer. It is to be emphasized that the specification of state in terms of the area and curvature of a selected dividing surface is a somewhat abstract procedure, not to be confused with more concrete attempts to treat the transition layer as a separate entity having some definite small value ζ for its thickness.[4]

Having chosen some particular dividing surface, it becomes possible, as we have seen in Section 3, to express the total energy E of a two-phase system as the sum of the energies E' and E'', which would be computed for the two phases if they remained strictly homogeneous right to the geometrical dividing surface, plus an additional correction term E^s resulting from the actual presence of the transition layer. And similar decompositions can be carried out for other quantities having extensive magnitudes such as entropy S, and the masses $m_1 \cdots m_h$ of the different components of the system. It is to be emphasized in this connection that the values of the correction terms, such as E^s, S^s, $m_1^s \cdots m_h^s$, which are introduced by this procedure will depend on the particular choice that is made for the location of the dividing surface. Indeed, it will be noted that the values of such terms may be positive or negative according as that choice leads to a deficiency or excess for the sum of the values computed for the two phases as compared with the actual value of the quantity in question for the system as a whole. It should be specially kept in mind that the quantities E^s, S^s, m_1^s, etc., are not the energy, entropy, mass, etc., for some specific thin layer of substance between the two phases, but are correction terms as defined.[4]

Although it is possible to choose one or another of many different possible dividing surfaces for

[4] See remarks made in Section 15 with regard to the somewhat unsatisfactory treatment given by J. Rice to the question of the location of the Gibbs surface of tension. By picturing the transition layer as having a definite thickness with a uniform distribution of surface energy throughout, he introduces a conception of the transition layer that does not agree with the conception of Gibbs which he is trying to illuminate.

the specification of state, it is to be emphasized that the most general results obtained by Gibbs are all dependent on the actual choice of the surface of tension as the one employed. This choice is made in order to reduce the fundamental expression, for the variation in energy δE, as given by (5.1), to the much simpler form (5.3), on which all further deductions are based. Hence, it is always to be presumed that the values of quantities appearing in the equations of Gibbs are taken with reference to the surface of tension, unless an explicit statement is made to the contrary, as is meticulously carried out by Gibbs. As an example, it may be noted that the Kelvin relation (6.2), connecting pressure difference between the phases $(p'-p'')$, with surface tension σ and radius of curvature r, can be taken as strictly correct only when we use the values of σ and r for the surface of tension, a matter of importance when the radius is small enough so that the exact location of the surface of tension has an appreciable effect. As another example, it is to be noted and emphasized that the dependence of surface tension on temperature and potentials given by (6.9) holds in general only when we use the values for the superficial densities of entropy and matter S_S, Γ_1, Γ_2, $\cdots$ that are computed with reference to the surface of tension. It is very important not to misunderstand the essential role played by the surface of tension in the Gibbs development.

8. Possibilities for Simplified Treatments

As has just been emphasized, the general results of Gibbs are obtained with the help of the reduction of Eq. (5.1) to the simplified form (5.3) through the choice of the surface of tension as the dividing surface employed. It will be noted, however, that the same reduction of (5.1) to the form (5.3) would be automatically achieved, for any choice of dividing surface, so long as applications are restricted to the behavior of plane surfaces, since the last two terms in (5.1) become zero if the curvatures c_1 and c_2 are not allowed to vary from zero. It is for this reason that simplified treatments are possible for plane surfaces with other and sometimes more illuminating choices for dividing surface. For example, that surface may be given such a location as to make the surface density of some particular component equal to zero, e.g., the main component of the liquid phase.

This possibility of giving specially adapted treatments in the case of plane surfaces of separation is important, since most experimental studies of surface tension have been made with surfaces which are essentially plane. In giving such treatments, however, it is appropriate, following Gibbs, to attach a special suffix to symbols for surface densities to indicate their computation with respect to some special dividing surface. It is also to be emphasized that we must still use the surface of tension even for plane surfaces when we wish to employ Eq. (6.9) to calculate changes in surface tension that involve changes in curvature.

Thermodynamic treatments of surface tension which do not emphasize the role of the surface of tension can be carried out. One such possibility was briefly discussed by Gibbs (reference 1, footnote on p. 267), and in two recent American texts, Epstein[5] and Keenan[6] have presented somewhat complete theories of surface phenomena without explicit introduction of the notion of surface of tension. Such treatments, however, as suggested by Gibbs (reference 1, footnote on p. 267), may not have sufficient generality for all purposes.

A simplified thermodynamic treatment of surface tension, which is useful for some purposes but not general enough for others, was given by Lewis and Randall.[7] Using our notation, their development is based on a definition of surface tension σ, in terms of thermodynamic potential F and surface areas, given by

$$dF=\sigma ds, \tag{8.1}$$

where it becomes evident later that they regard F as a function of the quantities p, T, m_1, $\cdots m_h$, and s, with p *the pressure* of the system. Comparing with (5.8), however, it is clear that a general treatment could be obtained only by including the possibility for different pressures

[5] P. S. Epstein, *Textbook of Thermodynamics* (John Wiley and Sons, Inc., New York, 1937), see Chapter XII.

[6] J. H. Keenan, *Thermodynamics* (John Wiley and Sons, Inc., New York, 1941), see pp. 434–447, 479–484.

[7] G. N. Lewis and M. Randall, *Thermodynamics* (McGraw-Hill Book Company, Inc., New York, 1923), see pp. 247–253.

p' and p'' in the two phases, and thus also including in accordance with the Kelvin relation (6.1) the possibility for curved as well as plane surfaces of separation. This explains the reason why O. K. Rice,[8] using the theory of Lewis and Randall to treat the effect of pressure on surface tension, finds a breakdown when he considers a one-component system where change in pressure at a given temperature would have to be correlated with change in curvature.

Our own further work will always be carried out in the light of the complete Gibbs theory.

II. DETAILED TREATMENT OF TRANSITION LAYER

9. Geometry of Transition Layer

We shall now endeavor to supplement our understanding of the Gibbs theory by undertaking a more detailed consideration of the nature of the transition layer. In doing this we shall limit the treatment to transition layers having spherical form, with values of the principal curvatures of the surface of tension which are kept equal when changes in curvature are made. We introduce this limitation partly to simplify our treatment, partly since the Gibbs treatment, as noted in connection with the reduction in form from (5.1) to (5.3), retains strict validity for highly curved surfaces only when they are spherical, and partly because of contemplated later application to spherical surfaces of small radius. We shall also restrict the treatment in the next section to one-component systems.

We shall regard the character of a spherical transition layer as determined by the area s and curvature c for the surface of tension, and shall treat the properties of the fluid within the transition layer as functions of the distance x from that surface. We shall measure this distance normal to the surface of tension and treat x as a variable, having positive values which increase from zero on the convex side of the surface of tension, and having negative values which decrease from zero on the concave side.

Taking r as the radius of the surface of tension, and ω as the solid angle subtended by the transition layer around the center of curvature, we can then write

$$s=\omega r^2 \tag{9.1}$$

as an expression for the area of the surface of tension, and can write

$$s(x)=\omega(r+x)^2 \tag{9.2}$$

as an expression for the area of any concentric surface of interest located within the transition layer at a distance x from the dividing surface. We use the same value of ω in the two expressions, since we shall assume it appropriate to neglect edge effects in the case of transition layers of large extent, and shall prescribe lateral boundaries determined by a conical surface having its apex at the center of curvature in the case of application to layers of small extent. Combining (9.1) and (9.2), and making use of the relation $c=1/r$ between the curvature and radius of the surface of tension, we can then write

$$s(x)=s[(r+x)^2/r^2]=s(1+cx)^2 \tag{9.3}$$

as a convenient expression for the areas of concentric surfaces within the transition layer.

Since we take the distribution of fluid within the transition layer as a function of x, the above expression for area now makes it possible to treat the whole layer as composed of a succession of infinitesimal layers, of area $s(1+cx)^2$ and thickness dx, within each of which we can take the condition of the fluid as uniform. Furthermore, for the volumes v' and v'' of the two fluid phases measured to the surface of tension, it now becomes convenient to introduce expressions of the form

$$v'=v_a'+s\int_{-a}^{0}(1+cx)^2dx,$$

and

$$v''=v_b''+s\int_{0}^{b}(1+cx)^2dx, \tag{9.4}$$

where we take the limits of integration at $x=-a$ and $x=b$ on the two sides of the surface of tension as sufficiently distant from that surface so that we can regard the condition of the fluid at those points as substantially the same as for the corresponding homogeneous phases, and can regard the remaining parts v_a' and v_b'' of the two volumes as filled with homogeneous distributions of fluid.

[8] O. K. Rice, J. Chem. Phys. **15**, 333 (1947).

10. Condition of Fluid within the Transition Layer

We must now inquire in more detail into conditions within the transition layer. In doing so, we shall treat the fluid within the layer by the usual methods of thermodynamics, and shall return briefly later to the question of the validity of giving thermodynamic treatment to the exceedingly small portions of non-homogeneous matter that will now concern us. (See Section 16.)

In making this application, we recognize that the behavior of the fluid at any point in the transition layer will be determined not only by effects resulting from the local condition of matter at that precise point, but also by effects arising from the non-homogeneous distribution of neighboring matter. To take account of this, we shall assume that we can treat the fluid, at any point in the layer, as subjected to an isotropic pressure corresponding to the local density and temperature, and also to a directed force associated with the external force field produced by the non-homogeneous distribution of neighboring matter.

In accordance with the usual methods of thermodynamics (reference 1, pp. 144–150), we may then require, as the condition for equilibrium, constancy throughout the layer for the *intrinsic* Gibbs potential for each component of the system, *augmented* by the external potential corresponding to the force field resulting from non-uniform distribution. Restricting the treatment for simplicity to one-component systems, we may then take the requirement for equilibrium throughout the system as given by

$$\mu_i+\phi=\text{const.}, \tag{10.1}$$

where μ_i is the intrinsic Gibbs potential for the fluid at any point in the system and ϕ is the external potential at that point corresponding to the externally produced force field. We shall find it most convenient to take these two potentials as reckoned per unit mass, e.g., per gram, of substance.

In accordance with the definition (reference 1, Eq. (104), p. 89) of the Gibbs potential as the differential rate of increase in the Helmholtz free energy of a system, per gram of substance added to a homogeneous phase at constant temperature, volume, and composition, we can take μ_i as given by

$$\mu_i=\psi+(p/\gamma), \tag{10.2}$$

where ψ is the Helmholtz free energy per gram, p the pressure, and γ the density of the fluid at the point considered. The appropriateness of this expression is evident since ψ is the free energy per gram of substance in a condition suitable for introduction into the system, and p/γ is the work needed per gram to carry out the introduction reversibly, at constant temperature and volume. Substituting (10.2) into (10.1), we may now write the condition for equilibrium in the more detailed form

$$\psi+(p/\gamma)+\phi=\text{const.}, \tag{10.3}$$

where the constancy applies to all points in the two phases and in the transition layer of the system that concerns us. Certain consequences that can be drawn from this equation will prove illuminating.

In the first place, it will be appreciated that the requirement stated by (10.3) is equivalent to the familiar criterion for equilibrium that the reversible, isothermal work needed for the transfer of an infinitesimal amount of substance from one point of a system to another should be equal to zero. It is immediately obvious that (10.3) will secure this result, since it permits us to assign the value zero,

$$\psi_2-\psi_1+(p_2/\gamma_2)-(p_1/\gamma_1)+\phi_2-\phi_1=0, \tag{10.4}$$

to an evident expression for the work per gram needed for such a transfer from points (1) to (2) in the system.

In the second place, it will be of interest to note that the full requirement for equilibrium given by (10.3) contains within it the special requirement needed for mechanical equilibrium in the interior of the non-homogeneous layer. To show this we may differentiate (10.3) with respect to position x within the transition layer, and write

$$\frac{d\psi}{dx}-\frac{p}{\gamma^2}\frac{d\gamma}{dx}+\frac{1}{\gamma}\frac{dp}{dx}+\frac{d\phi}{dx}=0 \tag{10.5}$$

as a necessary relation. We can evidently write, however,

$$d\psi=-pdv=(p/\gamma^2)d\gamma \tag{10.6}$$

for the dependence of the free energy of the fluid per gram on its specific volume v or density γ. Hence, on substituting in (10.5) we obtain a necessary condition for equilibrium, which can be written in the form

$$\frac{1}{\gamma}\frac{dp}{dx}+\frac{d\phi}{dx}=\frac{1}{\gamma}\frac{dp}{dx}-f_x=0, \qquad (10.7)$$

where $f_x=-d\phi/dx$ is seen to be the external force per gram acting in the x direction on the fluid. We at once appreciate that this result secures mechanical equilibrium through a balancing action of pressure gradient against external force.

Finally, it will be noted that the full condition for equilibrium given by (10.3) will reduce, in the homogeneous portions of the system where no external field of force has to be considered, to the simpler form

$$\psi'+(p'/\gamma')=\psi''+(p''/\gamma'')=\mu, \qquad (10.8)$$

where the single and double accents refer to the two homogeneous phases of the system, and μ is seen to be the Gibbs potential for the fluid in those phases. This result is of interest since it reasserts the accepted equality for the Gibbs potential in two homogeneous phases which are in equilibrium, and gives us a specific value for the constant in Eq. (10.3) which now permits us to rewrite that equation in the more explicit form

$$\psi+(p/\gamma)+\phi=\mu, \qquad (10.9)$$

where μ is the value of the Gibbs potential for the fluid in the homogeneous portions of the system.

11. Detailed Expressions for Changes in Mass and Free Energy

We are now ready to obtain detailed expressions for the changes in mass and in free energy which would accompany a particular, specified variation in the state of our system of two phases and transition layer. We shall need these expressions in the next section, where we shall derive the desired expressions for the magnitude of surface tension and for the location of the surface of tension.

We shall specify the particular variation in the state of the system to be treated by the requirement that we start from a state of equilibrium and make arbitrary variations δs and δc in the area and curvature of the surface of tension, keeping the temperature T of the system and the volumes v' and v'' of its two phases constant, and also keeping the homogeneous distributions of fluid pertaining to these phases unaltered by introducing whatever change δm in the mass of fluid in the system that is needed to secure this result. We select this particular variation in the state of the system in order to simplify the further treatment.

Since the specified variation in the state of the system is to be made without changes in the volumes v' and v'' of the two phases, we may begin by using the expressions for these quantities given by (9.4) to provide the following restrictions on the character of the variation

$$\delta v'=\delta v_a'+\delta s\int_{-a}^{0}(1+cx)^2dx+2s\delta c\int_{-a}^{0}(1+cx)xdx=0, \qquad (11.1)$$

and

$$\delta v''=\delta v_b''+\delta s\int_{0}^{b}(1+cx)^2dx+2s\delta c\int_{0}^{b}(1+cx)xdx=0. \qquad (11.2)$$

Furthermore, since the variation is to be made without change in the idealized homogeneous distributions of fluid assigned to the two phases, we can evidently write for the needed change in the mass of the system

$$\delta m=\gamma'\delta v_a'+\delta s\int_{-a}^{0}\gamma(1+cx)^2dx+2s\delta c\int_{-a}^{0}\gamma(1+cx)xdx+\gamma''\delta v_b''+\delta s\int_{0}^{b}\gamma(1+cx)^2dx+2s\delta c\int_{0}^{b}\gamma(1+cx)xdx, \qquad (11.3)$$

where γ', γ'', and γ denote the densities of fluid in the two phases and in the transition layer, respectively, and where we treat γ as an unaltered function of the distance x from the surface of tension. Multiplying Eq. (11.1) by γ' and Eq. (11.2) by γ'' and subtracting from (11.3),

we can rewrite this expression for δm in the desired form

$$\delta m = \delta s \int_{-a}^{0} (\gamma - \gamma')(1+cx)^2 dx + 2s\delta c \int_{-a}^{0} (\gamma - \gamma')(1+cx)x dx + \delta s \int_{0}^{b} (\gamma - \gamma'')(1+cx)^2 dx + 2s\delta c \int_{0}^{b} (\gamma - \gamma'')(1+cx)x dx. \quad (11.4)$$

Finally, since the total free energy of the system can be expressed in terms of the intrinsic free energy of the elements of fluid in the system, augmented when necessary by their potential energy in the field of force in the transition layer, we can evidently write for the change in free energy of the system

$$\delta A = \gamma'\psi'\delta v_a' + \delta s \int_{-a}^{0} \gamma(\psi+\phi)(1+cx)^2 dx - 2s\delta c \int_{-a}^{0} \gamma(\psi+\phi)(1+cx)x dx + \gamma''\psi''\delta v_b'' + \delta s \int_{0}^{b} \gamma(\psi+\phi)(1+cx)^2 dx + 2s\delta c \int_{0}^{b} \gamma(\psi+\phi)(1+cx)x dx, \quad (11.5)$$

where ψ', ψ'', and ψ denote the intrinsic free energy per gram of fluid in the two phases and in the transition layer, respectively, where ϕ denotes the potential energy per gram of fluid in the transition layer associated with the force field in that layer, and where we now regard ψ and ϕ, as well as γ, as unaltered functions of the distance x from the surface of tension. Multiplying Eq. (11.1) by $\gamma'\psi'$ and Eq. (11.2) by $\gamma''\psi''$ and subtracting from (11.5), we can rewrite this expression for δA in the desired form

$$\delta A = \delta s \int_{-a}^{0} (\gamma\psi + \gamma\phi - \gamma'\psi')(1+cx)^2 dx + 2s\delta c \int_{-a}^{0} (\gamma\psi + \gamma\phi - \gamma'\psi')(1+cx)x dx + \delta s \int_{0}^{b} (\gamma\psi + \gamma\phi - \gamma''\psi'')(1+cx)^2 dx + 2s\delta c \int_{0}^{b} (\gamma\psi + \gamma\phi - \gamma''\psi'')(1+cx)x dx. \quad (11.6)$$

It will have been appreciated that the derivations given for (11.4) and (11.6) involve the assumption that we can treat γ, ψ, and ϕ as functions of x which are unaltered by the variation. As a basis for the validity, or approximate validity, of this assumption, it will be noted that the condition of the fluid remains by hypothesis unaltered at the limits $x = -a$ and $x = b$, and can be expected to depend on position x as we pass through the transition layer in a manner only secondarily affected by infinitesimal changes in area and curvature.[9] The degree of approximate validity that might be found for the assumption, as we proceed from a treatment of the simple case of nearly plane surfaces to a treatment of the more complicated case of highly curved surfaces, remains to be investigated.

12. Detailed Expressions for Surface Tension and for the Location of the Surface of Tension

We are now ready to derive detailed expressions for surface tension and for a condition on the location of the surface of tension. This we shall do by comparing the consequences of the Gibbs treatment of the free energy of a two-phase system with the more detailed consequences of the treatment given in the preceding section.

On the one hand, in accordance with the general equation of Gibbs (5.6) giving the dependence of the free energy of such a system on the variables which determine its state, we see that we can write the simplified expression,

$$\delta A = \mu\delta m + \sigma\delta s, \quad (12.1)$$

for the change in free energy of a one-component, two-phase system, when we make variations in its fluid content and in its transition layer, keeping temperature and the volumes of the two phases constant. In applying this equation it will be appreciated that μ is the Gibbs potential for the fluid in the system, as could be calculated from the properties of either homogeneous phase with the help of Eq. (10.8), that σ is the surface tension as defined by Gibbs, and that there is no term dependent on change in curvature δc because of choice of the surface of tension as the dividing surface employed.

[9] A similar assumption is made by Gibbs (reference 1, p. 226), when he treats the distance λ between two different possible dividing surfaces as being unaffected by a variation in curvature.

On the other hand, by combining the expressions for δm and δA provided by Eqs. (11.4) and (11.6) in the preceding section, we see that we can also write the more detailed expression,

$$\begin{aligned}\delta A &= \mu\delta m \\ &+\delta s\left[\int_{-a}^{0}(\gamma\psi+\gamma\phi-\gamma'\psi'-\mu\gamma+\mu\gamma')(1+cx)^2dx\right. \\ &\left.+\int_{0}^{b}(\gamma\psi+\gamma\phi-\gamma''\psi''-\mu\gamma+\mu\gamma'')(1+cx)^2dx\right] \\ &+2s\delta c\left[\int_{-a}^{0}(\gamma\psi+\gamma\phi-\gamma'\psi'-\mu\gamma+\mu\gamma')(1+cx)xdx\right. \\ &\left.+\int_{0}^{b}(\gamma\psi+\gamma\phi-\gamma''\psi''-\mu\gamma+\mu\gamma'')(1+cx)xdx\right],\end{aligned} \tag{12.2}$$

for the change in free energy of the same system, when we make the variations in its fluid content and in its transition layer that were specified in Section 11, keeping temperature and the volumes of the two phases constant. And this expression can be considerably simplified, since with help of Eqs. (10.8) and (10.9) we see that we can introduce the substitutions

$$\begin{aligned}&(\gamma\psi+\gamma\phi-\gamma'\psi'-\mu\gamma+\mu\gamma') \\ &\quad=\gamma\psi+\gamma\phi-\gamma'\psi'-\gamma\psi'-\gamma(p'/\gamma')+\gamma'\psi'+p' \\ &\quad=\gamma[\psi+\phi+(p/\gamma)-\psi'-(p'/\gamma')]-p+p' \\ &\quad=p'-p,\end{aligned} \tag{12.3}$$

and, similarly,

$$(\gamma\psi+\gamma\phi-\gamma''\psi''-\mu\gamma+\mu\gamma'')=p''-p. \tag{12.4}$$

This then permits us to rewrite Eq. (12.2) in the simpler and physically more transparent form

$$\begin{aligned}\delta A &= \mu\delta m+\delta s\left[\int_{-a}^{0}(p'-p)(1+cx)^2dx\right. \\ &\qquad\left.+\int_{0}^{b}(p''-p)(1+cx)^2dx\right] \\ &\quad+2s\delta c\left[\int_{-a}^{0}(p'-p)(1+cx)xdx\right. \\ &\qquad\left.+\int_{0}^{b}(p''-p)(1+cx)xdx\right].\end{aligned} \tag{12.5}$$

This result appears reasonable since we can regard the first term $\mu\delta m$ as expressing the increase in free energy associated with introduction of fluid to be used in the formation of increased transition layer, and can regard the remaining terms as expressing the mechanical work associated with increase in the volumes $s(1+cx)^2dx$ of the differential layers under pressure p within the transition region, and with decrease in the volumes v_a' and v_b'' containing homogeneous distributions of fluid under pressures p' and p''.

We may now compare the consequences of the Gibbs treatment and the more detailed treatment. Since Eqs. (12.1) and (12.5) can both be taken as applying to the same system and same variation in state, it is evident by identifying coefficients in the two expressions that we can now write

$$\begin{aligned}\sigma &= \int_{-a}^{0}(p'-p)(1+cx)^2dx \\ &\qquad+\int_{0}^{b}(p''-p)(1+cx)^2dx,\end{aligned} \tag{12.6}$$

and

$$\begin{aligned}0 &= \int_{-a}^{0}(p'-p)(1+cx)xdx \\ &\qquad+\int_{0}^{b}(p''-p)(1+cx)xdx.\end{aligned} \tag{12.7}$$

The first of these Eqs. (12.6) gives a detailed expression for the surface tension σ in terms of the distribution of fluid pressures p', p'', and p in the two phases and in the transition layer. The second of the Eqs. (12.7) gives detailed expression to the consequences arising from the simplifications introduced by Gibbs through choice of the surface of tension as the particular dividing surface to be used. The development which we have given for Eq. (12.5) would be valid for any choice of dividing surface, provided s and c were taken as the area and curvature thereof. But, when we specify with Gibbs that the surface of tension is to be used, it is evident that this choice requires the value zero for the coefficient of δc in Eq. (12.5). The necessary condition for this is given by our Eq. (12.7), and, with any specific dependence of p on position in the transition layer, this equation pre-

scribes a specific location for the surface of tension within that layer.

We regard these two equations as important for increasing our insight into the mechanisms underlying surface phenomena, and for providing supplementary information useful in making applications of the Gibbs theory. With the help of Eq. (12.6), we can correlate actual values of surface tension with the pressures that exist in the transition layer, including the negative pressures that would prevail in regions filled with liquid of reduced density. And with the help of Eq. (12.7), we can make estimates as to the location of the surface of tension for use in cases where the actual consequences of the Gibbs theory depend thereon.

We shall now take these more detailed equations as the starting point for deducing two relations which have already been obtained by the treatment of Gibbs. This can serve to increase our confidence in the validity of the more detailed treatment.

13. Deduction of the Kelvin Relation

We may first use Eqs. (12.6) and (12.7) to obtain a deduction of the Kelvin relation connecting the pressures in the two homogeneous phases with surface tension and curvature. Multiplying (12.7) by c and subtracting from (12.6), we see that we can rewrite the expression for surface tension in the following forms.

$$\sigma=\int_{-a}^{0}(p'-p)(1+cx)dx+\int_{0}^{b}(p''-p)(1+cx)dx$$

$$=\int_{-a}^{0}\frac{p'-p}{2c}d(1+cx)^2+\int_{0}^{b}\frac{p''-p}{2c}d(1+cx)^2$$

$$=\left|\frac{p'-p}{2c}(1+cx)^2\right|_{-a}^{0}+\left|\frac{p''-p}{2c}(1+cx)^2\right|_{0}^{b}$$

$$+\frac{1}{2c}\int_{-a}^{b}\frac{dp}{dx}(1+cx)^2dx$$

$$=\frac{p'-p''}{2c}+\frac{1}{2c}\int_{-a}^{b}\frac{1}{\gamma}\frac{dp}{dx}\gamma(1+cx)^2dx$$

$$=\frac{p'-p''}{2c}+\frac{1}{2c}\int_{-a}^{b}f_x\gamma(1+cx)^2dx, \qquad (13.1)$$

where, in agreement with Eq. (10.7), f_x is the external force per gram acting in the x direction on the fluid in the transition layer. We see, however, since the external force acting on any element of the fluid is due to attraction or repulsion from neighboring elements, that the total integral in (13.1) will have to be zero because of the equality of action and reaction. Hence, we may drop the last term from (13.1) and rewrite the result in the form

$$p'-p''=2c\sigma=2\sigma/r, \qquad (13.2)$$

already given for the Kelvin relation by Eq. (6.2).

14. Deduction of Gibbs Expression for Change in Surface Tension

a. Lemma on Changes in Pressure

We shall next wish to use our equations to derive the Gibbs relation connecting changes in surface tension with changes in temperature and potential. To do this we shall first need to prove a lemma on the changes in fluid pressure that would accompany changes in temperature and potential.

Let us take a system at equilibrium, consisting of two phases and a spherical transition layer, filled with a one-component fluid which is distributed at some given temperature T, in accordance with the condition on equilibrium (10.9) given by

$$\psi+\frac{p}{\gamma}+\phi=\mu, \qquad (14.1)$$

where p and γ are the pressure and density of the fluid, and ψ and ϕ its free energy and potential per gram, at any distance x measured normal from the surface of tension, and where μ is the Gibbs potential of the fluid as determined in either homogeneous phase having a value independent of x. And let us consider the change to a slightly varied equilibrium distribution which would be brought about by small changes, dT and $d\mu$, in the temperature and Gibbs potential for the system.

To examine the detailed consequences of such a change, let us first fix our attention on a particular element of the fluid originally located at some point x in the system, and let us denote by

δx the displacement which it receives normal to the surface of tension as a consequence of the change to the varied equilibrium distribution. Using the symbol δ to designate differences which involve the change δx in position, and reserving the symbol d to designate differences which apply at a given position, we can then evidently write, correct to the first order,

$$\delta\psi = -S_m dT + (p/\gamma^2)\delta\gamma, \qquad (14.2)$$

as an expression for the change in free energy per gram of fluid in the element (reference 1, Eq. (88)) where S_m is the entropy per gram, and can write

$$\delta p = (dp/dx)\delta x + dp, \qquad (14.3)$$

as an expression for the change of fluid pressure in the element, where (dp/dx) is the rate of change of pressure with position in the original distribution, and dp is the difference between the varied and original fluid pressures at the point $x+\delta x$, and can write

$$\delta\phi = (d\phi/dx)\delta x, \qquad (14.4)$$

as an expression for the change in the external potential of the element, where $(d\phi/dx)$ is the rate of change of potential with position in the original distribution, and we regard $\delta\phi$ as determined correctly to the first order by change of position in the unvaried field. Furthermore, in addition to such equations derived by considering changes in the displaced element of fluid, it is evident, from the general condition on equilibrium given by (14.1), that we can also write

$$\delta\psi - (p/\gamma^2)\delta\gamma + (\delta p/\gamma) + \delta\phi = d\mu, \qquad (14.5)$$

since an equation of the same form as (14.1) will have to hold at all points in the varied system with the constant μ replaced by $\mu+d\mu$.

Substituting from (14.2–4) into (14.5), we now obtain the result

$$-S_m dT + \frac{1}{\gamma}dp + \frac{1}{\gamma}\frac{dp}{dx}\delta x + \frac{d\phi}{dx}\delta x = d\mu, \qquad (14.6)$$

and noting that the last two terms on the left-hand side will cancel in accordance with the condition for mechanical equilibrium given by (10.7), we can rewrite this in the form

$$dp = S_v dT + \gamma d\mu, \qquad (14.7)$$

where S_v is seen to be entropy per unit volume of the fluid at any point of interest. This is the desired lemma connecting the change in pressure at any point with changes in temperature and potential.

Equation (14.7) has the same form as is known to apply to a homogeneous phase in the absence of external field. (See 6.10.) The present equation, however, applies throughout our system at points of varying external potential, and the quantity μ in the equation is not the intrinsic Gibbs potential at the point in the system under consideration, but that applying to the homogeneous parts of the system. Hence, a special derivation of our lemma was necessary.

b. Deduction of Gibbs Expression

We are now ready to use our detailed equations (12.6) and (12.7) to derive the Gibbs expression for change in surface tension. Differentiating the expression for surface tension given by (12.6), we can begin by writing

$$\begin{aligned} d\sigma = &\int_{-a}^{0} (dp'-dp)(1+cx)^2 dx \\ &+ \int_{0}^{b} (dp''-dp)(1+cx)^2 dx \\ &+ 2dc\int_{-a}^{0} (p'-p)(1+cx)x\,dx \\ &+ 2dc\int_{0}^{b} (p''-p)(1+cx)x\,dx \\ &- 2cdx_t\int_{-a}^{0} (p'-p)(1+cx)\,dx \\ &- 2cdx_t\int_{0}^{b} (p''-p)(1+cx)\,dx \\ &+ p'dx_t - p''dx_t, \end{aligned} \qquad (14.8)$$

where dx_t is the differential change in the position of the surface of tension in the positive x direction. We note however, that only the first two terms in this expression will survive, since the sum of the next two terms will be zero in accordance with (12.7), and the remaining terms will cancel in accordance with the expressions for σ given by the first line of (13.1) and by (13.2).

Hence, substituting the expression for dp, given by our lemma (14.7), we now obtain

$$d\sigma = \int_{-a}^{0} [(S_v' - S_v)dT + (\gamma' - \gamma)d\mu](1+cx)^2 dx + \int_{0}^{b} [(S_v'' - S_v)dT + (\gamma'' - \gamma)d\mu](1+cx)^2 dx. \tag{14.9}$$

And, finally, noting the definition of surface densities given by (6.8) in terms of the differences between the actual values of quantities and those computed on the basis of completely homogeneous distributions, as discussed in Section 3, we now see that we can rewrite this equation in the form

$$-d\sigma = S_s dT + \Gamma d\mu, \tag{14.10}$$

which for a one-component system agrees with the Gibbs expression (6.9) connecting the changes in σ, T, and μ with the superficial densities S_s and Γ for entropy and mass of the single component, calculated for the surface of tension. This completes our illustration of the use of the more detailed treatment to derive, for the special case treated, important results which can also be derived by the certainly valid methods of Gibbs.

15. Possibilities for Detailed Treatments of Transition Layers

In bringing this article to its conclusion, two further points need discussion. In the present section we discuss the general possibilities for giving detailed treatment to transition layers. And in the following section we consider the validity of the particular treatment that we have given.

First of all it may again be emphasized as in Section 7 that the thermodynamic treatment of Gibbs was developed, presumably purposely, in such a manner as to reduce detailed consideration of the structure of the transition layer to the minimum essential for the treatment, namely, to the bare assumption that all the properties of the transition layer would be determined by the area and curvature of an idealized geometrical dividing surface. This has the advantage that the results of the treatment have a wide range of applicability without reference to the structure of the transition layer. It also carries, however, the concomitant disadvantage that such a treatment provides less physical insight into underlying mechanisms, and less theoretical foundation for calculating the values of parameters needed for specific application than we might like to have and be able to procure, Hence, it is also appropriate to be interested in more detailed treatments.

For purposes of discussion, we may roughly distinguish three methods of giving more detailed treatment to transition layers: firstly by the application of simple mechanical principles to the behavior of particles in the neighborhood of a boundary between phases, secondly by the application of the usual principles of thermodynamics to the infinitesimal portions of fluid composing a transition layer as has been essayed in the foregoing, and thirdly by application of the full methods of modern statistical mechanics to a study of the average behavior of matter at points within the transition layer.

The application of simple mechanical principles to particles in the neighborhood of a boundary between phases has a long past history which includes the original theoretical work of Young, Laplace, Gauss, and Poisson and later work of more recent investigators. Their treatments were carried out on the assumption of the existence of short-range forces between neighboring particles, and led to the general idea of a resultant "surface tension," and to correct conclusions as to the constancy of angle of contact between solids and liquids, and as to the equilibrium shapes of boundary surfaces.

The application of thermodynamics to the infinitesimal portions of fluid composing a transition layer has not usually been carried out in the past in any systematic manner, but has consisted in the qualitative use of thermodynamic terms such as pressure, temperature, and energy density in giving a rough description of the internal character of the transition layer. As an example we may mention the treatment given by J. Rice[10] in the well-known volume of commentaries on the work of Gibbs, to the question of the location of the surface of tension within the

[10] See article *L* by J. Rice in *A Commentary on the Scientific Writings of J. Willard Gibbs* (Yale University Press, New Haven, 1936), Vol. I, pp. 529–533.

transition layer. By ascribing a definite thickness ζ to the transition layer, and assuming that σ represents a surface energy per unit area which is actually uniformly distributed throughout the layer so defined, he comes to the conclusion that the surface of tension would lie midway at the distance $\zeta/2$ from his two postulated boundaries. It is evident, however, that such an analysis is inadequate[11] and leads to a result not in agreement with our Eq. (12.7), It is hoped that the systematic thermodynamic analysis of the transition layer attempted in this article will prove a useful step in the understanding of surface phenomena.

The application of the full methods of modern statistical mechanics to a study of the transition layers between phases must be regarded as an ultimate goal of great importance. Indeed, as will be mentioned again later, detailed thermodynamic treatments of the transition layer, of the kind that we have given, can in some ways be regarded as temporary procedures which may receive further justification and extension from the later application of statistical methods. Nevertheless, it is apparent that many complexities and difficulties stand at present in the way of such a development. Some steps in the direction of applying statistical mechanics to the transition region have already been taken by Fowler and Guggenheim,[12] where the existence of difficulties is well illustrated by the many simplifying approximations which they have had to introduce, including, finally, the assumption that the molecular densities at the boundary between a liquid and vapor phase would have strictly constant values right up to a geometrical surface of sharp discontinuity.

16. Validity of Detailed Treatment

We must now inquire specially into the validity of applying usual thermodynamic methods in treating the distribution of fluid in a thin transition layer, as was done in developing the detailed treatment of Part II. This is important, since it is planned to make later use of the consequences of the treatment as given by Eqs. (12.6) and (12.7).

We have ample empirical justification for applying the usual methods of thermodynamics to a distribution of fluid in an external field of force, when the distribution is sufficiently uniform and the external forces are of such an origin that we can treat the system as composed of substantially homogeneous macroscopic elements, having dimensions large enough to cover many intermolecular distances, but at the same time also small enough to make the internal condition of the fluid and the intensity of the external force acting on it sensibly constant throughout any element. It is natural to feel the need of further inquiry, however, when we apply these same methods to a situation where the average condition of the molecules composing the fluid must be regarded as changing by substantial amounts within distances of the order of the separation between molecules, and the average forces acting on them must be regarded as resulting from the short-range influence of neighboring molecules.

To make the problem specific, let us return to the fundamental equation (10.3) on which we have based our detailed treatment of the transition layer,

$$\psi+\frac{p}{\gamma}+\phi=\text{const.} \tag{16.1}$$

In the first place, we may then inquire what meaning can be ascribed to the macroscopic quantities, ψ, p, γ, and ϕ, occurring in this equation when we apply it to microscopic layers of fluid in the transition region which have a thickness only of the same order as that of the distance between molecules. In the second place, we may inquire what justification there is for regarding the equation as still valid when applied to such microscopic regions. We can only make a few remarks on these points.

With regard to the meaning of the quantities in (16.1), it is clear that such quantities find their first entrance into theory as macroscopic thermodynamic variables having values which can be directly determined by large-scale measurements. Nevertheless, since it is well known in the case of large-scale systems that the values of such macroscopic variables can be given

[11] Note remarks made in footnote 4 as to the unsatisfactory character of the treatment given by Rice.

[12] R. H. Fowler and E. A. Guggenheim, *Statistical Thermodynamics* (Cambridge University Press, Teddington, 1939), pp. 445–450.

a statistical mechanical interpretation as the average values of appropriate microscopic quanties of molecular character, it can be hoped that a similar interpretation will be possible in the case of microscopic portions of a system. Thus, it might be natural to begin by taking the quantity γ, at any point x in the transition layer, as the time average of the density of fluid at that point, and then proceed by assigning to p and ψ the values of pressure and of free energy per gram which would be exhibited by fluid in bulk at the density γ and at the temperature of interest. The interpretation of ϕ presents more difficulty, since it involves some kind of successful distinction between very short-range molecular forces which depend on the immediate local condition of the fluid and only slightly longer range molecular forces which depend on the change in condition with position. It would seem reasonable, however, to expect that ϕ could be interpreted as an appropriate average of that part of the energy per gram at any point, which depends on the derivatives of γ with respect to x.

With regard to the validity of (16.1), it seems rational for the present to extend the application of this macroscopically verified equation to microscopic regions, and for the future to expect that such an extension will find added statistical mechanical support, substituting appropriate averages of the kind suggested above into the equation. In addition, we may again call attention to the successful use of the consequences of (16.1) to derive, at least for a special case, significant results which can also be derived by the method of Gibbs. This outcome can, of course, not be taken as a sufficient criterion for the validity of (16.1) but can nevertheless increase our confidence therein.

For the time being, it would seem a sensible procedure to make tenative use of the consequences of our detailed treatment when we need them to supplement the consequences of the less detailed treatment of Gibbs.

THE JOURNAL OF CHEMICAL PHYSICS VOLUME 16, NUMBER 8 AUGUST, 1948

Ionization Processes on Tungsten Filaments

I. The Electron Affinity of the Oxygen Atom*

MAX METLAY†‡ AND GEORGE E. KIMBALL
Department of Chemistry, Columbia University, New York, New York

(Received April 16, 1948)

The electron affinity of the oxygen atom was determined to be 53.8±0.8 kcal./mole by measuring the ratio of ions to electrons leaving a hot tungsten filament in contact with nitrous oxide gas at a low pressure. Previous investigations of this quantity yielded discordant results. A possible reason for this disagreement is set forth.

INTRODUCTION

DIRECT experimental determinations of the electron affinity of the oxygen atom have been made by Vier and Mayer,[1] Lozier,[2] and Hanson.[3] These workers obtained, respectively, values of 70.8±2, 51±5, and 46±9 kcal./mole. This investigation was undertaken in an attempt to resolve these differences. The method used,

* Publication assisted by the Ernest Kempton Adams Fund for Physical Research of Columbia University.

† Part of a dissertation submitted in partial fulfillment of the requirements for the degree of Doctor of Philosophy at Columbia University.

‡ Present address: Northwestern University, Evanston, Ill.

[1] D. T. Vier and J. E. Mayer, J. Chem. Phys. **12**, 28 (1944).
[2] W. Lozier, Phys. Rev. **46**, 268 (1934).
[3] G. Hanson, Phys. Rev. **48**, 476 (1935).

that of Vier and Mayer, has been successful in determinations of the electron affinities of the atoms of chlorine,[4,5] bromine,[6] and iodine.[7] In this method, molecules containing the atom, X, whose electron affinity we wish to measure, are allowed to dissociate on the surface of a hot tungsten filament:

$$AX_n \rightarrow nX + A. \quad (1)$$

The resulting X atoms react with the electrons emitted from the filament according to the reaction

$$X + e^- \rightarrow X^-. \quad (2)$$

The negative of the energy change of this reaction at 0°K, $-\Delta E_0$, is the electron affinity of X. From measurements of the relative electron and ion currents from the filament, the equilibrium constant of this reaction, and hence the electron affinity, can be calculated.

One of the requirements for the success of the method is an accurate knowledge of the rate of formation of X atoms at the filament. Vier and Mayer[1] used oxygen molecules as their source of oxygen atoms. The dissociation of these molecules is far from complete, and difficulty arises in the computation of the extent of the dissociation. In addition, the possibility of the formation of O_2^- cannot be disregarded. Other carriers, such as CO, CO_2, and SO_2, have the disadvantage of possibly changing the filament characteristics. Others, such as NO, are not completely dissociated at filament temperatures. In order to avoid these difficulties, we have used nitrous oxide as the carrier gas. We believe that N_2O dissociates completely into N_2 and O at the filament temperatures used, 2000°K to 2400°K, since dissociation is substantially complete at 1200°K.[8]

TABLE I. Electron affinity of the oxygen atom with N_2O as carrier.

Run	T, °K	P, μ	$i_i/i_e \times 10^3$	$-\Delta E_0$
I	2192	3.1	3.7	53.2
	2186		3.2	52.5
	2210		3.0	52.7
	2260		1.0	49.3
II	2131	12.2	30	54.6
	2134		16	52.0
	2202		16	54.0
	2305	11.4	7	53.4
	2292		8.9	54.1
	2289		14	56.1
	2342		9.3	55.8
	2342		4.4	52.3
III	2177	11.9	24	55.1
	2273		10	54.0
	2213		19	55.1
	2213		15	54.1
	2106		55	56.5
IV	2268	11	9.5	54.4
	2266		5.7	51.3
	2136		27	55.2
	2163		21	54.2
	2181	8.4	17.5	55.3
	2177		22	56.3
	2138	7.7	25	55.0
	2168		16	55.0
	2278		3.6	51.6
	2278		6.2	54.1
V	2092	6.6	16	53.4
	2111	4.6	11	53.9
	2202		5.3	53.3
	2202		5.9	53.8
	2276		3	52.9
	2279		1.8	50.6
	2082		17	54.8
				53.8 av.
				a.d. = 1.3
				P. E. = 0.2

THEORY

It has been shown by McCallum and Mayer[4] that if a gas at temperature T_r and pressure P_r, composed of molecules of mass m_r containing n atoms X whose electron affinity is to be measured, is completely decomposed at a filament at the temperature T_s and gives an ion current i_i and an electron current i_e, then the electron affinity, $-\Delta E_0$, is given by

$$-\Delta E_0 = RT_s \ln\left[\frac{2^{5/2}\pi^{3/2}k^{5/2}}{h^3}\frac{m_e m_r^{1/2}}{n} \times \frac{i_i}{i_e}\frac{T_r^{1/2}T_s^2}{P_r}\frac{Q_x'}{Q_i'}\right] \quad (3)$$

where m_e is the mass of the electron, Q_x' and Q_i' are the internal partition functions for the atoms X and the ions X^-, and the other symbols have their usual significance. This equation also applies even if the carrier molecules are not com-

[4] K. J. McCallum and J. E. Mayer, J. Chem. Phys. **11**, 56 (1943).
[5] J. J. Mitchell and J. E. Mayer, J. Chem. Phys. **8**, 282 (1940).
[6] P. M. Doty and J. E. Mayer, J. Chem. Phys. **12**, 323 (1944).
[7] P. P. Sutton and J. E. Mayer, J. Chem. Phys. **3**, 20 (1935).
[8] L. S. Kassel, *The Kinetics of Homogeneous Gas Reactions* (Chemical Catalog Company, New York, New York, 1932).

TABLE II. Results of the calculation of the electron affinity of the oxygen molecule, calculated on the assumption of the reaction $O_2+e^-\rightarrow O_2^-$, and of the oxygen atom, with oxygen as carrier gas.

T, °K	P, μ	$i_i/i_e\times10^4$	$-\Delta E_0(0)$	$-\Delta E_0(O_2)$
2052	6.65	80	72.5	66.0
2151	5.3	21	68.5	64.8
2306	4.45	3.0	62.7	61.5
		2.4	61.7	
2386	4.1	1.9	62.4	61.9
		1.2	60.3	
2170	4.8	46.2	73.1	69.2
2207	0.67	6.15	70.3	70.3
2396	0.67	0.31	61.8	62.5
		0.26	61.0	
2282	0.67	2.05	67.4	68.1
				65.5 av.
				a.d. = 2.8

pletely dissociated into atoms, as long as all the atoms X are completely dissociated from the rest of the molecule. Equation (3) can, therefore, be used for the electron affinity of oxygen with N_2O as the carrier, since the N_2O molecule can be assumed to dissociate into N_2 and O.

In the work of Vier and Mayer, in which O_2 was used as the carrier, the assumption of complete dissociation at the filament could not be made. If a fraction β of the carrier is dissociated, Eq. (3) can be corrected for incomplete dissociation by replacing P_r by βP_r. Vier and Mayer calculated β by assuming that temperature equilibrium was reached between the carrier O_2 and the filament. This, however, introduces a possible error into the results.

Vier and Mayer have used the following expressions for Q_x' and Q_i' for oxygen atoms and ions:

$$Q_x'=5+3\exp(-226.2/T_s)+\exp(-324.5/T_s)$$
$$Q_i'=6.0. \qquad (4)$$

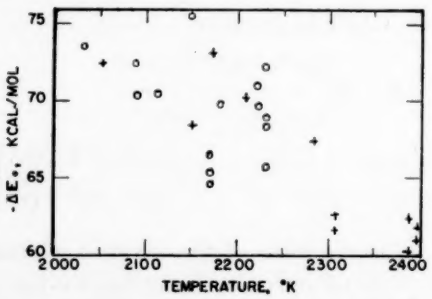

FIG. 1. Electron affinity of O, calculated on the assumption of the reaction $O+e^-\rightarrow O^-$, plotted against filament temperature, for runs with oxygen as carrier gas. This experiment +; Vier and Mayer ○.

Using these expressions and evaluating the numerical constants, the electron affinity of oxygen in kcal./mole is

$$-\Delta E_0=4.574\times10^{-3}T_s[\log10^4 i_i/i_e-\log P_r+2\log10^{-3}T_s-\log n-\log\beta+\tfrac{1}{2}\log M+4.722], \qquad (5)$$

if P_r is expressed in microns, and where M is the molecular weight of the carrier. In deriving this equation, a term $0.09342\times10^{-4}T_s$ has been approximated by the constant value 0.020.

With N_2O as the carrier gas, we have used $n=1$ and $\beta=1$. With O_2 as the carrier, $n=2$ and β has been calculated in the way described by Vier and Mayer.

If we assume the observed ion current to be due to O_2^- ions, formed as a results of the reaction

$$O_2+e^-\rightarrow O_2^-, \qquad (6)$$

we set $n=1$ and $\beta=1$ and assume as a first approximation that $Q_x'=Q_i'$. The numerical constant in Eq. (5) is then 4.568.

EXPERIMENTAL

Previous papers have described the essential features of the apparatus. The Pyrex reaction tube contained a central tungsten filament, of 0.02 cm diameter, a radial nickel grid, and a nickel plate with two guard rings, all approximately co-axial. A water cooled solenoid was placed around the outside of the tube. Since this tube was also used for an investigation of fluorine, the tungsten helix that was used to keep the filament taut was nickel plated, and all other metal parts in the tube were constructed of nickel. All tungsten leads were encased in glass.

The measurements consisted of the determination of ion current, electron current, filament temperature, and pressure. With the plate at a positive potential with respect to the filament, electrons and negative ions are collected on the plate, and the plate current is the sum of the current due to ions and of that due to electrons. This current is measured with a Leeds and Northrup type HS galvanometer with a sensitivity of 2.3×10^{-10} amp./mm. On passing a current through the solenoid, a magnetic field with B approximately 0.03 weber/m² (300 gauss)

is produced parallel to the filament. This field is sufficient to deflect the electrons to the radial grid, while the ions are practically unaffected. The plate current is then equal to the negative ion current, and the electron current can be found by difference. For each value of the filament temperature, several values of the plate voltage were used, ranging in value from 6 to 45 volts positive with respect to the positive end of the filament. The grid was normally kept 3 volts negative with respect to the plate. The effect of changing solenoid current was occasionally checked. Any current of more than four amperes gave satisfactory results, in that the ratio of the plate current with the magnetic field to that without field was less than 10^{-5} in vacuum, and i_i did not change with solenoid current in the presence of gas. Most measurements were taken at about six amperes solenoid current.

The temperature of the filament was determined by means of the R/R_{293} function for tungsten as tabulated by Jones and Langmuir.[9] Since the diameter of the wire changes during the run, the assumption of a linear change of diameter with time was made. The runs were kept to less than thirty minutes so that this assumption produces only a small error in the calculated temperature. The diameter was determined before and after each run as follows. The voltage and current were measured at several temperatures between 1900°–2300°K in vacuum. From these, the temperature was determined by means of the diameter-independent $VA^{\frac{1}{2}}/l$ function given by Jones and Langmuir. From this temperature, and the resistance, R_{293} and the diameter could be calculated. These diameters agreed within 0.5 percent with diameters obtained by weighing and measuring filaments, both before insertion in the reaction tube and after removal from the tube after a series of runs.

Pressure measurements were made by means of a quartz fiber gauge which had been calibrated with dry air against a McLeod gauge. Damping at the fiber was observed by means of a telescope with a graduated eyepiece. The gauge was suspended from the reaction tube by a glass helix and was surrounded by mineral oil to minimize

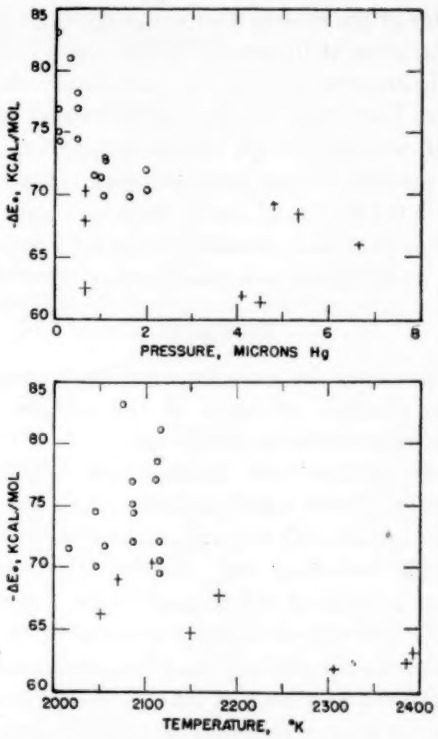

FIG. 2. Electron affinity of O_2, calculated on the assumption of the occurrence of the reaction $O_2+e^- \rightarrow O_2^-$, plotted against filament temperature and against pressure. This experiment +; Vier and Mayer ○.

the effect of external vibrations. The calibration was reproducible to within 10 percent.

The nitrous oxide, of 98 percent purity, was obtained from the Matheson Co. It was purified by condensing it into a liquid nitrogen trap and pumping off any non-condensible gases. The nitrous oxide was then distilled off while the trap was kept cold with dry ice-acetone mixture, leaving behind any more condensible impurities. This procedure was repeated three times. The nitrous oxide was then transferred to a two-liter reservoir bulb which was connected to the system by a capillary leak.

The error in the measurement of the filament temperature is less than 10°, on the basis of the reproducibility of measurements made in vacuum and the calculation of the temperature by several different methods. An error of 10° in a single temperature measurement would lead to an error of 0.5 percent or 0.25 kcal./mole in the electron affinity calculated from that measurement. The pressure measurements are in error by less than 10 percent, as calculated from the

[9] H. A. Jones and I. Langmuir, Gen. Elec. Rev. **30**, 312 (1927).

behavior of the quartz fiber gauge during calibration. An error of 10 percent in the pressure would result in an error of 0.5 kcal./mole in the electron affinity. The error in the current ratio ranged from 10 percent at high temperatures to as much as 50 percent at low temperatures. This would result in 0.5 to 3 kcal./mole error in $-\Delta E_0$. This leads to a precision measure of ± 0.8 for measurements at temperatures greater than 2100°K.

RESULTS

Table I lists the experimental results and calculated electron affinities of the oxygen atom with nitrous oxide as carrier gas.

Table II lists the results with oxygen as carrier gas. This table includes the calculated electron affinity of O_2, computed on the assumption that reaction (6), $O_2+e^- \rightarrow O_2^-$, is the dominant source of the observed ions, and it also lists the calculated electron affinity of 0, computed on the assumption that the ions formed are O^-. Figure 1 is a plot of the calculated electron affinity of 0 as a function of temperature. The data of Vier and Mayer are included for comparison. Figure 2 includes plots of the calculated electron affinity of O_2 as a function of pressure and of temperature.

DISCUSSION OF RESULTS

Figure 1 shows that the runs with oxygen give substantially the same results as those of Vier and Mayer but that an extension of the experimental temperature range introduces a decided dependence of the calculated electron affinity on temperature. This indicates that some assumption in the calculation of the electron affinity is not justified and that the calculated electron affinity is presumably not the true electron affinity of the oxygen atom. Figure 2 shows that there is no dependence of the calculated electron affinity of O_2 on either pressure or temperature. Therefore, it seems possible that the ions observed were actually O_2^-. However, other experimental determinations of the electron affinity of O_2 have resulted in values of 3 kcal./mole[10] and 8 kcal./mole.[11] Although an estimation of this quantity from the heat of dissociation and heat of solution of HO_2 is 62 kcal./mole[12] the values obtained seem to be unreasonably high. The results are not sufficiently clear for a conclusive interpretation to be made.

The results of the runs with N_2O as carrier gas are free of any trend with temperature over a range of 2092–2340°K and with pressure from 4 to 12 microns. The average value of 53.8 ± 0.8 kcal./mole agrees within experimental error with the results of Lozier and of Hanson.

ACKNOWLEDGMENT

The authors wish to express their thanks to Dr. Joseph E. Mayer, at whose suggestion this work was commenced, and whose generous advice has contributed greatly to its completion.

CONCLUSION

1. We have shown that the results of the measurements using oxygen gas as the carrier cannot be interpreted as giving the correct electron affinity of oxygen atom. They may possibly give the electron affinity of oxygen molecule, but this appears to be unlikely.

2. The electron affinity of the oxygen atom is 53.8 ± 0.8 kcal./mole, in agreement with the results of Lozier and of Hanson.

---

[10] N. E. Bradbury, J. Chem. Phys. **2**, 627 (1394); *ibid.*, **2**, 835 (1934).
[11] L. B. Loeb, Phys. Rev. **48**, 684 (1935).
[12] J. Weiss, Trans. Faraday Soc. **31**, 966 (1935).

THE JOURNAL OF CHEMICAL PHYSICS VOLUME 16, NUMBER 8 AUGUST, 1948

Ionization Processes on Tungsten Filaments

II. The Absorption of Fluorine on Tungsten*

MAX METLAY†‡ AND GEORGE E. KIMBALL
Department of Chemistry, Columbia University, New York, New York

(Received April 16, 1948)

Fluorine is found to form an adsorbed film on tungsten stable to temperatures above 2600°K. This causes a low accommodation for the thermal dissociation of fluorine. The adsorption is compared to that of oxygen on tungsten.

INTRODUCTION

THIS investigation was begun as an attempt to measure the electron affinity of fluorine by the method described in the preceding paper[1] of passing fluorine gas at a given pressure over a hot tungsten filament and measuring the relative currents of negative ions and electrons emitted from the filament. It soon became evident, however, that the current of negative ions was much smaller than would be expected from any reasonable estimate of the electron affinity of fluorine and that this discrepancy decreased as filament temperature was raised. Further investigation has led to the conclusion that the fluorine gas is not completely dissociated, predictions, based on the equilibrium constant for the dissociation,[2] to the contrary. This paper is an attempt to elucidate this behavior.

The apparatus and techniques used were those described in Part I.

EXPERIMENTAL OBSERVATIONS

The following experimental observations form the basis for the picture given here of the interaction of fluorine and tungsten at high temperatures.

1. A tungsten filament which had been exposed to fluorine for several minutes was slowly heated in vacuum and electron emission measured as a function of temperature. The temperature was raised to 2650°K, then slowly lowered. The electron emission on lowering the temperature was much greater at a given temperature than before heating but was not as high as the emission of tungsten which had never been exposed to fluorine. The work function of the fluorine covered tungsten is in the neighborhood of 5.6 e.v., but the data were not sufficiently reproducible to allow an accurate estimate of this quantity. The results are shown in Fig. 1.

2. Under the assumption that all fluorine molecules hitting the filament leave as atoms, ions, or molecules in equilibrium at the temperature of the filament, the electron affinity of fluorine, as calculated from Eq. (I-3), is given by

$$-\Delta E_0 = 4.574\times10^{-3}T_s(\log 100 i_i/i_e - \log P_r + 2\log T_s + 3.338\times10^{-5}T_s + 7.711), \quad (1)$$

where P_r is the pressure of fluorine gas in the filament chamber, in microns.

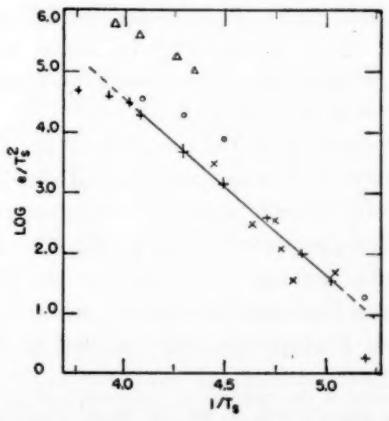

FIG. 1. Log electron emission over T^2 plotted against the reciprocal of the filament temperature. + temperature raised, filament fluorine covered in vacuum, ○ temperature lowered, immediately after above run, × in the presence of fluorine gas, and △ clean tungsten in vacuum.

* Publication assisted by the Ernest Kempton Adams Fund for Physical Research of Columbia University.

† Part of a dissertation submitted in partial fulfillment of the requirements for the degree of Doctor of Philosophy at Columbia University.

‡ Present address: Northwestern University, Evanston, Illinois.

[1] M. Metlay and G. E. Kimball, J. Chem. Phys. **16**, 774 (1948), hereinafter referred to as I.

[2] G. M. Murphy and J. E. Vance, J. Chem. Phys. **7**, 806 (1939).

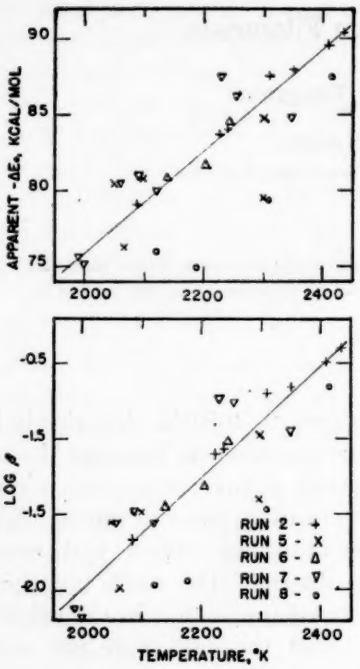

FIG. 2. Apparent electron affinity of fluorine, and logarithm of fraction of fluorine molecules dissociated, plotted against filament temperature.

If it is assumed that the fraction β of the molecules hitting the filament is dissociated, P_r in Eq. (1) must be replaced by βP_r, as in Part I. Using 95 kcal./mole[3] as an assumed value of the electron affinity of fluorine, we may calculate β from (1) as

$$-\log\beta=(95+\Delta E_0)/4.574\times10^{-3}T_s. \qquad (2)$$

The values of β for the various runs are listed in Table I, and $\log\beta$ is plotted against temperature in Fig. 2. It is shown clearly there that the fraction of molecules dissociated increases exponentially with temperature.

3. The decrease in the diameter of the filament for different runs was measured. Table II lists, for each of several runs, the temperature T_s, the fluorine pressure P_s, the number z_w of tungsten atoms leaving the filament per cm² per second, and the ratio of z_F to z_w, where z_F is the number of F atoms striking one cm² of filament in one second in the form of F_2. It is seen that there is no appreciable trend of z_w with temperature or with pressure.

[3] This value is the average of the results of Mayer and Helmholtz, Zeits. f. Physik **75**, 19 (1932), who find $-\Delta E_0=95.3$ kcal./mole, from calculations of Born cycles, and of Ionov, Comptes Rendus Acad. Sci. U.R.S.S. (Doklady), **28**, 512 (1940), who obtains $-\Delta E_0=94.7$ kcal./mole, from an investigation of the dissociation products of alkali fluorides on tungsten.

INTERPRETATION OF RESULTS

Roberts[4] presents evidence for the following picture of the adsorption of oxygen on tungsten in the temperature range 1100°K and 1700°K. The oxygen is first adsorbed in the form of a stable atomic layer, each adsorbed molecule occupying two adjacent tungsten atoms. When this layer is complete, the surface will contain about 8 percent of isolated tungsten atoms, which are not sites for adsorbed oxygen atoms. Adsorption then continues as molecules are adsorbed in the holes in the first layer. When these are filled, any further adsorption will be of molecules into a mobile third layer deposited on the first two layers. On heating the tungsten to 1700°K, the top two layers desorb, leaving only the stable atomic layer and the holes.

We shall now examine the experimental results described above in the light of this picture. It is

TABLE I. Experimental results for fluorine.

Run	T, °K	P, μ	$-\Delta E_0$	$-\log\beta$	β
2	2083	4.5	79.1	1.66	0.022
	2311	5.6	87.6	0.70	0.20
	2240	6.1	84.1	1.06	0.087
	2227	6.7	83.8	1.10	0.079
	2435	5.7	90.5	0.40	0.40
	2348	5.3	88.0	0.66	0.22
	2411	5.0	89.6	0.49	0.32
5	2067	3.0	76.3	1.98	0.01
	2300	2.8	79.5	1.40	0.04
			84.8	0.97	0.11
	2048	2.4	80.5	1.55	0.028
	2100	2.5	80.8	1.48	0.033
6	2206	2.1	81.7	1.32	0.048
	2243	1.9	84.5	1.02	0.096
	2139	1.1	80.9	1.45	0.035
7	1991	0.7	75.7	2.12	0.0076
	2000	1.1	75.2	2.17	0.0068
	2120	1.1	80.0	1.55	0.028
	2230	1.7	87.5	0.73	0.186
	2255	2.3	86.2	0.76	0.174
	2350	3.6	84.8	0.95	0.11
	2060	2.0	80.5	1.54	0.029
	2090	2.5	81.0	1.47	0.034
8	2309	1.2	79.5	1.47	0.034
	2414	1.4	87.7	0.66	0.22
	2122	1.8	76.0	1.96	0.011
	2181	3.4	75.0	1.94	0.012

[4] J. K. Roberts, *Some Problems in Adsorption* (Cambridge University Press, 1939).

evident from the study of electron emission as a function of the temperature of the fluorine coated filament that an extremely stable layer is formed which does not desorb below 2600°K. This corresponds to Roberts' first layer. It would be expected that any holes in this film would be filled by fluorine molecules, corresponding to Roberts' second layer. At elevated temperatures, these might either desorb as such, followed by dissociation, or they might dissociate in situ, leaving one atom adsorbed and desorbing the other atom of the molecule. This latter process would cause the surface to be completely covered by the stable atomic first layer.

The investigation of the fraction of the fluorine molecules dissociated seems to indicate that the fluorine is adsorbed onto a layer corresponding to Roberts' third layer. The precise nature of this layer, in the case of fluorine, is not yet clear.

A plausible explanation of the high rate of loss of tungsten is inherent in this picture. The fluorine atoms are sufficiently small as compared to the internuclear distance of tungsten so that an occasional atom or molecule from the second layer can slip between the atoms of the first layer, form chemical bonding with the tungsten, and sufficiently weaken the remaining tungsten-tungsten bonds so that the tungsten fluoride thus formed is readily evaporated.

TABLE II. Rate of loss of tungsten from the filament.

Run	T, °K	P, μ	z_w	zp/z_w
2		6	7.0×10^{15}	566
3		2.4	8.4×10^{15}	190
7A	1990	1.0	7.3×10^{15}	90
7B	2120	1.2	1.1×10^{16}	72
7C	2250	2.4	1.25×10^{16}	128
7D	2350	3.0	1.03×10^{16}	194
7E	2075	2.4	1.13×10^{16}	140

CONCLUSION

Fluorine is found to form a very stable atomic layer on the surface of tungsten, which does not desorb below 2600°K. A less stable layer is believed to adsorb over the first layer. The fraction of the fluorine dissociated on the surface of the tungsten is exponential in temperature, and the rate of loss of tungsten from the surface is independent of temperature and of pressure, in the range 2000°K to 2400°K, and 1 to 6 microns of mercury pressure.

THE JOURNAL OF CHEMICAL PHYSICS VOLUME 16, NUMBER 8 AUGUST, 1948

The Energy Levels and Thermodynamic Functions of the Fourth Power Oscillator

JOHN E. KILPATRICK AND MYRA FERGUSON KILPATRICK
Department of Chemistry, The Rice Institute, Houston, Texas

(Received May 20, 1948)

The first six characteristic numbers of the reduced wave equation $\psi''+(\lambda-\xi^4)\psi=0$ have been calculated by a method of numerical integration. These values have been compared with the corresponding values obtained from the first, second, and third Wentzel-Kramers-Brillouin approximations. For the fourth, fifth, and sixth characteristic numbers, the third W.K.B. approximation is correct within 0.0001. The four thermodynamic functions $-(F-H_0)/RT$, $(H-H_0)/RT$, S/R, and C/R have been calculated over the range $h\nu_0/kT=0$ to 10. A previously reported maximum in the heat capacity function, C/R, does not exist.

THE potential $V(x)=ax^4$ is intermediate between the square law potential of the simple harmonic oscillator and the rectangular potential of the particle in a one-dimensional box with infinitely high walls. For this reason alone the energy levels of the fourth power oscillator are of interest. In addition, some molecules may contain a vibration with a fourth power potential. For example, the twisting motion of the bridge structure in the aluminum halide dimers and in diborane may be of this type. Bell[1] has discussed the energy levels and the heat capacity of the fourth power oscillator. There are, how-

[1] R. P. Bell, Proc. Roy. Soc. **A183**, 328 (1944).

TABLE I.

Trial λ	$I(\lambda)$	N	$d\lambda/dN$	Corrected λ (λ_n)
1	3.046 9			1.060 5
2	3.109 0			
3	3.171 9			
4	3.236 2			3.799 8
1.000 000	3.047 164			
1.060 5	3.050 871 3	1.000 067 6	2.03	1.060 363
1.060 363	3.050 864 6	1.000 000 8	2.01	1.060 361
3.799 8	3.223 352 8	2.000 038 4	3.30	3.799 673
7.414 4	3.449 31	2.989 65	3.943	7.455 2
11.612	3.680 88	3.992 60	4.417	11.644 7
16.234	3.893 93	3.994 03	4.806	16.262 7
7.455 2	3.451 616	2.999 869	3.943	7.455 72
11.644 9	3.682 524	4.000 033	4.417	11.644 75
16.234	3.894 075	4.994 215	4.806	16.261 8
21.214	4.089 277	5.995 249	5.140	21.238 4

ever, a number of errors in his work which invalidate some of his results.

NUMERICAL INTEGRATION

The wave equation for the fourth power oscillator

$$(d^2\psi/dx^2)+(8\pi^2m/h^2)(E-ax^4)\psi=0 \quad (1)$$

is readily transformed into the reduced equation

$$(d^2\psi/d\xi^2)+(\lambda-\xi^4)\psi=0 \quad (2)$$

by the substitutions

$$\xi=(8\pi^2ma/h^2)^{1/6}x, \quad (3)$$

$$\lambda=(1/a)(8\pi^2ma/h^2)^{2/3}E. \quad (4)$$

The numerical method given by Milne[2] is very convenient for the solution of this equation. The auxiliary differential equation

$$(d^2w/d\xi^2)+(\lambda-\xi^4)w-\lambda w^{-3}=0, \quad (5)$$

which differs from Eq. (2) by the addition of the last term $(-\lambda w^{-3})$, is set up. The initial conditions $w(0)=1$ and $w'(0)=0$ are imposed in order to simplify the solution of Eq. (5). The following relationship exists between ψ and w for all values of λ:

$$\psi(\xi)=Cw(\xi)\sin\left\{\lambda^{\frac{1}{2}}\int_{-\infty}^{\xi}w^{-2}d\xi\right\}. \quad (6)$$

Equation (5) is not a characteristic value equation; for all values of λ, w increases slowly from its initial value of unity while $|\xi|<\lambda^{\frac{1}{4}}$, then increases very rapidly for $|\xi|>\lambda^{\frac{1}{4}}$. As ξ approaches $-\infty$, ψ approaches zero; however, as ξ approaches $+\infty$, ψ approaches zero only if

$$\lambda^{\frac{1}{2}}\int_{-\infty}^{\infty}w^{-2}d\xi=N\pi, \quad (7)$$

where N is an integer. Fortunately, the integral

$$I(\lambda)=\int_{-\infty}^{\infty}w^{-2}d\xi \quad (8)$$

is not very sensitive to the value of λ. Equation (5) can be integrated numerically for a number of trial values of λ; the values of λ that will make N of Eq. (7) an integer can then be determined by interpolation. These values of λ are the characteristic numbers (eigenvalues) of Eq. (2), and the corresponding functions $\psi(\xi)$ from Eq. (6) are characteristic functions (eigenfunctions).

It is advantageous to use the best approximations available for trial values of λ. Initially we used the four decimal values $\lambda_0=1.0605$ and $\lambda_1=3.7998$ which were calculated by Milne[2] by this same method. For the higher quantum states, we used the values given by the first Wentzel-Kramers-Brillouin approximation:[1,3]

$$\lambda_{In}=2.185069(n+\tfrac{1}{2})^{4/3}, \quad (n=0, 1, 2, 3, \cdots). \quad (9)$$

For each trial value of λ, Eq. (5) was integrated numerically by a method also devised by Milne.[4,5]

An interval of 0.1 in ξ was used. The necessary starting values of w were calculated from the expansion

$$w=1+\frac{1}{30}\xi^6-\frac{\lambda}{420}\xi^8+\frac{\lambda^2}{9450}\xi^{10}+\frac{315-4\lambda^3}{1,247,400}\xi^{12}+\cdots, \quad (10)$$

which was obtained with the aid of the initial conditions $w(0)=1$ and $w'(0)=0$, Eq. (5), and Maclaurin's series.

[2] W. E. Milne, Phys. Rev. **35**, 863 (1930).

[3] J. L. Dunham, Phys. Rev. **41**, 713 (1932).

[4] W. E. Milne, Am. Math. Mo. **40**, 322 (1933).

[5] Marchant Methods MM 216A, Marchant Calculating Machine Company, Oakland, California (1943).

The integration of Eq. (5) was carried out by means of five point open and closed Milne-Steffensen[4] double integration formulas. At the end of every five complete cycles ($\Delta\xi=0.5$) an over-all check on the accumulated error in w was made by means of the eleven point closed formula:[6]

$$w_{i+10}=2w_{i+5}-w_i+h^2\sum_{n=0}^{10}C_nw''_{i+n}, \quad (11)$$

$$\begin{aligned}
C_0=C_{10}&=\ 2{,}144{,}850/38{,}320{,}128\\
&=0.055\ 971\ 890,\\
C_1=C_9&=\ 44{,}122{,}500/38{,}320{,}128\\
&=1.151\ 418\ 388,\\
C_2=C_8&=59{,}426{,}250/38{,}320{,}128\\
&=1.550\ 784\ 225,\\
C_3=C_7&=150{,}630{,}000/38{,}320{,}128\\
&=3.930\ 832\ 381,\\
C_4=C_6&=\ 98{,}902{,}500/38{,}320{,}128\\
&=2.580\ 954\ 323,\\
C_5&=247{,}551{,}000/38{,}320{,}128\\
&=6.460\ 077\ 586.
\end{aligned}$$

The symbol h is the tabular interval; in this case, $\Delta\xi=0.1$.

Sufficient figures were carried in each integration to give $w^{-2}(\xi)$ to the desired accuracy, which was six, four, and five decimal places, respectively, in the three series of integrations that were performed. Since $w(\xi)$ is a symmetric function and increases rapidly with ξ after $\xi>\lambda^{\frac{1}{2}}$, it was necessary to integrate Eq. (5) only from $\xi=0$ to about 3.0. The integrals $I(\lambda)$ were evaluated by both Simpson's rule and Weddle's rule.

In Table I are given the various trial values of λ, the corresponding values of $I(\lambda)$, N, $d\lambda/dN$, and the derived characteristic numbers (λ_n). The first four rows are from Milne.[2] These values were used to calculate $d\lambda/dN$ for use with our integrations with Milne's values of λ_0 and λ_1.

As can be seen from Table I, some of the corrected λ's were used as trial λ's in reintegrations of Eq. (5) in order to effect a check and improvement in their values. In the integration with trial $=11.6449$, the seven point closed double integration formula

$$w_{i+6}=w_{i+5}+w_{i+1}-w_i+h^2\sum_{n=0}^{6}C_nw''_{i+n}, \quad (12)$$

$$\begin{aligned}
C_0=C_6&=\ 787/12096=0.065\ 062\ 831,\\
C_1=C_5&=12162/12096=1.005\ 456\ 349,\\
C_2=C_4&=\ 9789/12096=0.809\ 275\ 794,\\
C_3&=15004/12096=1.240\ 410\ 052,
\end{aligned}$$

which was calculated by one of us,[7] was used in place of the five point closed formula.[4] This provided an answer to the question of whether the five point closed integration formula was sufficient to give $w(\xi)$ to the desired accuracy. Apparently the answer is in the affirmative, for the value of λ_3 was changed only slightly. The last digit of the corrected λ's given in Table I is probably not significant.

It was discovered later in this work that the third W.K.B. approximation (see below) apparently provides very good values for the higher characteristic numbers. An elaborate integration was begun, with a trial $\lambda_{10}=50.256\ 255$, in which eight decimal places were carried and a nine point closed integration formula used. About two-thirds of the way through this integration it was discovered that the five, seven, nine, and eleven point integration formulae gave results in each cycle differing in the sixth or seventh decimal place of w. This behavior is decidedly not characteristic of a smooth function, but indicates the presence of rapidly oscillating higher derivatives. Numerical differences showed that this is just the situation in the fourth and sixth derivatives. Curiously enough, the number of such oscillations in the higher derivatives of w is about the same as would be expected in the corresponding derivatives of ψ. This was found to be true for the lower quantum states also. Although w appears to be smooth and continuously concave upward, the oscillatory nature of ψ is hidden in the higher derivatives of w.

This effect does not invalidate the integrations for the values of λ which are given. It does set an upper limit on the accuracy that may be attained (for a given integration interval h) and prevents Milne's method from being used on the higher quantum states.

[6] This equation was calculated from the coefficients given by H. E. Salzer, J. Math. Phys. **24**, 135 (1945).

[7] Marchant Methods MM 216B, Marchant Calculating Machine Company, Oakland, California (1946).

THE WENTZEL-KRAMERS-BRILLOUIN SOLUTION

Although much work has been done in recent years on the W.K.B. solution to the wave equation,[3, 8, 9–12] it seems that no comparisons have been made between the exact energy levels of a particular wave equation and the levels given by the higher approximations of the W.K.B. method.

For the potential $v(x)=a|x|^q$, is quite practicable to carry the W.K.B. solution out to the third approximation. In the case of the harmonic oscillator, of course, the exact values of the energy levels are given by the first approximation of the W.K.B. method. It was thought that a comparison of the numerically integrated values of the characteristic numbers for the fourth-power oscillator with those given by the W.K.B. method would be considerable interest.

Dunham[3] has given the expression for the first three W.K.B. approximations to the energy levels of the wave equation

$$-\frac{h^2}{8\pi^2 m}\frac{d^2\psi}{dx^2}+V(x)\psi=E\psi \tag{13}$$

in the form

$$(n+\tfrac{1}{2})2\pi\left(\frac{h^2}{8\pi^2 m}\right)^{\frac{1}{2}}=\oint(E-V)^{\frac{1}{2}}dx$$
$$-\frac{1}{32}\frac{h^2}{8\pi^2 m}\oint V''^2(E-V)^{-5/2}dx$$
$$-\frac{1}{2048}\left(\frac{h^2}{8\pi^2 m}\right)^2\oint[49V'^4(E-V)^{-11/2}$$
$$-16V'V'''(E-V)^{-7/2}]dx. \tag{14}$$

In the terms of the local momentum variable

$$p=[2m(E-V)]^{\frac{1}{2}}, \tag{15}$$

this equation assumes a somewhat simplified form:

$$n+\tfrac{1}{2}=\frac{1}{h}\oint p\,dx+\frac{1}{h}\left(\frac{h}{2\pi i}\right)^2\frac{1}{8}\oint(p')^2p^{-3}dx$$
$$+\frac{1}{h}\left(\frac{h}{2\pi i}\right)^4\left[-\frac{1}{32}\oint(p'')^2p^{-5}dx\right.$$
$$\left.+\frac{15}{128}\oint(p')^4p^{-7}dx\right]. \tag{16}$$

Titchmarsh (see reference 12, pp. 136, 137) has pointed out that this is only apparently an expansion in powers of $h/2\pi i$. For example, with the potential $V(x)=a|x|^q$, the substitutions:

$$\xi=\left(\frac{8\pi^2 ma}{h^2}\right)^{1/(q+2)}x, \tag{17}$$

$$\lambda=\frac{1}{a}\left(\frac{8\pi^2 ma}{h^2}\right)^{q/(q+2)}E, \tag{18}$$

reduce Eqs. (13) and (16) to

$$\frac{d^2\psi}{d\xi^2}+(\lambda-|\xi|^q)\psi=0 \tag{19}$$

and

$$n+\tfrac{1}{2}=\frac{1}{2\pi}\left\{\oint(\lambda-|\xi|^q)^{\frac{1}{2}}d\xi\right.$$
$$-\frac{q^2}{32}\oint(\lambda-|\xi|^q)^{-5/2}|\xi|^{2q-2}d\xi$$
$$+\left[\frac{11q^4}{2048}\oint(\lambda-|\xi|^q)^{-11/2}|\xi|^{4q-4}d\xi\right.$$
$$-\frac{q^3(q-1)}{128}\oint(\lambda-|\xi|^q)^{-9/2}|\xi|^{3q-4}d\xi$$
$$\left.\left.-\frac{q^2(q-1)^2}{128}\oint(\lambda-|\xi|^q)^{-7/2}|\xi|^{2q-4}d\xi\right]\right\}. \tag{20}$$

The parameter $h/2\pi i$ has disappeared in the reduced W.K.B. expansion of Eq. (20). Dunham[3] has indicated that the W.K.B. approximations to the energy levels of an oscillator become better as the mass of the oscillator increases. This cannot be true in general, however, since mass does not appear in Eq. (20). The characteristic numbers or reduced energy levels from Eq. (20)

[8] G. D. Birkhoff, Bull. Am. Math. Soc. **39**, 681 (1933).
[9] R. E. Langer, Bull. Am. Math. Soc. **40**, 545 (1934).
[10] E. C. Kemble, Phys. Rev. **48**, 549 (1935).
[11] R. E. Langer, Phys. Rev. **51**, 669 (1937).
[12] E. C. Titchmarsh, *Eigenfunction Expansions* (Clarendon Press, Oxford, 1946).

are the same for all oscillators with a given q. Any particular level must be in error by some percentage which is independent of the mass of the system.

The contour integrals of Eq. (20) are readily evaluated in terms of the gamma-function

$$n+\tfrac{1}{2}=\frac{1}{2\pi}\left\{\frac{4}{q}\frac{\Gamma\left(\frac{3}{2}\right)\Gamma\left(\frac{1}{q}\right)}{\Gamma\left(\frac{3}{2}+\frac{1}{q}\right)}\lambda^{[\frac{1}{2}+(1/q)]}\right.$$

$$-\frac{q}{8}\frac{\Gamma\left(-\frac{3}{2}\right)\Gamma\left(2-\frac{1}{q}\right)}{\Gamma\left(\frac{1}{2}-\frac{1}{q}\right)}\lambda^{-[\frac{1}{2}+(1/q)]}$$

$$-\frac{q^2(q-1)(2q+3)}{1536}\frac{\Gamma\left(-\frac{5}{2}\right)\Gamma\left(2-\frac{3}{q}\right)}{\Gamma\left(-\frac{1}{2}-\frac{3}{q}\right)}$$

$$\left.\times\lambda^{-3[\frac{1}{2}+(1/q)]}\right\}. \quad (21)$$

For the case which we have investigated, $q=4$, ($V(x)=ax^4$), Eq. (21) reduces to

$$n+\tfrac{1}{2}=0.55641\ 78941\lambda^{3/4}$$
$$-0.04767\ 24852\ 5\lambda^{-3/4}$$
$$+0.01195\ 42906\ 9\lambda^{-9/4}. \quad (22)$$

If only the first term on the right-hand side of Eq. (22) is retained, we have the so-called W.K.B. first approximation. The inclusion, in addition, of the second term gives the second W.K.B. approximation. The complete equation gives the third approximation. We have designated λ as a function of n from these three approximations as λ_{In}, λ_{IIn}, and λ_{IIIn}, respectively.

It can be seen from Table II that the values of λ_{In} agree fairly well with those of the true characteristic numbers. For the fourth power oscillator, λ_{In} seems to be a lower limit to λ_n, although this point has not been proved. Titchmarsh[12] has given several equations which place upper and lower bounds on λ_n. These limits are actually too broad to be of any use in this case but do involve definite integrals closely related to the contour integrals of the first and second W.K.B. approximations. For example, Titchmarsh's equation (7.2.3), which places an upper bound on λ_n, is equivalent in the case of the fourth power oscillator to the first W.K.B. approximation, with the term $\frac{1}{2}$ replaced by unity. The second approximation, λ_{II}, is much better than the first approximation. The improvement, however, is not very marked in λ_{II0} and λ_{II1}. The third approximation gives perfect agreement with the characteristic numbers obtained by numerical integration, for $n=3$, 4, and 5, within their probable uncertainty. For $n=2$, either there is a small error in λ_2(num. int.) or λ_{II2} is slightly better than λ_{III2}. Only a slight improvement is observed in λ_{III1} over λ_{II1}, and λ_{III0} is actually worse than λ_{II0}. It is interesting to note that the higher W.K.B. approximations improve in accuracy much more rapidly with increase in n than does the first approximation.

TABLE II.

n	λ_{In}	λ_{IIn}	λ_{IIIn}	λ_n (numerical integration)
0	0.867 145	0.980 766	0.951 643	1.060 361
1	3.751 920	3.810 330	3.808 377	3.799 673
2	7.415 988	7.455 795	7.455 282	7.455 72
3	11.611 525	11.644 990	11.644 779	11.644 75
4	16.233 615	16.261 937	16.261 829	16.261 83
5	21.213 653	21.238 438	21.238 375	21.238 4
6	26.506 336	26.528 515	26.528 474	
7	32.078 464	32.098 626	32.098 598	
8	37.904 472	37.923 021	37.923 001	
9	43.963 948	43.981 173	43.981 158	
10	50.240 152	50.256 266	50.256 255	
11	56.719 057	56.734 223	56.734 214	
12	63.388 708	63.403 054	63.403 047	
13	70.238 771	70.252 400	70.252 395	
14	77.260 210	77.273 205	77.273 201	
15	84.445 040	84.457 470	84.457 466	
16	91.786 147	91.798 070	91.798 067	

Bell[1] calculated, by means of a numerical difference method, the values of the first four characteristic numbers: $\lambda_0=1.09$, $\lambda_1=3.81$, $\lambda_2=7.36$, and $\lambda_3=11.40$. His errors are about the magnitude that he assigned (2 percent). In addition, he calculated the first five λ's from both the first and second W.K.B. approximations. He also gives the single value, $\lambda_{III0}=1.15$, but

without the equations from which it was calculated. There are several errors, some of which may be typographical, in his W.K.B. work: (a) there is a missing factor of $1/2\pi$ in the second term of his Eq. (4); (b) the integral of his Eq. (6) is correct in form but is incorrectly evaluated numerically ($I_2=2.39628$, not 2.636); (c) there is a numerical error in his evaluation of λ_{II2} of about 0.06. The net effect of all of these errors led Bell to the erroneous conclusion that the second W.K.B. approximation is no improvement on the first. His bad value for λ_{III0} probably discouraged him from a further investigation of the third approximation.

TABLE III.

x	$-(F-H_0)/RT$	$(H-H_0)/RT$	S/R	C/R
0	∞	0.7500	∞	0.7500
0.1	1.8486	0.7148	2.5634	0.7481
0.2	1.3631	0.6827	2.0457	0.7451
0.3	1.0921	0.6522	1.7443	0.7411
0.4	0.9085	0.6232	1.5317	0.7365
0.5	0.7724	0.5954	1.3678	0.7312
0.6	0.6662	0.5688	1.2350	0.7256
0.7	0.5805	0.5431	1.1236	0.7196
0.8	0.5096	0.5184	1.0279	0.7132
0.9	0.4499	0.4944	0.9443	0.7064
1.0	0.3990	0.4712	0.8702	0.6991
1.1	0.3551	0.4488	0.8040	0.6915
1.2	0.3170	0.4271	0.7442	0.6834
1.3	0.2837	0.4061	0.6898	0.6748
1.4	0.2543	0.3858	0.6401	0.6656
1.5	0.2284	0.3661	0.5945	0.6560
1.6	0.2054	0.3471	0.5525	0.6457
1.7	0.1849	0.3288	0.5137	0.6349
1.8	0.1666	0.3111	0.4777	0.6234
1.9	0.1502	0.2941	0.4443	0.6114
2.0	0.1356	0.2777	0.4133	0.5988
2.2	0.1106	0.2469	0.3574	0.5719
2.4	0.0903	0.2186	0.3089	0.5430
2.6	0.0738	0.1928	0.2666	0.5124
2.8	0.0604	0.1694	0.2298	0.4806
3.0	0.0495	0.1483	0.1978	0.4481
3.2	0.0405	0.1294	0.1699	0.4152
3.4	0.0332	0.1125	0.1457	0.3826
3.6	0.0272	0.0976	0.1248	0.3507
3.8	0.0223	0.0844	0.1066	0.3197
4.0	0.0182	0.0727	0.0910	0.2900
4.2	0.0149	0.0626	0.0775	0.2619
4.4	0.0122	0.0537	0.0660	0.2355
4.6	0.0100	0.0460	0.0560	0.2109
4.8	0.00821	0.0392	0.0475	0.1882
5.0	0.00672	0.03356	0.04028	0.16735
5.5	0.00408	0.02242	0.02650	0.12305
6.0	0.00248	0.01485	0.01733	0.08896
6.5	0.00150	0.00976	0.01126	0.06339
7.0	0.00091	0.00638	0.00729	0.04462
7.5	0.00055	0.00415	0.00470	0.03109
8.0	0.00033	0.00268	0.00301	0.02146
8.5	0.00020	0.00173	0.00193	0.01470
9.0	0.00012	0.00111	0.00123	0.00999
9.5	0.00007	0.00071	0.00078	0.00675
10.0	0.00004	0.00045	0.00049	0.00454

THERMODYNAMIC FUNCTIONS

The molal thermodynamic functions

$$-(F-H_0)/RT,\ (H-H_0)/RT,\ S/R,\ \text{and}\ C/R$$

were calculated as functions of the variable $x=h\nu_0/kT$. In this equation ν_0 represents the frequency that would be observed in a transition between the two lowest energy levels of a fourth power oscillator. The energy levels (E_n) of any particular fourth power oscillator are proportional to the corresponding characteristic numbers (λ_n) of the reduced equation. Therefore, we have

$$\frac{E_n-E_0}{kT}=\frac{\lambda_n-\lambda_0}{\lambda_1-\lambda_0}\frac{E_1-E_0}{kT}=\frac{\lambda_n-\lambda_0}{\lambda_1-\lambda_0}x. \qquad (23)$$

The partition function is given by the summation

$$Q=\sum_{n=0}^{\infty}\exp\left(-\frac{\lambda_n-\lambda_0}{\lambda_1-\lambda_0}x\right). \qquad (24)$$

From $x=0.5$ to $x=10.0$ the partition function and its derivatives were summed directly, with enough figures carried to give the thermodynamic functions to six significant figures. The thermodynamic functions were then rounded to four decimal places in the final tables up to $x=5.0$, and to five decimal places from $x=5.0$ to 10.0.

The values of λ_n that were used in these summations are as follows: (a) for λ_0, λ_1, λ_2, λ_3, λ_4, and λ_5, the values determined by numerical integration and given in the last column of Table II, (b) for λ_6 and higher λ_n's, the approximations λ_{IIn}, rounded to four decimal places. These values of λ_{IIn} agree with those of λ_{IIIn} within that extent, and probably represent λ_n to better than 0.0001.

For $x=0.5$, it was necessary to sum the partition function and its derivatives to the term in λ_{16}. For $x<0.5$, direct summation became too laborious. The summations in this range were made by means of the Euler-Maclaurin summa-

tion formula. First the summation

$$Q_I = \sum_{n=0}^{\infty} \exp\left(-\frac{\lambda_{In}-\lambda_0}{\lambda_1-\lambda_0}\right)$$
$$= \exp\left(\frac{\lambda_0-\lambda_{I0}}{\lambda_1-\lambda_0}\right)$$
$$\times \sum_{n=0}^{\infty} \exp\left(-\frac{\lambda_{In}-\lambda_{I0}}{\lambda_{I1}-\lambda_{I0}}\left[\frac{\lambda_{I1}-\lambda_{I0}}{\lambda_1-\lambda_0}x\right]\right) \quad (25)$$

was evaluated, through the Euler-Maclaurin term in the fifth derivative of the exponential. This partition function is based on the same zero of energy as the correct partition function [Eq. (24)] and has the same independent variable, x (*not* $(E_{I1}-E_{I0})/kT$). It differs from the correct partition function in that it contains the W.K.B. first approximation characteristic numbers instead of the true λ_n's. Since the final expression for Q_I is rather complicated and is probably not of general interest, it will not be given here.

For large values of n, λ_{In} approaches λ_n asymptotically; even for moderate values of n, λ_{In}, and λ_n do not differ very much. The partition function Q_I leads, therefore, to nearly correct values of the thermodynamic functions when x is small. This residual error was removed by subtracting from Q_I a sufficient number of exponentials in λ_{In} and replacing them with corresponding exponentials in λ_n:

$$Q = Q_I - \sum_{n=0}^{\sim 6} \exp\left(-\frac{\lambda_{In}-\lambda_0}{\lambda_1-\lambda_0}x\right)$$
$$+ \sum_{n=0}^{\sim 6} \exp\left(-\frac{\lambda_n-\lambda_0}{\lambda_1-\lambda_0}x\right). \quad (26)$$

The values of the thermodynamic functions obtained in this manner agreed with those obtained by direct summation within 0.0001 at $x=0.5$. The values for smaller values of x should therefore be correct. Table III gives a summary of the four thermodynamic functions as functions of x.

It can be seen from the data given in Table III that the fourth power oscillator thermodynamic functions vary (qualitatively) with x in about the same way as do the corresponding functions of the harmonic oscillator. The most striking difference is that, as was pointed out by Bell,[1] the high temperature limiting value of the heat capacity function (C/R) and the heat content function $[(H-H_0)/RT]$ is 0.75 instead of unity.

Bell gave a short table of C/R. There is a considerable systematic error in his calculation, however. He found a maximum in C/R in the neighborhood of $x=1.0$. This maximum does not exist. Not enough details are given for us to determine the source of his error; it does not lie in the somewhat rough λ_n's that he used. A partition function summed over Bell's set of λ_n's yields a heat capacity function in good agreement with our work.

TRANSITION PROBABILITIES

After the characteristic numbers $\lambda_0=1.060361$, $\lambda_1=3.799673$, and $\lambda_3=11.64475$ were determined, the corresponding functions $w(\xi, \lambda)$ were inserted in Eq. (6). The indicated integration was performed up to each tabular value of ξ. In this way we obtained the unnormalized characteristic functions ψ_0, ψ_1, and ψ_3 at intervals of 0.1 in ξ. These functions were normalized and the transition integrals evaluated:

$$\int_{-\infty}^{\infty} \psi_0\psi_1\xi d\xi = 0.6008, \quad (27)$$

$$\int_{-\infty}^{\infty} \psi_0\psi_3\xi d\xi = 0.0325. \quad (28)$$

The third harmonic transition integral is only 5.4 percent of the fundamental integral. These values differ considerably from those given by Bell: 1.41 and 0.015, respectively.

THE JOURNAL OF CHEMICAL PHYSICS VOLUME 16, NUMBER 8 AUGUST, 1948

Photo-Chemical Studies. XL. The Mechanism of the Photo-Chemical Decomposition of Acetone[1]

W. ALBERT NOYES, JR. AND LEON M. DORFMAN
Department of Chemistry, University of Rochester, Rochester, New York

(Received April 16, 1948)

The data now available indicate quite strongly that the photo-chemical decomposition of acetone proceeds mainly if not entirely by a free radical mechanism. The various steps are reviewed and the evidence for them given. At high pressures where wall effects may be neglected certain definite conclusions are possible. In the region where some reactions are both homogeneous and heterogeneous the proof for all steps is not available and would be difficult to obtain. The analyses for some of the known products are not satisfactory for the small amounts formed. Nevertheless, it is believed that the steps proposed are adequately substantiated, and that the difficulties of obtaining further information are so great as probably not to warrant more effort along certain lines.

THE first quantitative experiments on the photo-chemical decomposition of acetone vapor seem to have been performed by Porter and Iddings,[2] but the first work studying the effects of many variables is due to Damon and Daniels.[3] Since this early work many articles have been published. The data are often in apparent conflict, and the present article is being written to present a consistent mechanism for the photo-chemical decomposition of acetone and to show that most of the undisputed facts are in accord with this mechanism. Certain points have not been proved beyond a reasonable doubt because of experimental difficulties, but strong support for their validity is found from many sources.

The present article does not contain a complete bibliography of the photo-chemical decomposition of acetone. Such a review article covering work through 1946 has been published recently by Davis,[4] and frequent reference will be made to it.

THE PRIMARY PROCESS (PRELIMINARY)

Three different primary dissociation processes for the photo-chemical decomposition of acetone vapor have been proposed:

$$CH_3COCH_3+h\nu=C_2H_6+CO, \quad (1)^{5-7}$$

$$CH_3COCH_3+h\nu=CH_3+COCH_3, \quad (2)^{7-9}$$

followed by

$$a\ COCH_3=a\ CO+a\ CH_3 \quad (3)^{8}$$

(where a is the fraction of the initially formed $COCH_3$ radicals which retain enough energy following (2) to dissociate immediately and $(1-a)$ is the fraction which attain thermal equilibrium with the surroundings and whose reactions follow a pattern dependent on temperature and other experimental conditions)

$$CH_3COCH_3+h\nu=2\ CH_3+CO. \quad (4)^{7}$$

In addition to the preceding reactions, another primary process must be included

$$CH_3COCH_3+h\nu=CH_3COCH_3'. \quad (5)$$

Reaction (5) is necessary because acetone exhibits a weak blue fluorescence[10] which possesses some discrete structure.[11]

Recent work[12] indicates that ethane is formed

[1] This work was supported by Contract N6onr-241, Task I, with the Office of Naval Research, United States Navy.

[2] C. W. Porter and C. Iddings, J. Am. Chem. Soc. **48**, 40 (1926).

[3] G. H. Damon and F. Daniels, J. Am. Chem. Soc. **55**, 2363 (1933).

[4] W. Davis, Jr., Chem. Rev. **40**, 201 (1947).

[5] R. Spence and W. Wild, J. Chem. Soc. 352 (1937); 590 (1941).

[6] M. H. Feldman, M. Burton, J. E. Ricci, and T. W. Davis, J. Chem. Phys. **13**, 440 (1945).

[7] F. W. Kirkbride and R. G. W. Norrish, Trans. Faraday Soc. **27**, 404 (1931).

[8] D. S. Herr and W. A. Noyes, Jr., J. Am. Chem. Soc. **62**, 2052 (1940).

[9] M. S. Matheson and W. A. Noyes, Jr., J. Am. Chem. Soc. **60**, 1857 (1938).

[10] See R. E. Hunt and W. A. Noyes, Jr., J. Am. Chem. Soc. **70**, 467 (1948) for a description of fluorescence and for a bibliography of the subject.

[11] G. W. Luckey, A. B. F. Duncan, and W. A. Noyes, Jr., J. Chem. Phys. **16**, 407 (1948).

[12] L. M. Dorfman and W. A. Noyes, Jr., J. Chem. Phys. **16**, 557 (1948).

mainly, if not solely, by reaction between methyl radicals. Under conditions of low light intensity and relatively high pressure the amount of CH_4 may exceed the amount of C_2H_6 very considerably. These facts do not exclude reaction (1) completely, but indicate that it is of minor importance compared to dissociation into radicals. It is unnecessary to assume that (1) occurs during the fluorescence act.[11] For these and other reasons to be given later reaction (1) is neglected in the following discussion.

It will be necessary to state very clearly the meaning of the primary quantum yield (ϕ). Every molecule which absorbs a quantum must undergo either one or the other of reactions (1), (2), (4), or (5). Reaction (4) would be difficult to distinguish from (2) followed by (3). This point will be discussed later. The following facts are pertinent: (a) At temperatures below 100°C biacetyl is known to be one of the products;[5] (b) at temperatures above 100°C very close to one molecule of carbon monoxide is formed per absorbed quantum;[8] (c) under otherwise comparable experimental conditions the yield of carbon monoxide at 25°C is greater at 2537A than it is at 3130A;[8] (d) at temperatures of 60°C and above, the photo-chemical decomposition of acetone at 2537A in the presence of iodine vapor indicates a primary yield very close to unity;[13] (e) at 80° and 90°C at 3130A in the presence of iodine vapor the yield of CH_3I is about 0.85 molecule per quantum.[14]

Fact (a) can best be explained by assuming some formation of CH_3CO in the primary process. Hence a part of the primary process at least must follow (2).

Fact (c) makes it necessary to assume that a is dependent on wave-length and facts (a), (b), and (c) make it necessary to assume that a and perhaps also ϕ are dependent on temperature. Temperature dependence for ϕ is also strongly indicated by the decrease in fluorescence efficiency with increase in temperature when 3130A is the exciting radiation.[10]

Fact (d) indicates that ϕ at 2537A is probably close to unity at all temperatures. No supporting fluorescence data are available at this wave-length. Fact (e) does not lead to positive conclusions, although it tends to support the statement that ϕ is less than unity at 3130A at 80°C. This is particularly true since some CH_3I would doubtless be formed from CH_3 radicals resulting from the dissociation of CH_3CO. The yield of CH_3COI was always considerably below the yield of CH_3I.

The fate of the excited molecules produced by (5) at 3130A (tentatively it can be assumed that none is formed at 2537A) is uncertain. They may do one of the following: (a) fluoresce; (b) be transferred to another electronic state by collision;[5,10] (c) be deactivated by collision; (d) "predissociate by collision." The absolute fluorescence efficiency is not known but is probably below 0.05 at moderate pressures.[3] Transfer to another electronic state, probably through the agency of collisions, is strongly indicated by the fluorescence data[10] and by the long lifetimes of the molecules responsible for fluorescence.[15] The validity of the latter point as applied to fluorescence in the gas phase has not been established since the data were obtained for solid acetone.

The distinction between (c) and (d) cannot be obtained from fluorescence data since either process leads to fluorescence quenching. It is at this point that the greatest ambiguity arises both in defining the primary quantum yield and in determining the magnitude of the primary yield.

It is concluded from the above discussion that process (1) occurs to such a minor extent as to be unimportant, that process (4) satisfactorily represents the facts at temperatures above 100°C, and that the following must be included in the reaction mechanism at temperatures below 100°C: (2), (3), (5). It is further necessary to conclude that a is dependent on wave-length.

It is now necessary to define the primary quantum yield in terms of Eqs. (2), (3), and (5), assuming that (5) may be followed in some instances by (2) and perhaps (3). It seems best to do this in terms of rate of formation of methyl radicals. As will be shown later, there are no reactions, either primary or secondary, other than (2), (3), and the thermal decomposition of CH_3CO radicals, which lead to the formation of CH_3 radicals. Similarly, reaction (3) and the

[13] S. W. Benson and G. S. Forbes, J. Am. Chem. Soc. 65, 1398 (1943); cf. reference 4.
[14] E. Gorin, J. Chem. Phys. 7, 256 (1939).
[15] W. E. Kaskan and A. B. F. Duncan, J. Chem. Phys. 16, 223 (1948).

thermal decomposition of CH_3CO radicals seem to be the only ones which lead to CO formation. This neglects reaction (4) at low temperatures (see below). It makes no difference whether there is a delay of a fraction of a second following absorption and before dissociation except that such a delay might make ϕ pressure dependent.

It is possible to write

$$CH_3COCH_3+h\nu=CH_3+COCH_3; \quad (+d(CH_3)/dt)_1=\phi I_a. \quad (6)$$

(Reaction (6) is taken to represent all molecules which dissociate immediately or eventually to give CH_3+COCH_3.)

$$COCH_3=CO+CH_3; \quad (+d(CH_3)/dt)_2=a\phi I_a=(+d(CO)/dt)_1, \quad (7)$$

$$COCH_3=CO+CH_3; \quad (+d(CH_3)/dt)_3=k_1(COCH_3)=(+d(CO)/dt)_2. \quad (8)$$

It could be considered that the fraction $a\phi$ of the absorbing molecules follows reaction (4), thus leading to the same rate equations. Equation (8) represents the thermal decomposition of $COCH_3$ radicals which have come to thermal equilibrium with the surroundings. It is evident that if $T<100°C$.

$$+d(CH_3)/dt\cdot(1/I_a)=\phi+a\phi+k_1(COCH_3)/I_a, \quad (9)$$

$$+d(CO)/dt\cdot(1/I_a)=a\phi+k_1(COCH_3)/I_a=\Phi_{CO}, \quad (10)$$

$$+d(CH_3)/dt\cdot(1/I_a)-\Phi_{CO}=\phi. \quad (11)$$

Under some conditions $+d(CH_3)/dt$ can be determined from the quantum yields of the products, thus permitting an evaluation of ϕ. The value so obtained is subject to considerable error because of the way in which the data must be treated. At low temperatures, however, the recombination of CH_3 and $COCH_3$ to form CH_3COCH_3 makes the determination of ϕ subject to even greater uncertainties. These matters will be treated further after consideration has been given to the secondary reactions.

SECONDARY REACTIONS

The secondary reactions during photo-chemical acetone decomposition may be obtained by a consideration of the reactions of CH_3 and $COCH_3$ radicals. There seem to be no secondary reactions involving CO at the temperatures used in most of the experimental work.

The following compounds are known to be produced during the reaction: CH_4, C_2H_6, CO, $(CH_3CO)_2(B)$,[5] $CH_3COCH_2CH_3(E)$.[16] The first three are the ones for which analyses are practicable in most of the work. An additional compound $(CH_2COCH_3)_2(D)$, is certainly formed whenever the CH_4 yield is high. It has been identified among the products of the thermal reaction of CH_3 radicals with acetone,[17] but it has never been possible to identify it positively in the small quantities in which it is produced during the photo-chemical reaction. One other compound is theoretically possible at low temperatures: $CH_3COCH_2COCH_3$. However, the amount of this compound should be small at room temperature, and it should not be formed at all at temperatures over 100°C where the $COCH_3$ radical is quite unstable. Still other products identified at high temperatures[16] need not be considered here.

Two points need special emphasis before starting a discussion of secondary reactions. Some of the reactions involve combinations of radicals and hence depend on the second power of radical concentrations at pressures such that diffusion to the walls is unimportant. If the various radical reactions are sufficiently rapid so that the radicals to a good approximation may be considered not to diffuse out of the light beam, quantitative conclusions are possible *provided* the shape of the light beam is known. However, the calculations prove to be extremely difficult if the beam is not parallel. Moreover, even with a parallel beam the number of quanta absorbed per unit volume per second will progressively decrease with increase in distance from the window through which the light is incident on the cell. While it is theoretically possible to derive an exact expression when I_a varies in this manner,[18] the labor is very great, and the results are not accurate unless the radical recombination

[16] A. O. Allen, J. Am. Chem. Soc. **63**, 708 (1941). Methyl ethyl ketone was identified by Allen at temperatures of 250–350°C. It should be formed whenever CH_4 is produced in appreciable quantities, but a quantitative analysis for it in the presence of a large amount of acetone is very difficult.

[17] F. O. Rice, E. L. Rodowskas, and W. R. Lewis, J. Am. Chem. Soc. **56**, 2497 (1934).

[18] Cf. W. A. Noyes, Jr., Cold Spring Harbor Symposium in Quant. Biol. **3**, 37 (1935).

reactions are very fast. In most of the work on acetone the percentage absorption is sufficiently low to permit use of a mean value of I_a in the light beam to a good first approximation.

These considerations make a quantitative treatment of much of the photo-chemical work on acetone impossible. It has been necessary to base most of the quantitative tests of the mechanism on data obtained with parallel or nearly parallel light beams with sufficiently accurate intensity measurements to permit a calculation of mean I_a. The latter is expressed in quanta absorbed per cm³ per second.

Only qualitative conclusions are possible in the intermediate pressure region (roughly 10 mm to 50 mm) where homogeneous reactions between radicals and diffusion of radicals to the walls are both important. At very low pressures data are scarce.

TABLE I. Quantum yields at 122°C.*

Run No.	9	4b	4a	11	12
$\Phi_{C_2H_6}$ (fnd.)	0.60	0.27	0.25	0.17	0.17
$\Phi_{C_2H_6}$ (calc.)	0.67	0.34	0.34	0.19	0.19
Φ_{CH_4} (fnd.)	0.41	1.06	1.21	1.11	1.32
Φ_{CO} (assumed)	1.0	1.0	1.0	1.0	1.0
I_a (quanta/sec./cm³ $\times 10^{-12}$)	2.86	0.203	0.201	0.0875	0.0743
P (mm)	117.4	107.2	107.4	123.2	115.1

* See reference 12.

Reactions (6)–(8) will be followed by

$$2\ COCH_3 = (COCH_3)_2 \quad ; k_2(COCH_3)^2 \tag{12}$$

$$2\ CH_3 = C_2H_6 \quad ; k_3(CH_3)^2 \tag{13}$$

$$CH_3 + COCH_3 = CH_3COCH_3 \quad ; k_4(CH_3)(COCH_3) \tag{14}$$

$$CH_3 + CH_3COCH_3 = CH_4 + CH_3COCH_2 \quad ; k_5(CH_3)(A) \tag{15}$$

$$2\ CH_2COCH_3 = (CH_2COCH_3)_2 \quad ; k_6(CH_2COCH_3)^2 \tag{16}$$

$$CH_3 + CH_2COCH_3 = CH_3COCH_2CH_3 \quad ; k_7(CH_3)(CH_2COCH_3) \tag{17}$$

$$CH_3CO + CH_2COCH_3 = CH_3COCH_2COCH_3 ; k_8(CH_3CO)(CH_2COCH_3). \tag{18}$$

(A) = concentration of acetone.

Certain relationships are now evident by imposing the conditions for material balance:

$$N_{CH_3} = 2\,N_{C_2H_6} + N_{CH_4} + N_E + N_A', \tag{19}$$

where N_{CH_3} = number of CH_3 radicals produced, $N_{C_2H_6}$ = number of ethane molecules formed, N_{CH_4} = number of methane molecules formed, N_E = number of molecules of methyl ethyl ketone formed, N_A' = number of molecules of acetone reformed.

$$2\,N_{CO} + 2\,N_B + N_{AA} = N_{CH_3} - N_A' = 2\,N_{C_2H_6} + N_{CH_4} + N_E, \tag{20}$$

where N_B = number of molecules of biacetyl produced, N_{AA} = number of molecules of acetyl acetone produced.

$$N_{CH_4} = N_E + 2\,N_D + N_{AA}, \tag{21}$$

where N_D = number of molecules of $(CH_2COCH_3)_2$ produced.

At low temperatures CH_4, C_2H_6, CO, $(CH_3CO)_2$, $CH_3COCH_2CH_3$, $(CH_2COCH_3)_2$, and $CH_3COCH_2COCH_3$ can all be formed, and in addition some of the radicals can recombine to form acetone. If the first three are determined experimentally, five unknowns remain with only three equations relating them. Indeed, in the absence of a knowledge of ϕ, N_{CH_3} must also be considered as an unknown. Consequently, a gas analysis for the easily determinable gases will not serve to permit even an indirect calculation of the yields of all of the products.

Certain experimental conditions may be chosen which do make a quantitative treatment of the system possible provided accurate values of N_{CH_4}, $N_{C_2H_6}$, and N_{CO} are available.

Condition 1

Light intensity sufficiently high to make N_{CH_4} negligible compared to $N_{C_2H_6}$: If $N_{CH_4} = 0$, $N_E = N_D = N_{AA} = 0$. Hence,

$$N_B = N_{C_2H_6} - N_{CO}, \tag{22}$$

$$N_{CH_3} = 2\,N_{C_2H_6} + N_A'. \tag{23}$$

Values of N_B calculated from Eq. (22) will not be very accurate unless $N_{C_2H_6}$ and N_{CO} are known with very high accuracy.

Condition 2

Temperatures over 100°C: Under these conditions the $COCH_3$ radical is sufficiently unstable to reduce the rate of formation of $(COCH_3)_2$ to a negligible value. Hence,

$$N_D = N_{C_2H_6} + N_{CH_4} - N_{CO}, \quad (24)$$

$$N_E = 2\,N_{CO} - 2\,N_{C_2H_6} - N_{CH_4}. \quad (25)$$

N_D and N_E calculated in this way will be subject to considerable error.

In the following discussion the quantum yield Φ_X of the species X is defined by the expression

$$d(X)/dt \cdot (1/I_a) = \Phi_X, \quad (26)$$

where $d(X)/dt$ is the local rate of formation (or disappearance) of X in the light beam, and I_a is the number of quanta absorbed per cubic centimeter per second in the light beam. It should be noted particularly that the differential is an absolute and not a net rate. Actually, this is not the experimentally determined quantum yield which is

$$N_X/V_L \int_0^t I_a dt = \Phi_X', \quad (27)$$

where N_X represents the total number of molecules of X formed (or disappeared) in the entire reaction system and V_L is the volume of the light beam. I_a in (27) is the mean number of quanta absorbed per cubic centimeter per second in the light beam. For a rigorous treatment $V_L \int_0^t I_a dt$ should be replaced by an integral $\int_0^t \int_0^{V_L} I_a dV dt$. This integral can only be obtained if I_a is known as a function of V.

One is justified in placing

$$d(X)/dt \cdot (1/I_a) = \Phi_X = N_X/V_L \int_0^t I_a dt \quad (28)$$

if the species X for which the quantum yield is being determined does not itself undergo further reaction. Thus if the compound $(CH_2COCH_3)_2$ reacts with CH_3 radicals (which it certainly would if its concentration became high) Eq. (27) could be used to calculate the net quantum yield of its formation. However, $(CH_2COCH_3)_2$ is a stable compound and will immediately begin to diffuse out of the light beam as soon as it is formed. Consequently, its concentration in the light beam cannot be calculated in any simple manner as would be possible for short-lived free radicals. This question is unimportant except when it would be desired to use steady-state equations for some of the products which might undergo further reaction. Thus biacetyl is known not to build up to a very high concentration,[19] probably because it reacts either with free radicals or with excited acetone molecules, and its rate of formation could be equated to its rate of disappearance after long exposures. However, this could only be done in deriving a rate equation if due account is taken of the fact that (barring thermal reactions) the formation and the disappearance occur mainly in the light beam.

For the reasons just given a quantitative treatment of the photo-chemical decomposition of acetone must be based on studies during which the percentage decomposition is very small, i.e., during the early stages of the reaction and long before the rates of disappearance of products become appreciable. The theoretical treatment of a situation in which the products are allowed to accumulate is almost impossible unless the light beam fills the entire vessel, and there is no dead volume such as a McLeod gauge. These restrictions reduce even further the data which can be considered for a quantitative test of the reaction mechanism.

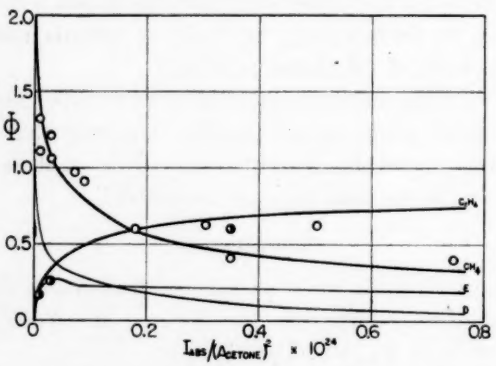

FIG. 1. The quantum yields of methane (○) and of ethane (◑) as a function of $I_a/(A)^2$. The curves are the theoretical ones from Eqs. (33) and (34). The theoretical yields for ethyl methyl ketone (E) and for biacetonyl (D) as obtained from calculated values of the yields of methane and of ethane by means of Eqs. (24) and (25) are also shown. Each of the two points for $\Phi_{C_2H_6}$ near the origin represents two results.

[19] G. M. Almy and S. Anderson, J. Chem. Phys. **8**, 805 (1940).

TEST OF THE MECHANISM AT TEMPERATURES OVER 100°C

It is wise to subject the proposed mechanism to as many tests of validity as possible. One of these has already been published[12] and may be stated as follows (by reference to Eqs. (13) and (15)):

$$\Phi_{C_2H_6}{}^{\frac{1}{2}}/\Phi_{CH_4}=(k_3I_a)^{\frac{1}{2}}/k_5(A), \qquad (29)$$

where (A) is the concentration (or pressure) of acetone. This equation has been found to be obeyed within experimental error both at 25°C and at 122°C, thus furnishing evidence that ethane and methane are formed by the reactions indicated.

Another relationship (from Eqs. (13), (16), and (17)) would be

$$\Phi_{C_2H_6}\Phi_D/\Phi_E{}^2=k_3k_6/k_7{}^2. \qquad (30)$$

Φ_D and $\Phi_E(T>100°C)$ in this equation may be obtained indirectly from Eqs. (20) and (21), since $N_B=N_{AA}=0$. Making the proper substitutions gives the following result:

$$\frac{\Phi_{C_2H_6}(\Phi_{C_2H_6}+\Phi_{CH_4}-\Phi_{CO})}{(2\Phi_{CO}-2\Phi_{C_2H_6}-\Phi_{CH_4})^2}=k_3k_6/k_7{}^2=\text{const.} \qquad (31)$$

Any errors in individual quantum yields will be badly magnified in ascertaining whether a true constant is obtained from Eq. (31). This equation is valid only at temperatures such that the yield of biacetyl is negligible, whereas Eq. (29) is valid at any temperature. Of course, Eq. (30) should be valid at any temperature, but the necessary yields for determining its validity are not available.

Only one series of runs[12] is available for testing Eq. (31). The constant varies from 0.5 to 1.6, but the nature of Eq. (31) is such that good constancy could scarcely be expected. Thus an error of 0.01 in determining the fraction of C_2H_6 in the reaction products will cause an error of at least 0.03 in $\Phi_{C_2H_6}$. With the small amounts of gas obtained at low intensities, duplicate runs frequently differ by as much as 0.03 in the fraction of C_2H_6 and other gases.

As will be shown in later paragraphs, there is another way of evaluating $k_3k_6/k_7{}^2$ from quantum yields of methane alone. Neither method can claim high accuracy, although the equations of the theory undoubtedly give the correct trend to the results. In order to show the difficulty of applying Eq. (31) and to show that, in general, it gives results within experimental error of the found values, some comparisons are made in Table I. The calculated values are based on $k_3k_6/k_7{}^2=2.0$ (see Table II).

TABLE II. The calculation of $k_3k_6/k_7{}^2$ at 122°C.

Run No. and ref.	Temp. °C	Press mm	(A) Molecules per cm³	I_a Quanta/cm³/sec.	Φ_{CH_4}	$k_3k_6/k_7{}^2$ (dimensionless)
$6A$[19]	126	194	4.69×10^{18}	16.4×10^{12}	0.40	1.2
9[12]	122	117	2.87	2.86	0.41	—
$7A$[19]	120	205	5.01	2.20	0.91	3.9
$8A$[19]	120	233	5.72	2.30	0.97	—
$9A$[19]	127	152	3.67	2.40	0.60	7.1
$10A$[19]	122	95	2.32	2.70	0.62	0.5
$11A$[19]	126.5	109	2.63	2.10	0.63	1.0
$4b$[12]	121.2	107	2.62	0.203	1.06	1.6
$4a$[12]	122	107	2.62	0.201	1.21	—
11[12]	123	123	3.00	0.0875	1.11	0.1
12[12]	123	115	2.81	0.0743	1.32	0.7
					Mean	2.0

In Table I $\Phi_{C_2H_6}$ is calculated by assuming Φ_{CH_4}, as taken from the smooth curve in Fig. 1, to be correct. Any more precise test of the mechanism would involve obtaining data of greater precision than has hitherto been possible.

A complete expression relating Φ_{CH_4} to intensity and acetone pressure is

$$0=K_a{}^2(4K_b-1)\left\{\frac{(\Phi_{CH_4}I_a/(A))^2}{I_a(2-\Phi_{CH_4})}\right\}^2+K_a\left\{\frac{1-\Phi_{CH_4}}{2-\Phi_{CH_4}}-4K_b\right\}\times\left\{\frac{(\Phi_{CH_4}I_a/(A))^2}{I_a(2-\Phi_{CH_4})}\right\}+K_b, \qquad (32)$$

where $K_a=k_3/k_5{}^2$, $K_b=k_3k_6/k_7{}^2$.

K_a at 122°C has been obtained[12] from a straight line plot of $\Phi_{CH_4}/\Phi_{C_2H_6}{}^{\frac{1}{2}}$ *vs.* $(A)/I_a{}^{\frac{1}{2}}$ and has the value 9.8×10^{24} molecules sec. cm^{-3}. It is now possible to solve for K_b from quantum yields of CH_4 under various experimental conditions. Some of the data were reported previously,[12] and some have been obtained by Davis.[19a]

Table II shows the results of the calculations. Runs 9 and $8A$ gave negative values, and Run $4a$ gave an extremely high value.

[19a] W. Davis, Jr., J. Am. Chem. Soc. **70**, 1867 (1948).

It should be noted that the data in Table II cover a more than 200-fold change in intensity. In view of the sensitivity of K_b to values of Φ_{CH_4} and I_a, the constancy of K_b is as good as can be expected. As can be seen from Fig. 1, probably the values of K_a and K_b may not be the best ones for fitting the data, but the accuracy is such as not to warrant a more extended treatment. The use of $(1-\Phi_{CH_4})$ and of $\Phi_{CH_4}^4$ amplifies errors considerably.

Since K_a and K_b have been determined, it is now possible to calculate Φ_{CH_4} as a function of $I_a/(A)^2$. If I_a is expressed in quanta per cm^3 per second and (A) is in molecules per cm^3, the resulting equation for $T=122$°C is

$$672.3\Phi_{CH_4}^4x^2+68.6\Phi_{CH_4}^3x+\Phi_{CH_4}^2(2-147x)-8\Phi_{CH_4}+8=0, \quad (33)$$

where $x=(I_a/(A)^2)\times10^{24}$. Figure 1 shows the experimental points and the theoretical curve taken from Eq. (33). It is evident that the equation gives the correct trend to the results and reproduces them within experimental error.

It is also possible to establish an equation for $\Phi_{C_2H_6}$ in terms of $(A)/I_a^{\frac{1}{2}}$

$$7\Phi_{C_2H_6}^2+2.24\Phi_{C_2H_6}^{\frac{1}{2}}y+\Phi_{C_2H_6}(0.204y^2-15)-\Phi_{C_2H_6}^{\frac{1}{2}}2.56y+8=0, \quad (34)$$

where $y=((A)/I_a^{\frac{1}{2}})\times10^{-12}$. Figure 1 shows the theoretical curve and the experimental points for $\Phi_{C_2H_6}$ as a function of $I_a/(A)^2$. The experimental points are not very numerous in this instance.

Thus the mechanism embodied in Eqs. (6)–(8) and (12)–(18) accounts for the yields of CO, CH_4, and C_2H_6 within experimental error. It should be noted particularly, however, that data must be carefully obtained or the resulting equations cannot be employed. Thus I_a expressed in quanta absorbed per cubic centimeter per second is critical, and a diverging or converging light beam will make exact calculations impossible.

A few words may be said concerning the primary process at temperatures over 100°C. All authors agree that Φ_{CO} under these conditions is approximately 1 and varies little if at all with temperature.[20] This could be explained in one of the following ways: (a) Reaction (4) with one molecule of CO and two CH_3 radicals being formed per quantum absorbed; (b) reactions (6) and (7) with ϕ and a both unity; (c) reactions (6)–(8) with $\phi=1$, $a<1$, and k_1 sufficiently large to make the decomposition of the $COCH_3$ radical very rapid compared to other reactions it might undergo. No definite way of deciding between these possibilities is available. However, the data of Gorin[14] show quite definitely that some $COCH_3$ radicals are produced in the primary process at temperatures of 80–90°C. The energy of activation for reaction (8) is not known precisely but has been estimated at from 10 to 18 kcal.[4] Thus (8) will have a very high temperature coefficient and would be expected to be very rapid at temperatures over 100°C. This could mean merely that the $COCH_3$ radicals formed by (6) would be less apt to lose energy at high temperatures than at low. The data are in agreement with possibility (b) above, but (c) cannot be excluded.

The equivalent of reaction (15) may occur in mixtures of acetone and other organic molecules. Thus Leermakers[20] has shown that considerable quantities of CH_4 are produced in mixtures of acetone and dimethyl ether. This fact adds further support to the mechanism.

A word about the low pressure case with diffusion of radicals to the walls as the predominating process may be said. The unknown here is the possible reaction of methyl radicals with acetone adsorbed on the walls. The meager data on this point[20] tend to the belief that at 403°C the amount of ethane produced even at a pressure of 12.6 mm is negligible but that the C_2H_6/CH_4 ratio increases with decreasing temperature. At 122°C it seems probable that a large fraction of the CH_3 radicals which diffuse to the walls forms C_2H_6 rather than CH_4, but more data are needed on this point.

TEST OF THE MECHANISM AT TEMPERATURES NEAR 25°C

Reference to Eqs. (19)–(21) shows that there are too many unknowns to be calculated from analyses for CO, C_2H_6, and CH_4. However, it is possible to choose experimental conditions such that $\Phi_{CH_4}\ll\Phi_{C_2H_6}$. When methane is formed, it has been shown that the same type of mechanism

[20] See reference 4 for a summary. References 19 and 8 have data on this point, but the data of J. A. Leermakers, J. Am. Chem. Soc. 56, 1900 (1934) are most significant since they cover the temperature range 163–405°C.

holds for CH_4 and for C_2H_6 formation at 25°C as at 122°C.[12] Thus reactions (15) and (13) seem to be correct at both temperatures. Indeed the data are more extensive at 25°C and prove the validity of these two equations particularly well at that temperature.

From Eqs. (12) and (22) it is seen that

$$\Phi_B = k_2(COCH_3)^2/I_a = \Phi_{C_2H_6} - \Phi_{CO}, \quad (35)$$

when Φ_{CH_4} is negligible. Similarly, from Eqs. (7) and (8)

$$\Phi_{CO} = k_1(COCH_3)/I_a + a\phi. \quad (36)$$

Hence,

$$(\Phi_{CO} - a\phi)/(\Phi_{C_2H_6} - \Phi_{CO})^{\frac{1}{2}} = k_1 I_a^{\frac{1}{2}}/k_2^{\frac{1}{2}}. \quad (37)$$

It should be noted that k_1 and k_2 should be independent of wave-length, whereas a probably depends on wave-length since the residual energy left in the $COCH_3$ radical will depend on the energy taken up by the absorbing molecules.

The following data are taken from earlier work:[8]

	$\Phi_{C_2H_6}$	Φ_{CO}	I_a
3130A	0.19	0.11	10
2537	0.36	0.28	10

($P = 100$ mm, $T = 25$°C, I_a is in arbitrary units, where 1 unit is approximately 2×10^{12} quanta per cm³ per second.)

Substituting the appropriate values in Eq. (37) and equating for the two different wave-lengths gives

$$0.17 = (a\phi)_{2537} - (a\phi)_{3130}. \quad (38)$$

Of course it is impossible to get individual values by this method. The previous value[8] for the difference in Eq. (38) obtained by making certain assumptions with regard to the constants was 0.15.

An examination of the proposed mechanism shows that there are only two reactions which lead to the disappearance of acetone molecules: (6) and (15). There is also one reaction which leads to reformation of acetone molecules: (14). With these facts in mind it is seen that

$$\frac{k_4^2(CH_3)^2(COCH_3)^2}{k_2(COCH_3)^2 k_3(CH_3)^2} = \frac{k_4^2}{k_2 k_3} = \frac{(\phi + \Phi_{CH_4} - \Phi_A)^2}{\Phi_{C_2H_6}\Phi_B}, \quad (39)$$

where Φ_A is the quantum yield of acetone disappearance. Φ_A cannot be measured directly, and it can be calculated only when $\Phi_{CH_4} = 0$, i.e., when the intensity is high and preferably when the pressure is low. Under such conditions

$$\Phi_A = 2\,\Phi_{C_2H_6} - \Phi_{CO}. \quad (40)$$

Taking the data preceding Eq. (38) and making the proper substitutions in Eq. (39), one finds either

$$\pm 1.377(\phi_{3130} - 0.27) = \phi_{2537} - 0.44. \quad (41)$$

If the minus sign is chosen, $\phi_{2537} = 0.13$ if $\phi_{3130} = 0.5$. Since the quantum yields of acetone disappearance are sometimes greater than 0.5 at both 3130 and 2537A,[8] the values of ϕ_{3130} and ϕ_{2537} must both be greater than 0.5. The positive sign is the only one which leads to a physically acceptable result. Hence,

$$\phi_{2537} = 1.377\phi_{3130} + 0.068. \quad (42)$$

If $\phi_{2537} = 1$, $\phi_{3130} = 0.68$. The accuracy of this figure is difficult to estimate, but it should be within ± 0.15 and indicates that the primary quantum yield at 3130A is significantly less than 1. This is in general agreement with the existence of fluorescence. However, ϕ_{3130} must be temperature dependent, as indicated by the fluorescence and photo-chemical data,[10] and reach a value close to unity at 100°C.

Another approximation may be made to arrive at a value of ϕ. In earlier work[8] it was assumed that at relatively low pressures reactions (12) and (13) occurred mainly on the walls, a conclusion supported by the work of Anderson and Rollefson,[21,22] whereas the reformation of acetone was a rapid reaction which occurred mainly in the gas phase. The following data are taken from previous work[8] at 25°C and a

[21] H. W. Anderson and G. K. Rollefson, J. Am. Chem. Soc. **63**, 816 (1941).

[22] E. W. R. Steacie and B. de B. Darwent, J. Chem. Phys. **16**, 230 (1948) have shown that the character of the wall surface does not affect the C_2H_6/CO ratio. This would not have been expected if wall recombinations of free radicals occur. On the other hand, for rapid reactions, such as $CH_3CO + CH_3CO$ with a very low activation energy the character of the walls may not be too important. The data in the region where wall reactions may be important do not lead to very definite conclusions. On the other hand, it is impossible to explain the increase in C_2H_6/CO ratio at low pressures without heterogeneous formation of biacetyl.

TABLE III. Summary of various constants.*

Constant	$T=0°C$	$T=25°C$	$T=120°C$
ϕ_{3130}	0.5	0.7 (100 mm) 0.8 (25 mm)	1.0
ϕ_{2537}	1.0	1.0	1.0
a_{3130}		0.07	
a_{2537}		0.22	
k_3/k_5^2		1.37×10^{27}	9.8×10^{24}
k_2k_6/k_4^2			2.0
$k_1/k_2^{\frac{1}{2}}$		4.8×10^{-8}	
k_4^2/k_2k_3		1.1	

* The energy of activation for reaction (5) is 6500 cal. (see reference 12).

pressure of 25 mm:

	$\Phi_{C_2H_6}$	Φ_{CO}	I_a
3130A	0.24	0.098	10
2537	0.36	0.235	10

$$\frac{k_4(CH_3)(COCH_3)}{k_2'(COCH_3)k_3'(CH_3)}=\frac{\phi-2\Phi_{C_2H_6}+\Phi_{CO}}{\Phi_{C_2H_6}(\Phi_{C_2H_6}-\Phi_{CO})}, \quad (43)$$

where k_2' and k_3' are the constants for wall combination to form $(COCH_3)_2$ and $(CH_3)_2$, respectively. Placing $\phi_{2537}=1$, ϕ_{3130} is found to be 0.78, a reasonably good check with the value found from Eq. (42). Perhaps ϕ should increase with decrease in pressure (see below).

Returning to Eq. (39) and assuming $\phi_{2537}=1$ (which is a very reasonable assumption from all standpoints), it is seen that

$$k_4^2/k_2k_3=1.1. \quad (44)$$

The constants in Eq. (44) are all constants for association reactions of radicals and would be expected to have small temperature coefficients. If it is assumed tentatively that $k_4^2/k_2k_3=1.1$ at 0°C, one can make use of data from earlier work[8] at a pressure of 110 mm to calculate ϕ_{3130} at that temperature. The following quantum yields were used: $\Phi_{C_2H_6}=0.19$, $\Phi_{CO}=0.045$. From Eq. (39) one finds $\phi_{3130}=0.51$ at 0°C. This is a further indication that ϕ is temperature dependent.

A possible explanation of the temperature dependence of ϕ may be offered. At 2537, where $\phi=1$, direct dissociation of the acetone molecule may be assumed to occur upon absorption of radiation. At 3130 the following steps may be visualized:

$$A+h\nu=A' \quad ; \text{ rate}=I_a, \quad (45)$$

$$A'=CH_3+COCH_3; \text{ rate}=k_9(A'), \quad (46)$$

$$A'+A=2A \quad ; \text{ rate}=k_{10}(A')(A'). \quad (47)$$

A' might undergo other processes, such as fluorescence, but these need not be considered here. This leads to the definition of ϕ as follows:

$$\phi=1/(1+k_{10}(A)/k_9). \quad (48)$$

ϕ would thus be pressure dependent. Since fluorescence would be a competing process for (46), it cannot be stated that ϕ should become unity at zero pressure, but the trend toward increased values at lower pressures seems to be definite. Data on this point are inadequate. If k_{10} is assumed to have zero activation energy, an activation energy for k_9 is estimated to be about 5000 cal. Thus ϕ would be very close to unity at temperatures above 100°C, as required by the data.

Little can be said about a. From Eq. (36) and the data preceding Eq. (38) one can show that

$$a_{3130}=(a_{2537}-0.17)/0.68. \quad (49)$$

Thus if a_{2537} is given the value previously calculated[8] of 0.22, $a_{3130}=0.073$ at 25°C. The dependence of a on temperature cannot be estimated from present data.

As pointed out recently by Steacie and Darwent,[22] the C_2H_6/CO ratio at 25°C obtained by various authors increased with increase in I_a. This is in accord with the mechanism proposed in the present article. If the values of ϕ and a at 3130A are accepted as 0.70 and 0.073, respectively, the maximum value of C_2H_6/CO at infinite intensity would be 5.2. At 2537 with $\phi=1.0$ and $a=0.22$, C_2H_6/CO would have a maximum value of 2.8. To account for the ratio of 3.6 observed by Anderson and Rollefson,[21] a would have to be 0.18 if $\phi_{2537}=1$. If the mercury sensitized reaction follows the same pattern, a_{2537} would have to be 0.14 to account for the results of Steacie and Darwent. However, there is sound reason to believe that a for the sensitized reaction should be somewhat lower than for the unsensitized reaction. In view of the type of arc used, Anderson and Rollefson[21] probably were also dealing at least partially with a mercury sensitized reaction. When an excited mercury atom collides with a CH_3COCH_3 molecule to form CH_3+CH_3CO, the laws of conservation of energy and conservation of momentum must be obeyed. Thus part of the energy will be imparted

to the mercury atom as kinetic energy, and the kinetic energy of the CH_3CO radical, as well as possibly its vibrational energy, may be appreciably lower than that of a radical produced by absorption of 2537A radiation directly by an acetone molecule. In the absence of further information we may accept $\phi_{2537}=1$, $a_{2537}=0.22\pm0.05$ at 25°C.

In conclusion, it is well to give a summary of the various constants concerning the mechanism which have been evaluated.

The mechanism proposed in this article accounts for the following points:

(a) The variation of the C_2H_6/CO ratio with pressure, with intensity, with temperature, and with wave-length;
(b) the increase in the CH_4/C_2H_6 ratio with decreasing intensity and increasing pressure;
(c) variation of quantum yields of C_2H_6, CO, and CH_4 with temperature and pressure;
(d) the effect of wave-length on the CO yield;
(e) the formation of all known products;
(f) qualitatively for fluorescence and its variation with temperature. This point and its relationship to primary quantum yield merit further study.

It is believed that the mechanism does not disagree with any experimental facts so far available. In particular it agrees qualitatively with Fig. 2 of the second article by Spence and Wild,[5] who were the first to point out that the C_2H_6/CO ratio really falls on a family of curves, one for each pressure as a function of intensity.

The mechanism makes no pretense of describing acetone decomposition except in the early stages before products have been allowed to accumulate. With large percentage decomposition there must be secondary reactions which would change the composition of the gaseous products. Also the effect of the walls has not been included in detail. Such effects are almost certainly not of importance except at pressures below 50 mm and in any case could not be included easily in any quantitative theory. Many of the effects previously ascribed to the walls are undoubtedly due to variations in intensity and in pressure. The importance of obtaining data in such a fashion that the number of quanta absorbed per unit volume per second is as constant as possible is obvious from the nature of the mechanism.

The authors wish to express their appreciation to Dr. W. Davis, Jr., who first derived Eq. (32).

THE JOURNAL OF CHEMICAL PHYSICS VOLUME 16, NUMBER 8 AUGUST, 1948

The Vapor Pressure and Heat of Sublimation of Graphite*

LEO BREWER, PAUL W. GILLES,** AND FRANCIS A. JENKINS
*Department of Chemistry, Radiation Laboratory,*** *and Department of Physics, University of California, Berkeley*

(Received April 19, 1948)

The heat of sublimation of graphite and the heats of dissociation of CO and C_2, which have been the subject of much controversy in recent years, have been unambiguously established by the direct determination of the total vapor pressure of graphite by an equilibrium effusion method and by the determination of the partial pressure of C_2(gas) in equilibrium with graphite.

The heat of sublimation of graphite to C(g) is found to be $\Delta H_0=170.39\pm0.20$ kilocalories per mole at 0°K. The heat of sublimation of graphite to C_2(g) is found to be $\Delta H_0=233.1\pm7$ kilocalories per mole. The heats of dissociation of C_2 and CO have been shown to be 4.7 ± 0.3 and 11.109 ± 0.01 electron volts, respectively. The accommodation coefficient of carbon gas on graphite at high temperatures is found to be about 0.3 and vaporized carbon gas is shown to be in the ^3P ground electronic state.

* Abstracted in part from the thesis submitted by Paul W. Gilles in partial satisfaction of the requirements for the degree of Doctor of Philosophy in Chemistry at the University of California. Presented before the Inorganic and Physical Division of the American Chemical Society at the 113th National Meeting at Chicago, April 19, 1948.

** du Pont Fellow in Chemistry, 1946–1947; present address: Chemistry Department, The University of Kansas, Lawrence, Kansas.

*** This document is based in part on work performed under Contract No. W-7405-eng-48 for the Atomic Energy Commission.

INTRODUCTION

THE vapor pressure of graphite and the heat for the reaction

$$C(\text{graphite}) = C(g), \quad (1)$$

have been the subject of considerable controversy for a great many years.[1] The sum of the reactions

$$CO(g) = C(g) + O(g), \quad (2)$$

$$C(s) + \tfrac{1}{2}O_2(g) = CO(g), \quad (3)$$

$$O(g) = \tfrac{1}{2}O_2(g), \quad (4)$$

yields reaction (1) and the sum of the heats of these reactions must be the heat of reaction (1). Herzberg[2] showed in 1937 that a consideration of various predissociations in carbon monoxide leads to several definite values, one of which must be the heat of dissociation of this molecule. It was not possible for him to make an unequivocal choice from these values. Since the heats of reactions (3) and (4) are accurately known, each possible value for the heat of dissociation of CO leads to a possible value for the heat of sublimation of graphite. The purpose of this work has been to obtain data that make possible the correct choice of the value for the heat of sublimation of graphite, and incidentally thereby, the proper choice for the CO dissociation energy.

Previous values for the heat of sublimation calculated from vapor pressure data obtained from rates of vaporization of graphite filaments and rings have been criticized on the grounds that sublimation may have taken place to an excited gaseous state, that the accommodation coefficient may have been very low, and that the relative gaseous concentrations of C(gas) and C_2(gas) were unknown.[1] The value obtained in the present work is not subject to these same objections since the vapor pressure measurements were obtained by an equilibrium method, that of the effusion of a gas through a small knife-edged orifice. As is indicated by the constancy of the vapor pressure values with variation of hole size, the vapor pressure determined by this method is not dependent on the accommodation coefficient. This method also insures that the gas will be in its equilibrium state. Also the independent measurement of the C_2(gas) partial pressure has eliminated any uncertainties due to C_2. The determination of this last quantity along with the heat of formation of C_2(gas) will be discussed first.

[1] F. R. Bichowsky and F. D. Rossini, *Thermochemistry of Chemical Substances* (Reinhold Publishing Corporation, New York, New York, 1936), p. 230, gives early references; L. H. Long and R. G. W. Norrish, Nature **158**, 238 (1946) gives later ones.

[2] G. Herzberg, Chem. Rev. **20**, 145 (1937).

THE HEAT OF FORMATION OF C_2(GAS)

The process of the formation of gaseous diatomic carbon from the solid can be studied independently of the formation of monatomic carbon vapor, by spectroscopic observations of the intensities of the molecular bands of C_2.

If one measures the intensity of a single spectral line, he has a quantity that is proportional to the total rate of decay of the excited state of the molecule and therefore to the concentration or pressure of the molecules in this excited state. If he measures the temperature coefficient of this intensity, he has a measure of how rapidly the pressure of the excited species is varying with temperature, a quantity that is related to the heat of formation of the excited gaseous state. The heat of formation of the equilibrium gaseous state of C_2 can be calculated from the heat of formation of the excited state and can be used with values of the free energy function, $(\Delta F - \Delta E_0)/T$, for the reaction,

$$2C(\text{graphite}) = C_2(\text{equilibrium gas}), \quad (5)$$

to calculate the pressure of C_2(gas) in equilibrium with graphite.

Experimental

For the production of the C_2 vapor, a special high temperature graphite tube resistance furnace, shown in Fig. 1, was constructed somewhat similar to one made by King.[3] The innermost part of the furnace was a hollow graphite tube of either National Carbon C-18 graphite or National Regular Spectroscopic Electrode Material, AGKS-ANJ-889.

The tube was supported at each end by a split graphite bushing, bored so that the tube fitted snugly. The outside of the bushing was tapered

[3] A. S. King, Trans. Am. Electrochem. Soc. **56**, 97 (1929).

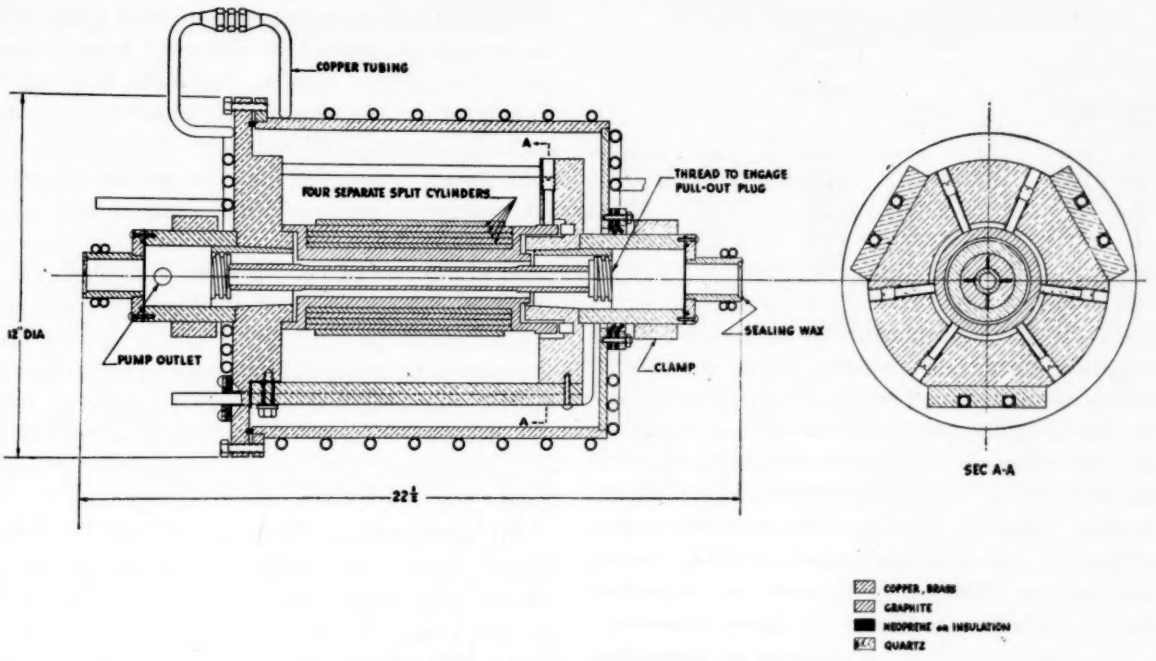

FIG. 1. High temperature carbon tube furnace.

so that when it was forced into the tapered copper end-plate it tightened on the tube, giving good electrical contact. This shape and position of the bushing permitted longitudinal thermal expansion and contraction of the graphite tube without destroying the electrical contact. The other parts of the furnace were for insulation, cooling, and sealing purposes. The furnace was designed and constructed in such a way that the tube could be heated in a vacuum or in a gaseous atmosphere at any pressure less than one atmosphere. The outstanding feature of the design of this furnace is the ease with which a burnt-out tube can be replaced. By removing the window holders and inserting a threaded piece of aluminum into the square threads on the bushings, one can remove a spent tube in a very few minutes.

The tube is heated by low voltage alternating current led in by the massive copper clamps. Furnace currents of about 700 to 800 amp. were obtained from a 90 amp., 220-volt, 60-cycle source through a step-down transformer.

Because of the heat losses through the graphite bushings to the copper parts at the ends, a tube with straight outer walls showed a short hot zone in the center and a large temperature gradient out toward the ends. To equalize the temperature along the length of the tube and to make it thus suitable for equilibrium measurements, the outer diameter of the tube was decreased in certain places to such a degree that the temperature was nearly constant over a long region and then fell off quite rapidly through cylindrical graphite diaphragms inserted into the tube near its ends. The tendency for a loss of carbon vapor by diffusion out the ends was counteracted by adjusting the diameter of the tube so that the temperature just inside the diaphragm was about 30° to 50° higher than in center of the tube. The diaphragms, in addition to defining the hot zone, also helped to decrease the diffusion loss because of their small, $\frac{1}{4}$-inch opening. The temperature used in the calculations was that of the long center zone. This procedure was shown experimentally to be correct in several early runs in which the temperature differences between ends and center increased during the course of the experiment. The C_2 spectral intensities taken with the large temperature differences agreed with those taken with small differences if central temperatures were used.

Argon was added to the furnace as an inert gas in order to decrease diffusion of carbon out

TABLE I. Experimental intensity data and their Σ-treatment.

Exposure	Temp. (°K)	I	4.576 log$I$	$\frac{-2600\,\Delta C_p}{T}$	$\frac{-2.303}{(\Delta C_p - R)\log T}$	Σ
4	2683	2.4	1.739	7.559	77.267	−86.565
3	2733	5.9	3.528	7.420	77.448	−88.396
5	2793	18.2	5.766	7.261	77.660	−90.686
2	2828	31.0	6.823	7.171	77.782	−91.775
6	2858	51.9	7.843	7.096	77.885	−92.828
1	2918	72.1	8.502	6.950	78.089	−93.541
7	2963	289.	11.262	6.844	78.238	−96.343

the ends of the tube and in order thereby to lengthen the life of the tube. Argon was chosen rather than helium because its large molecular weight helped prevent loss of carbon vapor by thermal diffusion. Despite the presence of gas in the furnace, at high temperatures rapid volatilization occurred, leading ultimately to arcing within the tube and subsequent breaking. Arcing was always detectable as soon as it started because of a drop in current of about 50 percent.

An experiment was performed to show that the argon which was added only decreased the diffusion out of the tube and did not alter the equilibrium pressure of diatomic carbon vapor inside the tube. Two spectrograms were taken at the same temperature of 2850°K, one with an argon pressure of 48.5 cm and the other with a pressure of 9.1 cm. The intensities were the same in the two exposures to within the limit of measurement of the tracings, which was about one percent. This experiment also showed that the effect of pressure broadening of lines was negligible. Self-absorption of emitted light by the vapor was considered and found to be negligible in these experiments. For example, if the number of dispersion electrons per molecule, or the f value, is taken as unity for C_2, the maximum error caused by self-absorption can be calculated to be 10^{-6} percent. The f value would not be expected to be appreciably greater than unity and is probably less than 0.1.

After the tube had been prepared to give the desired temperature distribution, the furnace was heated for a few minutes in a vacuum to above 2500°C to rid the tube of gaseous impurities. Then argon was added to the desired pressure. The current through the furnace was increased until the desired temperature was reached, following which ten to fifteen minutes was allowed for the furnace to reach equilibrium. After temperature measurements had been made with an optical pyrometer at different points along the tube, a five minute exposure was taken. Temperature measurements were made after each exposure as well as before. The current was then raised or lowered and the process repeated for another exposure. Since temperature equilibrium existed within the furnace no discrete lines would be observed if light from the wall of the furnace was allowed to enter the spectrograph. A thin piece of metal with a $\frac{1}{16}$-inch hole was placed between the furnace and spectrograph and it diaphragmed out any light from solid material in the furnace. Since the work was done in a darkened room, only light from the gas inside the tube entered the spectrograph.

All spectrograms were taken with a small Hilger glass constant-deviation spectrograph of 50-cm focal length and a dispersion of from 20 to 200A/mm Eastman Number 33, Panchromatic, and 103a-F plates were used. Developing was done with Eastman M-Q developer for one to two minutes. The plates were calibrated by means of a tungsten bulb running at constant current from storage batteries and screens calibrated for transmission. The screens were placed some distance in front of the slit of the spectrograph and were rocked in an apparatus in an

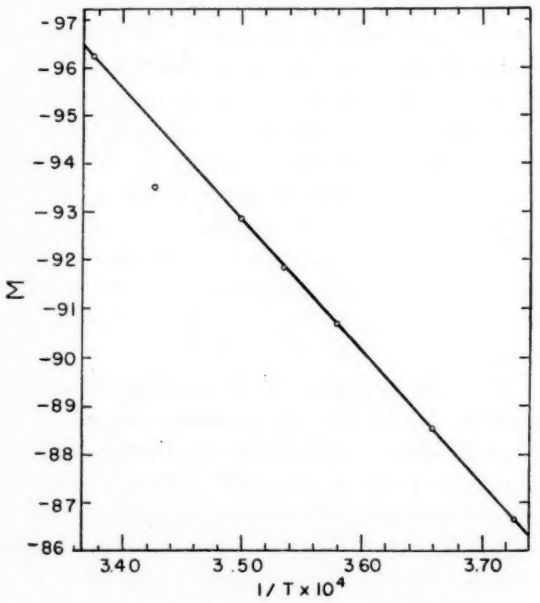

FIG. 2. Σ *vs.* $1/T$ plot for the reaction 2C(graphite) $= C_2(^3\Pi_g$ excited state).

TABLE II. Pressure of C_2(g) above graphite.

T°K	$\left(\frac{F-E_0}{T}\right)$ graphite	$\left(\frac{F-E_0}{T}\right)C_2$	$\left(\frac{\Delta F-\Delta E_0}{T}\right)_{2gr=C_2}$	$\frac{\Delta E_0}{T}$	$\frac{\Delta F}{T}$	log$P$	P(atmos.)
2000	−5.38	−56.331	−45.57	116.5	71.0	−15.5	3×10^{-16}
3000	−7.38	−59.666	−44.91	77.7	32.8	−7.16	7×10^{-8}
4000	−8.92	−62.102	−44.26	58.3	14.0	−3.06	9×10^{-4}
5000	−10.20	−64.032	−43.63	46.6	2.98	−0.65	2.2×10^{-1}

elliptical motion so that an average transmission was obtained. Photographic densities were measured with a Zeiss recording microphotometer.

Calculations and Results

In the experiments, the resolving power of the apparatus was insufficient, and the intensity was too low to allow the measurement of an individual band line in the spectrum. In this work the peak intensity of the 0−0 head of the C_2 Swan bands at λ5165 was used. The furnace spectra were examined to see if lines arising from impurities lying close to the head could contribute to the intensity and thereby cause an error. None was found.

The uncertainties arising when one uses the head of the band are due to the possibility of inclusion of a different number of lines in the head at different temperatures of the furnace, to the change of the line of maximum intensity with temperature, and to the uncertainty as to what state one takes as his "average" upper state in the calculation of the excitation energy.

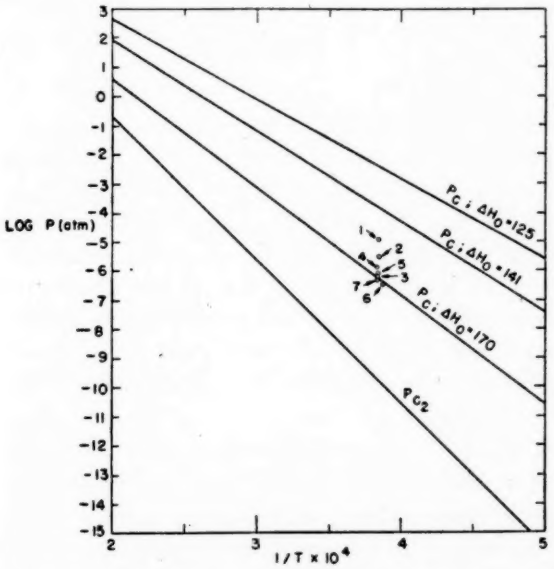

FIG. 3. Vapor pressure of graphite. The circles give the experimental vapor pressure from effusion measurements. The lowest curve gives the pressure of C_2(g) in equilibrium with graphite. The upper three curves give what the pressure of C(g) would be if the heat of sublimation were 125.03, 141.25, or 170.39 kcal./mole. The last is indicated as the correct one.

The microphotometer tracings of the heads of the C_2 bands indicated that the number of lines included in the heads did not change with the temperature. A calculation of the line of maximum intensity at the extreme temperatures indicated that it changed by only one rotational quantum number. None of the above effects was considered to cause an appreciable error.

In the 0−0 band the head occurs at a J' value of about 13. At 3000°K the line of maximum intensity is $J'=24$. Within 1.5A of the head are found lines corresponding to $J'=5$ through $J'=21$ which are the only lines to contribute appreciably to the peak intensity as determined by measuring the contour of individual atomic lines. The rotational energies in the excited state corresponding to the rotational quantum numbers of 5 and 21 are 52.5 and 808 cm^{-1}, respectively, or 0.15 and 2.13 kcals./mole. If one then considers that the head originates from a single "average" state he must assign to this state a rotational energy between these limits. A value of 1.2±0.5 kcal. was chosen as the additional excitation energy due to rotation of the molecule in the upper state.

The partial pressure of C_2 gas can be related to the intensity of emission, I, since I is proportional to the concentration of C_2 gas which is in turn proportional to p/T from the perfect gas law. For the reaction,

$$2C(\text{graphite}) = C_2(\text{excited gas state}), \quad (6)$$

by setting

$$\Delta H_T = \Delta H_{2600°K} + \Delta C_p(T-2600), \quad (7)$$

and integrating the van't Hoff isochore, one

obtains

$$-4.576\log p = -4.576\log kTI = (\Delta H_{2600°K})/T - 2600\Delta C_p/T - 2.303\Delta C_p \log T + M, \quad (8)$$

where p is the pressure exerted by the molecules of C_2 in the excited state, k is a proportionality constant, I is the intensity of the band head, and M is a constant. A plot of Σ, defined by the relation

$$\Sigma = -4.576\log I + 2600\Delta C_p/T + 2.303(\Delta C_p - R)\log T = (\Delta H_{2600°K})/T + M + 4.576\log k, \quad (9)$$

against $1/T$ must be a straight line of slope $\Delta H_{2600°K}$ and intercept $M+4.576\log k$. The experimental data and the details of the calculation of Σ are given in Table I.

The ΔC_p used in the calculations was taken as -7.8 e.u. This figure was obtained by taking the difference between $5R/2=4.97$, the heat capacity at constant pressure of the single "average" gaseous state we are considering, and 12.8, which is twice the heat capacity of solid graphite, as determined by extrapolating to the temperatures of the experiments the data of Worthing[4] covering a temperature range from 1200°K to 2100°K. Although such an extrapolation may give an uncertain value, the terms involving ΔC_p do not change rapidly with temperature and do so in opposite directions, so that together they amount to only a slight correction to the intensity term.

Figure 2 gives a plot of Σ against $1/T$. The point falling out of line is the first point that was taken and it deviates from the others because the temperature changed greatly during the exposure. The line on the graph is the one obtained from a least squares reduction of Σ and $1/T$ values, giving zero weight to the first exposure. The slope of this line, 277.8 kcal./mole, is the heat at 2600°K for reaction (6). The probable error, taking equal weighting for all points except the discarded point, is calculated to be ± 1.4 kilocals.

The heat at 2600°K for the reaction

$$2C(\text{graphite}) = C_2(\text{ground gas state}) \quad (10)$$

may be obtained from the above heat by subtracting from it the energy of excitation of the excited gas state. As discussed previously, the rotational energy is 1.2 ± 0.5 kcal./mole, the vibrational contribution is zero, and the electronic excitation of C_2 is 19,377 cm^{-1} or 55.4 kcal./mole. Thus we obtain for reaction (10),

$$\Delta H_{2600°K} = 277.8 - 1.2 - 55.4 = 221.2 \text{ kcal./mole.} \quad (11)$$

To obtain the heat of the last reaction at absolute zero, one must use the heat capacities to get the change of the heat with temperature. As pointed out, the heat capacity of a gas in a single quantum state is that of a monatomic gas, $5R/2$, and its heat content change with temperature is simply $5R\Delta T/2$. For solid carbon, Wagman, Kilpatrick, Taylor, Pitzer, and Rossini[5] give 5.814 kcal./mole as the difference of heat content between 1500° and 0°K. An integration of Worthing's heat capacity curve together with its extrapolation gave 6.597 kcal./mole as the difference in heat content of graphite at 2600°K, and 1500°K. From these two values one finds that 12.411 kcal./mole is the difference in heat content of graphite at 2600°K and 0°K. Therefore, for reaction (10)

$$\Delta H_{0°K} = \Delta H_{2600°K} - 5(2600)R/2 + 2(12.411) = 233.1 \text{ kcal./mole.} \quad (12)$$

A consideration of the magnitude of the possible errors in the temperature measurements indicated that if the temperature were incorrect in one direction at one end of the temperature range and in the other direction at the other end, the heat could be in error by about 15 kcal./mole. Since such a situation is not at all likely, the error in the heat attributable to the temperature is probably not over five kcal./mole. The uncertainties produced by the intensity measurements were about of the same order of magnitude as by the temperature measurements. Although the probable error is only ± 1.4 kilocals, the absolute uncertainty is thus set at ± 7.0 kilocals.

Since at 0°K the equilibrium gaseous state of C_2 is the ground state we have for reaction (5),

$$\Delta E_{0°K} \cong \Delta H_{0°K} = 233.1 \pm 7.0 \text{ kcal./mole.} \quad (13)$$

[4] A. G. Worthing, Phys. Rev. **12**, 199 (1918).

[5] Wagman, Kilpatrick, Taylor, Pitzer, and Rossini, J. Research Nat. Bur. Stand. **34**, 143 (1945).

TABLE III. Experimental vapor pressure and heat of sublimation of graphite.

Run No.	$T°K$	Time (hrs)	Hole area (cm^2)	Wt. carbon collected (mg)	P (atmos.)	$\log P$	$\frac{\Delta F}{T}$	$\frac{\Delta E_0}{T}$	ΔE_0
1	2603	3.50	0.0884	1.971	1.153×10^{-5}	−4.938	22.60	54.49	154.85
2	2603	1.60	0.0884	0.234	3.00×10^{-6}	−5.523	25.27	62.16	161.80
3	2613	3.83	0.0884	0.132	7.08×10^{-7}	−6.150	28.14	65.03	169.92
4	2608	3.67	0.0884	0.216	1.21×10^{-6}	−5.917	27.08	63.97	166.83
5	2598	4.62	0.0319	0.073	8.97×10^{-7}	−6.047	27.67	64.56	167.73
6	2583	3.28	0.0322	0.021	3.59×10^{-7}	−6.445	29.49	66.38	171.46
7	2603	3.50	0.0325	0.033	5.25×10^{-7}	−6.280	28.74	65.63	170.83

The vapor pressure of graphite as C_2 is calculated in Table II from this value of the heat and values of the free energy function, $(\Delta F-\Delta E_{0°K})/T$ for reaction (5). The values given by Kelley[6] and Gordon[7] for the free energy functions of graphite and C_2(gas), respectively, have been used in Table II. The pressure of C_2 in equilibrium with graphite at different temperatures given in the last column in Table II is plotted as the lowest curve in Fig. 3.

The same general spectroscopic procedures that were used in the determination of the heat of formation of C_2(gas) can also be employed in the study of other substances such as CH, CN, and CS. The heat of formation of CH is related to the heat of sublimation of graphite through a series of reactions similar to reactions (1), (2), (3), and (4), including the heats of dissociation of CH and H_2. Since Herzberg[8] gives values for these last two quantities, a determination of the heat of formation of CH would lead to a value for the heat of sublimation of graphite. Preliminary experiments were performed to accomplish this determination but in the presence of hydrogen the graphite tubes disintegrated so rapidly, presumably because of the formation of the relatively stable acetylene, that no reliable results were obtained.

THE VAPOR PRESSURE OF GRAPHITE AND HEAT OF FORMATION OF C(Gas)

Of the several values that Herzberg[2] gave as possible heats of dissociation of CO, all but three are admittedly much too low. These three are 256.18, 227.04, and 210.82 kcal./mole on the basis of the latest constants advocated by the National Bureau of Standards.[9] The heats for reactions (3) and (4) are given as −27.202 and −58.586 kcal./mole[10], respectively, and by combining these with the possible heats of dissociation of CO one sees that one of the following three values must be the heat of sublimation of graphite: 170.39, 141.25, or 125.03 kcal./mole. By using these values with values of the free energy functions for solid graphite and gaseous monatomic carbon from Kelley[6] and Gordon,[7] one can calculate what the vapor pressure would be at any temperature corresponding to each of these three heats. The results of this calculation are presented in graphical form in Fig. 3. It is apparent that at low pressures the pressure of C_2(gas) is negligible in comparison with the pressure of C(gas) irrespective of which of the possible heats of sublimation is correct.

Marshall and Norton[11] carried out experiments on the rate of loss of weight of graphite rings heated inductively and reported that the heat of sublimation of graphite is 177 kcal./mole. Later Marshall and Johnston[12] measured the weight loss from graphite cylinders and claimed that the results indicated a very low accommodation coefficient for graphite. Since if the accommodation coefficient is very low, any vapor pressure measurement based on rates of vaporization will be too low, leading to a heat of sublimation too large; others[1] have used the argument of low accommodation coefficient to question the results of work leading to the highest value for the heat.

[6] K. K. Kelley, U. S. Bur. Mines Bull. 383, 32 (1935).
[7] A. R. Gordon, J. Chem. Phys. **5**, 350 (1937).
[8] G. Herzberg, *Molecular Spectra and Molecular Structure* (Prentice-Hall, Inc., New York, New York, 1939).
[9] American Petroleum Institute Research Project 44 at the National Bureau of Standards. Selected values of hydrocarbons. Table β (part 9) conversion factors—units of molecular energy, March 31, 1945.
[10] See reference 9, Table O*w*, August 31, 1946 and Table 00*w*, June 30, 1946.
[11] A. L. Marshall and F. J. Norton, J. Am. Chem. Soc. **55**, 431 (1933).
[12] Private Communication from H. L. Johnston; see G. Herzberg, J. Chem. Phys. **10**, 306 (1942).

An equilibrium method of measuring vapor pressures and one not dependent on the measurement of rate of vaporization is one in which the material to be studied is heated in an inert vessel completely closed except for a small hole in the top. Inside the vessel equilibrium exists and the quantity of substance effusing through the hole can be calculated from the kinetic gas theory if the pressure is known. Conversely, if the quantity transported is measured, the pressure of that species inside the crucible can be calculated.

Experimental

The inert effusion vessel used was equivalent to a tantalum carbide cylinder with a small hole through the upper surface. It consisted of a graphite crucible which fitted snugly inside a tantalum crucible which had been carburized on the inner surfaces. The tantalum crucible acted as the heating element in the high frequency induction furnace. The holes through the covers of the graphite and tantalum crucibles were coaxial, of the same size, and tapered in such a manner that they acted together as a single thin-edged hole. The graphite crucible was filled with Acheson graphite powder, grade No. 38, to one quarter to one half of its height. The graphite crucible was of National Carbon C-18 material and had an internal diameter of about $\frac{1}{2}$ inch and a height of about 1.2 inches with $\frac{1}{16}$-inch walls. Two different sized holes, one about $\frac{1}{16}$ inch and one about $\frac{1}{8}$ inch, were used.

A series of thin molybdenum and tantalum spirals or cylinders surrounding the crucibles and a series of disks of the same metals supported on $\frac{1}{16}$-inch metal pins served to decrease heat loss outward and downward from the crucibles. Heat flow out the top was decreased by having above the crucibles a series of tantalum disks each of which had a hole in the center. The size of the hole increased regularly with the distance of the disk from the top of the crucible so that an unobstructed cone was available for the escape of the carbon vapor. Above these shields was a thin platinum collector plate suspended in a water-cooled copper holder. The geometry was such that 5.09 percent of the vapor leaving the hole was collected.

The crucibles and all the molybdenum and tantalum shielding were contained in a zircon crucible about 5.5 inch tall, 2.25 inch diameter at the bottom and about 2.5 inch diameter at the top. The zircon crucible rested on a zircon stand inside a Pyrex tube that was water cooled on the outside. The Pyrex tube was connected with a ground glass joint to the vacuum system consisting of a mechanical pump and two oil diffusion pumps in series. At the beginning of an experiment the pressure in the system was about 1 to 2×10^{-5} mm and during the heating rose to about 2 to 3×10^{-4} mm as read on a Knudsen gauge.

Energy was supplied to the crucible from a closely wound water-cooled coil of copper tubing which surrounded the jacket carrying water to cool the Pyrex tube. The coil was in series with a 20-kw spark gap converter delivering about 100 amp. at a frequency of about 16,000 cycles/sec. and with several other coils which were part of a controlling device for maintaining constant temperature in the crucible. The temperature inside the crucible was read with a calibrated optical pyrometer focused through a hole in the collector plate and on the hole in the top of the crucibles. Because of the relatively high emissivity of graphite and the small ratio of hole area to total inside area, no deviation from blackbody conditions was assumed. The temperature measurements were corrected for reflection and absorption by the windows of the vacuum system.

Before a series of runs the apparatus was heated to outgas as much as possible the metallic parts and the graphite. The first four runs were made with an effusion hole about $\frac{1}{8}$ in. in diameter. In the last three runs the hole was about $\frac{1}{16}$ in. diameter. Although the first run was intended to be an outgassing one, enough data were taken to obtain a measurement. Before the first run with the smaller hole the apparatus was heated for about 1.3 hours at a temperature about 50 degrees higher than that for the succeeding runs.

The procedure was to heat fairly rapidly to the temperature of the experiment, to adjust the controlling devices and to allow vaporization to occur for several hours. The carbon was burned off the platinum plate in a micro-combustion apparatus and was determined by the weight of CO_2 which was collected. The authors are very

grateful to Mr. Charles Koch who carried out all these micro-determinations of carbon. A spectroscopic analysis of the deposit indicated that the main impurity, silicon, was less than 0.1 percent.

Results

The data are given in Table III. The accuracy of the weights given in column 5 is indicated by the results of a blank burned to test the sensitivity of the analysis which was estimated to be ± 0.004 mg. The blank registered 0.005 mg. The pressures in column 6 were calculated from the fraction of the total material transported that was collected and from the effusion equation,

$$p = z(MT)^{\frac{1}{2}}/44.383a \cdot t, \qquad (14)$$

where p is the pressure in atmospheres of the species of molecular weight M, z is the number of moles effusing out of the crucible in time t through a hole of area a. The values of $\Delta F/T$ in column 8 have been calculated from this pressure. The value of $(\Delta F - \Delta E_{0°K})/T$ for reaction (1) is the same for each of these temperatures and is -36.89 as calculated from the values of Kelley[6] and Gordon.[7] Column 9 gives values of $\Delta E_{0°K}/T$ obtained by substracting -36.89 from the values in column 8. The last column contains the value of $\Delta E_{0°K}$ calculated from each experiment. The data are also presented as the circles in Fig. 3.

Both the table and graph indicate that the apparent vapor pressure decreases with the time of heating at high temperature. This phenomenon is probably caused by volatilization of tars remaining in the material from the binder used in the graphitization process. These tars are organic substances which if deposited on the collector plate, would register as carbon in the burning analysis. With long heating at high temperatures the tars gradually vaporize and consecutive measurements of vapor pressure show a decrease toward the true equilibrium vapor pressure of graphite. It is worth while to note that whereas this difficulty will appear in any effusion or vaporization method, because one has no way of knowing precisely the gaseous species he is observing, he may proceed with much more certainty in the tube furnace and spectroscopic experiments because there he is absolutely certain of the molecules he is observing and he knows even in which particular energy states they are.

TABLE IV. Sublimation points of graphite in degrees Kelvin.

Pressure(atmos.)	10^{-10}	10^{-8}	10^{-6}	10^{-4}	10^{-2}
C(g)	2060	2320	2650	3090	3705
C_2(g)	2562	2855	3227	3715	

The purpose of changing the hole size in the effusion measurements was to check the magnitude of the accommodation coefficient. If the latter were very small then, irrespective of the size of the hole, all the material vaporizing should finally escape and the observed vapor pressure would be a function of the hole size. The last three runs with the smaller hole should have given apparent vapor pressures higher than the first four experiments in case the accomodation coefficient were very low. This is not the case and therefore these data indicate a relatively high accommodation coefficient.

Vapor pressures obtained by the effusion method will be correct if the accommodation coefficient is large compared to the ratio of hole area to total area inside the crucible. The agreement between the experiments with the different size holes indicates that this condition was met. The ratio of hole area to total area was 4.03×10^{-3} in the first runs and 1.46×10^{-3} in the last runs. The accommodation coefficient therefore must be greater than 4×10^{-3}, and the vapor pressures obtained are the true equilibrium vapor pressures.

In view of the facts that the vapor pressure measurements were of the equilibrium type and that the measured heat of sublimation is very nearly one of the values obtained from a consideration of the CO dissociation data, there seems to be no good reason to suppose that carbon gas left the crucible in the ^5S state as proposed by Schmid and Gero.[13] Shenstone[14] has recently found the ^5S state to be 33735.2 cm^{-1} above the ground state ^3P. The observation of emission from this state eliminates the possibility of its being a strongly metastable state. The fair agreement of the rates of vaporization work with this research indicates that carbon

[13] R. Schmid and L. Gero, Zeits. f. Physik **99**, 281 (1936).
[14] A. G. Shenstone, Phys. Rev. **72**, 411 (1947).

evaporates from the solid as monatomic gas in the ground electronic state.

The data obtained in the present work indicate that the heat of sublimation of graphite is about 170 kcal./mole and it is expected that the value of 170.39±0.20 kcal./mole obtained from the CO spectroscopic data is more nearly correct than any other experimental value.

Calculations based upon values of $(\Delta F - \Delta E_{0°K})/T$ calculated from data of Kelley[6] and Gordon[7] and upon the heats of formation of gaseous C and C_2 indicate that at 4640°K one atmosphere of C(g) would be in equilibrium with solid graphite; at 5390°K the pressure of C_2(g) above solid graphite would be one atmosphere; and that at 4630°K the combined pressure of C(g) and C_2(g) would be one atmosphere in equilibrium with solid graphite. These temperatures are not necessarily realizable sublimation points because the melting point of graphite may be lower. There is no reliable determination of the melting point, but if it does lie lower than the temperatures given, then the true boiling points of liquid carbon will be higher. Table IV gives the temperatures in degrees Kelvin at which the indicated species reach the indicated partial pressures in equilibrium with graphite. These temperatures have been calculated in the same manner as that used for the above sublimation points. The ratio of the partial pressure of C_2(g) to the partial pressure of C(g) in equilibrium with graphite increases regularly with increasing temperature and is given approximately by the following values: $10^{-4.94}$ at 2000°K, $10^{-3.65}$ at 2500°K, $10^{-2.81}$ at 3000°K, $10^{-2.22}$ at 3500°K, $10^{-1.79}$ at 4000°K, and $10^{-1.47}$ at 4500°K.

Correlation With Other Work

As noted above, Johnston[12] has reported that preliminary measurements have indicated that the accommodation coefficient of carbon gas on graphite might be very low. We are not familiar with all the details of this work, but Simpson[15] has recently performed experiments of a similar type and has concluded that they indicate that the accommodation coefficient is very close to unity. Comparison of our equilibrium vapor pressure data with the data of Marshall and Norton[11] obtained by measurement of the rate of evaporation of graphite indicates that the accommodation coefficient is not less than 0.3. Experimental uncertainties do not allow us to fix it any closer to unity. Therefore, one may summarize by stating that the accommodation coefficient of carbon gas on graphite at high temperatures is close to unity and can be given a rough value of about 0.3.

The only other recent experiments on the vapor pressure of graphite are those of Basset[16] and of Ribaud and Begue.[17] Their results have been interpreted by others[1] as supporting a much higher vapor pressure than the present work indicates. The work by Basset was performed on graphite rods of fair purity which he heated to high temperatures in high pressures of argon. His outgassing procedure was performed at a lower temperature than the experiments and probably, therefore, was not sufficient to dispose of the residual tars. His temperature readings, furthermore, were taken with an optical pyrometer which could conceivably give temperature indications far too low because of smoke or particles in the argon. Ribaud and Begue tried to obtain the temperature of sublimation of graphite at several pressures of argon by observing the maximum temperatures of a graphite crucible packed in lampblack, when they increased the high frequency power supplied inductively to the crucible. Such an experiment need not necessarily give a true sublimation point because if insufficient power were available, it would give only the temperature at which the rate of heat loss from the crucible by conduction, convection, radiation, and evaporation is equal to the power input. In addition, their experiments are subject to the same criticism as are those of Basset.

These possible errors are in such a direction that if they exist the observed temperatures would be too low, or the observed vapor pressures would be too high. It is in this direction that the work of these others differs from the results of the present work.

[15] O. C. Simpson and R. J. Thorn, private communication of work to be published soon.

[16] J. Basset, Brennstoff-Chemie **23**, 127 (1942).

[17] G. Ribaud and J. Begue, Comptes Rendus **221**, 73 (1945).

THE HEATS OF DISSOCIATION OF C_2 AND CO

The values for the heats of formation of C(g) and C_2(g) are related to the heat of dissociation of C_2 through the equations

$$2C(\text{graphite}) = C_2(g), \quad (5)$$

$$C_2(g) = 2C(g), \quad (15)$$

$$2C(\text{graphite}) = 2C(g). \quad (1)$$

Here, the sum of the first two equations yields the last, and the sum of the heats for the first two must be the heat of the last. That is, the sum of the heat of dissociation of C_2 and the heat of formation of C_2(g) must be twice the heat of formation of C(g). The heat of dissociation of C_2 is not known but Herzberg[18] has pointed out that vibrational levels in the ground state have been observed as high as $v=11$. This vibrational level has an energy above the C_2 ground state of about 16,441 cm^{-1} or about 47.00 kcal./mole. The heat of dissociation of the C_2 molecule must be greater than this energy. By adding to the 47.00 kcal./mole the heat of formation of C_2(g), 233.1 kcal., one obtains 280.1 kcal. as the lower limit for twice the heat of formation of C(g). This value eliminates 125.03 as the heat of formation of C(g) and makes 141.25 very improbable since at $v=11$ the vibrational spacing is still large and it does not seem reasonable that the spacing would go to zero after this vibrational level. This evidence indicates, in conformity with the vapor pressure measurements, that the heat of formation of C(g) is 170.39 kcal./mole.

This discussion is based on the assumption that C_2 in the $^3\Pi$-ground state dissociates to atoms in the normal state. This seems like a safe assumption since very few cases are known in which the ground state of a molecule does not dissociate to normal atoms. Furthermore, since the correlation rules between atomic and molecular states do not permit a $^3\Pi$-state to dissociate into any S state, the ground state of C_2 cannot be dissociating into carbon atoms in the ^5S state.

By taking this heat of formation of C(g) and the heat of formation of C_2(g) one can calculate the heat of dissociation of C_2 to be $340.78-233.1=107.7$ kcal./mole or 4.7 volts. Three recent estimates of this value have been made. A Birge-Sponer[19] linear extrapolation of the vibrational energy level spacings based upon only a few levels gives about 6.8 volts as the heat of dissociation. Herzberg[18] claimed that this value is about 3.6 volts. Gaydon[20] has stated that it would not be difficult to make a graphical extrapolation to about five volts. The present results indicate that the Birge-Sponer extrapolation gives too large a value, probably because only a few vibrational levels can be used, and that Gaydon's estimate is nearly correct.

Having the heat of formation of C(gas), one may use the thermochemical cycle represented in Eqs. (1), (2), (3), and (4) to choose the correct value for the heat of dissociation of CO. This procedure gives 11.109 ev as the energy of dissociation of CO corresponding to a heat of sublimation of carbon of about 170 kcal./mole.

The Birge-Sponer extrapolation of the vibrational levels of the ground state for this molecule gives 11.2 ev for D_{CO}. This extrapolation is based upon a large number of levels and gives very close agreement with the experimental value determined in this work. Gaydon[20] very recently has discussed at some length the problem of the energy of dissociation of CO. He has discussed the Birge-Sponer extrapolations, the predissociations in CO, the rule of non-crossing of potential energy curves, the photo-dissociation of CO, electron impact experiments, the dissociation energy of CO^+, the dissociation energies of CN and C_2N_2, and theoretical considerations of the bond energies of some organic molecules. He concludes that none of these data is definitely contradictory to a heat of dissociation of 11.11 ev for CO, and that several of them strongly indicate this value to be correct. Thus his conclusions are in agreement with the results of the present work. The present experiments show also that Gaydon is probably correct in his contention that the Birge-Sponer method of extrapolating the vibrational energy level spacings can be quite useful in helping one fix the dissociation energies of many diatomic molecules.

[18] G. Herzberg, Phys. Rev. **70**, 762 (1946). N. L. Singh, Ind. J. Phys. **19**, 167 (1945) would reduce the highest observed level in the Swan system to $v=9$, which reduces lower limit of heat of sublimation slightly.

[19] R. T. Birge and H. Sponer, Phys. Rev. **28**, 259 (1926).

[20] A. G. Gaydon, *Dissociation Energies* (Chapman and Hall, Ltd., London, 1947).

The Vibrational Spectrum and Thermodynamic Functions of Acrylonitrile

FREDERICK HALVERSON, ROBERT F. STAMM, AND JOHN J. WHALEN
Stamford Research Laboratories, American Cyanamid Company, Stamford, Connecticut

(Received April 21, 1948)

The infra-red spectra of gaseous and liquid acrylonitrile have been studied from 2.5μ to 25μ with a spectrometer using LiF, CaF_2, NaCl, and KBr prisms. The Raman spectrum of the liquid has been obtained, including intensity and polarization data. A normal coordinate calculation of the non-planar frequencies has been made, using force constants from related molecules. This information permits a complete assignment of the fifteen fundamental frequencies and a calculation of the thermodynamic quantities for the molecule.

I. INTRODUCTION

THE acrylonitrile (or vinyl cyanide) molecule has the structural formula

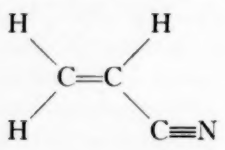

and may be treated as a substituted ethylene. Its vibrational spectrum is of considerable interest since the molecule is small enough to allow a complete assignment of normal vibration frequencies, and yet is large enough to exhibit several interesting features of more complicated molecules. Furthermore, assignment of the fundamental frequencies permits the calculation of thermodynamic functions which should be of extensive use for such a chemically important molecule.

Previous Raman[1,2] and infra-red[3] measurements have been reported for acrylonitrile, but our data are sufficiently different in some cases as to require another choice of normal frequencies.

II. OBSERVED SPECTRUM

The acrylonitrile used for obtaining these spectra had been prepared by the dehydration of hydracrylonitrile, and was purified by vacuum distillation just prior to using. Its index of refraction was $n_D^{22.5}=1.3902\pm0.0002$ and its density was $d_{24}=0.8024\pm0.0003$ g/cc.[4]

[1] B. Timm and R. Mecke, Zeits. f. Physik **97**, 221 (1935).
[2] A. W. Reitz and R. Skrabal, Monats. f. Chem. **70**, 398 (1937).
[3] H. W. Thompson and P. Torkington, J. Chem. Soc. **1944**, 597.
[4] Literature values are $n_D^{22.5}=1.3898\pm0.0002$ and $d_{24}=0.8017$ g/cc given by H. S. Davis and O. F. Wiedeman, Ind. Eng. Chem. **37**, 482 (1945).

Infra-Red Absorption

(*a*) *Vapor Phase.* The infra-red spectrum shown in Fig. 1 was obtained using a Perkin-Elmer spectrometer Model 12A with LiF, CaF_2, NaCl, and KBr prisms. For the region 4000 to 2000 cm^{-1} a multiple reflection cell with a variable path length of 1, 2, 3, or 4 meters was used, the spectrum in Fig. 1 being that for a 2 meter path. Measurements were made at 27°C with an acrylonitrile partial pressure of about 110 mm of Hg. For the region 2000 to 400 cm^{-1} the small housing of the spectrometer was filled with acrylonitrile vapor at pressures ranging from 110 mm to about 5 mm of Hg, the path length being 40 cm. No absorption bands were observed from 400 to 600 cm^{-1} even at a pressure of 110 mm. The spectrum in Fig. 1 is for a partial pressure of 110 mm, with lower pressure inserts for the bands at 954 and 972 cm^{-1}.

The observed bands are listed in Table I, together with a type designation. Bands are termed type *A*, *B*, or *C* depending on whether the *Q* branch is observed to be weak, absent, or strong, relative to the *P*- and *R*-branches. In some cases overlapping bands (atmospheric water vapor and carbon dioxide) do not permit a sharp distinction, and so the apparent band type is listed as a question mark. In cases where a *Q* branch is not observed, the band center is taken as the average of the *P*- and *R*-branch values.

The *P*-branch (3115 cm^{-1}) of the band at 3125 cm^{-1} has some asymmetry relative to the *R*-branch, as though some additional absorption were present other than the single band. A shoulder appears at 2984 cm^{-1} on the *P*-branch of the strong band at 3042 cm^{-1} when the path

length is 3 meters, but there is not sufficient structure to determine the band type. It is assumed that the 2984 cm^{-1} absorption represents a *P*-branch, and so a band center is estimated at about 2994 cm^{-1}. The *P* branch of the atmospheric CO_2 band at 2350 cm^{-1} is overlapped by a weak acrylonitrile band with peaks at 2278 cm^{-1} and 2295 cm^{-1}. Whether it is an *A* or *B* type band is not apparent. The absorption at 1085 cm^{-1} has the appearance of a weak type *C* band, superimposed on a type *A* band at 1096 cm^{-1}.

The absorption bands at 954 cm^{-1} and 972 cm^{-1} are very intense so that even a few millimeters pressure with a 40 cm path length causes 50 percent absorption. Part of the fine structure associated with these bands was resolved as shown in Fig. 1, with the frequency values given in Table II. The fine structure frequency values for the analogous band at 683 cm^{-1} are given in Table III. Measurements down to 655 cm^{-1} were made with a NaCl prism; below that point a KBr prism was used which did not resolve the fine structure. Although the frequencies in Tables II and III are given to a tenth wave number, the absolute values are good to only ± 2 cm^{-1} and the relative values to only ± 0.2 cm^{-1}.

(*b*) *Liquid Phase.* The spectrum shown in Fig. 2 was obtained using the same spectrometer as for the vapor and using a 0.1 mm cell at room temperature. Other measurements were made in the region 800–900 cm^{-1} with the cell cooled to about $-30°C$, but no appreciable changes in intensities of the bands resulted. No discrete absorption bands were found in the region 400–600 cm^{-1}. Band centers are listed in Table I.

RAMAN EFFECT

A number of Raman spectra were obtained using a grating spectrograph and other accessories which have been described previously.[5]

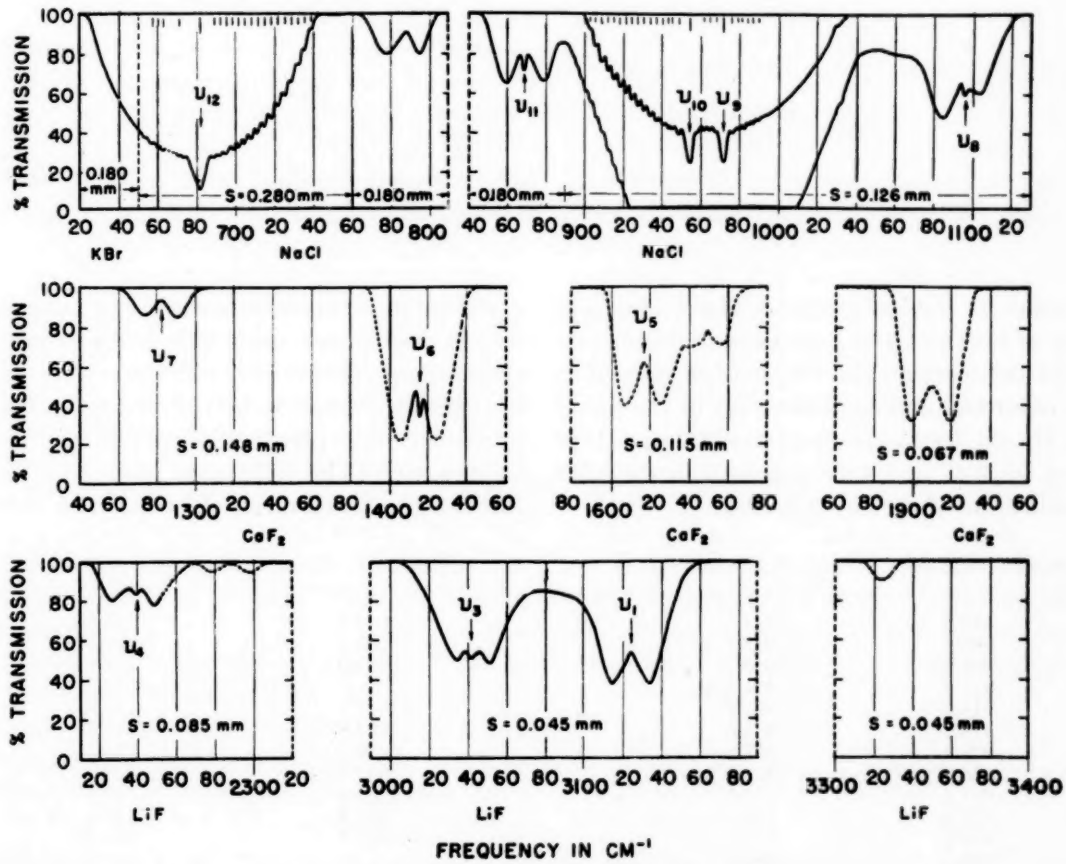

FIG. 1. Infra-red spectrum of acrylonitrile vapor.

[5] R. F. Stamm, Ind. Eng. Chem. Anal. Ed. **17**, 318 (1945).

TABLE I. Observed infra-red absorption by acrylonitrile.

Vapor			Liquid		Vapor			Liquid		Vapor			Liquid	
683	*Q*	*C*	690	*S*	1607	*P*				2889	*P*			
							B	1609	*M*			*B*	2885	*W*
777	*P*				1625	*R*				2911	*R*			
		B	804	*W*										
794	*R*													
					1641	?				2984	*P*			
							?	1648	*W*			?	2990	*M*
860	*P*				1658	?				—				
869	*Q*	*A*	871	*M*										
879	*R*													
					1899	*P*								
							B	1940	*S*	3035	*P*			
					1919	*R*				3042	*Q*	*A*	3033	*S*
										3052	*R*			
954	*Q*	*C*	960											
			↕	*VS*										
972	*Q*	*C*	980											
								2174	*VW*					
													3068	*S*
1033	?		1035	*W*										
					2226	*P*							3091	*W*
					2239	*Q*	*A*	2228	*M*					
1085	*Q, P*	*C*			2247	*R*								
1096	*Q*	*A*	1094	*M*										
1104	*R*									3115	*P*			
												B	3125	*M*
										3134	*R*			
1273	*P*				2278	*P*								
		B	1288				?	2280	*W*				3210	*W*
1291	*R*				2295	*R*								
										3330	?	?	3323	*W*
			1325?	*VW*				2465	*VW*					
			1376?	*VW*				2580	*VW*				3557	*M*
								2697	*W*					
1406	*P*													
1416	*Q*	*A*	1415	*S*										
1424	*R*							2795	*VW*				~3650	*M*

Excitation by the indigo triplet (4358, etc.) and the use of Eastman 103-J plates proved sufficient to yield the fundamental frequencies (as well as a few overtones and combinations) in the liquid state. On the long exposures, $\Delta\nu\nu$3032 and 2228 excited by 4047 and 4078 appeared in the 4358 region in spite of the $NaNO_2$ filter.

Polarization measurements were made both by the double and single exposure method. For the former, "Polaroid" cylinders were used.[6] For the latter, two horizontal H-11 arcs backed by machined, Cr plated elliptical reflectors served as a source. The light from the arcs passed through blackened metal slots and then through

TABLE II. Structure on bands at 954 and 972 cm^{-1}.

903.5	943.3
906.1	945.4
909.2	948.7
912.2	954.3 St.
915.2	961.8
918.3	964.6
921.4	967.6
924.5	971.5 St.
927.7	975.7
930.9	979.7
934.1	981.1
937.3	984.1
940.5	986.7
	989.5

TABLE III. Structure on band at 683 cm^{-1}.

657.8	705.0
660.1	708.3
663.0	711.6
—	715.0
671.3	718.4
682.8 St.	721.8
689.2	725.5
692.3	729.0
695.5	732.3
698.5	735.8
701.7	739.6

[6] B. L. Crawford, Jr., and W. Horwitz, J. Chem. Phys. **15**, 268 (1947).

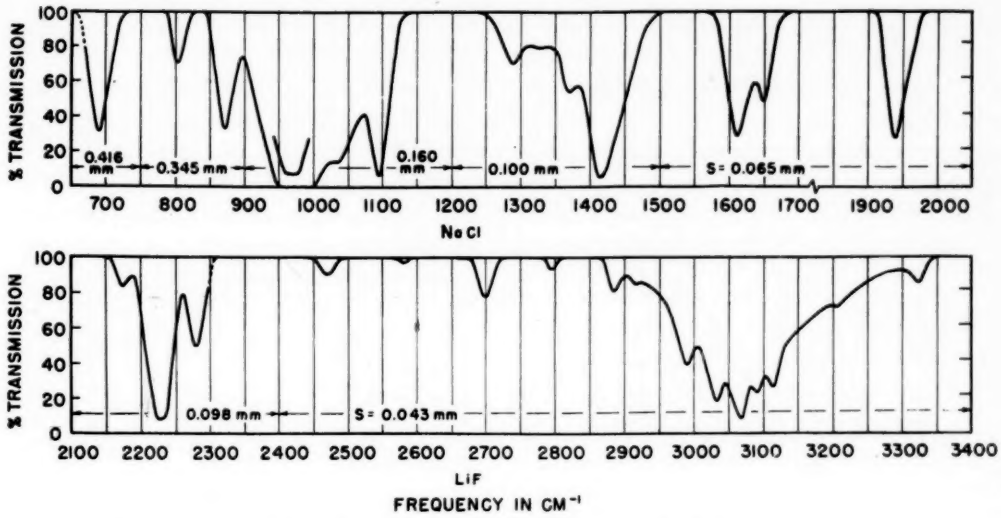

FIG. 2. Infra-red spectrum of liquid acrylonitrile.

glass filters to the liquid which was contained in a horizontal tube of square cross section with a strain-free window of good optical quality fused onto the end. Between the condensing lens and the slit was placed a Wollaston prism (made of $NH_4H_2PO_4$) having an aperture 4 cm×4 cm and a semi-angle of divergence of 0.04 radian at 4400A. No depolarizer was used between the Wollaston and the slit. Instead, the polarizing properties of the spectrograph were determined at λλ4471, 4713, and 5016A using a fairly large bore He tube as a source in conjunction with the condensing lens and Wollaston prism. The appropriate correction factors were then applied to the experimentally-determined, single-exposure ρ values to obtain the corrected values. No value was obtained for $\Delta\nu 362$. The values for $\Delta\nu\nu 970$ and 1094 are larger than the theoretical limit of 6/7 (0.86) even though 1094 is supposed to be polarized. This is occasioned by their low intensities and diffuse characters. (An additional reason for the high ρ value for 1094 will be mentioned later.)

The Raman frequencies are given in Table V. These values are corrected for vacuum and are accurate to within ± 2 cm^{-1}. The intensities (determined microphotometrically) are given on a scale of 1 to 100 with 2228 being given a value of 100; they have not been corrected for irregularities in plate sensitivity.

Enlarged reproductions of the Raman spectrum and of the single-exposure polarized spectra are given in Fig. 3 along with the corresponding microphotometer tracings. The two spectra which show $\Delta\nu 362$ have too much background to be suitable for reproduction.

III. THEORETICAL CONSIDERATIONS

The acrylonitrile molecule is presumably planar, belonging to symmetry point group C_s, and having fifteen normal vibrational degrees of freedom. The representation of this point group (which has the vibrational motions as its basis) in terms of its irreducible components, is $\Gamma_{vib}=11A'+4A''$, where type A' is symmetric and type A'' is antisymmetric with respect to reflection in the molecular plane. Selection rules permit all the vibrational frequencies to be active both in infra-red absorption and in the Raman effect.

Although no data are available for the molecular parameters, estimates can be made which are sufficiently accurate for qualitative discussions. A diagram of the molecule is given in Fig. 4, together with abbreviations used to designate the atoms and angles involved. For our purposes we assume

$$r(C-H)=1.08A, \quad r(C=C)=1.35A,$$
$$r(C-C)=1.49A, \quad r(C\equiv N)=1.17A$$

and $\alpha_3=\beta_{56}=120°$. These dimensions yield as the principal moments of inertia $I_A\simeq 19$, $I_B\simeq 174$, and $I_C=I_A+I_B\simeq 193$ (in units of 10^{-40} g cm^2) about the axes designated as A and B in Fig. 4,

and the C-axes perpendicular to the molecular plane. These moments are only approximate, although I_A seems about right for the observed rotational spacing.

The infra-red absorption bands for the vapor should have contours characteristic of the orientation of the vibrating electric moment with respect to the principal axes. A description of the band envelopes for this type of molecule may be obtained from the computations of Badger and Zumwalt[7] on unsymmetrical rotator molecules. For a planar molecule with $I_A \ll I_B$, I_C, vibrations in which the electric moment change is parallel to the A-axis should give rise to type "A" bands with three peaks, the central one being weak relative to the others. Vibrations in

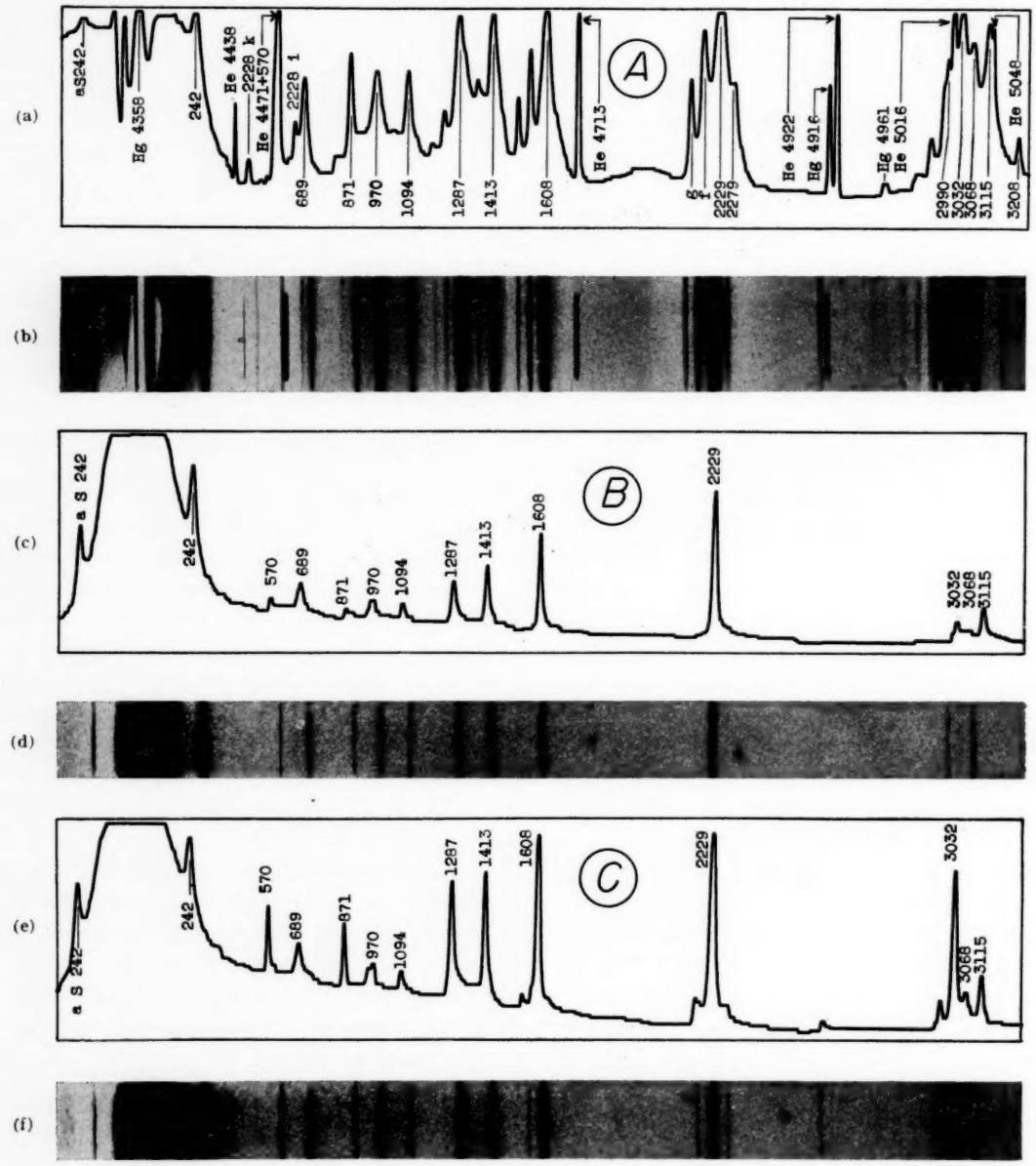

FIG. 3. Raman spectra of acrylonitrile (liquid). (A) Spectrum with helium reference spectrum. The stronger lines are excited by Hg e, f, and g. (B) and (C) are polarized spectra using natural light incident on sample and represent i_σ and I_π, respectively, with $\rho_n = i_\sigma / I_\pi$.

[7] R. M. Badger and L. R. Zumwalt, J. Chem. Phys. 6, 711 (1938).

which the moment is parallel to the B-axis should yield type "B" bands with two peaks and a minimum between them. Vibrations in which the moment is parallel to the C-axis should yield type "C" bands with three peaks, the central one being very strong relative to the other two. And finally, vibrations in which the moment makes an arbitrary angle with the principal axes should yield band envelopes which are linear combinations of the A, B and C type intensity distributions, with coefficients proportional to the squares of the components of the moments along the respective axes; these are termed hybrid bands. Consequently the a'' vibrations[8] should give rise to pure type C bands, while the a' vibrations may give rise to types A or B, or hybrids of the two, depending on the particular vibrations. Hybrid bands, however, may appear to be type B bands because of the low intensity of the Q branch and because of incomplete resolution. Perhaps the purest type A band is the one at 2239 cm^{-1} caused primarily by a stretching of the C≡N bond. Bands at 786 and 1282 cm^{-1} do not show Q branches, although run under conditions which resolve the peaks for bands at 869 and 1416 cm^{-1}.

In the Raman effect lines arising from a'' vibrations should be completely depolarized, i.e., should show a depolarization factor of 6/7 when unpolarized incident light is used, and scattering is observed at 90°. Raman lines arising from a' vibrations, however, may show any depolarization factor, ρ_n, $\leqslant 6/7$, although pure deformation vibrations are expected to show a relatively high factor.[9]

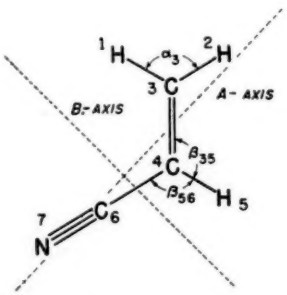

FIG. 4. Structural parameters for acrylonitrile.

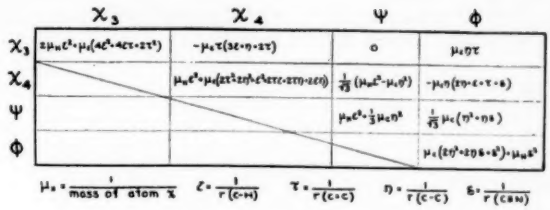

FIG. 5. G matrix for non-planar vibrations of acrylonitrile assuming $\alpha_3=\beta_{56}=120°$ (symmetrical about diagonal).

A normal coordinate treatment of the a' (planar) vibrations would involve an equation of eleventh degree which is too large to handle conveniently. The a'' (non-planar) vibrations, however, require only a fourth degree equation which is amenable to treatment. Furthermore, an indication of the frequency values of the out-of-plane vibrations will be of material help in assigning some of the low frequency vibrations. As valence force coordinates (VFC) for such a treatment, we take the angle between the bisector of the HC^3H angle and the C=C axis (χ_3), the analogous angle between the bisector of the HC^4C^6 angle and the C=C axis (χ_4), the angle of torsion about the C=C bond (ψ), and the C−C≡N angle (ϕ). Wilson's technique[10] was used for setting up the secular equation, and the G matrix ($2T=\dot{S}'G^{-1}\dot{S}$, where S represents the VFC) obtained is given in Fig. 5. The F matrix ($2V=S'FS$) used with the G matrix in obtaining the secular equation, $|GF-\lambda E|=0$, for the a'' vibrations of the acrylonitrile molecule is given in Fig. 6.

Approximate values of the force constants in the F matrix may be estimated from values for related molecules. F_{33} is taken as 0.23×10^{-11},

F	χ_3	χ_4	Ψ	Φ
χ_3	F_{33}	f_{34}		
χ_4	f_{34}	F_{44}		
Ψ			$F_{\psi\psi}$	
Φ				$F_{\phi\phi}$

FIG. 6. F matrix for non-planar vibrations of acrylonitrile.

[8] Small letters are used for the symmetry species of a normal vibration, corresponding to the capital letter for the general symmetry class.

[9] M. Wolkenstein and M. Eliashevich, C. R. Acad. Sci. U.R.S.S. **41**, 366 (1943). The fuzziness and high depolarization factor of the lowest lying Raman line in acrylonitrile supplies some experimental support for these theoretical considerations.

[10] E. B. Wilson, Jr., J. Chem. Phys. **7**, 1047 (1939); **9**, 76 (1941).

TABLE IV. Probable regions for vibrational frequencies.

Type	Description	Approximate region	Description	Approximate region
	3 C—H stretching	3000 cm^{-1}	1 C=CH_2 wagging	1100 cm^{-1}
	1 C≡N stretching	2240 cm^{-1}	1 C—C stretching	900 cm^{-1}
	1 C=C stretching	1630 cm^{-1}	1 C=C—C bending	450 cm^{-1}
A'	1 =C—H_2 deformation	1400 cm^{-1}	1 C—C≡N bending	360 cm^{-1}
	1 C=C—R bending	1290 cm^{-1}		
A''	1 C=CH_2 wagging (χ_3)	940 cm^{-1}	1 C=C HR wagging (χ_4)	964 cm^{-1}
	1 C—C≡N bending (ϕ)	357 cm^{-1}	1 C=C torsion (ψ)	632 cm^{-1}

F_{44} as 0.25×10^{-11} and f_{34} as $+0.03\times10^{-11}$ ergs per radian^2 from the values for vinyl chloride.[11] $F_{\psi\psi}$ is taken as 0.47×10^{-11} ergs per radian,^{2} an average of the values for ethylene dibromide[12] and vinyl chloride.[11] $F_{\phi\phi}$ is taken as 0.344×10^{-11} ergs per radian^2 as given for methyl cyanide.[13] All interaction constants except f_{34} are neglected since no consistent data are available for them. With these values for the force constants, the frequencies calculated for the a'' vibrations are those given in Table IV. Exact agreement between these calculated frequencies and the observed ones should not be expected, since force constants were only estimated and interaction constants were neglected.

Probable spectral regions for the frequencies of the fifteen normal vibrations of acrylonitrile are given in Table IV, together with a description of the principal mode of motion involved in each. In some cases, of course, two or more of these modes may be interacting strongly. For example, the modes designated as the C=CHR out-of-plane wagging (referred to later as ν_9) and the C=C bond torsion (ν_{12}) involve both coordinates χ_4 and ψ to a large extent, with χ_4 making the slightly larger contribution to ν_9 (about 8 percent larger) and *vice versa* for ν_{12}.

IV. ASSIGNMENT OF OBSERVED FREQUENCIES

We shall designate the fifteen normal vibrations arranged in order of descending frequencies by the numbers one to fifteen. Thus the first three will be those associated primarily with the stretching of the C−H bonds, which are expected to have frequencies in the vicinity of 3000 cm^{-1}. The two strong vapor phase infra-red bands at 3125 cm^{-1} and 3042 cm^{-1} are assigned to the fundamental vibrations ν_1 and ν_3, respectively. Each of these bands shifts downward about 10 cm^{-1} on going to the liquid. In view of this, the fundamental ν_2 is taken to be 3068 cm^{-1} for the liquid, and estimated at about 3078 cm^{-1} for the vapor (perhaps accounting for the asymmetry in the "P" branch of the band at 3125 cm^{-1}). The variations in intensities of absorption by these vibrations on going from the vapor to the liquid state are also indicative of rather strong intermolecular forces.

The band at 2239 cm^{-1} in the vapor (at 2229 cm^{-1} in the liquid) must be associated with ν_4, the stretching of the C≡N bond. An absorption band with a similar contour occurs at 869 cm^{-1}, which must be caused by a vibration with its transition moment in the same direction. This latter band is assigned to ν_{11}, the stretching of the C−C bond. Little or no shift is observed for this band on going to the liquid state (logical behavior for stretching of an internal bond).

The stretching of the C=C bond, ν_5, is assigned to the band at 1615 cm^{-1}, which also shows little shift with a change of state (1608 cm^{-1} in the liquid). The CH_2 deformation, ν_6, is assigned the frequency 1416 cm^{-1}. The vibration ν_7, essentially the in-plane wagging of the olefinic C−H group (involving changes in β_{56} and β_{35} of Fig. 4), is associated with the vapor band at 1282 cm^{-1} and the slightly higher liquid frequency, 1287 cm^{-1} (average of 1286 and 1288 cm^{-1}).

The in-plane wagging of the CH_2 group, ν_8, is assigned the frequency 1094 cm^{-1} in the liquid

[11] K. S. Pitzer and N. K. Freeman, J. Chem. Phys. **14**, 586 (1946).
[12] C. Manneback as quoted by M. de Hemptinne, Trans. Faraday Soc. **42**, 5 (1946).
[13] B. L. Crawford and S. R. Brinkley, J. Chem. Phys. **9**, 69 (1941).

TABLE V. Vibrational assignments for acrylonitrile.

Descriptive assignments†			Gas Infra-red			Liquid Infra-red		Liquid Raman			Average	Infra-red T & T* Gas	Infra-red T & T* Liquid	Raman** Liquid
ν_{15}	a'	C−C≡N bend						242	.72	16	242	ν_{14}		238
												ν_{15}		305
ν_{14}	a''	C−C≡N bend						362	—	—	362			
												ν_{12}		517
ν_{13}	a'	C=C−C bend						570	.18	4.1	570			561
														628
ν_{12}	a''	C=C torsion	683	*C*	*S*	690	*S*	688	.875	3.0	689	ν_{13} 690		688
	A'	$\nu_{13}+\nu_{15}$	786	*B*	*W*	804	*M*				804	791	805	
ν_{11}	a'	C−C stretch	869	*A*	*M*	871	*M*	871	.22	4.7	871	870	873	878
													907	
ν_{10}	a''	H_2C=C wag	954	*C*	V.S.							954		
						960–980	*VS*	970	.94	2.8	970		960–980	965
ν_9	a''	HRC=C wag	972	*C*	V.S.							971		
	A'	$\nu_{14}+\nu_{12}$	1033	?	?	1035	*W*				1035		1038	
	A''	$3\nu_{14}$	1085	*C*	*S*									
						1094	*S*	1094	.91	2.8	1094			
ν_8	a'	CH_2 rock	1096	*A*	*W*							ν_8 1095	1097	1099
														1205
ν_7	a'	C−H rock	1282	*B*	*W*	1288	*M*	1286	.31	14	1287	ν_7	1288	1275
	A'	$\nu_{10}+\nu_{14}$				1325?	*VW*				1325		1330	
		$2\nu_{12}$				1376?	*VW*				1376		1372	
ν_6	a'	CH_2def.	1416	*A*	*M*	1415	*S*	1412	.34	20	1413	ν_6 1421	1420	1406
	A'	$\nu_{11}+2\nu_{14}$						1588	*P*		1588			
ν_5	a'	C=C stretch	1615	*B*	*M*	1609	*S*	1607	.23	36	1608		1610	1607
	A'	$\nu_6+\nu_{15}$	1650	?	*W*	1648	*M*	1648	*D*		1648		1650	
	A'	$\nu_9+\nu_{10}$	1909	*B*	*M*	1940	*M*				1940			
	A'	$2\nu_8$				2174	*W*				2174			
ν_4	a'	C≡N stretch	2239	*A*	*W*	2228	*S*	2228	.30	100	2228	ν_4	2232	2224
	A'	$\nu_6+\nu_{11}$	2286	?	*V.W.*	2280	*M*	2278	*P*		2279		2283	
	A'	$\nu_4+\nu_{15}$				2465	*VW*				2465			
	A''	$\nu_5+\nu_9$				2580	*VW*				2580			
	A'	$\nu_6+\nu_7$				2697	*W*				2697			
	A'	$\nu_4+\nu_{13}$				2795	*VW*				2795			
			2894	*B*		2885	*W*				2885			
			2994	?		2990	*W*	2989	*P*		2990			2989
ν_3	a'	C−H stretch	3042	*A*	*S*	3033	*S*	3032	.21	45	3032			3036
ν_2	a'	C−H stretch	(3078?)		?	3068	*S*	3068	.51	7.5	3068			
	A'	$\nu_4+\nu_{11}$				3091					3091			
ν_1	a'	C−H stretch	3125	*B*	*S*	3114	*S*	3116	.80	14	3115			3115
	A'	$2\nu_5$				3210		3207			3208			
	A'	$\nu_4+\nu_8$	3330	?	*W*	3323					3323			
	A'	$\nu_5+\nu_9+\nu_{10}$				3557±7					3557			
						3650±7					3650			

† Present paper.
* Thompson and Torkington, reference 3.
** References 1 and 2.

and 1096 cm^{-1} in the vapor. This is complicated by the appearance of a weak type *C* band at 1085 cm^{-1}, which is believed to be the third harmonic of a fundamental at 362 cm^{-1} (symmetry A'') lying on top of the fundamental ν_8 (symmetry a'). The A'' harmonic probably gains some intensity by interaction with the intense type "*C*" bands at 972 cm^{-1} and 954 cm^{-1}. In the Raman spectrum, however, the line at 1094 is comparable in intensity to the doublet at 960–980 cm^{-1}, and presumably is caused by the fundamental itself. This super positioning of A'' and a' frequencies could cause ρ to be high (as high as 0.86) if A'' has considerable intensity. However, it seems better to say that the third harmonic of 362 will be very weak in Raman effect and that the erroneous value for ρ is

TABLE VI. Thermodynamic functions for acrylonitrile.

Absolute temperature	C_P^0	$(H^0-H_0^0)/T$	$-(F^0-H_0^0)/T$	S^0
298.16	15.24	10.79	54.68	65.47
300	15.30	10.82	54.75	65.56
400	18.36	12.33	58.07	70.40
500	20.95	13.80	60.97	74.78
600	23.11	15.18	63.61	78.79
700	24.90	16.44	66.05	82.49
800	26.43	17.60	68.31	85.91
900	27.75	18.66	70.46	89.12
1000	28.88	19.62	72.49	92.11

caused by experimental difficulties. We therefore disregard the value of ρ for this line and assign 1094 to an a' frequency.

The bands at 972 cm^{-1} and 954 cm^{-1} are extremely intense type *C* bands in infra-red absorption, and are assigned to ν_9 (C=CHC wagging) and ν_{10} ($C=CH_2$ wagging) respectively, corresponding to the calculations in Table IV. In the liquid the bands occur at slightly higher frequencies. This very intense infra-red absorption by out-of-plane C−H wagging vibrations is compatible with a relatively polar C−H bond[14] as well as the increase in frequency on going to the liquid state. The frequency ν_{12}, torsion about the C=C bond, is assigned to the strong type *C* band at 683 cm^{-1}. Its intensity is reasonable when compared to the intense bands for ν_9 and ν_{10}, and when consideration is given to the interaction of coordinates ψ and χ_4 in producing ν_{12} and ν_9. The polarized Raman lines at 570 cm^{-1} and 242 cm^{-1} must be assigned to the planar vibrations ν_{13} (C=C−C bending) and ν_{15} (C−C≡N bending), respectively. This leaves 362 cm^{-1} as the frequency of the out-of-plane C−C≡N bending vibration, ν_{14}. The combination of $\nu_{13}+\nu_{15}$ explains the infra-red band in the liquid at 805 cm^{-1} very nicely. In the vapor, however, this band appears at a lower frequency, 786 cm^{-1}, and if the same assignment is to hold, one or both of ν_{13} and ν_{15} must be lower in the vapor phase. In view of the intermolecular forces present, such a shift is reasonable for bending vibrations.

Our assignment of observed frequencies, together with a comparison of data given by other observers, is given in Table V. Only the band centers are listed.

[14] G. W. Wheland, *The Theory of Resonance* (John Wiley and Sons, Inc., New York, New York, 1944), pp. 135–136.

V. THERMODYNAMIC FUNCTIONS

Since the fundamental frequencies have been determined, and since the moments of inertia have been estimated, the thermodynamic functions for the vapor may be calculated. Values obtained for the temperature range 298.16–1000°K using the tables given by Aston,[15] are given in Table VI in terms of calories per mole per degree. The translational and rotational contributions were obtained using the working equations given by Wagman *et al.*[16] Values of 560, 362, and 238 cm^{-1} were estimated for the vapor phase frequencies ν_{13}, ν_{14}, and ν_{15} for use in the calculations, and $I_A \cdot I_B \cdot I_C$ was taken as 634×10^{-117} g^3 cm^6.

[15] J. G. Aston, in Taylor and Glasstone, *Treatise on Physical Chemistry* (D. Van Nostrand Company, Inc., New York, New York, 1942), Vol. 1, pp. 655–658.

[16] D. Wagman, J. E. Kilpatrick, W. J. Taylor, K. S. Pitzer, and F. D. Rossini, J. Research Nat. Bur. Stand. **34**, 143 (1945).

Dielectric Behavior of Solutions of Electrolytes in Solvents of Low Dielectric Constant. III. The Influence of Constitution on Dielectric Absorption*

H. A. STROBEL** AND H. C. ECKSTROM***
Metcalf Research Laboratory, Brown University, Providence, Rhode Island

(Received April 26, 1948)

Using a calorimetric method, a study of the influence of constitutional factors on the dielectric absorption of a variety of long chain salts in benzene solution has been made. In a series of octadecyltributylammonium salts, absorption at a given concentration proved dependent on the constitution of the anion and increased for the following anions in the order of their naming: formate, nitrate, chloride, iodide, and thiocyanate. Two salt series in which the chloride and thiocyanate anions were combined with different cations showed a marked dependence of absorption and of calculated aggregate dimensions on the size of the positive ions. All salt solutions below about 0.005 molar behaved as monodisperse systems; at about 0.01 molar additional varieties of ion clusters appeared to become stable and the systems were highly polydispersed; at somewhat higher concentrations there was evidence that a few types of aggregates were predominating and that the complexity was being reduced. On the basis of Debye theory, critical frequencies, average aggregate radii, and dipole moments have been evaluated wherever feasible. The results are in good agreement with such polarization and conductance data as are available.

IN the previous papers of this series,[1,2] an apparatus employing a calorimetric method for the measurement of dielectric absorption was described, and data obtained from several representative electrolytes in non-polar solvents were presented and discussed. That work has recently been extended to include a study of the influence of constitutional factors on the absorption and association of a variety of long chain salts in benzene.

Three systems of quaternary ammonium salts were investigated in benzene solution at 25°C: (1) a relatively soluble octadecyltri-*n*-butylammonium series consisting of the nitrate, formate, thiocyanate, picrate, iodide, and chloride; (2) a chloride series comprising octadecyltri-*n*-butylammonium and dioctadecyldi-*n*-butammonium chloride; and (3) a thiocyanate series in which the data for the dioctadecyldimethyl- and octadecyltributylammonium thiocyanates run currently were added to those for the tetra-*n*-butylammonium and dioctadecyldi-*n*-butylammonium salts run by Sharbaugh. In addition to these three series, tri-*iso*amylammonium picrate, whose behavior in benzene and diphenyl methane solution has already been reported,[2] was again studied in benzene and then investigated in anisole to ascertain what influence a slightly polar medium would have. The Debye polar molecule theory[3] has formed the basis for the consideration of the present results.

EXPERIMENTAL

Materials

Commercial, thiophene-free benzene was washed several times with portions of concentrated sulfuric acid until the washings were almost free of color. After one or two sodium hydroxide washes, the benzene was shaken several times with small amounts of water until neutral to litmus, then put aside to dry over calcium chloride. Several days' refluxing over sodium lead alloy served to remove the last traces of water before the solvent was distilled. The specific conductance was about 10^{-13} ohm^{-1} cm^{-1}.

* This paper is based in part on a portion of a thesis submitted by H. A. Strobel in partial fulfillment of the requirements for the degree of Doctor of Philosophy in the Graduate School of Brown University, October, 1947, and in part on work supported by a grant from the Research Corporation.

** Metcalf Fellow, Brown University, 1946; General Electric Coffin Fellow, 1946–47. Present address: Duke University, Durham, N. C.

*** Present address: Research Laboratory, Stanolind Oil and Gas Company, Tulsa, Oklahoma.

[1] Sharbaugh, Schmelzer, Eckstrom, and Kraus, J. Chem. Phys. **15**, 47 (1947).

[2] Sharbaugh, Eckstrom, and Kraus, J. Chem. Phys. **15**, 54 (1947).

[3] P. Debye, *Polar Molecules* (Dover Publications, New York, 1945).

Eastman anisole, which all distilled between 154 and 155° [4] was further purified by several hours' refluxing over molten sodium metal and was then stored over sodium. All runs were made with anisole freshly distilled from the metal. The lowest specific conductance obtained was 10^{-11} ohm^{-1} cm^{-1}.

Tri-*iso*amylammonium picrate, prepared and purified by Dr. D. T. Copenhafer[5] of this laboratory, was further recrystallized from 95 percent ethyl alcohol. M.p., 127.5–128.5°.

Tetra-*n*-butylammonium triphenylborohydroxide and dioctadecyldimethylammonium thiocyanate were available at the laboratory.[6] The former had a m.p. of 147–148.5°, while the latter was characteristically observed to melt over a wide range.

Octadecyltri-*n*-butylammonium iodide was prepared in an evacuated sealed tube by the reaction of *n*-octadecyl iodide and a 30 percent excess of tri-*n*-butylamine with a small amount of isopropyl alcohol added as solvent. After a week at 70°, the mixture was removed and the alcohol evaporated. Purification was effected by one recrystallization from hexane and a small amount of isopropyl alcohol, and several recrystallizations from the alcohol alone. On standing in a closed, dark bottle, the compound showed gradual oxidation and had to be recrystallized occasionally. M.p., 100–101°.

Octadecyltri-*n*-butylammonium nitrate was prepared from the iodide by metathesis with silver nitrate in hot 80 percent ethanol. It was recrystallized from hexane to which isopropyl alcohol was added dropwise until a clear solution resulted at the boiling point. M.p., 88.5–89.5°.

Octadecyltri-*n*-butylammonium thiocyanate was obtained from the nitrate by reaction with an equivalent quantity of potassium thiocyanate in absolute alcohol. It was also recrystallized from hexane to which a small amount of isopropyl alcohol was added. M.p., 66–67°.

Octadecyltri-*n*-butylammonium chloride was made by agitation of an alcohol solution of the corresponding iodide with an excess of washed silver chloride for about twelve hours. Recrystallization was effected from hexane and a small amount of isopropyl alcohol. Filtration of the salt was avoided by centrifuging. The salt sintered at about 52° and had an m.p. of 56–57.5°.

Octadecyltri-*n*-butylammonium formate was prepared by metathesis of the nitrate with an excess of dry potassium formate[7] in absolute methanol. After filtering out the precipitated potassium nitrate and evaporation of the solvent, the quaternary ammonium formate was leached from the residue with benzene. Hexane to which a little acetone was added was used for recrystallizing. Centrifuging was again employed to collect the salt. M.p., 89.5–90°.

Method and Equipment

The dipole or absorption conductivities of the solutions being investigated were determined by the calorimetric method, employing the apparatus and procedure described in the first paper of this series.[1]

In that paper it was shown, where Ohm's law is valid, that the specific conductance at any frequency is given by

$$\kappa_\omega = \kappa_0 + \Delta\kappa = V_0^2 t_0 \kappa_0 / V_\omega^2 t_\omega, \qquad (1)$$

where κ is the specific conductance in ohm^{-1} cm^{-1}, $\Delta\kappa$ is the absorption conductivity, V is the peak voltage across the thermometer cell, t is the time of rise of the solution through a standard length of capillary, and the subscripts 0 and ω refer to the audio calibration frequency and to any other frequency, respectively. When Ohm's law fails, as was found at very low frequencies for the more dilute solutions included in the present study,[8] Eq. (1) becomes inapplicable. The difficulty lies in the fact that $V_0^2 t_0 \kappa_0$ is now dependent on the field strength. For this case, it is

[4] All temperatures hereafter are in degrees centigrade, corrected for stem exposure.

[5] D. T. Copenhafer, Thesis, Brown University (1942).

[6] The preparation of the borohydroxide is detailed in D. L. Fowler and C. A. Kraus, J. Am. Chem. Soc. **62**, 1143 (1940), and the preparation of the thiocyanate is described in L. Strong, thesis, Brown University (1940).

[7] Supplied by Dr. H. L. Pickering of this laboratory. He prepared the formate by the reaction of a very small excess of dry potassium carbonate with distilled formic acid. The mixture was kept in a molten condition on a hot plate for a few hours and subsequently cooled with constant stirring. It was then placed in a desiccator over P_2O_5 and pumped with a Hyvac for two days. M.p., 171–172°.

[8] The results showing the variation of conductivity with field strength are given in an accompanying paper: H. A. Strobel and H. C. Eckstrom, J. Chem. Phys. **16**, 827 (1948).

possible to take advantage of the constancy of $V_0^2 t_0 \kappa_0$ for each cell for *most other* solutions. The average value of this quantity for each cell, which has been designated A, may then be substituted in Eq. (1) to give $\kappa_\omega = A/V_\omega^2 t_\omega$. Values of the κ_ω calculated in this manner are less reliable than those obtained from Eq. (1).[9] For the thermometer cell of largest capacity, which was always used with the more dilute solutions, A had a value of 5.1×10^{-3}.

One important change has been made in the apparatus. In place of the custom-built voltmeter tubes used previously, two types of commercial u.h.f. tubes have proved satisfactory: (1) RCA 957 triodes (with plate and grid linked) and (2) RCA 9005 diodes. The diodes were used throughout most of this study. Calibration at 60 cycles against a Weston model 341 voltmeter showed V_{peak}^2 values furnished by the voltmeter tubes to be low by a factor of 1.015. All calculations have been made using corrected voltages.

THEORY

Of the variety of physical interpretations proposed to account for the familiar observation of dependence of dielectric properties on the frequency of the applied field, the Debye theory is representative and has had the widest application. Since that theory has often been presented in detail elsewhere, only results of particular interest for this paper will be described here.

In terms of quantities measurable by the present method, it has been shown[2] that the a.c. part of the loss factor, here termed $\Delta\epsilon''$, is a measure of the energy absorbed per cycle and is given by

$$\Delta\epsilon'' = 1.8\times10^{12}\Delta\kappa/\nu, \qquad (2)$$

where $\Delta\kappa$ is in ohm^{-1} cm^{-1} and ν is in cycles per second.

From Debye theory, one finds that $\Delta\epsilon''$ [10] has a maximum value at a critical frequency ν_c; for a spherical particle of radius a obeying Stokes hydrodynamics, ν_c becomes

$$\nu_c = kT(\epsilon_\infty+2)/8\pi^2\eta a^3(\epsilon_0+2),$$

where η is the macroscopic viscosity and kT has its usual significance. In addition, where $\nu^2 \ll \nu_c^2$, it should be noted that Eq. (2) may be modified by being rewritten in terms of ν_c to give

$$\Delta\kappa = (\epsilon_0-\epsilon_\infty)\nu^2/1.8\times10^{12}\,\nu_c.$$

It is often found experimentally that the region of absorption is broader and that the loss-factor maximum is considerably smaller than predicted by theoretical treatments assuming a single type of particle. This deviation may, in many cases, be represented satisfactorily by the use of a single parameter α as suggested by the Coles.[11] In the present investigation, α has been calculated by the following expression relating the observed $\Delta\epsilon_{\max}''$ to that predicted by theory:

$$\Delta\epsilon_{\max}'' = (1/2)(\epsilon_0-\epsilon_\infty)\tan[(1-\alpha)\pi/4]. \qquad (3)$$

A further quantity of interest whose magnitude may be calculated from absorption data is the dipole moment of the average polar cluster. Assuming a monodisperse system, Debye[12] developed an equation providing such information for dilute solutions in non-polar solvents. For the more general case where a broad absorption region is observed and $\alpha\neq0$, one can obtain a similar equation by modifying the Debye formulation of the molar polarization as a function of the frequency. The starting equation for the general case is then

$$[(\epsilon^*-1)/(\epsilon^*+2)]M_1/d_1 = A+B/[1+(i\omega t)^{1-\alpha}], \qquad (4)$$

where A includes the solvent polarization and the distortion polarization of the solute,

$$B = (4\pi N f_2/3)(\mu^2/3kT),$$

ϵ^* is the complex dielectric constant of the solution, M_1 is the molecular weight of the solvent and d_1 its density, f_2 is the mole fraction of solute, $N=6.02\times10^{23}$, μ is the dipole moment in e.s.u., and the other symbols have been defined.

Two assumptions have been made: (1) that the loss is proportional to f_2, and (2) that Debye's $1/(1+i\omega t)$ should be replaced by $1/[1+(i\omega t)^{1-\alpha}]$ for cases where $\alpha\neq0$. Since the use of α is mathe-

[9] If invariant experimental conditions are maintained, the differences among the specific heats, coefficients of expansion, and densities of the solutions are sufficiently small, so that A may be estimated with an accuracy of ±5 percent.

[10] $\Delta\epsilon''$ is identical with ϵ'', when ionic conductance is neglected in the latter.

[11] K. S. Cole, and R. H. Cole, J. Chem. Phys. **9**, 341 (1941).

[12] P. Debye, Physik. Zeits. **35**, 101 (1934).

TABLE I. Constants measured at 25°C for all solutions investigated.*

Salt	$c\times10^2$	$f_2\times10^3$	d	η	ϵ_0	κ_0	P_1 or P_2
$Bu_4N\Phi_3BOH$	0.103	0.0921	0.8735	0.610	2.299	7.89×10^{-10}	5080
Oct_2Bu_2NSt	0.333	0.299	0.8735**	0.618	2.309	5.82×10^{-11}	2170
Oct_2Me_2NSCN	0.723	0.649	0.8735	0.652	2.286	7.21×10^{-11}	740
i-Am_3NHPi	9.31	8.53	0.8830	0.680	3.93	3.66×10^{-8}	2240
i-Am_3NHPi***	10.36	11.68	0.9958	1.104	6.35	2.08×10^{-7}	1390
$OctBu_3NNO_3$	0.193	0.173	0.8735	0.610	2.278	3.81×10^{-10}	680
$OctBu_3NNO_3$	1.39	1.25	0.8742	0.640	2.311	1.21×10^{-8}	610
$OctBu_3NNO_3$	1.73	1.56	0.8745**	0.650**	2.346	2.14×10^{-8}	740
$OctBu_3NNO_3$	2.26	2.04	0.8748**	0.668	2.416	4.91×10^{-8}	1160
$OctBu_3NNO_3$	2.54	2.29	0.8750	0.675	2.459	7.51×10^{-8}	1310
$OctBu_3NI$	0.160	0.143	0.8735	0.606	2.276**	3.70×10^{-10}	—
$OctBu_3NI$	0.260	0.234	0.8735**	0.608**	2.280	7.80×10^{-10}	690
$OctBu_3NI$	1.33	1.20	0.8741	0.625	2.314	1.61×10^{-8}	690
$OctBu_3NI$	1.45	1.31	0.8742	0.628	2.333	2.02×10^{-8}	860
$OctBu_3NI$	1.75	1.59	0.8743	0.633	2.378	3.47×10^{-8}	1150
$OctBu_3NCl$	1.38	1.24	0.8736	0.629	2.299	7.78×10^{-9}	480
$OctBu_3NCl$	1.75	1.58	0.8736	0.634	2.309	1.46×10^{-8}	500
$OctBu_3NCl$	2.57	2.33	0.8738	0.661	2.421	4.66×10^{-8}	1080
$OctBu_3NSCN$	1.38	1.24	0.8737	0.626	2.364	3.23×10^{-8}	1240
$OctBu_3NSCN$	1.50	1.35	0.8738	0.628	2.376	4.10×10^{-8}	1280
$OctBu_3HCOO$	1.39	1.26	0.8740**	0.635	2.301	1.13×10^{-8}	740
Oct_2Bu_2NCl	1.73	1.57	0.8735	0.647	2.393	3.78×10^{-8}	1340
C_6H_6			0.8735	0.606	2.272	10^{-13}–10^{-14}	26.62 (P_1)
$C_6H_5OCH_3$			0.9894	1.006	4.30	1–3 $\times10^{-11}$	57.33 (P_1)

* The solvent was benzene, unless otherwise indicated. Symbols: Bu, butyl; Am, amyl; Oct, octadecyl; Φ, phenyl; St, stearate; Pi, picrate.
** Estimated quantities.
*** Anisole was the solvent.

matically equivalent to assuming a logarithmically symmetrical distribution of relaxation times about $\omega\tau=1$, the generalization of Debye's development is made at this point, following the treatment of the Coles.[11] In addition, the following approximations have been made: $d_{12}\cong d_1$, $\Delta\epsilon''\ll\epsilon_0$, and $f_2\ll f_1\cong1$, where d_{12} is the solution density, and ϵ_0 and f_1 are the audiofrequency dielectric constant of the solution and mole fraction of the solvent, respectively.

By resolving into real and imaginary components, one may solve Eq. (4) for μ; he obtains

$$\mu=\left\{[M_1/f_2d_1][3kT/4\pi N][3/(\epsilon_0+2)]^2[\Delta\epsilon''] \times\left[\frac{1+(\omega\tau)^{2(1-\alpha)}+2(\omega\tau)^{1-\alpha}\cos(1-\alpha)\pi/2}{(\omega\tau)^{1-\alpha}\sin(1-\alpha)\pi/2}\right]\right\}^{\frac{1}{2}}. \quad (5)$$

When $\alpha=0$, the term in the last bracket reduces to $(1+(\omega\tau)^2)/\omega\tau$ and Eq. (5) is identical with Debye's except that he approximated ϵ_0 by the dielectric constant of the solvent. When $\omega\tau\cong1$, as will be true for the calculations made for the present examples of poly-disperse systems, the term in the last bracket becomes

$$(\epsilon_0-\epsilon_\infty)/\Delta\epsilon_{max}''.$$

Equation (5) has been used in these two forms for the calculation of dipole moments. It should be noted that the dipole moment ascertained in this way is characteristic of the particles in solution only for monodisperse systems; where the system contains a variety of polar clusters, the moment is an average value, weighted not only by the distribution of particle moments but of particle sizes.

RESULTS

In Table I all the physical quantities pertinent to the Debye theory are listed for each of the solutions and pure liquids investigated. All dielectric constants were measured relative to the 2.272 value assumed for benzene at 25°C.[13] As in the previous study,[2] the audiofrequency dielectric constants of the more concentrated solutions were found to vary with the frequency. An investigation of this behavior is now under way. Since all the ϵ_0's asymptotically approached a constant value at 7500 cycles per second, the dielectric constants at that frequency seem more

[13] This value is an average of the carefully determined value of C. P. Smyth, *Dielectric Constant and Molecular Structure* (Chemical Catalog Company, New York, 1931), and that of J. A. Geddes and C. A. Kraus, Trans. Faraday Soc. **32**, 585 (1936).

TABLE II. Constants calculated on the basis of the Debye theory.

Salt	Molarity $C\times10^2$	Critical frequency ν_c (Mc)	Relaxation time τ (sec.)	Molecular radius a(A)	Dipole moment μ(D)
$Bu_4N\Phi_3BOH$	0.103	400	4.0×10^{-10}	6.1	14.4
Oct_2Bu_2NSt	0.333	210	7.4×10^{-10}	7.3	9.0
Oct_2Me_2NSCN	0.723	870	1.8×10^{-10}	4.5	4
i-Am_3NHPi	9.31	490	2.3×10^{-10}	4.8	10.4
i-Am_3NHPi**	10.4	590	1.4×10^{-10}	3.4	—
$OctBu_3NNO_3$	0.193	500	3×10^{-10}	6	5
$OctBu_3NNO_3$	1.39	50*	3×10^{-9}	12	4.6
$OctBu_3NNO_3$	1.73	30*	5.2×10^{-9}	14	5.3
$OctBu_3NNO_3$	2.26	5.2	2.9×10^{-8}	24	6.8
$OctBu_3NNO_3$	2.54	4.4	3.4×10^{-8}	26	7.3
$OctBu_3NI$	0.160	300	5×10^{-10}	6	5
$OctBu_3NI$	1.33	25	6.3×10^{-9}	15	5.0
$OctBu_3NI$	1.45	21	7.4×10^{-9}	16	5.6
$OctBu_3NI$	1.75	8.3	1.9×10^{-8}	21	6.7
$OctBu_3NCl$	1.38	40*	4×10^{-9}	11	3.8
$OctBu_3NCl$	1.75	14.3	1.1×10^{-8}	18	4.0
$OctBu_3NCl$	2.57	1.6	9.5×10^{-8}	36	6.5
$OctBu_3NSCN$	1.38	11.0	1.4×10^{-8}	19	7.0
$OctBu_3NSCN$	1.50	9.3	1.7×10^{-8}	20	7.3
$OctBu_3NHCOO$	1.39	50*	3×10^{-9}	12	4.0
Oct_2Bu_2NCl	1.73	2.3	6.7×10^{-8}	32	7.3

* Estimated from graphs of $\Delta\epsilon''$ *vs.* $\ln\nu$.
** Anisole solution.

nearly correct and have been listed in the table and used in calculations. For all solutions, except where indicated, benzene was the solvent. Refractive indices at 25° were found to differ only slightly in the fourth decimal place from that of the solvent in all cases and are not tabulated. Molar polarizations were calculated on the basis of the Clausius-Mosotti relationship. The symbols used are c, molarity; f_2, mole fraction; x_0, specific conductance at 1000 c.p.s.; ϵ_0, dielectric constant at 7500 cycles; d, density; η, viscosity (centipoises); P_2, molar polarization of solute (cc) and P_1 molar polarization of the solvent (cc).

In Table II are summarized the constants calculated from Debye theory for all the solutions. The experimentally observed and theoretically predicted loss factor maxima are collected together with the calculated values of the parameter α in Table III. For these calculations ϵ_∞ for the benzene solutions has been taken as 2.272, the assumed dielectric constant of the solvent, rather than 2.244, the square of the D-line index of refraction of the solution used by Sharbaugh. This change seems justified since benzene is known to be non-polar; the difference between the figures must then be due to atomic polarization contributions, which should not be included in the orientation losses of solutions. It will be noted that critical frequencies and dipole moments are lowered and particle sizes increased, especially for the more dilute solutions, by this modification in procedure.

DISCUSSION

A. Slightly Soluble Salts

Three of the salts which appeared to be interesting, tetrabutylammonium triphenylborohydroxide, dioctadecyldibutylammonium stearate and dioctadecyldimethylammonium thiocyanate,

TABLE III. Theoretical and experimental absorption maxima.

Salt	Molarity $C\times10^2$	$\frac{\epsilon_0-\epsilon_\infty}{2}$	$\Delta\epsilon_{max}''$	α
$OctBu_3NNO_3$	0.190	—		0.0
	1.39	0.019	0.008*	0.49
	1.73	0.031	0.012	0.53
	2.26	0.072	0.026	0.56
	2.54	0.093	0.041	0.47
$OctBu_3NI$	0.160	—	—	0.0
	1.33	0.021	0.009	0.49
	1.45	0.030	0.011	0.55
	1.75	0.053	0.019	0.56
$OctBu_3NCl$	1.38	0.013	0.005*	0.49
	1.75	0.018	0.009	0.43
	2.57	0.074	0.038	0.40
$OctBu_3NSCN$	1.38	0.046	0.016	0.56
	1.50	0.052	0.020	0.53
Oct_2Bu_2NCl	1.73	0.061	0.028	0.45
$OctBu_3NHCOO$	1.39	0.014	0.007*	0.43

* Estimated from plots of $\Delta\epsilon''$ *vs.* $\ln\nu$.

TABLE IV. Equivalent loss factors* at 21 Mc for several dilute solutions.

Salt	Molar conc. $\times 10^3$	Equiv. loss factor at 21 Mc ($\Delta\epsilon''_E$)
Oct_2Me_2NSCN	7.23	50
$OctBu_3NNO_3$	1.93	100
$OctBu_3NI$	1.60	190
Oct_2Bu_2NSt	3.33	1000
$Bu_4N\Phi_3BOH$	1.03	1600

* The conventional loss factor has been multiplied by the factor $1000/c$, where c is the molarity, to put it on a mole basis.

proved difficulty soluble in benzene at 25°, and only dilute solutions, i.e., those below 0.005 molar, could be studied. Since the heating constant A and large cell-heating corrections figure in the dielectric loss calculations for such dilute solutions, the data from these salts must be considered with caution.

Tetrabutylammonium triphenylborohydroxide was the first of these salts and was selected to determine the magnitude of absorption of a salt with high dipole moment and with two large ions of about equal size. The second, the stearate, was investigated to ascertain the effect of having long chains in both cation and anion, while the third, dioctadecyldimethylammonium thiocyanate, was included to supply additional information as a member of the thiocyanate series to be discussed later. A single solution of each was studied near the limit of solubility.[14]

It is helpful in the discussion of the results for the solutions of these three salts to consider as well the data for two other dilute solutions studied in the present work, the approximately 0.002 molar solutions of octadecyltributylammonium nitrate and iodide. All five salts behaved as monodisperse systems in these solutions, yielding linear plots of $d(\ln\Delta\epsilon'')$ *versus* $d\ln\nu$ with a slope of unity as predicted by Debye theory for frequencies well below the critical. The calculated aggregate radii, dipole moments, and critical frequencies for these systems will be found in Table II. In addition, the equivalent loss factors at 21 Mc have been collected in Table IV.

From the results in Tables II and IV, it is evident that the two approximately equal-sized octadecyltributylammonium nitrate and iodide molecules behave similarly in dilute solution. On the other hand, the borohydroxide salt is a little larger by virtue of having three phenyl groups in place of an octadecyl chain and has given rise to slightly larger particles in solution. For the borohydroxide, a distinct increase in the spacing of the centers of charge in the particles has appeared, for its dipole moment is 14.4 Debyes in contrast to moments of about 5 Debyes for the other two salts. This marked increase is reflected in the very much higher equivalent loss factor of the borohydroxide. It is interesting to note that Geddes and Kraus,[13] found a moment of 19.6 Debyes for this salt by a limiting polarization method; the ratio of their limiting molar solute polarization to the present value, 1:0.61, is in good agreement with the ratio of the squares of the moments, 1:0.62, and thus is in accord with theory.

For the other two salts the data show very different behavior. As is suggested by the three long chains, the dioctadecyldibutylammonium stearate solution contained particles considerably greater in size than those found in the other solutions. The dipole moment also proved to be higher than the moments of the single long chain salts. Such properties are reflected in the high equivalent loss factor. In striking contrast are the significant quantities for the dioctadecyldimethylammonium thiocyanate. Although its

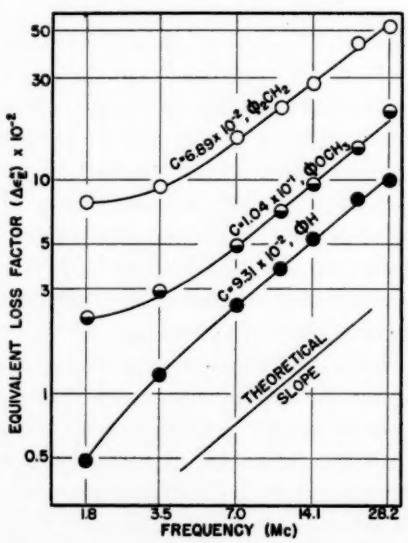

FIG. 1. Equivalent loss factor as a function of frequency for i-Am_3NHPi in C_6H_6, Φ_2CH_2, and ΦOCH_3.

[14] The thiocyanate proved so weak an electrolyte that even the 0.007 molar solution investigated was effectively in this dilute grouping.

molecular size is greater than that of the single long chain salts in this group, in solution its particles were less than half as large. Its weakness as an electrolyte in benzene solution is further confirmed by its small dipole moment and loss factor. These results confirm conductance measurements which have shown that long chain substituted ammonium ions, with at least two methyl groups, permit very close approach of anions and, consequently, tight binding.[15]

B. Tri-Isoamylammonium Picrate

This salt was extensively investigated by Sharbaugh[2] as a typical example of a weak electrolyte in benzene and diphenylmethane. Further study was initiated to determine what effect a slightly polar medium, such as anisole, would have on the dielectric behavior of the salt. Two solutions at about 0.1 molar were studied, one in benzene duplicating the most concentrated solution of Sharbaugh, the other in anisole.

For the first, the physical constants were found to be slightly different from those determined by Sharbaugh, the most important difference being that for the molar polarization, P_2. Using the polarization values obtained for this salt by Geddes and Kraus[13] and the present P_2 values, one obtains a smooth plot of P_2 against concentration; Sharbaugh's P_2 value, on the other hand, necessitates a change in curvature of the plot that is hard to justify. Good agreement with Sharbaugh's results on the dielectric loss was found.

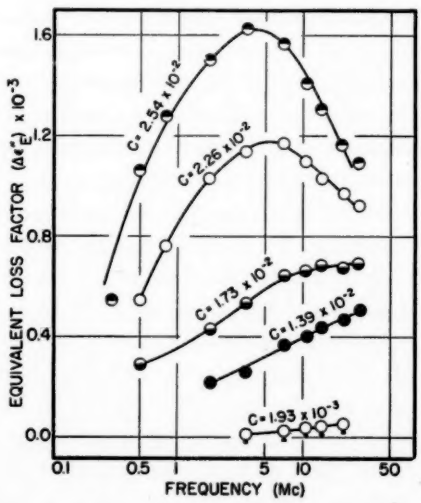

FIG. 2. Equivalent loss factor as a function of concentration and frequency for $OctBu_3NNO_3$ in C_6H_6.

[15] H. L. Pickering, thesis, Brown University (1947).

TABLE V. Salt series studied.

$OctBu_3N^+$	SCN^-	Cl^-
NO_3^-, $HCOO^-$	$Oct_2Bu_2N^+$	$Oct_2Bu_2N^+$
Cl^-, I^-	$OctBu_3N^+$	$OctBu_3N^+$
SCN^-, Pi^-	Bu_4N^+	

The changes in dielectric behavior introduced by shifting to an anisole solution were several. As might be expected solely on the basis of the increased viscosity, which was almost double that of the benzene solution, the dipole conductance and loss factor of the picrate in anisole were roughly twice those found for the salt in benzene. An examination of Fig. 1 with its plots of $d(\ln \Delta\epsilon'')$ *vs.* $d \ln \nu$ shows that even in a mildly polar solvent the salt gives rise to a monodisperse system, for the curves have the predicted 45° slope. The deviation from linearity at the lower frequencies probably reflects the greater errors in the range where one works with small differences. More marked changes have occurred in two other quantities; the molar polarization has been depressed from 2240 to 1390 cc, and the critical frequency has increased from 490 to 590 Mc in spite of the tendency of the greater viscosity of the anisole solution to lower ν_c. Both of these marked effects can be traced to the considerably smaller particle radius, which has dropped from the 4.8A observed in benzene to 3.4A. Since the extent of electrolytic dissociation is directly related to the polarity of the solvent, the observed effect is in the right direction.

C. The Variation in Dielectric Properties with Molecular Size and Shape

(1) *General Remarks.*—In order to obtain a more systematic picture of the influence of molecular shape and size on dielectric absorption, aggregate size, and (to some extent) on association, series of salts with the same anion or cation were studied. Three criteria governed the selection of the salts: (1) ease of preparation; (2) sufficient solubility so that a range of concentration could be studied; (3) possession of an ion or ions sufficiently large to bring the maximum in the

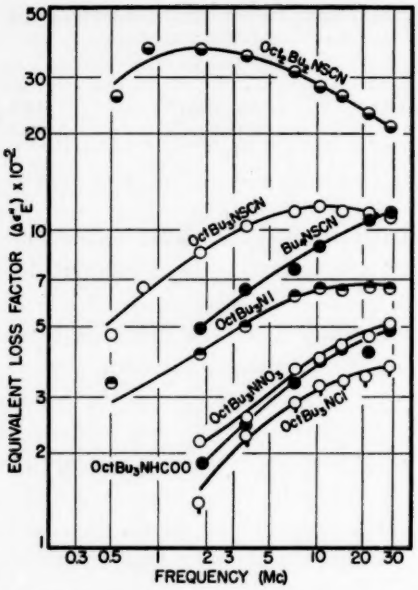

FIG. 3. Equivalent loss factor as a function of frequency for equimolar solutions of various salts in benzene. $C=1.4\times10^{-2}$ for all salts except Bu_4NSCN where $C=1.7\times10^{-2}$; Oct_2Bu_2NSCN and Bu_4NSCN data from Sharbaugh's work.

loss factor below 30 Mc at fairly low concentrations (0.01–0.05 molar).

Satisfying all these requirements was the octadecyltributylammonium salt series with solubilities for a given anion in general greater than 0.025 molar at 25°. In addition, short chloride and thiocyanate series provided information about cation influences. Sharbaugh's thiocyanate results are included in the latter series. The various combinations considered are compiled in Table V.

(2) *Octadecyltributylammonium Salts.*—The octadecyltributylammonium ion provided a convenient cation base for the study of anion influences on absorption and association. In all, six anions of various sizes and degrees of symmetry, both with respect to shape and charge, were examined. They were the completely symmetrical chloride and iodide ions, the linear thiocyanate ion, and the planar formate, nitrate, and picrate ions. The thiocyanate, formate, and picrate ions have unsymmetrical charge distributions, the negative charge being concentrated on the nitrogen and oxygen atoms.

While the differences in dielectric behavior for most of the anions in this series were small, the introduction of the very large picrate ion produced so marked a change in properties that a loss factor minimum rather than the usual maximum was observed in the band of frequencies available. An entirely similar behavior has been noted in preliminary investigations of closely related picrates. The existence of an equilibrium between two distinct particle types which have widely separated absorption regions, one at low frequencies and another at very high ones, is strongly suggested. Further information about the dielectric constant and absorption, particularly in the 10- to 1000-kc region, are needed to extend the usefulness of these results. Accordingly, the present data will be reserved until a complete report can be made in a succeeding paper.

To permit an effective correlation of differences in behavior produced by the combination of a variety of anions with the octadecyltributylammonium cation, absorption data were obtained at two or more concentrations for all but one of the salts. Since they exhibited similar properties as a function of concentration, a discussion of the characteristics of the ocatdecyltributylammonium nitrate concentration system can be considered representative.

Five nitrate solutions were studied in the range of concentration from 1.93×10^{-3} to 2.54×10^{-2} molar. (The results for the most dilute solution have already been discussed in connection with data obtained from solutions of slightly soluble salts.) As may be seen from Table II, with increasing concentration, the critical frequency dropped from about 500 to 4.2 Mc. The closely related ion aggregate size increased almost proportionately, the average particle radius expanding from 6 to 26A. As a result of both these trends, the equivalent loss factor maximum increased steadily with rising concentration. Both the shift of ν_c and the increase of $\Delta\epsilon_E''$ are well illustrated in Fig. 2.

The polarization data for the nitrate should be noted. Showing a behavior typical of the quaternary ammonium salts so far studied, it has a minimum at about 10^{-2} molar followed by a sharp rise that is just beginning to level off at the highest concentration. Such a behavior is consistent with the appearance of progressively larger aggregates and the gradual increase of the equivalent loss factor with rising concentration.

As interpreted theoretically for the limiting case by Fuoss,[16] a linear decrease in molar polarization with concentration is expected for dilute solutions if aggregation of dipoles into non-polar quadrupoles is taking place. If polar clusters of greater complexity become progressively more stable as the concentration is pushed higher, e.g., above 10^{-2} molar, the minimum and subsequent rise observed for these quarternary ammonium salts appear reasonable.

From the small dipole moments of $5\text{–}7\times10^{-18}$ e.s.u. calculated for these solutions (Table II), it is evident that the dipole centers of charge must be symmetrically located since they are separated on the average by little more than 10^{-8} cm. The ratios of the squares of the calculated dipole moments for the various concentrations, 1:0.88:0.56:0.47:0.52, compare satisfactorily with the ratios of the molar solute polarizations for these solutions, 1:0.87:0.53:0.40:0.47. In view of the "averaged" nature of the moments for the more concentrated solutions, the agreement with simple Debye theory is somewhat unexpected.

Further confirmation of the behavior inferred from the polarization and loss data is supplied by the tabulation in Table III of the variation of the parameter α with concentration. For the nitrate system in particular, in going from the most dilute solution to higher concentrations, the single type of particle ($\alpha=0$ at 0.0019 molar) is apparently replaced by several more complex varieties of ion clusters (α increases from 0.49 to 0.56 in the range 0.0139 to 0.0226 molar). At still greater concentrations, the variety of aggregates has seemingly been reduced as the equilibrium shifts toward a more stable type or types (α has decreased to 0.47 at 0.0254 molar). Curves plotted using these α's are in good qualitative agreement with the experimental data.

To adapt the preceding consideration of the nitrate to a qualitative treatment of other salts investigated in this octadecyltributylammonium series, it is only necessary to note that the polarization data give curves of the same form displaced relative to one another. That the Debye quantities have been shifted in like fashion may be confirmed from Table II. Thus, all the salts exhibited a decrease in critical frequency and an increase in loss factor maximum with increasing concentration. Similarly, all appeared to have very closely spaced and symmetrically located charges in their aggregates. In general, the values of α appeared consistent with a large variety of aggregate sizes that had originated somewhere below 10^{-2} molar and were tending to be displaced by fewer, more stable clusters somewhere above 10^{-2}.

In intercomparing the data for these salts, it should be remembered that the concentration will be an important factor. With that in mind, one may consider the relative sizes of the aggregates formed at equimolar concentrations—i.e., where there are an equal number of solute molecules per unit volume of solution for each salt. In the concentration range where the comparison is to be made, these systems are polydisperse, and the physical significance of the Debye a is somewhat uncertain, being perhaps best interpreted as an average aggregate radius. It seems desirable in comparing the systems to avoid the use of a, or the more preferable volume factor a^3; instead, one may employ the experimentally determined critical frequency, which, in Debye theory, is inversely proportional to the volume.

The shift of critical frequency with change of anion is clearly illustrated in Fig. 3, where the equivalent loss factors of several salts at 1.4×10^{-2} molar are graphed against the frequency on a logarithmic scale. For convenience in inspecting the data, the critical frequencies for the salts in this series at two concentrations, 1.4×10^{-2} and 1.75×10^{-2} molar, have been collected in Table VI. Additional columns give the ratios of critical frequencies at the two concentrations. At 1.4×10^{-2} molar, a wide range of aggregate sizes is in evidence, extending from the

TABLE VI. Critical frequencies for equimolar solutions.

Salt	$\nu_c(c=1.4\times10^{-2})$	Ratios	$\nu_c(c=1.75\times10^{-2})$	Ratios
$OctBu_3NOOCH$	50*	1.3	—	—
$OctBu_3NO_3$	50*	1.3	30*	2.1
$OctBu_3Cl$	40*	1	14.3	1
$OctBu_3I$	25	0.6	8.3	0.6
$OctBu_3SCN$	11	0.3	—	—

* Estimated from graphs of $\Delta\epsilon''$ *vs.* $\ln\nu$.

[16] R. M. Fuoss, J. Am. Chem. Soc. **56**, 1031 (1934).

approximately equal-sized formate and nitrate up to the thiocyanate aggregates, which are nearly five times larger. As would be expected because of its larger anion, the iodide salt aggregates are considerably larger than those formed by the chloride. Roughly, the same ν_c ratios hold for the 1.75×10^{-2} molar solutions, implying that association has advanced at about the same rate for three salts studied at both concentrations.

It would be interesting to establish whether the variation in aggregate sizes may not, in part, be ascribed to differences in the extent of association. That is only inexactly determinable, however, even if solvent interaction is ignored, since the whole concept of the size of ions in low dielectric constant solvents is relatively unexplored. From interatomic distances, ionic and van der Waals' radii, it is possible to estimate rough "volumes" for the anions. In order of decreasing volume, such calculations place the ions as follows: $NO_3^->HCOO^-$, I^-, $SCN^->Cl^-$ with the nitrate ion about twice as large as the chloride but only a little larger than the middle three. On the basis of that evidence, it appears that the nirate and formate salts associate somewhat less, and the thiocyanate salt associates somewhat more extensively than do the chloride and iodide salts.

(3) *Thiocyanate and Chloride Salts.*—A discussion of the influence of constitution on dielectric absorption would be incomplete without some consideration of different cations as well as different anions. Two further series with the thiocyanate and chloride anion common to all members supplied such information for the tetrabutylammonium, octadecyltributylammonium, and dioctadecyldibutylammonium cations.

Probably the most striking illustration of the influence of cation size on critical frequency and on the magnitude of the absorption is to be obtained from Fig. 3. There the equivalent loss factor data available for the thiocyanate series at about 1.4×10^{-2} molar have been included with the octadecyltributylammonium series plots so that an over-all picture might be given.

In comparing results obtained for the different cations, we find that at 1.4×10^{-2} molar the thiocyanates have the following ν_c's: tetrabutylammonium, 120 Mc;[17] octadecyltributylammonium, 11 Mc; and dioctadecyldibutylammonium, about 1.8 Mc. The ratios are approximately 100:10:1.6. For octadecyltributylammonium and dioctadecyldibutylammonium chloride at a slightly higher concentration, 1.75×10^{-2} molar, the critical frequencies were 14.3 and 2.3 Mc, respectively, again in the ratio of 10:1.6. The importance of cationic size is clearly evident here, for the substitution of each octadecyl group has reduced the critical frequency by a factor of about ten.

ACKNOWLEDGMENT

The authors are grateful to Professor Robert H. Cole for suggesting the modification, for the polydisperse case, of the equation used in calculating dipole moments from absorption data and for helpful discussion in the preparation of this paper.

[17] This figure was obtained by interpolation. See reference 2 for both the Bu_4NSCN and Oct_2Bu_2NSCN data.

THE JOURNAL OF CHEMICAL PHYSICS VOLUME 16, NUMBER 8 AUGUST, 1948

Dielectric Behavior of Solutions of Electrolytes in Solvents of Low Dielectric Constant. IV.A. Dielectric Absorption of Butyl Alcohol, B. The Second Wien Effect[1]

H. A. STROBEL[2] AND H. C. ECKSTROM[3]
Metcalf Research Laboratory, Brown University, Providence, Rhode Island

(Received April 26, 1948)

A. The absorption conductivity of *n*-butyl alcohol has been carefully determined by a calorimetric method, using two independent, specially purified samples. Its dielectric behavior proved in good agreement with Debye theory. The probable source of the error in earlier butyl alcohol measurements determined with the same apparatus was ascertained. A critical frequency of 305 Mc was calculated, which is about the average of most good literature values.

B. Several benzene solutions between 0.001–0.008 molar have shown increases in conductance with field strength at 60 cycles per second in accord with Onsager's theoretical treatment of the second Wien effect.

WHILE continuing the study of dielectric properties of solutions with the calorimetric dielectric absorption apparatus described in an earlier publication,[4] it also seemed desirable to consider two unsettled problems somewhat aside from the principal course of investigation: (a) the careful determination of the absorption conductivity and the critical frequency of pure *n*-butyl alcohol, and (b) the obtaining of further data to establish whether a systematic dependence of conductance on field strength could be observed at very low frequencies by use of the calorimetric method.

The first problem was posed by the general lack of agreement among the butyl alcohol dielectric absorption data recorded in the literature. During the last twenty years, the investigations of butyl alcohol have ranged from an examination of the dielectric properties at high frequencies (5–30 Mc) and a prediction of the behavior at greater frequencies through the use of the Debye equations, to actual study in the region of strong dielectric constant dispersion. Since all these researches have yielded values of the critical frequency ν_c, that quantity may be conveniently employed in the intercomparison of results. Even with widely differing techniques and procedures, careful work should have produced data in at least fair agreement; yet, most of the predicted and measured values of ν_c range from 185 to 385 Mc, while the value determined by Sharbaugh with the present apparatus lies at 1600 Mc.[4]

In spite of the disagreement, the extensive research into the dielectric properties of this alcohol have made it a useful standard for absorption work. It seemed worth while, therefore, to obtain a reliable set of data for the alcohol, and to seek an explanation of the very high critical frequency obtained by Sharbaugh.

The second problem arose quite naturally, since in using the calorimetric method, conductivities at a given frequency are often measured at several field strengths. Now, as a result of the work of Wien and others,[5,6] it is well known that departures from Ohm's law are found for all electrolyte solutions at high field strengths, though the deviations from the law become progressively smaller as the frequency increases. Two effects are operative to produce the increase of conductance with field strength that is observed. The first Wien effect is exhibited principally by strong electrolytes as ions are pulled from their retarding ion atmospheres; the second, with which this paper is concerned, results from increased dissociation of the solute and is displayed mainly by weak electrolytes.

Previous investigations with the dielectric

[1] This paper is based on a portion of a thesis submitted by H. A. Strobel in partial fulfillment of the requirements for the degree of Doctor of Philosophy in the Graduate School of Brown University, October, 1947.

[2] Metcalf Fellow, Brown University, 1946; Coffin Fellow, 1946–47. Present address: Duke University, Durham, North Carolina.

[3] Present address: Research Laboratory, Stanolind Oil and Gas Company, Tulsa, Oklahoma.

[4] Sharbaugh, Schmelzer, Eckstrom, and Kraus, J. Chem. Phys. **15**, 47 (1947); Sharbaugh, Eckstrom, and Kraus, J. Chem. Phys. **15**, 54 (1947).

[5] An extensive bibliography is available in a review article by H. C. Eckstrom and Ch. Schmelzer, Chem. Rev. **24**, 367 (1939).

[6] D. J. Mead and R. M. Fuoss, J. Am. Chem. Soc. **61**, 2047, 3589 (1939); *ibid.* **62**, 1720 (1940).

absorption apparatus in this laboratory did not succeed in definitely establishing the existence of such a dependence on field strength. An effect was reported, however, for the only two cases where determinations at very low frequencies were extended to fields greater than three kv/cm.[7]

To ascertain the conditions under which a second Wien effect can be observed with the present method and to estimate its magnitude, additional investigations have been made.

EXPERIMENTAL

Two entirely independent, specially purified samples of *n*-butyl alcohol, generously supplied by Commercial Solvents Corporation and U. S. Industrial Chemicals, Inc., were further treated in this laboratory by a week of shaking over activated alumina pellets to remove moisture and by subsequent distillation. No measurable difference in the dielectric constant or dipole conductivity of the final product was noted whether the butanol was distilled (a) under nitrogen at atmospheric pressure, (b) with air in the still at atmospheric pressure, or (c) from an icewater bath to a dry ice-isopropyl alcohol bath at the low pressures created by a Hyvac pump. One must conclude that the very small amounts of oxidation products, such as butyraldehyde, which might have been present produced no effect on dielectric properties detectable by the present technique. All specific conductances ranged from $2-4\times10^{-8}$ ohm^{-1} cm^{-1}.

Solvent benzene and the several salts used were prepared and purified as described in an accompanying paper.[8]

TABLE I. Average absorption conductivity and loss factor data for pure butanol.

Frequency (Mc)	Absorption conductivity $\Delta\kappa\times10^7$	Loss factor $\Delta\epsilon''$
1.827	0.91	0.089
3.504	3.3	0.17
7.045	13.6	0.35
10.512	30.9	0.53
14.090	58	0.74
21.135	125	1.17
28.180	225	1.44

[7] A. H. Sharbaugh, thesis, Brown University (1943).
[8] H. A. Strobel and H. C. Eckstrom, J. Chem. Phys. 16, 817 (1948).

The calorimetric method, the dielectric absorption apparatus, and necessary auxiliary equipment have been discussed briefly in the accompanying paper and are described in detail in Part I of this series.[4] Sixty-cycle current was furnished from the power mains by an arrangement consisting of a Variac connected either directly, or through a step-up transformer, to the cell circuit. All voltages at that frequency were read directly on a Weston 341 voltmeter.

The design of the calorimetric cells from which the Wien effect data were secured has already been described.[4] For such measurements the largest cell with a cell constant of 0.002326 and concentric cylindrical electrodes separated by about one millimeter was used. Since the outer electrode overlapped the inner one by 2–4 mm, appreciable edge effects probably existed.

Audiofrequency conductance measurements were made in the manner indicated previously (see reference 4, p. 55). For butyl alcohol, however, it was evident that some sort of electrode or glass absorption effect was operative in the audiofrequency conductance cells, and a slightly different procedure proved necessary. Using the same bridge method, the audiofrequency conductance, κ_0, of the butanol samples was measured in the *calorimetric cells* immediately after the absorption conductivity determinations. In that way one obtained κ_0's from which consistent loss data could be calculated. The success of the technique can probably be attributed to two factors: (a) the κ_0 of the alcohol sample actually in the calorimetric cell is measured;[9] and (b) absorption on electrode surfaces should be minimized since the layer of molecules next to those surfaces has been constantly renewed as a result of the dielectric heating of the fluid during the dipole or absorption conductivity determinations.

THEORY

In the accompanying paper it was shown that, for the present calorimetric method, the conductance κ at any frequency ω is given by

$$\kappa_\omega = V_0^2 t_0 \kappa_0 / V_\omega^2 t_\omega, \qquad (1)$$

[9] Exposure to air or to traces of substances that might not be removed in careful cleaning of the calorimetric cells readily affects the conductance of a pure, short-chain alcohol; however, no effect on dielectric properties could be ascertained by the present method.

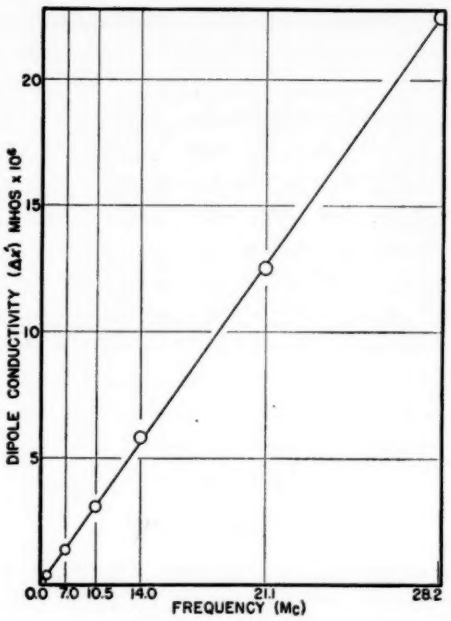

FIG. 1. Dipole conductivity of pure butanol as a function of frequency squared.

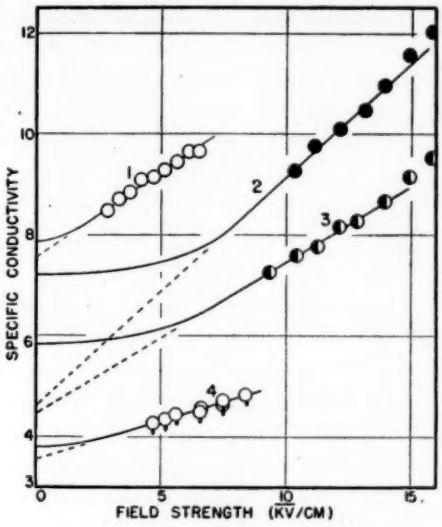

FIG. 2. Specific conductivity as a function of field strength at 60 c.p.s. for benzene solutions.

Linear extrapolation to zero field strength indicated by dashed extension.

$\kappa_E \times 10^{10}$	$\kappa_E \times 10^{11}$
1. 0.00104 molar $Bu_4N\Phi_3BOH$	2. 0.00723 molar Oct_2Me_2NSCN
4. 0.00193 molar $OctBu_3NNO_3$	3. 0.00333 molar Oct_2Bu_2NSt

where the subscripts 0 and ω refer to a 60-cycle reference frequency and any other frequency ω, respectively, V is the voltage across the calorimetric cell, and t represents the time of rise necessary for the production of a standard amount of heat Q. For most solutions, $V_0^2 t_0 \kappa_0$ is a constant for each cell and is denoted by A; for the more dilute solutions, on the other hand, Ohm's law has been observed to fail at 60 cycles, so that κ_0 and, consequently, $V_0^2 t_0 \kappa_0$ will vary with the field strength. At that frequency, the standard heat Q, generated in the system when Ohm's law is invalid, can be represented as

$$Q = V_E^2 t_E \kappa_E / z,$$

where the quantity κ_E is a type of time-average conductance at any particular field strength E. (In these measurements E has been obtained in peak kv/cm.) Thus, it is possible to determine κ_E as a function of field strength through use of an expression analogous to Eq. (1),

$$\kappa_E = A / V_E^2 t_E.^{10}$$

For the type of equivalent, highly associated electrolytes being considered in this paper, Onsager[11] found the following linear dependence of specific conductance κ on the average field strength $\bar{E}$:

$$\kappa/\kappa_0 = 1 + (e^3/4\epsilon_0 k^2 T^2)\bar{E}, \qquad (2)$$

where κ_0 is the conductance at very low fields, e the electronic charge, and ϵ_0 the audiofrequency dielectric constant. In order to compare the time average κ_E with the Onsager result, it will be helpful to consider the calorimetric method in more detail. For an alternating field of angular frequency ω, from Onsager's result the field dependence of κ will be of the form

$$\kappa = \kappa_0[1 + BE_m|\sin\omega t|],$$

where B is the Onsager slope and E_m is the peak value of the field. The heating per cycle, Q_c, obtained from the calorimetric measurements may then be formulated as

$$Q_c = 2\kappa_0 \int_0^{L/2} (1 + BE_m|\sin\omega t|)E_m^2 \sin^2\omega t dt,$$

where L is the period. By integrating this equation and multiplying through by the frequency, one obtains the heat per second Q'. But this may also be expressed $Q' = \kappa_E E_m^2/2$. Equating

[10] The substitution of A is made necessary only because calorimetric measurements cannot be made on these weakly conducting solutions at the very low voltages where $\kappa_E = \kappa_0$ and $V_0^2 t_0 \kappa_0$ is a constant.

[11] L. Onsager, J. Chem. Phys. 2, 599 (1934).

TABLE II. Constants observed and calculated for butanol.

Observer	$\kappa_0 \times 10^7$ (ohm^{-1} cm^{-1})	ϵ_0	Critical frequency ν_c (Mc.)	Molecular radius a(A)	Relaxation time τ (sec.)
Malsch*,[a]	—	18.4	185	2.6	—
Schmelzer*,[b]	2.6	17.5	200	2.6	—
Keutner[c]	3.1	—	288	2.4	1.17×10^{-10}
Strobel	0.3	17.4	305	2.4	1.06×10^{-10}
Keutner and Potapenko*,[d]	—	—	315	2.2	—
Filippov[e]	—	19.3	363**	—	—
Hackel[f]	1.4	17.2	385	—	8.8×10^{-11}
Sharbaugh***	0.56	17.7	1600	1.4	2.0×10^{-11}

* Data taken at 18 or 20°; all other data at 25°.
** Calculated from Filippov's data.
*** See reference 4, p. 54.
[a] J. Malsch, Physik. Zeits. **33**, 19 (1932).
[b] Ch. Schmelzer, Ann. d. Physik **28**, 35 (1937).
[c] E. Keutner, Ann. d. Physik **27**, 29 (1936).
[d] Keutner and Potapenko, Physik. Zeits. **40**, 100 (1939).
[e] M. I. Filippov, J. Phys. U.S.S.R. **1**, 479 (1939).
[f] W. Hackel, Physik. Zeits. **38**, 195 (1937).

TABLE III. Experimental slopes for second Wien effect.*

Salt	Molarity ($C\times10^3$)	Field strength range practicable av. kv/cm	Experimental slope/κ_0**
Bu_4NSCN***	3.66	1.9– 4.7	0.022
$OctBu_3NI$	1.60	4.7– 8.4	0.027
$OctBu_3NI$	2.60	3.7– 6.0	0.025
$OctBu_3NNO_3$	1.93	4.7– 8.4	0.029
$Bu_4N\Phi_2BOH$	1.03	2.8– 6.5	0.031
Oct_2Bu_2NSt	3.33	9.3–15.8	0.039
Oct_2Me_2NSCN	7.23	10.3–15.8	0.047

* Abbreviations used: Oct, octadecyl; Bu, butyl; St, stearate; Φ, phenyl.
** Corrected by multiplication by the factor $\frac{3}{4}$ as indicated in the section on theory.
*** Data obtained by private communication with Dr. Sharbaugh.

these two values of Q', it is apparent that

$$\kappa_E/\kappa_0 = 1 + 8BE_m/3\pi.$$

It remains to put the slope in terms of the average field strength $\bar{E}$. Since $\bar{E} = 2E_m/\pi$, the slope obtained using the calorimetric values κ_E will be 4/3 larger than the Onsager value B.

RESULTS

In Table I are listed the average values of the absorption or dipole conductivities and the calculated loss factors obtained for the samples of pure butanol. The absolute accuracy is estimated to be ±2 percent. Good agreement was obtained between the different samples when used in two different calorimetric cells. The datum at 28 Mc could be obtained only from one cell and may be less accurate.

For butyl alcohol, the following physical constants were measured at 25°: density, 0.8060 g/cm^3; specific conductance, $2-4\times10^{-8}$ ohm^{-1} cm^{-1}; audiofrequency dielectric constant ϵ_0, 17.42; viscosity, 2.56 centipoises; optical frequency dielectric constant, n^2, 1.960.

The experimentally observed conductance-field strength slopes, corrected as indicated in the preceding section, are collected in Table III. In addition, there is listed the field strength range over which measurements were practicable, which was determined by the requirement that rising times be within the span, 5–25 sec.

DISCUSSION

A. Butyl Alcohol

According to Debye theory, the absorption conductivity of polar molecules should increase linearly with the square of the frequency in a region where $\nu^2 \ll \nu_c^2$, ν being the frequency, and ν_c the critical frequency; Fig. 1 illustrates the validity of this equation for butyl alcohol. From the data ν_c has been calculated to be 305 Mc, which corresponds to a relaxation time of 1.06×10^{-10} second and a molecular radius of 2.4A. In Table II are collected the several values of pertinent constants that have been measured and calculated for butanol. The symbols κ_0 and ϵ_0 again denote the audiofrequency conductivity and dielectric constant.

It will be profitable to examine briefly the results of the other investigators with a view to finding possible sources for the discrepancies in the reported data. As suggested in the introduction, the critical frequency can serve as a convenient criterion of agreement. First, it should be considered that the other κ_0's were greater by factors of 5–10 than the present one, so that the relative purity of those samples is not assured and may account for some disagreement. Another factor is the temperature dependence of ν_c; values at 20°C are about 15 percent low according to Hackel (see reference f, of Table II), who investigated the influence of the temperature on dielectric properties from 20–40°C. Accordingly, the critical frequencies reported by Malsch and Schmelzer should be about 220 and 230 Mc, narrowing the spread somewhat, though the value of Keutner and

Potapenko becomes 360 Mc. Also the reduction of the 19.3 value observed for the audiofrequency dielectric constant by Filippov to about the average value 17.4 (neglecting the small temperature dependence) brings his ν_c down to 325 Mc.

The probable explanation of the high ν_c value determined by Sharbaugh was discovered in the course of measuring the audiofrequency conductivity (cf. experimental section). The usual procedure was found to yield κ_0's that were too low, which would give low dipole conductivities and a high ν_c.

B. Second Wien Effect

At 25°C in benzene Eq. (2) becomes

$$\kappa/\kappa_0 = 1 + 0.024\bar{E}.$$

An inspection of Fig. 2 reveals that the conductance-field curves are linear in accord with this equation (though their slopes differ) over the range through which data were taken. The slight deviation toward higher conductivities at about 15 kv/cm shown by curves (2) and (3) may be explained by the fact that a square term in $\bar{E}$ first becomes important at about that point.

The most interesting region of the curves is the rather flat initial portion. While no data was obtained there, it is known that the conductance-field curve must have its intercept on the conductivity ordinate at κ_0. Accordingly, the conductance has been represented as remaining almost constant for a time as $\bar{E}$ increases and then connecting smoothly with the known linear portion at higher fields. The presence of an ion atmosphere successfully accounts for the slow initial increase,[6] since the conductivity rises rapidly only when the ions move quickly enough so that an atmosphere has insufficient time to form. It seems evident that solutions of higher concentration showed no Wien effect at 60 c.p.s. because the field strength required for measurements (less than 3 kv/cm) was too low to force the conductance beyond the ion atmosphere region.

The corrected slopes in Table III are seen to be in fair agreement with the theoretical $0.024\kappa_0$ with the exception of the two values determined at much stronger fields. These results are subject to error because of the unavoidable edge effects mentioned earlier and because of the known imperfection of the 60-cycle wave form at the higher field strengths. In addition, both the slope of the curves and their relative distance above the $\bar{E}$ axis are affected by another type of error, the uncertainty of ± 5 percent in the heating constant, A, which was used in the calculation of κ_E. A more detailed discussion thus seems unjustified.

At higher frequencies (0.1–28 Mc) no evidence of a dependence of conductance on field strength has been observed. For the solutions that have been studied, the Langevin relaxation time, the time required to establish equilibrium between the charge distribution and the external field,[12] ranges from milliseconds for the dilute systems considered here down to 2 microseconds for the more highly conducting solutions. A second Wien effect might thus reasonably be expected for the more concentrated solutions below about 0.3 Mc where the period of the oscillation (2–6 microseconds) is sufficiently long to allow the effect to form. However, the field strengths used for such solutions at these higher frequencies were seldom as great as 2 kv/cm; the failure of any effect to appear does not seem surprising in view of the extent of the initial flat portion of the conductivity curves.

ACKNOWLEDGMENT

The authors are grateful to Professor Robert H. Cole for much helpful discussion in the preparation of this paper.

[12] Onsager, reference 11. The Langevin relaxation time, τ_L, is defined as $\tau_L = \epsilon_0/72\pi \times 10^{11}$ and equals $10.1 \times 10^{-14}/\kappa$ for benzene solutions.

Further Alkylbenzene Spectra to 1750A*

J. R. PLATT
Department of Physics, University of Chicago, Chicago, Illinois

AND

H. B. KLEVENS
Department of Biochemistry, University of Minnesota, St. Paul, Minnesota

(Received May 11, 1948)

The absolute absorption intensities of *n*-butyl-, secondary butyl-, and tertiary butylbenzene and of 1,3,5-trimethylbenzene (mesitylene) have been measured to about 1750A. Increased branching of the side chain shifts the 1900A and 2100A bands slightly to shorter wave-lengths but increases the total oscillator strength from 1.04 for *n*-butyl to 1.57 for tertiary butyl. The wave-length shifts are in the same direction, the intensity changes in the opposite direction from those observed in the 2600A bands of these same compounds. The mesitylene spectrum is about 1000 cm^{-1} to the red of the meta-xylene spectrum and its oscillator strength is reduced to 0.89, almost as low as that of benzene itself.

CONTINUING our earlier studies on alkylbenzene spectra in the far ultraviolet,[1] we have obtained the absorption curves of *n*-butyl-, secondary butyl-, and tertiary butylbenzene and of mesitylene to about 1750A in *n*-heptane solution in a 0.13 mm cell. The apparatus and techniques used were identical with those previously described. This is the first time absorption intensities have been measured below 2000A on these compounds, though the vapor spectrum of mesitylene in the 2000A–1000A region was obtained earlier in this laboratory.[2]

The compounds used here were Eastman Kodak Company samples which were purified by recrystallizing several times, then by distilling twice through a Podbielniak column of 50 equivalent plates, taking the center cut each time. The final constants were: mesitylene, n_D^{20} 1.4985, b.p. 165°C; *n*-butylbenzene, n_D^{20} 1.4890, b.p. 181°C; secondary butylbenzene, n_D^{20} 1.4898, b.p. 173°C; tertiary butylbenzene, n_D^{20} 1.4941, b.p. 169°C.

The spectra are qualitatively and quantitatively similar to those of the alkylbenzenes studied earlier, with a band of moderate intensity near 2100A and a strong allowed transition at shorter wave-lengths. The butylbenzene curves are shown in the top half of Fig. 1. The mesitylene curve is in the bottom half together with earlier curves for benzene with 0, 1, and 2 alkyl substituents in the meta sequence for comparison. Some of the main features of the new curves are tabulated in Table I.

The *n*-butyl curve coincides with the earlier ethylbenzene curve within the experimental error of about 10 percent at every point, and the oscillator strengths or *f*-values obtained from the integrated areas under the curves differ by only

TABLE I. Main features of spectra of butylbenzenes and mesitylene.

	n-butyl	Secondary butyl	Tertiary butyl	Mesitylene
	A. Forbidden transition			
Onset of absorption	2180A 45800 cm^{-1}	2170 46100	2160 46300	2270 44000
Peaks of component bands	46700 47600 48600 49500(?)	47000 47800 48700 49700(?)	47000 47900 48800 49700	44800 45700 46600
ϵ_{max}	7000	10800	9300	9500
Approx. oscill. strength, *f'* of this transition (to arbitary cut-off)	0.11 (2000A)	0.18 (1995)	0.16 (1985)	0.12 (2110)
	B. Allowed transition			
Peak	1890A 52900 cm^{-1}	1880 53100	1880 53200	1990 (double) 50300
ϵ_{max}	50000	70000	85000	46000
Components	51800 53000 54200(?) 55000(?)	52100 53100 54200(?)	52400 53300	49800 50900
Total oscill. strength, *f* of both transitions	1.04	1.37	1.57	0.89

* This work was assisted by the Office of Naval Research under Task Order IX of Contract N6ori-20 with the University of Chicago.

[1] J. R. Platt and H. B. Klevens, Chem. Rev. **41**, 301 (1947).

[2] W. C. Price (unpublished).

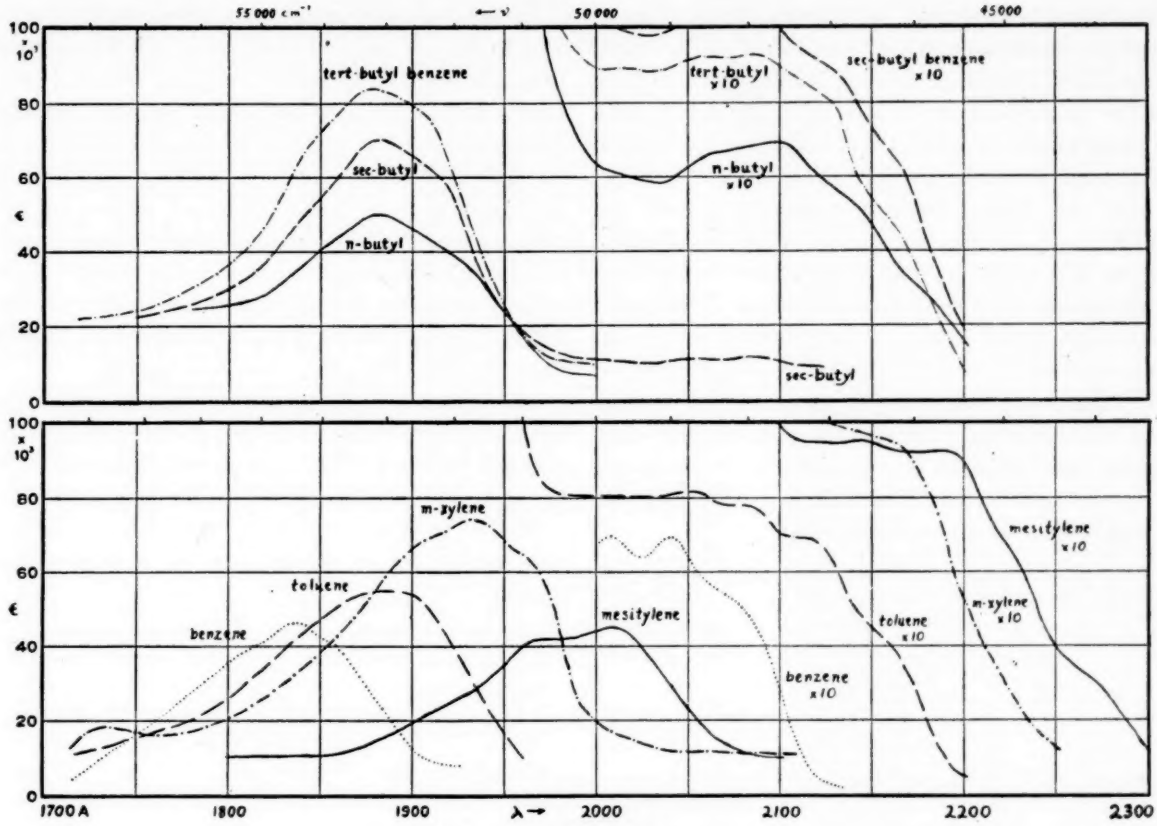

FIG. 1. Spectra of alkylbenzenes.

seven percent. This agreement supports the familiar rule that molar absorption is almost independent of the length of saturated side chains; and it therefore gives us some confidence in the consistency and reproducibility of our measurements.

The secondary butyl curve is shifted about 250 cm^{-1}, and the tertiary butyl curve about 350 cm^{-1} to shorter wave-lengths from the *n*-butyl curve. These shifts are in the same direction as the shifts observed in the 2600A bands of these same compounds[3, 4] but are larger, a phenomenon which we have observed in several other benzene derivatives. The intensity changes, on the other hand, vary in the opposite direction from the intensity changes in the longer wave-length bands, the ratio of the *f* values of tertiary to normal butyl being about 1.5 here, where in the 2600A bands the ratio is about 0.8.[4] Probably because of this crossover, the sequence is shuffled in the 2100A bands, with the secondary butyl curve lying above the other two in that region.

The crossover of intensities results in the curious fact that the 2600A bands in tertiary butylbenzene[4] are actually weaker relative to the 1900A bands, that is to say, *more forbidden*, than in benzene itself! This re-emphasizes the remark made earlier[1] that it is not merely loss of symmetry which causes the usual increase of intensity of the 2600A bands in substituted benzenes; for tertiary butylbenzene has quite low symmetry. The changes must evidently be understood in terms of specific electronic interactions of the substituent with the ring, which for some reason reduce the relative intensity in the present case.

Since the wave-length shift in the butylbenzenes is in the same direction as that observed in the 2600A bands, while the intensity change is in

[3] See, for example, F. A. Matsen, W. W. Robertson, and R. L. Chuoke, Chem. Rev. 41, 273 (1947).

[4] American Petroleum Institute Research Project 44 at the National Bureau of Standards. Catalog of Ultraviolet Spectrograms. Sequences of curves from several laboratories.

the opposite direction, it follows that at least two parameters must be assigned even to alkyl substituents in order to account for the changes in the three benzene-like bands. The same conclusion might have been reached from inspection of intensities alone in the earlier xylene curves, where the 1900A benzene-toluene-o-xylene sequence was in the same order as in the 2600A bands, but the meta-para order of intensities was reversed. Since the differences seem to be considerably larger than experimental error, it follows that no one-parameter interpretation of the changes in the alkylbenzene 2600A bands can be extended even approximately to the shorter wave-length bands. The need for more than one parameter in the 2600A bands has been remarked on by various authors.[3,5]

[5] Theodore Förster, Zeits. f. Naturforschung **2a**, 149 (1947).

In the meta sequence from benzene to mesitylene in Fig. 1, the red shifts with alkyl substitution are seen to be quite regular, about 1200–1500 cm^{-1} for each additional methyl group. These are several times as large as the shifts in the 2600A bands. The f value for mesitylene is low as it is for p-xylene, almost as low as for benzene itself. Symmetrical substitution with permanent dipole moment zero, seems to lead to low oscillator strength in these bands. In the 2600A bands, mesitylene has lower intensity than m-xylene, but p-xylene has higher.[4]

The spectra of N-trimethyl and B-trimethyl borazole have been obtained in this laboratory and will be compared in a subsequent paper with the spectrum of mesitylene, which they resemble.

We are indebted to Mr. Charles Rector for his able assistance in taking and in reducing the plates.

Erratum: Heats of Dissociation of the N_2 Molecule and the NH Radical

[J. Chem. Phys. 16, 602 (1948)]

GEORGE GLOCKLER
Department of Chemistry, University of Iowa, Iowa City, Iowa

The Figs. 1 and 2 should be interchanged leaving the legend as printed.

Letters to the Editor

THIS section will accept reports of new work, provided these are terse and contain few figures, and especially few halftone cuts. The Editorial Board will not hold itself responsible for opinions expressed by the correspondents. Contributions to this section should not exceed 600 words in length and must reach the office of the Managing Editor not later than the first of the month preceding that of the issue in which the letter is to appear. No proof will be sent to the authors. The usual publication charge ($4.00 per page) will not be made and no reprints will be furnished free.

Secondary Processes of Ion Production in the Mass Spectrometer

J. J. MITCHELL, R. H. PERKINS AND F. F. COLEMAN*
Beacon Laboratories of The Texas Company, Beacon, New York
June 1, 1948

IN the early days of mass spectrometer work, secondary production of ions was a common occurrence, primarily because of high gas pressures in the ionization chamber. Hogness and Lunn,[1] for instance, found that as the pressure of hydrogen in the ionization chamber was raised above 1 micron of mercury the ion intensity caused by H_2^+ decreased and that due to H_3^+ increased, both linearly with the pressure. They reasoned that the 48-volt electrons used to produce ions gave rise to metastable H_2^+ ions which then took part in the reaction:

$$H_2^+ + H_2 \rightarrow H_3^+ + H.$$

During some recent work in this laboratory, using the ratio of the $m/e=45$ ion intensity to $m/e=44$ ion intensity in CO_2 produced by burning various samples as a measure of their C^{13} to C^{12} ratios, the secondary production of HCO_2^+ was encountered at fairly low ionization chamber pressures.** Sample pressures were $150–225\times10^{-3}$ mm Hg on the high pressure side of the entrance leak so that the ionization chamber pressures were of the order of 5×10^{-4} mm Hg.

The failure of a drying agent in a CO_2 purification train and a resulting high water content gave rise to spuriously high C^{13} to C^{12} ratios when the ratio of the $m/e=45$ ion intensity to $m/e=44$ ion intensity was used as a measure of C^{13} content. Since such an effect would interfere seriously with the accuracy of this method of determining the C^{13}/C^{12} ratio, various gases were added to pure CO_2 to determine the magnitude and cause of the effect. Tables I and II show the results of adding water, hydrogen and rare gases to pure CO_2 in terms of excess ratio for the Type II and Type III ionization chambers made by the Consolidated Engineering Corporation. An electron energy of 50 volts was used in the first case and 70 volts in the second. Excess ratio is the difference between the ratio of $m/e=45$ to $m/e=44$ for the mixture in question and that for pure CO_2. This has been used since it appears certain from the results obtained with helium mixtures that the excess ratio is a measure of the amount of $(HC^{13}O_2^{16})^+$ present. Table III showing the effect of adding deuterium confirms this interpretation since no increase in $m/e=45$ ion intensity is observed, but instead an increase in $m/e=46$, corresponding to $(DC^{12}O_2^{16})^+$.

TABLE I. Effect of added gases on the $m/e=45$ to $m/e=44$ intensity ratio for CO_2.
(Type II ionization chamber)

Added gas	Mole % of added gas	Excess ratio ×100
H_2O	4.45	0.027
	5.0	0.020
	8.02	0.029
	9.0	0.012
	42.7	0.121
	62.3	0.097
H_2	50*	0.106
Argon	50*	−0.015
Average ratio for pure $CO_2\times100=1.178\pm0.011$.		

* Approximate.

From Tables I and II it will be seen that the effect is greater for the Type II ionization chamber than for the Type III. It is interesting to note that the results for hydrogen mixtures and for water mixtures in the Type III ionization chamber can be fitted by the relations

$$R=0.0098M$$

and

$$R=0.00104M,$$

where R is the excess ratio times 100 and M is mole percent of hydrogen in the first case and of water in the second, with standard errors of estimate of 0.007 and 0.006, respectively.

TABLE II. Effect of added gases on the $m/e=45$ to $m/e=44$ intensity ratio for CO_2.
(Type III ionization chamber)

Added gas	Mole % of added gas	Excess ratio ×100
H_2	8.99	0.018 ±0.007
	24.0	0.023 ±0.007
	49.5	0.047 ±0.008
	87.5	0.079 ±0.026
H_2O	7.8	0.011
	17.4	0.022
	37.0	0.030
	69.2	0.072
He	9.5	−0.003 ±0.005
	24.7	−0.005 ±0.004
	50.2	0.003 ±0.003
	50.3	0.004 ±0.010
	75.9	0.012 ±0.012
Average ratio for pure $CO_2\times100$.		
During H_2O measurements—1.167 ±0.008		
During H_2 measurements—1.150 ±0.006		
During He measurements—1.143 ±0.003		

In order to determine if the effect was similar to that reported by Hogness and Lunn for hydrogen, the $m/e=45$ to $m/e=44$ ratio was measured for a mixture containing 40.1 mole percent of hydrogen at three different sample pressures. As Fig. 1 shows, excess ratio, or HCO_2^+ relative ion intensity, increases in direct proportion to sample pressure and hence to pressure in the ionization chamber, in complete agreement with the results on H_3^+ from pure hydrogen.

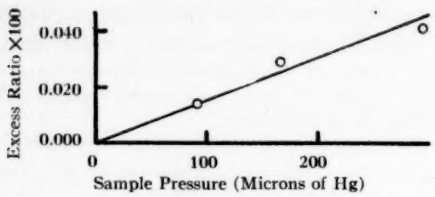

FIG. 1. Effect of sample pressure on the $m/e=45$ to $m/e=44$ ion intensity ratio for a hydrogen-CO_2 mixture.

TABLE III. Effect of addition of deuterium to CO_2.

Mole % of added gas	$(m/e=45)/(m/e=44)$ ×100	$(m/e=46)/(m/e=44)$ ×100
	Type II ionization chamber.	
0	1.179	0.412
50*	1.156	0.481
	Type III ionization chamber.	
0	1.155	0.407
51.3	1.153	0.429

* Approximate.

The authors wish to thank J. E. Mapes for aiding in the measurements made on hydrogen and helium mixtures in the Type III ionization chamber.

* Present address: U. S. Navy Electronics Laboratory, San Diego, California.
[1] T. R. Hogness and E. G. Lunn, Phys. Rev. **26**, 44–55 (1925).
** The mass spectrometer is a Model 21–102 built by Consolidated Engineering Corporation, Pasadena, California.

In Situ Study of the Thermal Decomposition of Ethylene Oxide by Infra-Red Spectrometry

G. L. SIMARD, J. STEGER, T. MARINER, D. J. SALLEY, AND V. Z. WILLIAMS*
American Cyanamid Company, Stamford, Connecticut
May 18, 1948

THE development of a high temperature seal[1] for sodium chloride plates to Pyrex made possible the construction of a cell for the direct study of homogeneous gas reactions by infra-red spectrometry. In order to evaluate this method for kinetic studies, the thermal decomposition of ethylene oxide was investigated. Firstly, decomposition products were identified from spectra recorded by wave-length scanning during reaction. Bands which persisted after complete decomposition were obviously from the spectra of final products. Bands which appeared and disappeared during reaction were from the spectra of intermediate products. The identity of the products was established in the usual manner from band positions, structures, and relative intensities. Secondly, quantitative measurements of reactant and products were made during reaction by continuous transmission recording at selected band positions. Products exhibiting strong pressure broadening could not be readily measured by infra-red and were analyzed by mass spectrometry on samples withdrawn from the reaction cell. The reaction was studied at 410°C, 440°C, and 470°C at initial ethylene oxide pressures of 200 mm and 400 mm.

Infra-red emission[2] was observed of sufficient intensity to be a useful adjunct to absorption spectra for the identification of products. Spectral bands were more prominent relative to background in emission than in absorption, and the techniques for emission minimized interference effects by atmospheric vapors.

The quasi-unimolecular nature of the decomposition, the activation energy, and the final products previously reported[3] were confirmed. Good agreement was found between the rates of decomposition of ethylene oxide determined from the spectrometer data and those from measurements of total pressures, provided the latter were based on the actual rather than on a theoretical ratio of the initial to the final reaction pressures.

Two intermediate products were identified, ketene and acetaldehyde. The formation of ketene had not been hitherto reported for this reaction. Both intermediates attained their maximum values at approximately the $\frac{1}{4}$ reaction life. The orders of concentration were about the same, but the maximum value for acetaldehyde persisted for a longer time than that for ketene. Formaldehyde, a postulated intermediate, was not found, although its presence to the order of 1 percent of sample composition could not be excluded. The conditions of investigation were not suitable for the detection of free radicals. Their presence could only be inferred from studies with added nitric oxide and from the induced decomposition of normally stable compounds by the reaction.

In addition to the principal final products, carbon monoxide and methane, small quantities of ethane, propane, and hydrogen were formed. The percent composition of carbon monoxide, ethane, and propane based on the total quantity of products was relatively constant during reaction, but the percent of methane increased and that of hydrogen decreased.

The results and experience obtained definitely established infra-red *in situ* measurements as a rapid and effective means for obtaining kinetic data. Identification and continuous measurement of each component during reaction can be made. As in the case of any research tool, certain limitations exist and coordination with other methods may be necessary depending on the particular reaction investigated. Obviously, substances exhibiting no infra-red adsorption cannot be measured. The overlapping of spectral bands may make direct identification of components difficult, or considerably lower the accuracy of measurements for weakly absorbing materials. Substances such as light gases may exhibit pressure broadening, and their measurement will consequently be difficult. Nevertheless, considerable data can be obtained in a relatively simple manner.

A complete presentation of the data and their implication on postulated mechanisms will be made at a later date.

* Present address: Perkin-Elmer Corporation, Glenbrook, Connecticut.
[1] G. L. Simard and J. Steger, Rev. Sci. Inst. **17**, 156 (1946).
[2] V. Z. Williams, G. L. Simard, and J. Steger, "Symposium on Molecular Structure and Spectroscopy," Ohio State University, June, 1946.
[3] W. Heckert and E. Mack, J. Am. Chem. Soc. **51**, 2706 (1929); C. Fletcher and G. Rollefson, J. Am. Chem. Soc. **58**, 2135 (1936); H. Thompson and M. Meissner, Trans. Faraday Soc. **32**, 1451 (1936).

A Comparison of the Ionization Cross Sections of H_2 and D_2

RICHARD E. HONIG
Research and Development Department, Socony-Vacuum Laboratories, Paulsboro, New Jersey

June 7, 1948

FROM recent mass spectrometric measurements, significant differences were reported[1] for the ion currents per unit sample pressure (sensitivities) of H_2^+ and D_2^+. The fact that the H_2^+ sensitivity was found to be higher by 10 to 40 percent apparently corroborated the assumption that the sensitivities of the three isotopic hydrogen molecules H_2, HD, and D_2 should be corrected by $M^{\frac{1}{2}}$ (where M = molecular weight) in order to compensate for their different flow rates. This correction cannot be reconciled with a previous theoretical analysis[2] of gas flow in the mass spectrometer, which showed that under conditions of molecular flow the sensitivity is proportional only to the partial pressure in the reservoir and does not depend on molecular weight.

In order to settle this point, the sensitivities of H_2^+ and D_2^+ were studied on a Consolidated Engineering mass spectrometer,[3] Model 21–101, at a nominal ionizing energy of 50 electron volts. After preliminary measurements had given erroneous and non-reproducible results, all operating conditions affecting H_2^+ and D_2^+ sensitivities were subjected to a close study. It was found that the temperature of the mercury diffusion pumps evacuating the mass spectrometer is a very critical parameter. In order to pump light gases properly, it was necessary to run the diffusion pumps at a temperature that was considerably higher than that used previously in routine operations. Figure 1 shows sensitivity as a function of pump temperature (heater voltage) for H_2^+ and CH_4^+. The poor pumping efficiency for H_2 at lower temperatures, as indicated by sensitivities above normal, is most surprising, but it agrees with observations recently made with oil diffusion pumps.[4] It is noteworthy that for a heavier molecule, such as CH_4, this effect is considerably smaller. This dependence of sensitivity on pump temperature explains why previously measured[1] ratios of H_2^+/D_2^+ sensitivities were apparently above unity. It also points out that line voltage fluctuations of ± 5 volts would account for ± 15 percent variations in H_2^+ sensitivity, as previously encountered, thus making impossible the accurate analysis of samples rich in hydrogen. After the pump heater voltage was raised from 52 to 65 volts (as shown in Fig. 1), long and short-term fluctuations of H_2^+ sensitivity were reduced to within the general instrumental accuracy.

Two other factors affecting H_2^+ sensitivity were found to be the ion accelerating potential E^+ and the complete establishment of equilibrium conditions. Figure 2 shows that the H_2^+ sensitivity is, for the instrument used, not a simple function of E^+, such as might be expected from theoretical considerations,[5] but has a pronounced plateau. The range of E^+ previously used is scanning H_2^+ (2500–2700 volts) is seen to give rise to a sensitivity variation of about ± 3 percent. To reduce this variation, the operating

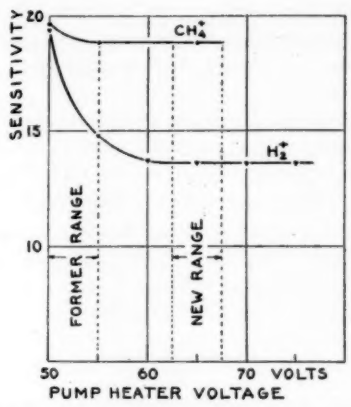

FIG. 1. Sensitivities of H_2^+ and CH_4^+ *vs.* pump heater voltage; ion accelerating potential $E^+ = 2650$ volts; *n*-butane sensitivity = 10.00 div./micron.

range for H_2^+ was shifted to about 2200 volts, where substantial changes in E^+ do not affect the sensitivity. A study made of the effects of sudden changes in electrostatic and magnetic fields and gas flow showed that even extreme changes require not more than 90 seconds for equilibrium conditions to be re-established.

Under these conditions of optimum reproducibility, ten separate sets of runs were made over a period of two weeks to compare H_2^+ and D_2^+ sensitivities. The gas samples used were carefully analyzed for the small amounts of N_2, O_2, and HD present, and sensitivities were corrected for these impurities. Each $H_2 - D_2$ pair was scanned at constant

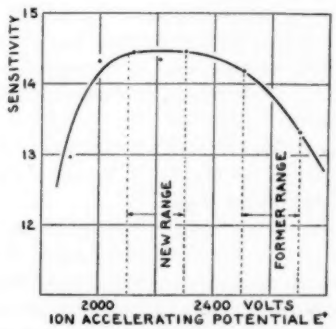

FIG. 2. Sensitivity of H_2^+ *vs.* ion accelerating potential E^+; pump heater voltage = 65 volts; *n*-butane sensitivity = 10.00.

magnetic field intensity. The average ratio obtained,

$$H_2^+/D_2^+ = 0.96_1 \pm 0.005$$

leads to the following conclusions:

(a) When measured under proper experimental conditions, the H_2^+ and D_2^+ sensitivities are essentially the same. The difference observed, about four percent, may well be due to instrumental discrimination. While the HD^+ sensitivity cannot be measured experimentally, it is reasonable to assume that it will lie between those of the other two isotopic molecules.

(b) Within four percent, the ionization cross sections (for 50 volt electrons) of H_2^+ and D_2^+, and probably HD^+, are the same, as should be expected from theoretical considerations.

(c) The theoretical analysis mentioned above appears to be corroborated by experiment. Ion currents are proportional to partial pressure in the reservoir, but not to flow rate, and no mass corrections should be made.

[1] N. Bauer and J. Y. Beach, J. Chem. Phys. **15**, 150 (1947).
[2] R. E. Honig, J. App. Phys. **16**, 646 (1945).
[3] H. W. Washburn, H. F. Wiley, S. M. Rock, and C. E. Berry, Ind. Eng. Chem., Anal. Ed. **17**, 74 (1945).
[4] R. J. Gibson, Jr., Rev. Sci. Inst. **19**, 276 (1948).
[5] N. D. Coggeshall, J. Chem. Phys. **12**, 19 (1944).

The Superconductivity of Lanthanum and Cerium[1]

W. T. Ziegler
State Engineering Experiment Station, Georgia School of Technology, Atlanta, Georgia
June 10, 1948

MEASUREMENTS have been made of the variation with temperature of the magnetic permeability of lanthanum and cerium, using an apparatus and method similar to that described by Horn and Ziegler.[2] Lanthanum was found to be a superconductor, while cerium did not become superconducting down to 2°K, the lowest temperature at which these metals were studied.

Two different samples of lanthanum were studied. Sample 1,[3] reported to contain 0.8 percent iron, exhibited a magnetic transition into superconductivity at 4.85 ± 0.15°K. Sample 2 (Hilger, Lab. No. 7259), reported to contain between 0.5 and 1 percent aluminum, silicon, and tungsten, showed a similar transition at 4.45 ± 0.10°K. In each instance the transition occurred over a range of less than 0.1°.

The sample of cerium[3] used was reported to contain 2.5 percent iron. No evidence for superconductivity in the material was observed down to 2°K, the lowest temperature reached. It is estimated that a transition of 10 percent of the material from the normal to a superconducting state could have been detected.

Lanthanum metal has previously been studied by Mendelssohn and Daunt,[4] using a magnetic method. These investigators reported a transition temperature of 4.71°K for a sample containing about 1 percent iron. Shoenberg,[5] also using a magnetic method, has reported that a lanthanum sample (Hilger, Lab. No. 7259), presumably identical with our Sample 2, was superconducting at 4.2°K. On the other hand, McLennan, Allen, and Wilhelm[6] have measured the electrical conductivity of "pure" samples of lanthanum and cerium from 300 to 1.9°K and reported that neither substance became superconducting.

Further work on these and other rare earth metals is underway and will be reported in the near future.

[1] This work was carried out with the assistance of the Office of Naval Research under Contract No. N6-ori-192, Task Order I.
[2] F. H. Horn and W. T. Ziegler, J. Am. Chem. Soc. **69**, 2762 (1947).
[3] Obtained from the Cooper Metallurgical Laboratory, 2135 Columbus Road, Cleveland 13, Ohio.
[4] K. Mendelssohn and J. G. Daunt, Nature **139**, 473 (1937).
[5] D. Shoenberg, Proc. Camb. Phil. Soc. **33**, 577 (1937).
[6] J. C. McLennan, J. F. Allen, and J. O. Wilhelm, Phil. Mag. (7) **10**, 500 (1930).

Immobilization of Solvent in Randomly Coiled Chain Molecules

Werner Kuhn and Hans Kuhn
Department of Physical Chemistry, University of Basel, Basel, Switzerland
June 7, 1948

IT has been generally accepted that chain molecules, dissolved in a proper medium, assume the shape of a statistical coil.[1]

The hydrodynamic behavior of a coil in a liquid has been studied first by W. Kuhn.[1] He has treated the limiting case in which the liquid inside the coil is completely immobilized if a translational motion of the coil is carried out or if the coil is suspended in a liquid with flow gradient. He has found that the intrinsic viscosity in this case is proportional to the square root of the degree of polymerization Z, and that the sedimentation constant s and the diffusion constant D are proportional to $Z^{\frac{1}{2}}$ and $Z^{-\frac{1}{2}}$, respectively.

$$\left.\begin{aligned}\eta_{sp}&\sim Z^{0.5}\\ s&\sim Z^{0.5}\\ D&\sim Z^{-0.5}\end{aligned}\right\}\quad\text{(complete immobilization).}\qquad(1)$$

M. L. Huggins[2] assumed a few years later free draining of the solvent through the coil, using Kuhn's result concerning the shape of the coil and his treatment of the hydrodynamic behavior of a completely drained road or filament (Perlenkettenmodell).[3] In this case, the intrinsic viscosity turns out to be proportional to Z,[2] the sedimentation constant independent on Z[4] and the diffusion constant proportional to Z^{-1}:[4]

$$\left.\begin{aligned}\eta_{sp}&\sim Z\\ s&\sim Z^{0}\\ D&\sim Z^{-1}\end{aligned}\right\}\quad\text{(free draining).}\qquad(2)$$

It has been pointed out[4] in 1943 that the cases (1) and (2) are two limiting cases. The low members in a homologous series of polymers approach the limit (2) (free draining), the highest members the limit (1) (complete immobilization). The correctness of this statement was proved by empirical data concerning diffusion,* sedimentation,** viscosity,*** and birefringence of flow.† These considerations have been confirmed and extended on the basis of experiments on macroscopic models, using a hydrodynamic similarity principle.[5,6]

In order to account for the hydrodynamic influence of partial immobilization upon the translational resistance of a statistical coil, the force $\mathbf{K}$ necessary to transport the coil through the liquid with a uniform velocity, u, was set up as

$$\mathbf{K}=\lambda_{\text{trans}}\eta_0 L u,\qquad(3)$$

η_0 is the viscosity of the solvent, and L the hydrodynamic length (end-to-end distance in the maximum extended chain). λ_{trans} is a numerical factor depending on the shape of the coil. On the basis of experiments on macroscopic models, λ_{trans} was found to be equal to

$$\lambda_{\text{trans}}=1\Big/\left(0.02+0.16\log^{10}\frac{A_m}{d_h}+0.1\left(\frac{L}{A_m}\right)^{\frac{1}{2}}\right),\qquad(3a)$$

d_h is the hydrodynamic thickness of the chain, and A_m the so-called length of the preferential statistical element (the

latter parameter is a constant for each homologous series and is equal to $A_m = \bar{h}^2/L$, $\bar{h}^2$ being the mean square distance between the ends of the chain).

Equations (3), (3a) include the two aforementioned limiting cases. For instance, in the case of large values of Z, it transforms to

$$\mathbf{K} = \eta_0 L u \Big/ \left(0.1\left(\frac{L}{A_m}\right)^{\frac{1}{2}}\right) = 10\eta_0 (L A_m)^{\frac{1}{2}} = 10\eta_0 (\bar{h}^2)^{\frac{1}{2}} u,$$

which is approximately equal to the resistance $\mathbf{K} = 3\pi\eta_0 (\bar{h}^2)^{\frac{1}{2}} u$ of a compact sphere of diameter equal to the average diameter of the coil (complete immobilization).

From Eqs. (3), (3a) can easily be obtained the following expressions for the sedimentation constant s and for the diffusion constant D[5, ††]

$$s = a_1 + b_1 (Z)^{\frac{1}{2}}, \tag{4}$$

$$D = (a_2 + b_2 (Z)^{\frac{1}{2}}) \frac{1}{Z}, \tag{5}$$

where the constants

$$a_1 = \frac{M_g}{N_L b} \frac{1 - v_{\text{part}} \rho_0}{\eta_0} \left(0.02 + 0.16 \log^{10} \frac{A_m}{d_h}\right), \tag{4a}$$

$$b_1 = \frac{M_g}{N_L b} \frac{1 - v_{\text{part}} \rho_0}{\eta_0} 0.1 \left(\frac{b}{A_m}\right)^{\frac{1}{2}}, \tag{4b}$$

$$a_2 = \frac{kT}{\eta_0 b} \left(0.02 + 0.16 \log^{10} \frac{A_m}{d_h}\right), \tag{5a}$$

$$b_2 = \frac{kT}{\eta_0 b} 0.1 \left(\frac{b}{A_m}\right)^{\frac{1}{2}} \tag{5b}$$

are independent upon the degree of polymerization Z. N_L is Loschmidt's number, M_g the molecular weight of the monomer unit, v_{part} the partial specific volume of the solute, ρ_0 the density of the solvent, k Boltzmann's constant, T the absolute temperature, and b the hydrodynamic length of the monomer unit (b is related to the hydrodynamic length L of the chain by the expression $L = b \cdot Z$). Equations (4) and (5) are found to be verified by the empirical data.

The partial immobilization is as important for rotational as for translational motions of the coil. Rotational experiments on models have shown that the rotational resistance and thus the rotational diffusion constant of random coils are given by simple expressions [analogous to (3), (3a)] as functions of A_m, d_h, and L.[5]

The motion of a particle suspended in a liquid with flow gradient is a translation superimposed by a rotation of the particle; therefore the rotational diffusion constant determines to a large extent the birefringence of flow and the viscosity of the solution.[3, 7]

By introducing the result of our rotational experiments on models into our earlier equation,[4] we obtain for the intrinsic viscosity[6, 8]

$$\frac{\eta_{sp}}{c} = \frac{A_m b^2}{48} \frac{N_L}{10^3} \frac{Z}{-0.05 + 0.12 \log^{10} \frac{A_m}{d_h} + 0.037 \left(\frac{bZ}{A_m}\right)^{\frac{1}{2}}} \text{‡, ‡‡} \tag{6}$$

(c concentration in base moles per liter).

The orientation and the value of the birefringence of flow can equally be described by expressions that take into account the partial immobilization of liquid inside the coil.[6]

P. Debye[11] and H. C. Brinkman[12] have recently also recognized the importance of partial immobilization on the viscosity, apparently without knowledge of our investigations in this field. The considerations of these authors are, as far as they have come to our knowledge, very similar to our own and represent to a considerable extent another expression of the same results. Thus the introduction of a "shielding ratio" by Debye corresponds entirely to our partial immobilization, and the cases (1) and (2) discussed in 1943 have again been found by Debye. Our expressions have the advantage of containing parameters that are determined by experiments on models, while the corresponding parameters of these authors refer to a non-realized spherical shape of the coils considered.

[1] W. Kuhn, Kolloid Zeits. **68**, 2 (1934).
[2] M. L. Huggins, J. Phys. Chem. **42**, 911 (1938).
[3] W. Kuhn, Zeits. f. physik. Chemie A **161**, 1 (1932); Kolloid Zeits. **62**, 269 (1932).
[4] W. Kuhn and H. Kuhn, Helv. Chim. Acta **26**, 1324 (1943).
* Reference 4, p. 1398.
** Reference 4, p. 1397.
*** Reference 4, p. 1443–44.
† Reference 4, p. 1420–21.
†† The linear relationship between the sedimentation constant and the square root of the degree of polymerization has already been recognized in our 1943 paper (reference 4, p. 1398).
‡ Equation (6) has been used already in reference 9, p. 85 and 92, reference 10, pp. 1573 and 1577.
‡‡ Reference 8 contains equally the corresponding quantitative expressions for branched chain molecules.
[5] H. Kuhn, Habilitationsschrift Basel (1946); preliminary report: H. Kuhn, Schweiz. Chem. Ztg. **28**, 373 (1945). Presented by W. Kuhn in lectures at Brooklyn Polytechnic Institute in New York, September 28, at the Harvard Medical School in Boston on October 9, 1946, and by H. Kuhn in a lecture at the California Institute of Technology on April 9, 1947.
[6] H. Kuhn and W. Kuhn, J. Polymer Sci., in print.
[7] P. Boeder, Zeits. f. Physik **75**, 258 (1932).
[8] W. Kuhn and H. Kuhn, Helv. Chim. Acta **30**, 1233 (1947).
[9] W. Kuhn and H. Kuhn, Helv. Chim. Acta **29**, 71 (1946).
[10] W. Kuhn and H. Kuhn, Helv. Chim. Acta **28**, 1533 (1945).
[11] P. Debye, Phys. Rev. **71**, 486 (1947).
[12] H. C. Brinkman, App. Sci. Res. A **1**, 27 (1947); Kon. Nederl. Akad. van Wetenschappen **50**, No. 6 (1947).

"Volume Effect" and Random Flights

R. C. Briant
Mellon Institute, Pittsburgh, Pennsylvania
June 14, 1948

THE so-called "volume effect" in flexible high polymer molecules has been a troublesome feature of high polymer theory since 1934.[1–3]

This note is to point out that the effect may be computed by elementary methods. In the random flight notation of Chandrasekhar[4] the probability of a flight of N randomly directed unit vectors from (x_1, y_1, z_1) to (x_2, y_2, z_2) (vector r_{12}) is

$$W_N(r_{12})dx_2dy_2dz_2 = (2\pi^2 |r_{12}|)^{-1} \int_0^\infty \sin(|\lambda||r_{12}|) \times (\sin|\lambda|/|\lambda|)^N |\lambda| d|\lambda| dx_2dy_2dz_2.$$

We write this in terms of the coordinates and abbreviate somewhat to

$$W_N(r_{12})dx_2dy_2dz_2 = W_N(x_1, x_2)dx_2.$$

A path from point 1 to point 2 in N steps is denoted $1\mathbf{N}2$.

Now the probability of a path of $S = L + M + N$ steps, $0\mathbf{L}1\mathbf{M}2\mathbf{N}3$, is

$$W_L(0, x_1) W_M(x_1, x_2) W_N(x_2, x_3) dx_1 dx_2 dx_3.$$

If the total number of steps S is fixed, then the middle section of M steps may range from the least integer greater than the distance from point 1 to point 2, denoted $\bar{r}_{12}$ up to $S-\bar{r}_{01}-\bar{r}_{23}$, where all the slack between 0 and 1 and 2 and 3 is taken up, and similarly for the other segments.

The probability of one of these events is (if $i+j+k=S$)

$$\sum_{i=\bar{r}_{01}}^{S-\bar{r}_{12}-\bar{r}_{23}} \sum_{j=\bar{r}_{12}}^{S-\bar{r}_{01}-\bar{r}_{23}} \sum_{k=\bar{r}_{23}}^{S-\bar{r}_{01}-\bar{r}_{12}} W_i(0, x_1)W_j \times(x_1, x_2)W_k(x_2, x_3)dx_1dx_2dx_3.$$

Now if point 1 and point 2 are within a certain critical distance of each other, we have what may be called a "loop" of vectors. A loop cannot occur if the vectors are the line of centers of a solid molecule.

If the last expression is integrated with respect to x_2, y_2, z_2 throughout a sphere of radius a centered at x_1, y_1, z_1 we have the probability that a loop of some size is formed.

This may be written

$$\int_{a_1x_2} \Sigma_{i_1j_1k} W_i(0, x_1)W_j(x_1, x_2)W_k(x_2, x_3)dx_1dx_2dx_3.$$

In the exact sense point 1 may be anywhere within a near-ellipsoidal solid of revolution with "foci" at points 1 and 3. If suitable asymptotic values are used point 1 may be anywhere. In either case, we integrate over the available range. This supplies the probability that at least one loop occurs somewhere on the path from 1 to 3. The complement to this is the probability that none occur. This is

$$\left\{W_S(0, x_3)-\int_{\infty,\, x_1}\int_{a_1x_2} \Sigma_{i_1j_1k} W_i(0, x_1)W_j \times(x_1, x_2)W_k(x_2, x_3)dx_1dx_2\right\}dx_3.$$

Details and applications to items in high polymer physics are being prepared.

[1] W. Kuhn, Kolloid Zeits. **68**, 2 (1934).
[2] R. Simha, J. Research Nat. Bur. Stand. **40**, 21 (1948).
[3] R. Simha, J. Polymer Sci. **3**, 227 (1948).
[4] S. Chandrasekhar, Rev. Mod. Phys. **13**, 1 (1943).

Free Electron Model for Absorption Spectra of Organic Dyes

HANS KUHN
Department of Physical Chemistry, University of Basel, Basel, Switzerland
June 7, 1948

A PAPER by N. S. Bayliss,[1] in which the absorption of polyenes is treated by a free electron model, has appeared recently in this Journal; the π-electrons belonging to the double bonds are assumed to have free mobility along the conjugated chain and to behave as a one-dimensional Fermi gas in a field of uniform potential energy. This model predicts values much too small of the wave-lengths of the absorption bands of polyenes; for instance, in carotene, according to Bayliss, the theoretical and experimental values of the wave-length of the first absorption band are 9700A and 4540A, respectively.

This discrepancy follows from the fact that in the ground state of a polyene molecule the π-electron gas just fills its first Brillouin zone, a zone which is produced by a periodicity of the potential energy along the chain due to the alternating "single" and "double" bonds. The electron jump corresponding to the first absorption band is a jump from the top of the first to the bottom of the second Brillouin zone; this process requires much more energy and, consequently, the absorption band appears at a much shorter wave-length than one would expect by a free electron model.

It has been shown recently[2] that a one-dimensional free electron gas model is, however, an appropriate approximation for a quantitative study of the absorption of a number of other colored substances, such as symmetric carbocyanine dyes, where the two resonating structures of the cation,

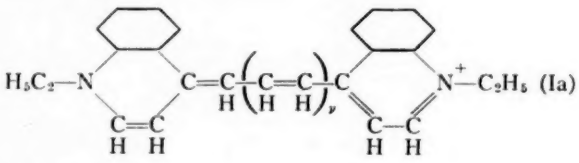

(Ia)

and

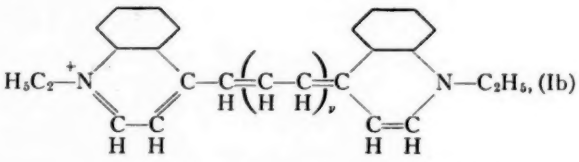

(Ib)

are equivalent. All C—C distances along the chain are equal, and the periodicity of "single" and "double" bond distances, which causes the appearance of the aforementioned Brillouin zone in the case of polyenes, is absent here.[3] There is a half-filled energy band in the ground state of the π-electron gas, and the electron jump corresponding to the first absorption band is a jump from the highest filled level to the next empty one. As these two levels are in the middle of an energy band, a free electron model is expected to give a reasonable approximation for their separation energy and consequently for the position of the peak of the corresponding absorption band.

Let us designate by Z the number of atoms that are linearly connected to the chain of resonating single and double bonds, and by l the bond distance between two neighbors of the chain. (In the case of a cyanine dye of structure (Ia), (Ib), where there is a chain of resonating single and double bonds between the two nitrogen atoms, Z is equal to $2\nu+9$ [see structure (Ia), (Ib)], and l is equal to 1.39×10^{-8} cm [i.e., equals the C—C distance in benzene].) The π-electrons are assumed to have free mobility along the zigzag chain of resonating single and double bonds (with inclusion of the area of the two nitrogen atoms at each end), i.e., along a line of total length $L=l(Z+1)$. The energy of the nth quantum state of this one-dimensional electron gas is then given by the expression[4]

$$E_n=\frac{h^2n^2}{8mL^2}=\frac{h^2n^2}{8ml^2(Z+1)^2}, \quad (1)$$

where h is Planck's constant and m the electronic mass. There are $N=Z+1=2\nu+10$ π-electrons belonging to the gas (each carbon atom in the chain contributes one electron, and the two nitrogen atoms altogether three); in the ground state, the $N/2$ levels of lowest energy are occupied by these electrons, each level containing two electrons. The first absorption band corresponds to a jump from the highest filled level with quantum number $n=N/2$ to the next higher level. From Eq. (1) can easily be obtained an expression for the wave-length λ_{vac} of the peak of this band.

$$\lambda_{vac}=\frac{8mc}{h}\frac{L^2}{N+1}=\frac{8ml^2c}{h}\frac{N^2}{N+1} \qquad (2)$$

(c = velocity of light). By introducing the numerical values of m, l, c, and h into (2) we obtain for some values of N (or ν):

$N=10(\nu=0)$ $\lambda_{vac}=5790$A (exp.$\lambda_{vac}=5900$A).
$N=12(\nu=1)$ $\lambda_{vac}=7060$A (exp.$\lambda_{vac}=7100$A)
$N=14(\nu=2)$ $\lambda_{vac}=8340$A (exp.$\lambda_{vac}=8200$A)
$N=16(\nu=3)$ $\lambda_{vac}=9590$A (exp.$\lambda_{vac}=9300$A).

The experimental values given in brackets are those obtained by Brooker and co-workers[3] from the spectra of dyes of structure (Ia), (Ib). These values are seen to be in good agreement with the theoretical values.

This one-dimensional free electron model can equally well be used for determining (in good agreement with the experiment) the position of the absorption peaks of a number of colored compounds, such as symmetric oxanole and cyanine dyes, triphenylmethane dyes, and aromatic hydrocarbons, such as anthracene, naphtacene and pentacene.[2]

The intensity of the absorption bands of these compounds, measured by the oscillator strength f, can easily be determined on the basis of our free electron model. For a molecule for which it can be assumed that its chain of resonating single and double bonds possesses all *trans*-configuration, such as symmetric cyanine of structure (IIa), (IIb),

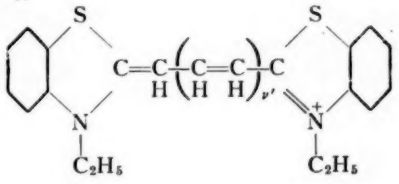

(IIa)

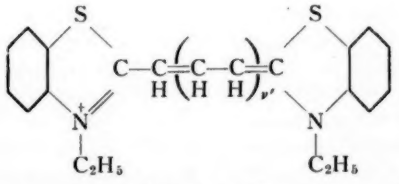

(IIb)

the oscillator strength of the first absorption band is found to be given by the equation:

$$f=\frac{4}{3\pi^2}\cos^2(\beta/2)\cdot\frac{N^2(N+2)^2}{(N+1)^3}. \qquad (3)$$

$180°-\beta$ is the valence angle between the chain members, and N, as mentioned above, the number of electrons belonging to the one-dimensional gas. (In the case of cyanines [see structure (IIa), (IIb)], N is equal to $2\nu'+6$, and $180°-\beta$ is equal to 124° (i.e., equals the C=C—C valence angle).) By introducing this value into (3), we obtain for some values of N (or ν'):

$N=6(\nu'=0)$ $f=0.71$ (exp.$f=1.2$)
$N=8(\nu'=1)$ $f=0.93$ (exp.$f=1.2$)
$N=10(\nu'=2)$ $f=1.14$ (exp.$f=1.6$)
$N=12(\nu'=3)$ $f=1.35$ (exp.$f=1.9$).

The experimental values in brackets, obtained from the data given by Brooker,[3] are in rough agreement with the theoretical values.

The problem of absorption of organic dyes and related compounds has been treated by earlier workers throughout on the basis of the bond orbital and molecular orbital method.[5] The wave functions of the π-electrons are considered in these latter treatments as simple combinations of atomic wave functions. The treatment proposed here, which is similar to Sommerfeld's treatment on metals,[6] does not refer to atomic wave functions, but considers a given π-electron as a particle in the potential field of the molecular frame. It is seen that this treatment is simpler and more powerful for the purpose considered here than the bond and molecular orbital treatments; according to the latter treatments, the position of the absorption peaks are dependent upon parameters that have to be determined empirically (in most cases from the position of the corresponding peaks in related compounds), while our equations do not contain such parameters.

[1] N. S. Bayliss, J. Chem. Phys. **16**, 287 (1948).
[2] H. Kuhn, Helv. Chim. Acta, in print; lecture at the chemistry colloquium in Basel, January 22, 1948.
[3] This Brillouin zone appears in non-symmetric cyanine dyes, where one of the two resonating structures that correspond to Ia and Ib is energetically preferred relative to the other. We thus expect by substituting a symmetric by a non-symmetric polymethine dye that there is a shift of the absorption band towards shorter wave-length. Such a shift has been found empirically by Brooker and co-workers [see L. G. Brooker, Rev. Mod. Phys. **14**, 275 (1942)—further references are given here] in a great number of examples.
[4] See, for instance, L. Pauling and E. B. Wilson, *Introduction to Quantum Mechanics* (McGraw-Hill Book Company, Inc., New York 1935), Section 14.
[5] A. L. Sklar, J. Chem. Phys. **5**, 669 (1937), **10**, 521 (1942); Rev. Mod. Phys. **14**, 233 (1942); K. F. Herzfeld and A. L. Sklar, Rev. Mod. Phys. **14**, 294 (1942); L. Pauling, in Gilman's *Organic Chemistry* (New York, 1938), p. 1864, Proc. Nat. Acad. Sci. **25**, 577 (1939); T. Förster, Zeits. f. Elektrochemie **45**, 548 (1939).
[6] See for instance: A. Sommerfeld and H. Bethe, *Handbuch der Physik*, Vol. **24**, second edition.

Monolayers Adsorbed on Metal Surfaces

A. R. MILLER
Royal Society Mond Laboratory, University of Cambridge, England
June 15, 1948

IN a recent paper, Halsey and Taylor[1] have considered the interpretation, in terms of statistical mechanics, of extensive measurements by Frankenburg[2] on the adsorption of hydrogen on tungsten powders. They quote the formula given by Fowler and Guggenheim[3] for the adsorption isotherm for a random distribution of particles (that is, an immobile film) on an array of localized[4] sites, taking account of closest neighbor interactions. Halsey and

Taylor point out, as is well known to be the case for an immobile film (each particle of which occupies one site on a localized array)[5] that this leads to a linear variation of heat of adsorption, q, with the fraction of the surface covered, θ. From the fact that Frankenburg's data does not follow such a law, they conclude that a theory of interactions on a surface in which all the sites involve the same energy of adsorption cannot account for the experimental results.

Their conclusion, in this respect, appears not to be well founded. Their rejection of interaction theories appears to be based primarily on the fact that the experimental results do not reproduce a linear variation of the heat of adsorption with the fraction of the surface covered. But this is not a characteristic of all possible types of adsorbed film, even for the kind of fixed interaction theory used in the case which they quote; such a linear variation is only to be expected on this theory for a random distribution, that is, an immobile film, of adsorbed particles, each of which occupies only one site on the surface. For *mobile* films[6] and for *all* films, mobile or immobile, *in which each adsorbed particle occupies more than one site*[7] on the array of the localized sites, the variation of the heat of adsorption may depart very much from a linear law in θ. Consequently, the experimental fact that a linear relation is not observed can provide no justification for rejecting out of hand an interaction theory.

Furthermore, it should be noted that the interaction theories to which reference has been made, and to one application of which Halsey and Taylor make appeal, assume that there is a *fixed* interaction energy between particles adsorbed on closest neighbor sites. It was pointed out by Roberts[8] that for an actual surface this will not be so; that, in fact, the surface provides a two-dimensional periodic potential field, the local sites postulated by Langmuir[9] being the potential minima of this field. It has been shown[10] that when this periodic variation of the potential field* provided by the surface and the variation with distance of the interaction energy between two adsorbed particles are taken into account, neither a mobile nor an immobile film gives anything like a linear variation of the heat of adsorption with the fraction of the surface covered. As this physical model is a much closer representation of an actual surface than the fixed interaction model which was used in the earlier theoretical treatments of adsorption, it can be concluded that for an actual surface a linear variation of q with θ is scarcely to be expected in any case. This is entirely neglected by Halsey and Taylor, and it provides an additional reason for doubting the validity of the conclusion which they seek to deduce from the absence of a linear variation. There is not space in a letter to consider all the effects of the periodic potential field provided by an actual surface but a qualitative discussion has been given elsewhere.[8] Miller and Roberts discussed theoretically a linear chain only, but by the use of other statistical methods it appears that the two-dimensional case can also be discussed and work is proceeding on this point.

Halsey and Taylor invoke the assumption that the energy difference between the lowest state in the gas phase and the lowest adsorbed state varies from site to site and that the interactions between adsorbed molecules can be neglected. It has been pointed out above that their argument depends on the neglect of a particular case of the fixed interaction theory and on the complete neglect of refinements of the theory which indicate that all adsorbed films give a variation of the heat of adsorption quite different from that which is the basis of their argument. Their rejection of theories which depend upon the interaction between adsorbed particles can scarcely be considered even to have been made plausible. Any effect which can be explained by the type of heterogeneity postulated by Halsey and Taylor is probably due to the fact that in the experiments which they discuss powdered metal is used and adsorbed gas on such a substratum forms a highly complex system.

[1] G. Halsey and H. S. Taylor, J. Chem. Phys. **15**, 624 (1947).
[2] W. G. Frankenburg, J. Am. Chem. Soc. **66**, 1827, 1838 (1944).
[3] R. H. Fowler and E. A. Guggenheim, *Statistical Thermodynamics* (Cambridge University Press, Teddington, England, 1939), Ch. X, p. 421.
[4] For a precise definition of the terms mobile and immobile films and of localized arrays of sites in this connection see J. K. Roberts, *Some Problems in Adsorption* (Cambridge University Press, Teddington, England, 1939), p. 22; A. R. Miller, Proc. Camb. Phil. Soc. **43**, 232 (1947); A. R. Miller, *The Adsorption of Gases on Solids* (Cambridge University Press, Teddington, England, in press), Section 2.2.
[5] J. K. Roberts, Proc. Camb. Phil. Soc. **34**, 399 (1938).
[6] J. S. Wang, Proc. Roy. Soc. **A161**, 127 (1937), Fig. 1; A. R. Miller, *The Adsorption of Gases on Solids* (Cambridge University Press, Teddington, England, in press), Sections 2.4 and 2.5.
[7] J. K. Roberts, Proc. Camb. Phil. Soc. **34**, 577 (1938), Fig. 4; A. R. Miller, Proc. Camb. Phil. Soc. **43**, 232 (1947), Figs. 2 and 5.
[8] J. K. Roberts, *Some Problems in Adsorption* (Cambridge University Press, Teddington, England, 1939), Section 2.7.
[9] I. Langmuir, J. Am. Chem. Soc. **40**, 1361 (1918).
[10] A. R. Miller and J. K. Roberts, Proc. Camb. Phil. Soc. **37**, 82 (1941).
* Still assuming, however, that the adsorption energy of a particle adsorbed at one of these minima is the same for all the sites.

Carbon-Carbon and Carbon-Hydrogen Bond Energies

GEORGE GLOCKLER
Department of Chemistry and Chemical Engineering, State University of Iowa, Iowa City, Iowa
June 14, 1948

WHEN the force constants (k(CC) and k(CH)) for the aliphatic structures given in Table I are plotted as a function of internuclear distance (R(CC) and R(CH)) as in Fig. 1, the well-known result is obtained that the larger force constants are found for the shorter bonds.[1] In order to obtain the corresponding carbon-carbon bond energies (D(CC)) and the average carbon-hydrogen bond energies (D(CH)), the atomic heats of formation (Q_a) of the molecules in Table I were calculated, using for the heat of sublimation of carbon $L(C)=5.888$ ev[2] or 7.334 ev.[3] For the D(CC):R(CC) curve only two points are known: $D(C_2(^3\Pi_u))=3.6$ ev from Herzberg[4] and D(diamond) $=L/2=2.944$ ev based on $L(C)=5.888$ ev. For the D(CH):R(CH) curve two known points are: $\bar{D}$(CH in CH_4) $=Q_a/4=3.88$ ev and $D(CH(^2\Pi_r))=3.47$ ev from Shidei.[5] Skinner[6] assumes a straight line relation for D(CH):R(CH). In the present calculations, however, the other points (C_2H_2, C_2H_4, C_2H_6) were found by dividing the corresponding Q_a values of these molecules in such a manner that *both* types of curve, D(CC):R(CC) *and* D(CH):R(CH) would have the same kind of curvature as the corresponding k(CC):R(CC) and k(CH):R(CH) curves. The procedure

TABLE I. Internuclear distances (R), force constants (k) and bond energies (D) of aliphatic carbon-carbon and carbon-hydrogen bonds.

	Substance	R(CC) A	k(CC) m.d./cm	D(CC)(ev) $L=7.334$	D(CC)(ev) $L=5.888$[f]	R(CH) A	k(CH) m.d./cm	D(CH)(ev) $L=7.334$	D(CH)(ev) $L=5.888$	Q_e(ev) $L=7.334$ (d)	Q_e(ev) $L=5.888$[f] (d)
1	C_2H_2	1.203[b]	1.56[b]	6.832	4.907	1.060[b]	0.59[b]	4.979	4.495	16.789	13.897
2	$C_2(^3\Pi_u)$	1.312[a]	0.95[a]	(5.54)	3.55[e]	—	—	—	—	—	—
3	C_2H_4	1.353[b]	0.82[b]	5.125	3.349	1.076[b]	0.53[b]	4.467	4.188	22.993	20.101
4	Diamond	1.545[c]	—	3.667	2.944	—	—	—	—	$L/2$	$L/2$
5	C_2H_6	1.569[b]	0.45[b]	3.535	2.922	1.098[b]	0.48[b]	4.212	3.834	28.807	25.925
6	CH_4	—	—	—	—	1.094[b]	0.50[b]	4.246	3.884	16.983	15.537
7	$CH(^2\Pi_r)$	—	—	—	—	1.120[a]	0.43[a]	(4.08)	3.47[g]	—	—

[a] G. Herzberg, *Molecular Spectra and Molecular Structure* (Prentice-Hall, Inc., New York, 1939).
[b] G. Herzberg, *Infrared and Raman Spectra* (D. Van Nostrand Company, Inc., New York, 1945).
[c] R. W. G. Wykoff, *The Structure of Crystals* (The Chemical Catalog Company, Inc., New York, 1931).
[d] F. R. Bichowsky and F. D. Rossini, *The Thermochemistry of the Chemical Substances* (Reinhold Publishing Corporation, New York, 1936).
[e] G. Herzberg, Phys. Rev. **70**, 764 (1946).
[f] H. D. Hagstrum, Phys. Rev. **72**, 947 (1947).
[g] T. Shidei, Jap. J. Phys. **11**, 23 (1936).

is arbitrary, but as a matter of fact very little choice is possible. It is believed that the values given in Table I are very good estimates of these bond energies. The CH-bond energies are, of course, average values with the exception of $D(CH(^2\Pi_r))$.

If a similar calculation is now made based on $L=7.334$ ev, then it is seen that $D(C_2(^3\Pi_u))\doteq 3.6$ ev and $D(CH(^2\Pi_r))=3.47$ ev no longer fit into the corresponding D(CC):R(CC) and D(CH):R(CH) curves, if curvatures like the k(CC):R(CC) and k(CH):R(CH) are to be maintained. In order to obtain proper energy-distance curves it is now necessary that $D(C_2(^3\Pi_u))=5.54$ ev and $D(CH(^2\Pi_r))=4.08$ ev. Obviously, these values do not check Herzberg[4] and Shidei.[5] It is conceivable that these investigators are wrong. However, several arguments will now be presented, indicating that the lower value of L(C)$=5.888$ ev is more acceptable, in spite of the fact that the latest experimental determination of L(C) seems to indicate the higher value:[3]

1. The D(CC):R(CC) and D(CH):R(CH) curves based on L(C)$=5.888$ ev have more nearly the curvature of the related k(CC):R(CC) and k(CH):R(CH) curves (Fig. 1).

2. A comparison of some molecular properties of the series of diatoms Be_2, B_2, C_2, N_2, O_2, F_2, Ne_2 shows that $D(C_2(^3\Pi_u))=3.55$ ev based on L(C)$=5.888$ ev fits better than $D(C_2(^3\Pi_u))=5.54$ ev based on L(C)$=7.334$ ev (Fig. 2).

TABLE II. Molecular properties of some first row elements.

	State	R (A)[a]	ω_e (cm^{-1})[a]	$x_e\omega_e$ (cm^{-1})[a]	k m.d./cm	D (ev)
Be_2	$^1\Sigma_g^+$	$\sim\infty$	~0	~0	~0	~0
B_2	$^3\Sigma_g^-$	(1.76)	(891)	(8.0)	(0.24)	(1.2)
C_2	$^3\Pi_u$	1.312	1642	11.71	0.95	3.56[e]
N_2	$^1\Sigma_g^+$	1.095	2360	14.45	2.29	9.76[d]
O_2	$^3\Sigma_g^-$	1.208	1580	12.07	1.17	5.08
F_2	$^1\Sigma_g^+$	1.435[b]	(790)	(8.0)	(0.34)	(~2.60)
Ne_2	$^1\Sigma_g^+$	$\sim\infty$	~0	~0	~0	~0

[a] G. Herzberg, *Molecular Spectra and Molecular Structure* (Prentice-Hall, Inc., New York, 1939.)
[b] M. T. Rogers, V. Schomaker and D. P. Stevenson, J. Am. Chem. Soc. **63**, 2610 (1941).
[c] G. Herzberg, Phys. Rev. **70**, 764 (1946).
[d] A. G. Gaydon, *Dissociation Energies and Spectra of Diatomic Molecules* (J. Wiley and Sons, Inc., New York, 1947).

3. The value of $\bar{D}$(CH in CH_4)$=3.88$ ev fits better into the series of hydrides CH_4, NH_3, OH_2, FH.[1] The higher value of 4.25 ev would produce a D(CH):R(CH) curve for these hydrides of quite different curvature than the corresponding k(CH):R(CH) curve.

4. The lower value of L(C)$=5.888$ ev fits appearance potential measurements.[2]

5. The removal energy of the first hydrogen atom from methane can be estimated from the curves of Fig. 1. The results based on L(C)$=5.888$ ev agree well with other work,[7-10] whereas similar calculations based on $L=7.334$ ev do not correspond at all. Since the distances R(CH in CH_4)$=1.094$A and $R(CH(^2\Pi_r))=1.121$A only differ by 0.027A, it was assumed that R(CH in CH_3) and R(CH in CH_2) are equally spaced between these values or R(CH in CH_3)$=1.103$A and R(CH in CH_2)$=1.112$A.

From a large plot of Fig. 1 the corresponding $\bar{D}$(CH) values can be found: $\bar{D}$(CH in CH_3)$=3.736$ ev and $\bar{D}$(CH

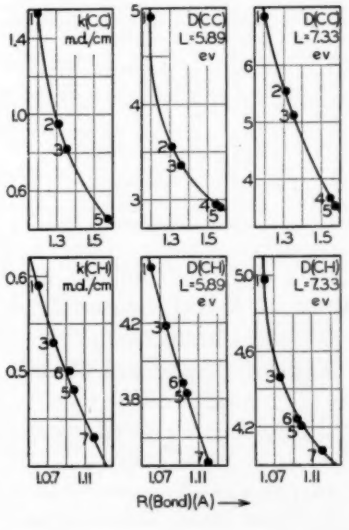

FIG. 1. Force constants (k; m.d./cm), bond energies (D; ev) of aliphatic carbon-carbon and carbon-hydrogen bonds as functions of internuclear distances (R; A^0). L = heat of sublimation of carbon = 5.89 or 7.33 ev; 1 = C_2H_2; 2 = $C_2(^3\Pi_u)$; 3 = C_2H_4; 4 = diamond; 5 = C_2H_6; 6 = CH_4; 7 = $CH(^2\Pi_r)$.

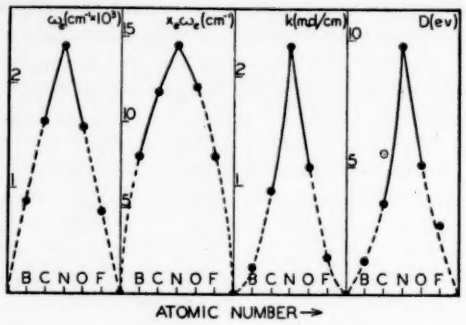

FIG. 2. Molecular constants of diatomic molecules Be_2, B_2, C_2, N_2, O_2, F_2, Ne_2.

in CH_2) = 3.593 ev. Hence the Q_a values of this series are:

$$C+4H\rightarrow CH_4+15.54 \text{ ev},$$
$$C+3H\rightarrow CH_3+11.21 \text{ ev},$$
$$C+2H\rightarrow CH_2+\ 7.19 \text{ ev},$$
$$C+\ H\rightarrow CH\ +\ 3.47 \text{ ev}.$$

And the removal energies of the consecutive hydrogen atoms of methane are:

$$CH_4\rightarrow CH_3+\ H-\ 4.33 \text{ ev},$$
$$CH_3\rightarrow CH_2+\ H-\ 4.02 \text{ ev},$$
$$CH_2\rightarrow CH\ +\ H-\ 3.72 \text{ ev},$$
$$CH\rightarrow C\ \ +\ H-\ 3.47 \text{ ev},$$

$$CH_4\rightarrow C\ \ +4H-15.54 \text{ ev}.$$

It is believed that these simple considerations lend weight to the lower value of the heat of dissociation $L(C) = 5.888$ ev.

[1] For literature references see G. Glockler, J. Chem. Phys. **16**, 600 (1948).
[2] H. D. Hagstrum, Phys. Rev. **72**, 947 (1947).
[3] L. Brewer, P. W. Gilles, and F. A. Jenkins, A.C.S. Meeting, Chicago, Illinois, April 19 (1948), Div. Phys. and Inorg. Chem., Paper No. 11.
[4] G. Herzberg, Phys. Rev. **70**, 762 (1946).
[5] T. Shidei, Jap. J. Phys. **11**, 23 (1936).
[6] H. A. Skinner, Trans. Faraday Soc. **41**, 465 (1945).
[7] K. Pitzer, Chem. Rev. **27**, 39 (1940).
[8] G. B. Kistiakowsky and E. R. Van Artsdalen, J. Chem. Phys. **12**, 469 (1944).
[9] D. P. Stevenson, J. Chem. Phys. **10**, 291 (1942).
[10] H. H. Voge, J. Chem. Phys. **4**, 581 (1936).

Interpretation of X-Ray Scattering from Solutions of Long-Chain Electrolytes on the Basis of a Spherical Micelle

M. L. CORRIN
Department of Chemistry, University of California, Berkeley, California
June 28, 1948

X-RAY diffraction measurements on isotropic aqueous solutions of long-chain electrolytes have been interpreted largely on the basis of a lamellar micelle;[1] thus "spacings" calculated by the Bragg equation have been assigned to various identity periods in this structure. Hartley,[2] however, has long maintained that the micelle must exist in spherical form. Recently a cylindrical model has been discussed by Harkins;[3] this latter is, however, characterized by Bragg law "spacings." It is indicated below (1) that the observed x-ray diffraction patterns can arise from a system of spherical micelles and (2) that Bragg law "spacings" may be meaningless.

Unfortunately no diffraction measurements have as yet been reported in which the absolute intensity of the scattered radiation is known as a function of the scattering angle. The position of the rather broad diffraction peaks has been studied as a function of electrolyte concentration; some qualitative observations have been made on the variation of relative intensities of these peaks, or bands, with concentration.[4]

The highly simplified model considered here is one of spherical micelles of uniform radius, a_0, whose short range order is characterized by a radial distribution function, $G(r)$. Ordinarily such distribution functions in liquid systems are calculated by means of the Fourier transform from diffraction data in which the absolute intensities of the scattered radiation are known as a function of the scattering angle.[5] Since in the present case no such data are available the reverse process will be employed; namely, the angular variation in intensity of the scattered radiation will be calculated on the basis of an assumed radial distribution function. All that can be expected from this treatment is qualitative agreement with respect to the form of the calculated and observed scattering curves. Under these conditions an extremely simple and highly approximate form of distribution function may be used.

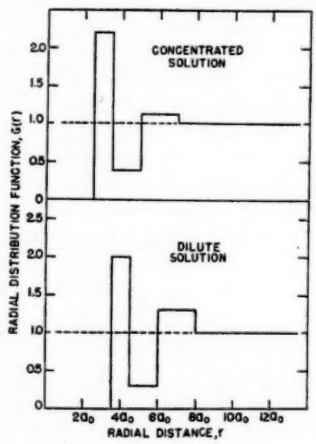

FIG. 1. Radial distribution functions for spherical micelles in concentrated and dilute solutions employed for the calculation of x-ray scattering. The radius of the micelle a_0, is taken as 16A.

Diffraction from two solutions of long-chain electrolyte, one dilute and the other concentrated, will be considered. The appropriate radial distribution functions employed are shown in Fig. 1 while the scattering curves calculated therefrom[6] are plotted in Fig. 2. These calculations are based upon a micelle 16A in radius and for Cu Kα radiation. The circles indicate those points for which the calculations were made.

These calculated scattering curves agree in form with those reported by Mattoon, Stearns and Harkins, while the relative intensities display the observed variation with concentration of long-chain salt. In a similar fashion the diffraction band observed at larger angles may be attributed to the short range ordering of hydrocarbon chains in the interior of the spherical micelle. On the basis of the model here considered, "spacings" calculated by the application of the Bragg equation to the position of the diffraction peaks are meaningless.[7]

It is thus shown that a lamellar model is not required to explain the x-ray diffraction patterns obtained from solutions of long-chain electrolytes. On a qualitative basis these patterns may be satisfactorily interpreted by recourse to a model of spherical micelles characterized with respect to relative position by a radial distribution function. This, of course, does not prove the validity of the spherical model. What it does indicate, in the light of our present experimental knowledge, is that x-ray measurements alone do not allow a decision between the lamellar and spherical models for micelles. Since a periodic structure cannot be demonstrated unambiguously, the "spacings" calculated

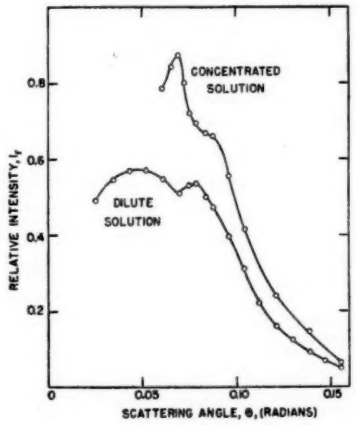

FIG. 2. The calculated scattered x-ray intensity curves for concentrated and dilute solutions of spherical micelles. Circles indicate those values which were calculated.

by the application of the Bragg equation to the diffraction patterns must be considered as of little significance.

The author would like to acknowledge helpful discussion and criticism by Dr. Bruno H. Zimm.

[1] P. Krishnamurti, Ind. J. Phys. **3**, 307 (1929); K. Hess, W. Philippoff and H. Kiessig, Kolloid Zeits. **88**, 40 (1939); J. W. McBain in *Advances in Colloid Science* (Interscience Publishers, Inc., New York, 1942); the work of numerous other investigators is cited in W. D. Harkins, R. W. Mattoon and M. L. Corrin, J. Am. Chem. Soc. **68**, 220 (1946).
[2] G. S. Hartley, *Aqueous Solutions of Paraffin Chain Salts* (Hermann et Cie, Paris, 1936).
[3] W. D. Harkins, J. Chem. Phys. **16**, 156 (1948).
[4] R. W. Mattoon, R. S. Stearns and W. D. Harkins, J. Chem. Phys. **15**, 209 (1947).
[5] N. S. Gingrich, Rev. Mod. Phys. **15**, 90 (1943).
[6] M. H. Pirenne, *The Diffraction of X-rays and Electrons by Free Molecules* (Cambridge University Press, New York, 1946).
[7] W. H. Zachariasen, J. Chem. Phys. **3**, 158 (1935).

Continuous Spectra and OH Absorption in Carbon Monoxide—Oxygen Explosions*

GEORGE A. HORNBECK
Applied Physics Laboratory, The Johns Hopkins University, Silver Spring, Maryland
June 11, 1948

THE use of a steel spherical bomb is not new to investigators in the field of combustion, but, in general, its use has been restricted for the purpose of obtaining pressure measurements, flame speeds, and experiments involving over-all radiation. The spectrum of an explosion of CO and oxygen of stoichiometric mixture is similar to a CO and oxygen flame in that the banded structure is superposed on a strong continuous background which extends throughout the visible into the ultraviolet. The intensity of this continuum frequently prevents sufficient contrast to allow resolution of the structural part of the spectrum; this single factor may account for the paucity of spectroscopic studies of combustion processes.

The brilliant flash which accompanies the explosion of CO and oxygen in a spherical bomb suggested the possibility of spectroscopic studies with an instrument of good dispersion without a prohibitive number of explosions. The steel bomb referred to in this discussion has a volume of 7 liters, and is equipped with two 1-in quartz windows diametrically centered. The mixture is ignited at the center of the sphere by a pair of tungsten electrodes connected to a common spark coil. The data are from spectrograms obtained with a Baird 2-meter grating spectrograph with 4A/mm dispersion. Figure 1 contains two curves founded on a series of single explosions in a bomb with a mixture of CO and oxygen in varying proportions. The carbon monoxide was commercially prepared and has 1.5 percent of nitrogen and hydrogen as impurities. Curve *A* shows the effect of increased oxygen on the intensity of the continuum. When the explosive mixture contained

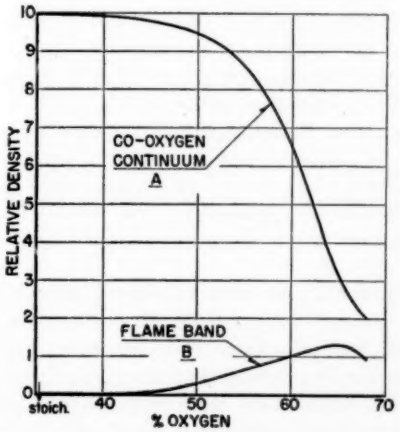

FIG. 1. Curve *A*: Density of the continuum at 3400A as a function of percent oxygen divided by the density at stoichiometric mixture. Curve *B*: The average density of several lines of a CO flame band of similar intensity (~3400A) above the density of the adjacent continuum. Thus, at 65 percent oxygen the density of a line would lie at about 1.3 above Curve *A*. The data for these curves are based on single explosions through a 2-meter grating spectrograph in the second order with a 25-micron slit on Eastman II-0 plates.

more than 68 percent oxygen, the intensity was too weak in a single explosion to be of any quantitative value in this problem. Curve *B* shows that explosions of increasing oxygen content afford greater contrast between the continuous background and the banded structure until the oxygen-CO ratio exceeds 2. It is interesting to note that the best mixture for spectroscopic studies of this combustion is the reverse of stoichiometric mixture; i.e., 2 parts oxygen and one part CO. It is hoped that further studies along this line will permit unambiguous identification of the molecules and radicals present in combustion and will furnish information on the processes involved.

Many investigators have been interested in obtaining OH in absorption in flames for the purpose of determining the concentration of the OH radical. However, in the past it was usually necessary to use the OH emission from a discharge tube in conjunction with a flame. The OH bands can readily be obtained in absorption in the CO-oxygen explosion. The determining factor for obtaining OH in absorption or in emission is the quantity of gas present in the bomb at the time of firing. The explosion of a stoichiometric mixture at one atmosphere pressure will yield OH in absorption, but the same mixture at any pressure less than 0.6 of an atmosphere will produce OH in emission. Figure 2 shows a portion of the OH band at 3064A in

FIG. 2. A portion of OH band at 3064A in absorption obtained on a 21-ft. grating spectrograph.

absorption taken on a 21-ft. grating spectrograph. In addition to the (0−0) OH band at 3064A, the (1−0), (2−0), and the (3−0) bands at 2811, 2609, and 2444A have been observed in absorption in this explosion.

Self-sustaining flames of CO and oxygen with various fuel ratios have been burned in an effort to produce spectra of high contrast but, due to the various degrees of combustion present in a fixed flame, the effect of increased oxygen content is less pronounced than in the explosive flame.

In conclusion I wish to express my appreciation to Dr. B. Lewis, Dr. von Elbe, and Dr. E. F. Fiock for valuable discussions. I am also indebted to Dr. R. C. Herman for helpful suggestions and general encouragement, and to Mr. B. W. Bullock for his assistance in experimental matters. I wish to thank Professor G. H. Dieke for his interest in this problem and for making available to me the 21-ft. Paschen spectrograph at The Johns Hopkins University.

* The work described in this paper has been supported by the Bureau of Ordnance, U. S. Navy, under Contract NOrd-7386.

Detonation Wave in Nuclear Explosives

P. CALDIROLA
Istituto di Fisica dell'Università di Pavia, Pavia, Italy
June 14, 1948

IT is known that the hydrothermodynamic theory of detonation developed by Chapman, Jouguet and R. Becker has been used successfully in order to study the detonation of gaseous, liquid and solid explosives.[1] The fundamental equations of the theory can be deduced, for detonation in steady conditions, in a plain and direct way by considering the process from a wholly macroscopic point of view by means of the application of general principles, i.e. laws of conservation of mass, momentum and energy, and the fundamental laws of thermodynamics. Starting from the observation that these principles are valid, independent of the kinetic elementary processes from which the detonation originates, we have thought to apply the hydrothermodynamic theory also in the case in which the explosion is determined by means of a chain process of nuclear fissions, such as that which takes place in a medium of uranium (isotope 235). The explosive material is supposed to occupy a perfectly smooth and rigid cylindrical tube having a sufficiently large diameter so that we consider negligible the effects on the walls of the container; we can also assume that the detonation thus proceeds parallel to the axis of the cylindrical tube. Although this schematization is somewhat different from the conditions realized in practice, nevertheless we believe that it can be used for a rough evaluation of the parameters, which characterize the detonation. In the mathematical theory of the process considered above, it is necessary to keep in mind an essential fact which differentiates the detonations having a nuclear origin from the ordinary ones: in nuclear explosives the temperatures produced are so high, that it is not possible to neglect the effect of the pressure and of the energy of radiation. It is therefore necessary to introduce terms in the equations of the theory taking account of the momentum and energy transferred by the radiation. If the radiation energy density is E_r, and the radiation pressure is $p_r=\frac{1}{3}E_r$, the hydrodynamic equations of the ordinary detonation theory shall be replaced by:

$$\begin{aligned}\rho_1 D&=\rho(D-W)\\ p_1+\rho_1 D^2&=(p+p_2)+\rho(D-W)^2,\\ p_1 D+\rho_1 D[E_1+(D^2/2)]&=(p+p_r)(D-W)+\rho(D-W)\\ &\quad\times[E+E_r+((D-W)^2/2)],\end{aligned}\tag{1}$$

where D is the velocity of the detonation wave, W, the velocity of the explosion products; ρ_1, p_1, E_1 and ρ, p, E the density, the pressure and the specific internal energy respectively, of the unexploded substance and of the explosion products.

To these equations we shall add the thermodynamic relation

$$E-E_1=\int_{T_1}^{T} c_v dT-q=\bar{c}_v(T-T_1)-q.$$

The explosion temperatures being extremely high, one can suppose

$$p_r=(aT^4/3)\gg p,$$

calling to mind the well known relation:

$$E_r=aT^4v$$

and from the preceding equations one deduces, therefore, the Rankine-Hugoniot curve

$$c_v(3/a)^{\frac{1}{4}}p^{\frac{1}{4}}+(7/2)pv\cdot(1/2)pv_1-q=0$$

where $v=(1/\rho)$, $v_1=(1/\rho_1)$.

For numerical computations, we observe that the energy liberated from the complete fission of 1 kg U_{235} is

$$q\approx 19.7\cdot 10^9 \text{ kcal./kg}=8.4\cdot 10^{14} \text{ kg}\cdot\text{cm/kg},$$

that the specific heat of the fission products (2 fission nucleus, 2 neutrons, 92 electrons for a single U_{235} atom) can be evaluated considering the mixture as a perfect non-degenerate gas

$$c_v=\tfrac{3}{2}R\frac{96\times 1000}{235}=1{,}21 \text{ kcal./°K}\cdot\text{kg}$$
$$=5{,}18\cdot 10^4 \text{ kg}\cdot\text{cm/°K}\cdot\text{kg}.$$

Assuming finally

$$a=7{,}81\cdot 10^{-21} \text{ kg/cm}^2\text{ °K},\quad \rho_1=18{,}7 \text{ kg/cm}^3,$$

Eq. (1) can be written

$$7{,}25\cdot 10^9 p^{\frac{1}{4}}+3{,}5pv-26{,}7p-8{,}40\cdot 10^{14}=0.$$

Supposing that, as in the case of the ordinary explosions, the stable state of the detonation process is analytically determined by the fact that, corresponding to it, the derivative ds/dv of the entropy must be taken equal to zero, one finds the values

$$p=9{,}0\cdot 10^{12} \text{ kg/cm}^2,\quad v=30{,}3 \text{ cm}^3,$$

from which by means of Eq. (1)

$$T=2{,}4\cdot 10^8 \text{ °K},\quad D=3{,}3\cdot 10^7 \text{ cm/sec.},\quad W=1{,}4\cdot 10^7 \text{ cm/sec.}$$

We will finally observe that the value found for the velocity D of the detonation wave is a little smaller than the value $U\approx 2\cdot 10^8$ cm/sec. or the mean velocity of the neutrons in thermal equilibrium at the temperature $T=2{,}4\cdot 10^8$ °K. The relationship between the velocities D and U is naturally determined by the mechanism from which the chain reaction takes place.

Although the preceding calculations have been established assuming some very rough hypothesis, nevertheless we believe that they can be interesting enough because they suggest a new starting point in order to attack the problem of the detonation of nuclear explosives.

[1] For a review see Stewart Paterson, Research 1, 221 (1948).

An Equation of State for Gases at Extremely High Temperatures and Pressures From the Hydrodynamic Theory of Detonation

STEWART PATERSON
Imperial Chemical Industries, Limited, Explosives Division, Stevenston, Scotland

June 23, 1948

I HAVE read the reply[1] of M. A. Cook to my criticisms[2] of his paper,[3] and realize that I was mistaken in supposing that he regarded his first method of solution as in practice more "general" than the second. As a matter of fact, I was more concerned with his claim that such a general solution was possible even in principle. Unfortunately, I can find no ground in his reply for revising my arguments regarding either this question or the detailed method of solution, but since these arguments have already been stated it seems unprofitable merely to repeat them.

My further point regarding the method of successive approximations as compared with step-by-step integration along an $\alpha(v_2)$ curve was largely mathematical. α is of course "well-defined," but it is a question here of determining it by the solution of certain equations. If one proceeds by a stepwise method from an assumed point in the (v_2, α) plane lying below Cook's curve, one does in fact derive two members of an integral family, of which Cook's curve is the envelope. This is just what one would expect on mathematical grounds. For various *physical* reasons, including that offered by Cook, it can be judged that these integral curves are on the whole unacceptable, but this did not appear to me to dispose of all interest attached to the question.

[1] M. A. Cook, J. Chem. Phys. **16**, 554 (1948).
[2] S. Paterson, J. Chem. Phys. **16**, 159 (1948).
[3] M. A. Cook, J. Chem. Phys. **15**, 518 (1947).

Testing of Colloidal Solutions by Dye Solubilization

JOSEPH M. LAMBERT AND WARREN F. BUSSE*
General Aniline and Film Corporation, Central Research Laboratory Easton, Pennsylvania

June 28, 1948

EXTENSIVE studies by McBain and collaborators[1-3] have elucidated dye solubilization phenomena which, in turn, gave valuable information on the structure of colloidal micelles. In some of their publications[2,4,5] solubilization data are given for commercial surface-active agents with the implication that dye solubilization is useful in evaluating the relative efficiency of such compounds. The experimental procedure which has been used at the Stanford Laboratory appears rather tedious since it involves the attainment of equilibrium conditions requiring periods in the order of days or even weeks.

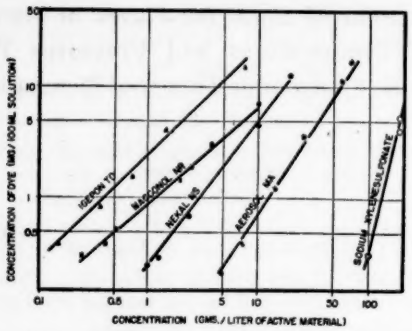

FIG. 1. Solubilization of 1-*o*-tolylazo-2-naphthol in aqueous solutions containing surface-active agents. Interaction: 15 min. at 50°C.

In our investigation, first a study was made in order to determine the rate of solubilization of water-insoluble azo dyestuffs under various experimental conditions. It was found that solubilization values sufficiently close to the equilibrium values could be attained within 15 minutes if the tests were made at 50°C and if the amounts of dye solubilized did not exceed certain limits. Subsequently, it was possible to work out a practical procedure which is reproducible and rapid and can be used for the routine evaluation and classification of different types of surface-active agents by dye solubilization.

A new method of presenting solubilization data proved useful; it consists of plotting the logarithm of the amount of dyestuff solubilized against the logarithm of the amount of surface-active agent in solution. Figure 1 shows the results obtained with 1-*o*-tolylazo-2-naphthol solubilized in solutions of the following commercial surface-active agents in distilled water:

Detergents—Igepon *TD* (General Aniline & Film Corporation); Nacconol *NR* (National Aniline & Chemical Company).

Wetting Agents—Aerosol *MA* (American Cyanamid & Chemical Company); Nekal *NS* (General Aniline & Film Corporation).

Hydrotropic Agent—Sodium Xylenesulfonate (Wyandotte Chemicals Corporation).

The values were obtained by admixing 100 mg crystallized dyestuff with 20 ml of each detergent solution contained in a test tube and pre-heated to 50°C in a constant temperature bath. After 15 minutes of interaction in the same bath, the solutions were filtered using No. 50 Whatman paper. The filtrates, as such, or after suitable dilution, were measured in a Fisher Electrophotometer in order to determine the amount of solubilized dye. Conventional standardization and calibration procedures were employed for this determination.

As can be seen in Fig. 1, characteristic solubilization isotherms for the different types of surface-active agents (each varying in concentration over a suitable concentration range) can be represented with good approximation by straight lines. The general equation for the isotherm is $S=Kc^n$ or $\log S=n\log c+\log K$ where S is the amount of dye solubilized (mg/100 ml of solution), c the concentration of detergent solution (grams/liter of active ingredient) and where K and n are constants which are characteristic for each solubilizing agent.

The procedure described makes possible the ready comparison of different surface-active agents. Useful and generally significant values can be obtained by determining the amount of surface-active agent required for solubilizing a certain amount, say 1 mg of dyestuff. Further details and other applications of the method will be published elsewhere.

* Present address: Institute of Textile Technology, Charlottesville, Virginia.

[1] J. W. McBain and M. E. L. McBain, J. Am. Chem. Soc. **58**, 2610 (1936).
[2] J. W. McBain, *Advances in Colloid Science I* (Interscience Publishers, Inc., New York, 1942), edited by E. O. Kraemer, pp. 99–142.
[3] J. W. McBain, K. E. Johnson, J. Am. Chem. Soc. **66**, 9 (1944).
[4] J. W. McBain, A. G. Wilder, and R. C. Merrill, Jr., J. Phys. Colloid Chem. **52**, 12 (1948).
[5] J. W. McBain and R. C. Merrill, Jr., Ind. Eng. Chem. **34**, 915 (1942).

Dissociation Energies of Nitrogen and Nitric Oxide

HOMER D. HAGSTRUM
Bell Telephone Laboratories, Murray Hill, New Jersey
June 30, 1948

IN a recent publication Glockler[1–3] has concluded from some semi-empirical relationships that $D(N_2)=9.764$ ev and $D(NO)=6.49$ ev. This is also the conclusion arrived at by Gaydon[4] through a rigorous application of the non-crossing rule in interpreting the band spectra of these molecules. It is the purpose of this letter to point out that these conclusions cannot account for an experimentally determined dissociation limit in NO^+ which is as well established as any determined by the electron impact method and which cannot be circumvented by the assumption of initial kinetic energy of the dissociation products as suggested by Gaydon and Glockler.

For N^+ ions from N_2 and from NO both the appearance potential *and* the initial kinetic energy have been measured with a mass spectrometer and with a retarding potential apparatus.[5–7] Both methods agree that N^+ ions of zero initial kinetic energy appear first at 24.3 ± 0.2 ev from N_2 and 21.8 ± 0.2 ev from NO. These data lead to the values $D(N_2)=9.75$, or 7.85, or 7.37 ev, and $D(NO)=7.25$, or 5.35, or 5.28 ev, etc., for various choices of the excitation of the products. Thus, although it is true that either of the spectroscopic values, 7.384 or 9.764 ev, proposed for $D(N_2)$ can be fitted to the electron impact results for N_2 alone, the value $D(NO)=6.49$ ev cannot be brought into agreement with the NO result. It would thus appear that the only set of values consistent with both electron impact and band spectroscopic results are $D(N_2)=7.384$ ev and $D(NO)=5.30$ ev.

The electron impact data referred to above are among those few for which a determination of the initial kinetic energy has been made (H^+ from H_2, N^+ from N_2 and NO,

C^+ from CO). They are not to be confused with, or treated on an equal footing with results obtained with the mass spectrometer alone (O^+ from O_2), or for which the ion peak shape is anomalous (O^+ from CO and NO).[5] The N^+ onset potentials in NO are not confused by the fact that there are two processes for the formation of N^+ ions as Gaydon suggests. The situation is entirely analogous to that found for C^+ ions from CO.

It is the opinion of this writer that the electron impact experiments should carry considerably more weight than the series comparisons presented by Glockler. It is also difficult to see the justification for the rigorous use of the non-crossing rule in view of the theoretical limitations on its applicability and evidences in band spectra of its violation. Glockler, although careful to point out that the rule is not violated for NO if $D(NO) = 6.49$ ev, is apparently willing to accept values of $D(CO)$ which involve violations for CO. Considerations relating to $D(CN)$ and $D(CN-CN)$ are based on experiments which are more readily reinterpreted than the electron impact experiments. Thus the diffuse spectra observed by Hogness and Liu-Sheng[8] in cyanogen might be interpreted differently as suggested by themselves and by Gaydon, and the result of Robertson and Pease[9] depends on the acceptance of a rather involved chain mechanism for the thermal reaction of hydrogen and cyanogen. Similarly, the Born-Haber cycle given by Glockler involves a number of questionable energetic quantities.

The occasion of this letter will also be taken to discuss interpretations of electron impact work to be found in Gaydon's book[4] which appear to this writer to be in error or concerning which new evidence is now available. The appearance potential for C^+ ions from CO at 22.8 ev has been determined for ions of zero initial kinetic energy so that one cannot attribute a part of this potential to undetected kinetic energy of the products.[10] The appearance potential for O^+ ions at the maximum of its kinetic energy distribution (27 ev) is not to be compared with the value for ions of zero initial kinetic energy $\left(23.5\ {}^{+0.0}_{-0.4}\ \text{ev}\right)$. The values 23.1 and 23.5 ev are not two independent appearance potentials but the experimental limits for a single one. C^- cannot be the other product in the process yielding O^+ from CO because C^- was looked for and not found.[5]

Concerning Gaydon's remarks about O_2 it may be pointed out that only the mass spectrometric result is available for the O^+ ion and there appears to exist no valid objection to the interpretation which has been given for the O^+ onset potential. The potential curve of O_2^+ involved in the dissociation process cannot be that of the ground state of the molecular ion as Gaydon assumes because the known r_e values of this state and the ground state of O_2 are nearly identical.

In connection with these discussions it is of interest to note the excellent agreement now obtained for the electron affinity of the oxygen atom by the method of ionization at a heated filament[11] with the electron impact result.[5,6] The present writer has had the opportunity to look at the original electron impact data for HCl,[12] referred to by Gaydon, and has found that if the data are evaluated by the vanishing current method rather than the now discredited linear extrapolation method used by Nier and Hanson, good agreement with the band spectroscopy of HCl is obtained.

[1] G. Glockler, J. Chem. Phys. **16**, 600 (1948).
[2] G. Glockler, J. Chem. Phys. **16**, 602 (1948).
[3] G. Glockler, J. Chem. Phys. **16**, 604 (1948).
[4] A. G. Gaydon, *Dissociation Energies and Spectra of Diatomic Molecules* (John Wiley and Sons, Inc., New York, 1947).
[5] H. D. Hagstrum and J. T. Tate, Phys. Rev. **59**, 354 (1941).
[6] W. W. Lozier, Phys. Rev. **44**, 575 (1933); *ibid.* **45**, 850 (1934); *ibid.* **46**, 268 (1934).
[7] E. E. Hanson, Phys. Rev. **51**, 86 (1937).
[8] T. R. Hogness and Liu-Sheng T'sai, J. Am. Chem. Soc. **54**, 123 (1932).
[9] N. C. Robertson and R. N. Pease, J. Chem. Phys. **10**, 490 (1942).
[10] H. D. Hagstrum, Phys. Rev. **72**, 947 (1947).
[11] M. Metlay and G. E. Kimball, J. Chem. Phys. **16**, 779 (1948).
[12] A. O. Nier and E. E. Hanson, Phys. Rev. **50**, 722 (1936).

The Influence of an Electric Field on the Depolarization Factors of Raman Lines*

A. E. Douglas
Physics Dept., Pennsylvania State College, State College, Pennsylvania
(May 20, 1948)

IT has been reported that the depolarization factors of some of the Raman lines of liquids are altered by an electric field.[1] It would seem that valuable information could be obtained by a detailed and quantitative investigation of this phenomena.

In order to investigate this effect two sample tubes containing flat brass electrodes were made. The space between the electrodes was 5 mm in one tube, and 2 mm in the other. The electric field was applied to the electrodes by means of tungsten wires sealed through the glass. The depolarization factors of the Raman lines of the sample were determined by means of a photoelectric recording spectrograph by a method which has been described previously.[2] To determine the effect of the electric field, the spectrograph was set at the Raman line under investigation and the change in intensity when the electric field was applied was measured directly by the galvanometer deflection. The effect of the field on both the strong and weak component was determined.

Measurements were made on the most highly polarized lines of benzene; cyclohexane; carbon tetrachloride and chlorobenzene and also on some of the less highly polarized lines. The field strength varied somewhat but most of the trials were made with a direct field of 20,000 volts per cm and then repeated with an alternating field of 70,000 volts per cm.

In no case did the applied field produce any noticeable change. Certainly, in no case did it change the depolarization factor of the highly polarized lines by more than 0.01. It is recognized that this result is in direct contradiction to the results published previously which lead one to expect a change in the depolarization factor of the order of 0.1. However, the method of measurement used here is direct and accurate and not subject to the many errors of the photographic method.

There still exists the possibility that measurable changes in the depolarization factor may occur at higher field

strengths. Such high fields can be applied to very few liquids and even in these cases, only under special conditions. Therefore it appears unlikely that the Raman spectrum of liquids in electric fields will yield much additional information.

* This research was carried out on Contract N60nr-269 Task V of the Office of Naval Research.

[1] S. C. Sirkar, Ind. J. Phys. **8**, 337 (1933).
[2] D. H. Rank, J. Opt. Soc. Am. **37**, 798 (1947).

Note on the Correlation through Anharmonic Force Theory of the Compressibility Modulus and Thermal Expansion Coefficient of KBr at Low Temperatures

CHARLES KITTEL
Bell Telephone Laboratories, Murray Hill, New Jersey
June 7, 1948

THE purpose of this note is to show that the temperature dependence of the compressibility modulus and volume of KBr at low temperatures may be understood approximately in terms of the theory of anharmonic lattice dynamics as formulated by Debye.[1]

Galt[2] has measured the elastic modulus c_{11} of KBr down to liquid helium temperatures, and he has also measured c_{12} down to 140°K. The modulus c_{12} was found to be approximately independent of temperature, and if we suppose that this independence continues down to 0°K we may deduce values of the compressibility modulus $K=(c_{11}+2c_{12})/3$ over the temperature range from the liquid helium region to room temperature, at which point the values join on to the earlier measurements of Slater[3] over the range 30°–75°C.

Since Galt's measurements appear to be the first which go down to temperatures such that $dK/dT\rightarrow 0$, it is of interest to see whether his results are intelligible in terms of anharmonic lattice interactions; as a check on the anharmonic constants one may also examine the thermal expansion data. The existence of a relation between the change δK in compressibility modulus and the change in volume, with increasing temperature, may be made plausible by the following very crude consideration. As a result of anharmonic terms, the compressibility modulus will be a function of the volume:

$$K=K_0+\delta K=K_0+K_1\Delta+\cdots,$$

where Δ is the fractional change of volume; now even if Δ is due to thermal expansion, we may expect that $\delta K/\Delta$ will be approximately constant.

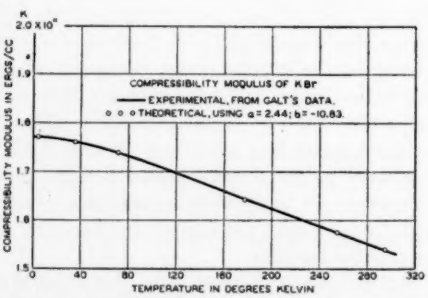

FIG. 1. Variation of compressibility modulus with temperature in KBr.

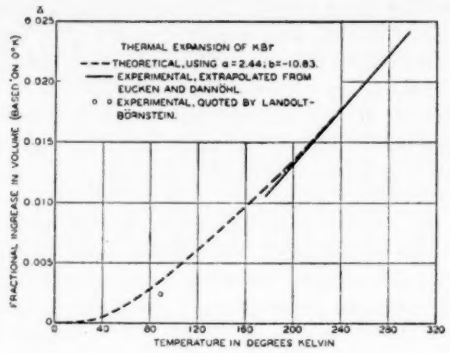

FIG. 2. Fractional increase in volume with temperature.

Debye expresses the effect of the anharmonic terms in the lattice interactions by supposing that the characteristic temperature Θ may be expressed as a power series in the fractional volume change

$$\Theta=\Theta_0[1-a\Delta+(b/2)\Delta^2+\cdots]$$

where $\Delta=(V-V_0)/V_0$. Debye then goes on to derive by straightforward methods certain approximate expressions for the compressibility modulus and for the thermal expansion coefficient as functions of the temperature and of the anharmonicity constants a and b. The expressions are too complicated to reproduce here.

Figure 1 shows an experimental curve for the compressibility modulus *vs.* T, derived from Galt's data, and the "best fit" theoretical values calculated from Debye's results using $a=2.44$, $b=-10.83$. For KBr, $\Theta_0=177$°K. The algebraic signs of a and b are physically plausible.

Figure 2 shows experimental values of the fractional volume increase *vs.* T and a theoretical curve calculated from Debye's results with the same values of a and b which gave the best fit to the compressibility data. The experimental data are taken from the Landolt-Börnstein tables and from an extrapolation to low temperatures of the high temperature measurements of Eucken and Dannöhl.[4] The volume was normalized so that the theoretical and experimental values of Δ were equal at 0°C.

The following conclusions may be drawn from this work:

(a) The Debye theory with anharmonic terms gives a satisfactory representation of the temperature variation of the compressibility modulus.

(b) Using the values of the anharmonicity constants determined by (a), the Debye theory gives correctly the slope of the curve of Δ *vs.* T: that is, it gives the thermal expansion coefficient.

I wish to express my thanks to Miss C. L. Froelich for computational assistance.

[1] P. Debye, in *Vorträge über die kinetische Theorie der Materie und Elektrizität*, by M. Planck *et al.* (B. G. Teubner, Leipzig, Germany, 1914); an equivalent treatment is given by E. Grüneisen, Handbuch der Physik **10**, 1–59 (1926).
[2] J. K. Galt, M.I.T. Research Laboratory of Electronics Technical Report No. 45, September 17, 1947, "Mechanical Properties of Alkali-Halide Crystals—NaCl, KBr, KCl": Phys. Rev. **73**, 1460 (1948).
[3] J. C. Slater, Phys. Rev. **23**, 488 (1924).
[4] A. Eucken and W. Dannöhl, Zeits. Elektroch. **40**, 814–821 (1934).